Republic of Iraq
Ministry of Higher Education & Scientific Research
University of Baghdad/ College of Education for Pure Sciences (Ibn al-Haitham)
Department of Chemistry

Spectroscopic and Structural Study of New Schiff Bases and Their Metal Complexes and Evaluation of Their Biological Activity

A thesis

Submitted to the Department of Chemistry, Collage of Education for Pure Sciences / Ibn Al Haitham University of Baghdad in Partial Fulfillment of the Requirements for the Degree of Doctor of Philosophy (Ph.D.) in Chemistry.

By

Shaimaa Ahmad Hassan Al-taee

B. Sc. in Chemistry 2002
M. Sc. in Chemistry 2012
(University of Baghdad)

Supervisor

Prof.Dr. Sajid Mahmood Lateef

1440 AH **2018 AD**

بسم الله الرحمن الرحيم

﴿نَرْفَعُ دَرَجَاتٍ مَنْ نَشَاءُ وَفَوْقَ كُلِّ ذِي عِلْمٍ عَلِيمٌ﴾

(صدق الله العظيم)

(سورة يوسف/ الآية 76)

Supervisor's certification

We certify that this thesis was prepared under our supervision at the department of chemistry, collage of education for pure sciences (Ibn Al Haitham) at the university of Baghdad in partial requirements for the degree of Doctor of Philosophy in chemistry.

Signature:

Name: Dr.Sajid M. Lateef

Title: professor

Member (Supervisor)

In view of the available recommendation, I forward this thesis for debate by the examining committee.

Signature

Name: Prof. Dr. Mohamad Jaber Al-Jeboori

Title: Professor

Address: Head of Department of Chemistry, College of Education for Pure

Science/(Ibn-Al-Haitham) University of Baghdad, Iraq.

Date: / / 2018

Examination committee certificate

We chairman and members of the examination committee, certify that we have studies this thesis presented by the student **Shaimaa Ahmed Hassan al-taee** and examined her in its contents and that, we have found its worthy to be accepted for the degree of the doctor of Philosophy in chemistry with ( ) .

Signature:

Name: Dr. Khalid Jawad Al Adilee

Title: Professor

Date: / / 2018

(Chairman)

Signature:

Name: Dr.Hasan Ahmed Hasan

Title: Asst.Prof.

Date: / / 2018

(Member)

Signature:

Name: Dr.Ibtihal Kadhim Kareem Dosh

Title: Asst.Prof.

Date: / / 2018

(Member)

Signature:

Name: Dr.Muna Sameer Al-Rawi

Title: Asst.Prof.

Date: / / 2018

(Member)

Signature:

Name: Dr.Lekaa Khalid Abdul Karem

Title: Asst.Prof.

Date: / / 2018

(Member)

Signature:

Name: Dr .Sajid Mahmood Lateef

Title: Professor

Date: / / 2018

Member (Supervisor)

I have certified upon the discussion of the examination committee

Signature:

Asst. Prof. Dr. Hasan Ahmed Hasan

Behalf / The Dean of collage of Education For Pure Sciences / Ibn al Haitham

Date: / / 2018

Dedication

Taught me the language in the stages of my studying....

To tired sleepless for me throughout the nights.....

To those who do not always forget and live on his memory

and he finished all that built me....

To the spirit of my father

To the spirit mother my eye sight

His words were given the best advice your best friend

To the good spirit

To the quiet Aura

To my heart resident

My husband Omar

To the tributaries of loyalty and fidelity

My Brothers and sister

Mohmod, Amar, Wafaa and my aunt's daughters

Goson,Maha

To the flowers and fruits of my heart

My children (Gada, Abd-AlRahman and Rawan)

Shaimaa

Acknowledgment

My great thanks to Allah the only one, the single for all this blessing during the pursuit of my academic and career goals.

I would like to express my sincere thanks with my appreciation to my supervisor (Prof.Dr. Sajid Mahmood Lateef) who obliged me by suggesting the subject of the research and bore the responsibilities of supervision. Therefore, I wish him everlasting health, happiness, success and long life.

Also my grateful thanks to the staff members of the collage of education for pure sciences Ibn Al Haitham especially Behalf / the Deen of collage Asst.Prof. Dr. Hasan Ahmed Hasan and to all my virtuous professors in the department of chemistry, especially the virtuous lecturer (Asst. Prof. Dr. Ismaeel Yaseen Majeed) for the guidance and advise him gave me during the research and study period.

I am deeply indebted to my family especially my husband omar for their support and patience during the years of my study and appreciation and my deep grateful thanks are due to all my friends.

I also extend my deep gratitude to the central service laboratory in the College of Education for Pure Sciences, Ibn-Al-Haitham / Baghdad University for cooperating with us in conducting the analyses related to the research and to all the higher studies students.

Shaimaa Ahmad Hssan Al-taee

Baghdad, Iraq

2018

Abstract

This work presented the synthesis of three ligands (L^1, L^2 and L^3) two from type (N,N) and one from (N,O) capable to form structures upon complexation with metal ions , these ligands are :

[L^1]….. Methyl (E)-(6-(((6-methoxybenzo[d]thiazol-2-yl)imino) (phenyl) methyl)-1H-benzo[d]imidazol-2-yl) carbamate .

[L^2]….. Methyl (E)-(6-((benzo[d]thiazol-2-ylimino) (phenyl) methyl)-1H-benzo[d]imidazol-2-yl) carbamate.

[L^3]…..Methyl (E)-(6-(((1,5-dimethyl-3-oxo-2-phenyl-2,3-dihydro-1H-pyrazol-4-yl)imino)(phenyl)methyl)-1H-benzo[d]imidazol-2-yl)carbamate.

These ligands were synthesized from reaction of one equivalent of (Mebendazole) with one equivalent for each 2-Amino-6-methoxy benzothiazole for first ligand [L^1], 2-Aminobenzothiazole for second ligand [L^2] and with 4-Aminoantipyrine for third ligand [L^3].

The reaction was carried out in ethanol (as a solvent), and reflux 30 hrs for all ligands.

The ligands were characterised by melting point measurement, elemental microanalysis C.H.N, FT-IR, UV, ^1H,^{13}C NMR and Mass

spectroscopy.

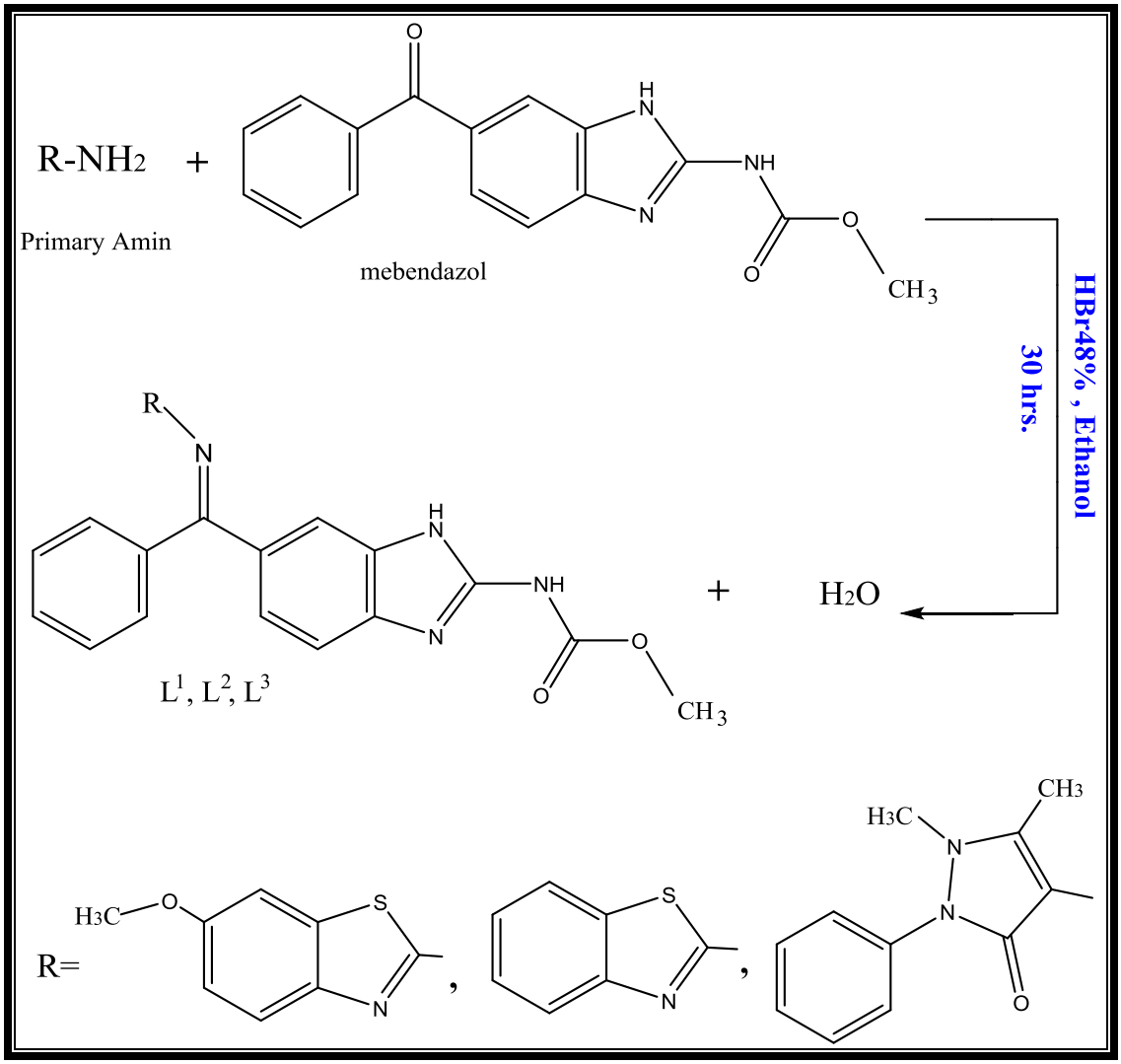

Scheme: Synthetic route for ligands L^1-L^3 .

The ligands were reacted with metal ions [VO(II), Mn(II), Co(II), Ni(II), Cu(II), Zn(II), Cd(II), and Hg(II)] refluxed in aceton for (L^1,L^2) and methanol about (L^3) to give the complexes of the general formula: $[M(L)_2(X)(Y)].H_2O$, Where;

L=L^1 and L^2

M=VO(II), X=0, Y=OSO_3^{-2},

M= Mn(II), Co(II), Ni(II), Cu(II), Zn(II), Cd(II) and Hg(II)

, X=Cl, Y=Cl,

$L=L^3$

$M=VO(II)$, $X=0$, $Y=OSO_3^{-2}$, $A=0$

$M=Mn(II),Co(II)$, $X=Cl$, $Y=H_2O$, $A=Cl$

$M=Ni(II)$, $X=Cl$, $Y=0$, $A=Cl$

$M=Cu(II),Cd(II),Zn(II),Hg(II)$, $X=Cl$, $Y=Cl$, $A=0$

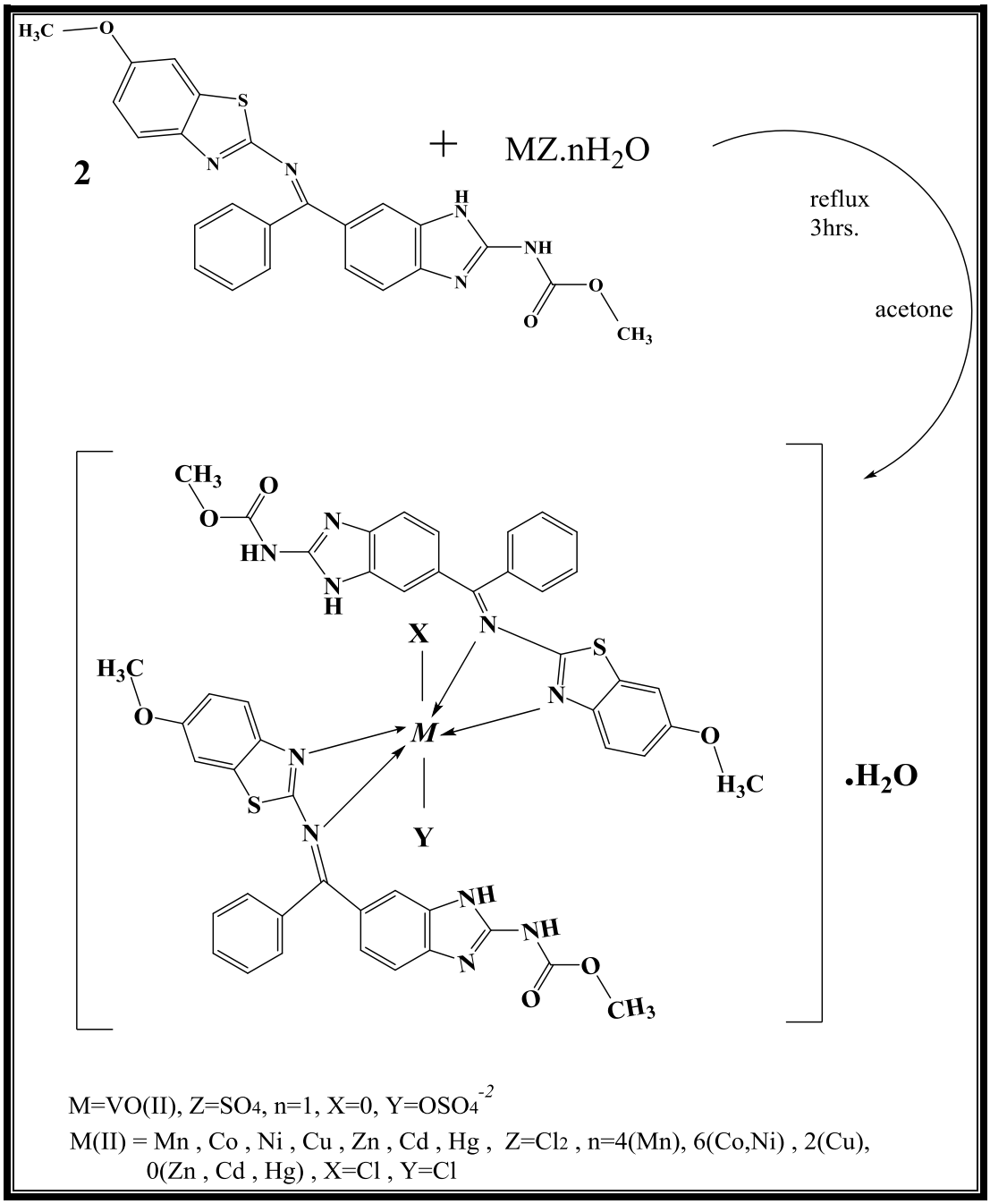

Scheme: Synthetic route of ligand [L^1] complexes.

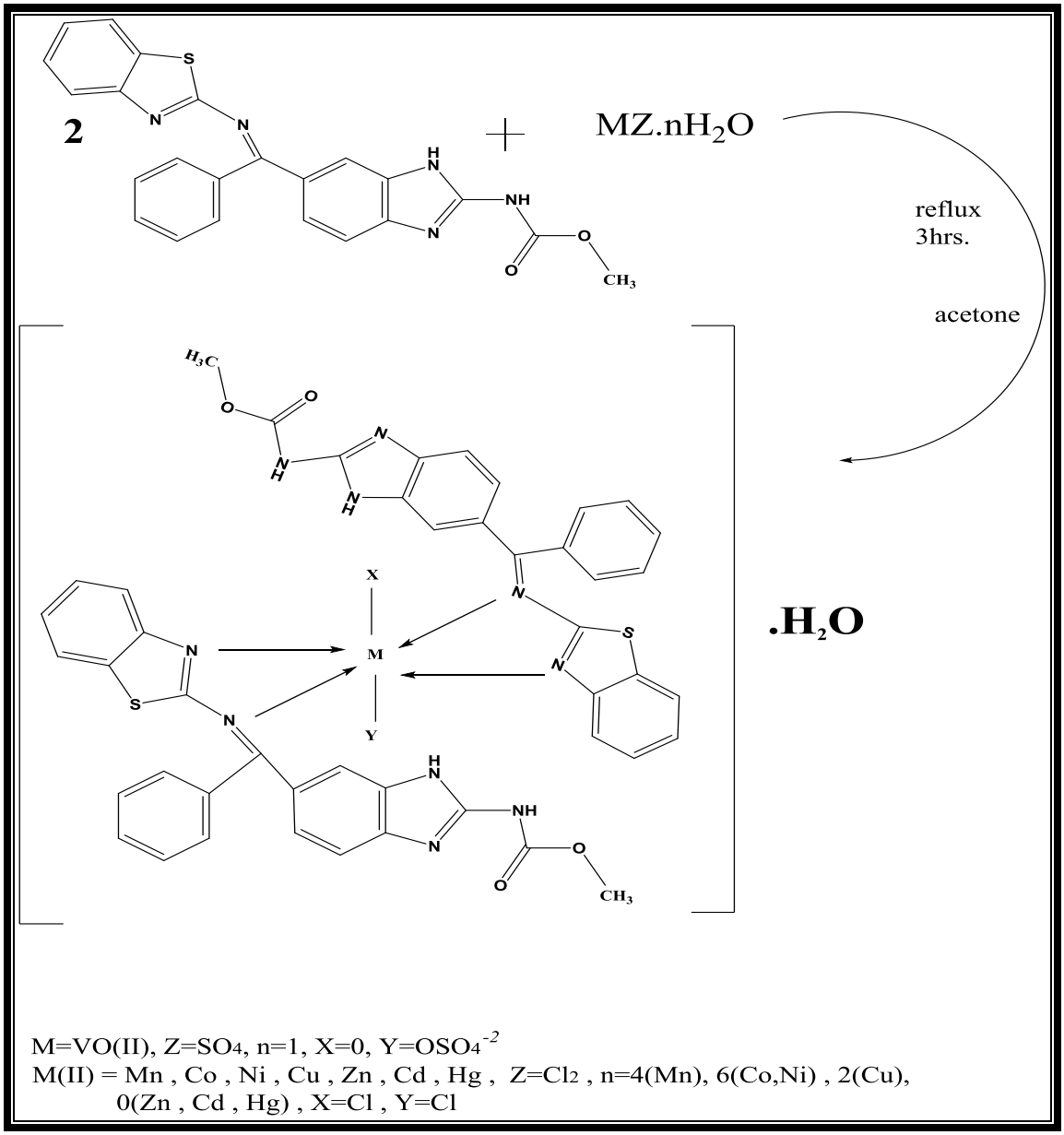

Scheme: Synthetic route of ligand [L^2] complexes.

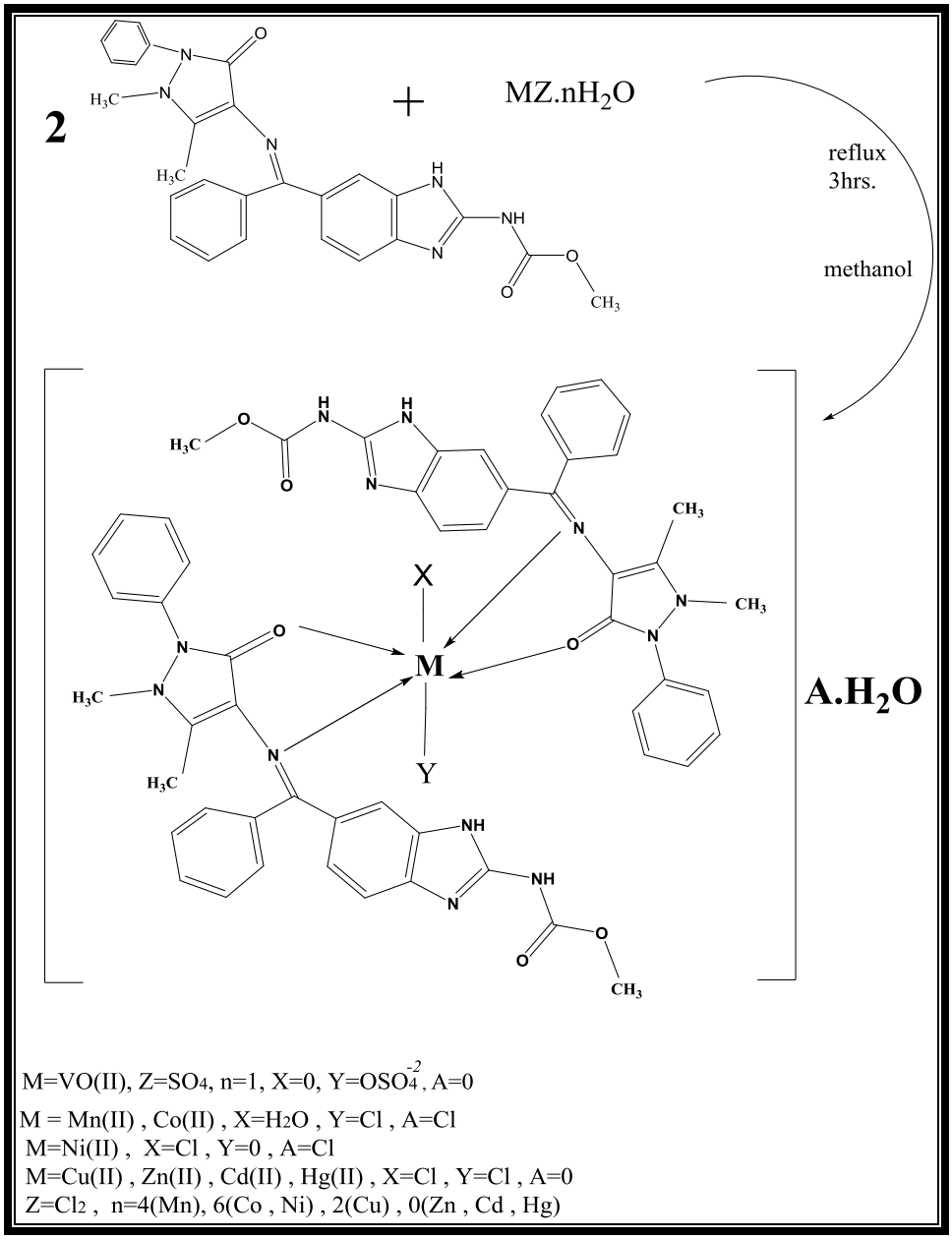

Scheme: Synthetic route of ligand [L^3] complexes.

These complexes were characterised by melting point measurement, elemental microanalysis C.H.N, A.A, chloride contents, magnetic susceptibility, thermal gravimetric analysis, FT-IR and U.V–Vis spectroscopy, along with conductivity measurement.

The FT-IR spectra of the complexes showed that, the potentially polydentate ligand acts as bicoordinate.

The UV–Vis spectra of the ligands and complexes were studied in order to elucidate the spatial arrangements of the ligand around the metal ions. The conductance measurements of the complexes in DMSO, and chloride contents revealed that, some of the complexes are ionic while others are non-electrolyte.

On the basis of elemental microanalysis, conductivity, magnetic moment and chloride contents measurements, thermal gravimetric analysis, FT-IR and UV–Vis spectroscopies are suggested an octahedral geometry for all complexes except complexe $[Ni(L^3)_2Cl]Cl.H_2O$ .It showed the shape trigonal bipyramidal .

Biological activities of ligands and their complexes were estimated for two types of bacteria (*Escherichia coli and Staphylococcus aureus*) and one type of fungi (*Candida albican*s).

The results shown biological activity against the types of bacteria and type of fungi mentioned previously for most of the synthesized complexes compared to ligands and starting materials.

List of Tables

List of Figures

List of Schemes

List of Abbreviations

List of Abbreviations	
MBZ	Mebendazole
BZC	benzimidazole carbamates
4-AAP	4-Aminoantipyrine
ABT	2-Aminobenzothiazole
AMBT	2-Amino-6-methoxy benzothiazole
A.A.	Atomic absorption
^{1}H-NMR	Proton Nuclear Magnetic Resonance
^{13}C-NMR	Carbon–13–Nuclear Magnetic Resonance
DMF	Dimethylformamide
DMSO	Dimethylsulfoxide
EDX	Energy- Disoersive X-ray Spectroscopy
EPR	Electron Paramagnetic Resonance
FAB	Fast Atom Bombarment
m.p.	Melting point
M.wt	Molecular Weight
B.M.	Bohr Magneton
FT-IR	Fourier Transform Infrared
U.V-Vis	Ultraviolet and visible
TGA	Thermo Gravimetric Analysis
DSC	Differential Scanning Calorimetry
λ	Wave length
ε_{max}	Molar absorptivity
Abs	Absorbance
Nm	Nanometer
$\bar{\nu}$	Wave Number

ppm	Part Per Million
MHz	Mega hertz

Chapter One

Introduction

(1) Introduction:

(1.1) Heterocyclic Compounds:

Compounds that possess a cyclic structure, contain one or more than one type of different atoms, substitute in the cycle, such as nitrogen, oxygen, sulfur and most of other known atoms [1]. The heterocyclic compounds are well known in organic chemistry. They have many important physiological functions in plants and animals, beside They have the important biological characteristics, for example penicillin, one of the antibiotics, as well as painkillers such as Phenobarbital and saccharin, which they consider heterocyclic compounds [2]. There are large number of heterocyclic compounds that can be synthesized in laboratory which could be containing important characteristics as factors [1].

Heterocyclic compounds are used in the dyes field, which it depends on components of heterogeneous aromatic diazo [3]. A heterocyclic system has a widely speared in the nature, especially in the natural products, nucleic acid, plants alkaloids and chlorophyll [4]. Furthermore, the heterocyclic compounds are very important in coordination chemistry because they can form stable complexes with most of the transition metals. These complexes could possess variety application in biological, clinical, analytical and pharmacological fields [5,6].

Heterocyclic compounds are important class of compounds in organic chemistry due to their biological activities like antimicrobial, antifungal, anti-inflammatory, analgesic and anticancer drugs [7].

Mebendazol, 4-aminoantipyrine and benzothiazole derivatives are one of the heterocyclic compounds, which are used in the field of medicinal chemistry because of their pharmacological, photographic and catalytic applications [8-10].

(1.2) Chemistry of Mebendazol (MBZ) :

Mebendazol (MBZ) belongs to the family of medicines called anthelmintics . For instance, benzimidazole carbamates (BZC), has especially useful against helminth infections. It is used principally to treat infections due to roundworms, hookworms, pinworms and whipworms. MBZ were widely used in veterinary medicines [11,12]. It has been well known that (BZC) such as mebendazole, cambendazole and carbendazim are important midications for the treatment of awide range of whipworms influences [13].

Mebendazol is a white powder, melting point about (286 -288)°C and thier stable molar mass equal 295.30 g/mol. The scientific name for mebendazolis (Methyl (5-benzoyl-1H-benzimidazol-2-yl) carbamate, its structure was shown in Fig. (1-1).

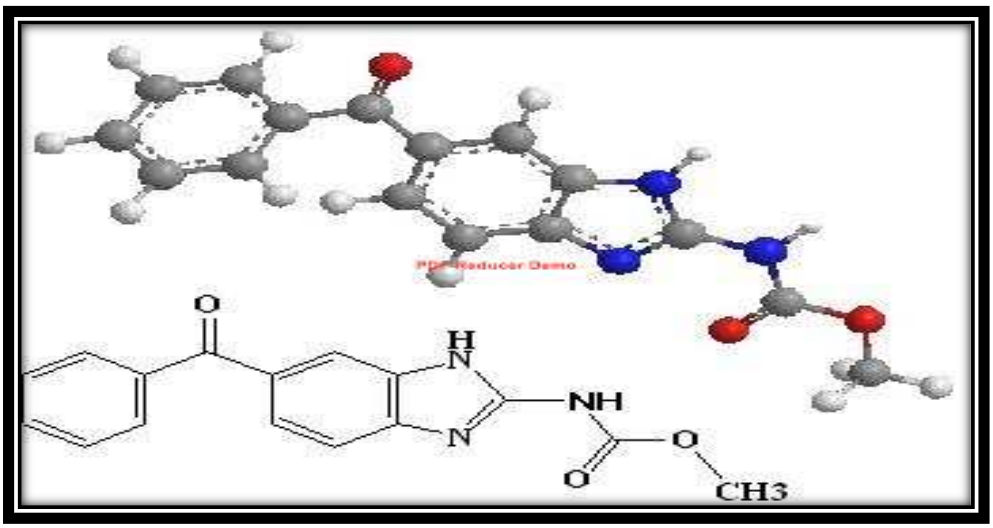

Fig. (1-1): Chemical structure of Mebendazol.

(1.3) Chemistry of 4–Aminoantipyrine (4–AAP):

4-aminoantipyrine (4–AAP) is doubly unsaturated five membered ring compound with three carbon and two nitrogen atoms. It also known as antipyretic agent [14] , which is consider one of the pyrazole derivatives. Numerous synthetic compounds containing pyrazole moiety have been

focused in the field of medicinal chemistry field [15] because of their pharmacological, photographic, catalytic and liquid crystals applications [9,14].

It is a yellow powder, melting point about (107-109)°C it is stable , sensitive for light and molar mass equal 203.245 g/mol [16]. The scientific name for 4-aminoantipyrine is (1-phenyl-2,3-dimethyl-4-amino pyrazole-5-one), their structure was shown in Fig. (1-2).

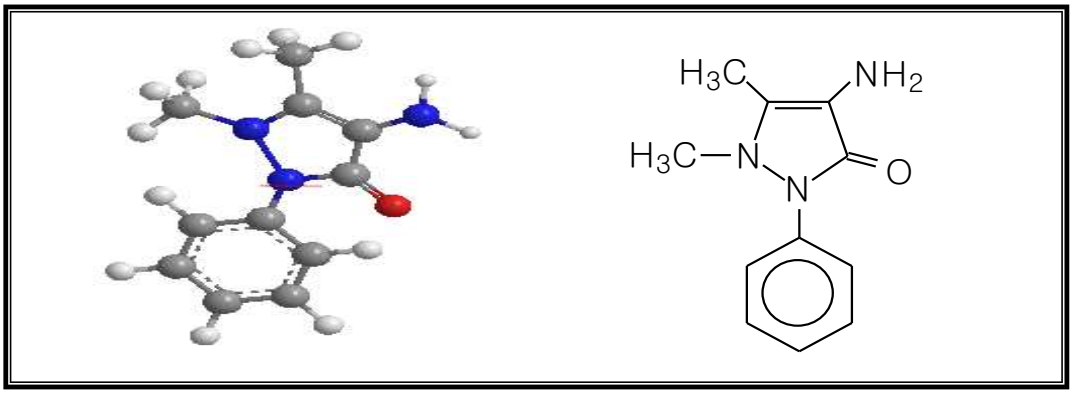

Fig. (1-2): Chemical structure of 4-aminoantipyrine.

4-Aminoantipyrine is a temperature reducing pyrazole derivatives. It is one of the synthetic drugs [14] and it can be used as an intermediate for the synthesis of pharmaceuticals especially antipyretic as well ant analgesic drugs [9, 17]. It's metal complexes have applications in analytical and pharmacological field [18]. It also used in preparation of azo dyes [19] and at last 4-aminoantipyrine and its formylation derivatives have biological activities like antimicrobial, antifungal, anti-inflammatory, antiviral, analgesic and antibacterial activities [20-22].

(1.4) Chemistry Benzothiazole derivatives:

Benzothiazole belongs to the family of bicyclic heterocyclic compounds having benzene ring fused with five-membered ring comprising nitrogen and sulfur atoms which can act as drugs,

benzothiazole based pharmaceuticals possess multiple applications [23]. Benzothiazole is an important scaffold with a wide array of interesting biologic [24]. For instance, antimicrobial [25], antimalarial [26], anticonvulsant [27], anthelmintic [28], analgesic [29], anti-inflammatory [30], antidiabetic [31] and antitumor [32] activities. Moreover, benzothiazoles are present in a range of marine or terrestrial natural compounds that have useful biological activities.

Benzothiazoles have been therapeutically useful in the treatment of various diseases such as ; neurodegenerative disorders, local brain ischemia, central muscle relaxants and cancer [33].

Substituted benzothiazoles like 2-aminobenzothiazoles and their derivatives were found to have wide range of applications as therapeutic, dyes and industrial chemicals.

(1.4.1) 2-Aminobenzothiazole (ABT):

It is a white or gray powder, melting point about (124-126)°C, stable molar mass 150.20 g/mol . The scientific name for 2-aminobenzothiazole is (1,3-Benzothaizol-2-amine). The structure was depicted in Fig. (1-3).

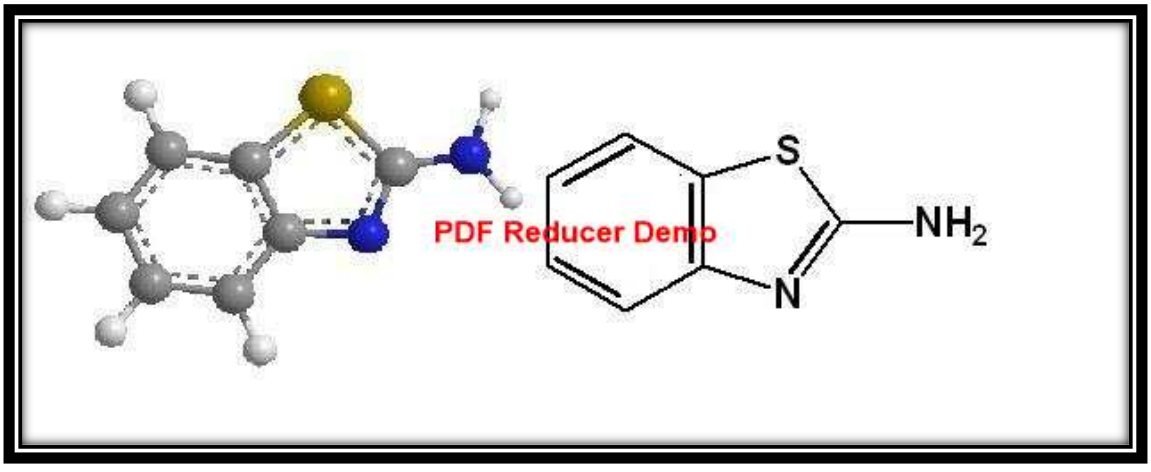

Fig. (1-3): Chemical structure of 2-Aminobenzothaizole.

(1.4.2) 2-Amino-6-methoxybenzothiazole (AMBT):

It is a gray powder, melting point about (165-167)°C, stable and molar mass 180.23 g/mol . The scientific name for 2-amino-6-methoxy benzothiazole is (6-methoxy-1,3-benzothaizol-2-amine), the structure was diaplayed in Fig. (1-4).

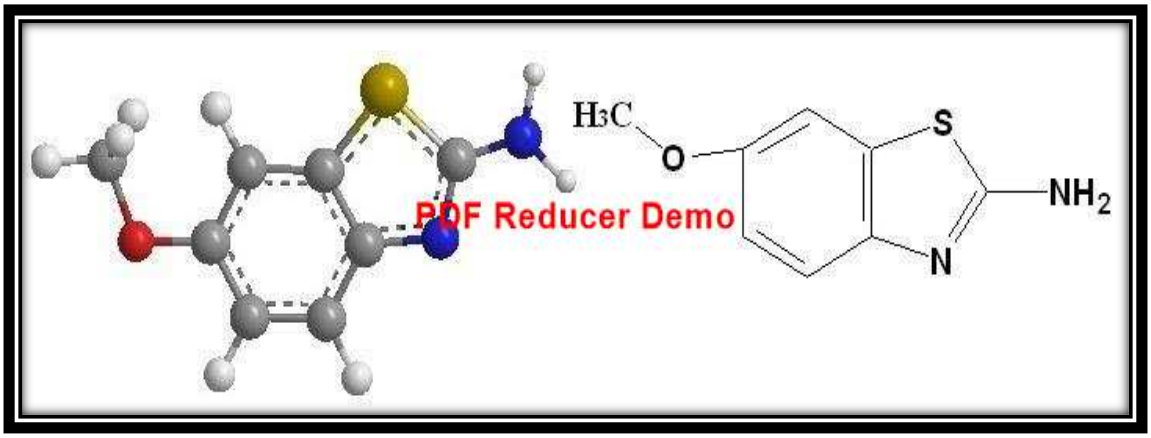

Fig. (1-4): Chemical structure of 2-Amino-6-methoxybenzothiazole.

(1.5) Schiff Bases:

Schiff bases are an important class in organic compounds [34]. They were first reported by Hugo Schiff in 1864 [35]. Schiff's bases are condensation products of primary amines with carbonyl compounds. The common structural feature of these compounds is the azomethine group with the general formula RHC = N-R_1, where R and R_1 are alkyl, aryl, cycloalkyl, or heterocyclic groups. Structurally, a Schiff's base (also known as imine or azomethine group) is a nitrogen analogue of an aldehyde or ketone in which the carbonyl group (>C = O) is replaced by an imine or azomethine group [36,37].

Schiff bases represent one of the most widely used families of organic compounds and their chemistry is essential material in many organic chemistry textbooks [38]. They possess easily synthesized route and

they are ability to form metal complexes with different metal ions. These facts making their chemists are very interested in synthesis and characterization of Schiff bases ligands and their complexes [39,40]. Schiff bases have many various names depending on the sources of carbonyl compound and primary amine. It's called aldimines, if its derived from aldehydes and ketimines, if it derived from ketones, while it's called aniles, benzanils and imines when the primary amine is aniline or one of its derivatives [41, 42].

(1.6) Synthesis of Schiff bases:

There are several reaction pathways to synthesis Schiff bases [42,43], but the most commonly pathway with acid catalyzed [44,45] . Condensation of carbonyl compounds and primary amines, with formation of characteristic(C=N) double bond usually called imine or azomethine group [38]. This reaction may be occurred in different conditions and in different solvents with elimination of water molecule. The presence of a dehydrating agent normally favors the formation of Schiff bases, as demonstrated in Scheme (1.1).

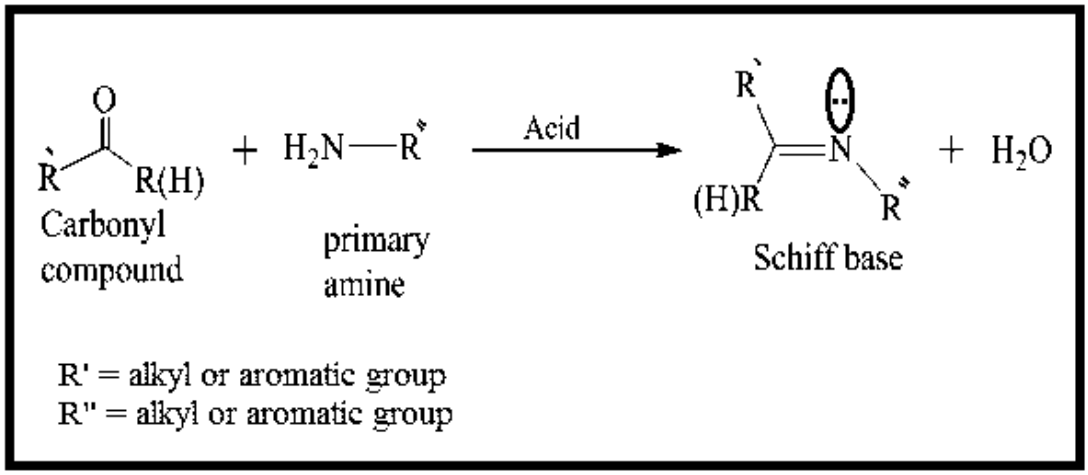

Scheme (1-1): Formation reaction of Schiff bases.

(1.7) Schiff bases complexes:

Schiff bases and their metal complexes have been synthesized due to their interesting and important properties, e.g., ability to bind toxic and heavy metal atoms, undergo tautomerism, exhibit catalytic reduction and photochromism [46]. The chemistry of Schiff bases metal complexes are interesting because these species display a variety of reactivity mode, besides they possess catalytic and biological activity [47]. Schiff bases can accommodate different metal centers involving various coordination modes thereby allowing successful synthesis of homo and hetero-metalic complexes with varied stereochemistry [48]. Schiff bases complexes containing different central metal atoms such as Cu, Ni, Co and Pd have been studied in great detail for their various crystallographic features, enzymatic reactions, steric effects, structure redox relationships, mesogenic characteristics, catalysis, magnetic properties and their important role in the understanding of the coordination chemistry of transition metal ions [49].

The transition metal complexes of Schiff base ligand with donor groups like N, O and S gained importance for more than two decades because of their usesing as models of biological systems [50,51], including antibacterial [52], antifungal, antitumor, and anti-inflammatory activities [53].

(1.8) General survey:

In 2011, M. Elnawawy and co- workers [54] synthesized newly Schiff base from mebendazole and 2-aminophenol (Scheme (1-2)) and its complexes with Fe(III), Co(II), Ni(II) and Zn(II) (Scheme (1-3)). All complexes were investigated by elemental micro analysis, molar conductivity, thermogravimetric analysis, magnetic moments, infrared and electronic spectra. The elemental analysis (C.H.N) showed the mole ratio

(L: M) is (1:2) in all complexes. The thermogravimetric analysis data exhibited the presence of coordinated and hydrated water molecules. The magnetic moment results show paramagnetic phenomena for Fe, Ni and Co complexes and diamagnetic Zn complexe. The IR spectral data of all prepared complexes displayed the proper coordination sites of the present Schiff base towards the metal ions. The electronic absorption spectral data of the prepared complexes confirmed the electronic transitions and the chemical structures. The antibacterial and antifungal activity of the Schiff base(I) and its complexes (Ia-d) was done in comparison with Penciling and Streptomycin for antibacterial Clotrimazole and Iitraconazole for antifungal as standard. All the six selected strains tow of bacteria and four of fungi namely; {*Staphylococcus aureus* and *Bacillus* (Gram +) and *Pseudomonas aeruginoca* and *Escherichia coli* (Gram-) and *Aspergillus fumigates*, *Geotrichum candidum*, *Candida albicans* and *syncephalastrum racemosum*} showed sensitivity to all derivatives and showed good activity against all the tasted bacterial and fungal except syncephalastrum racemosum..

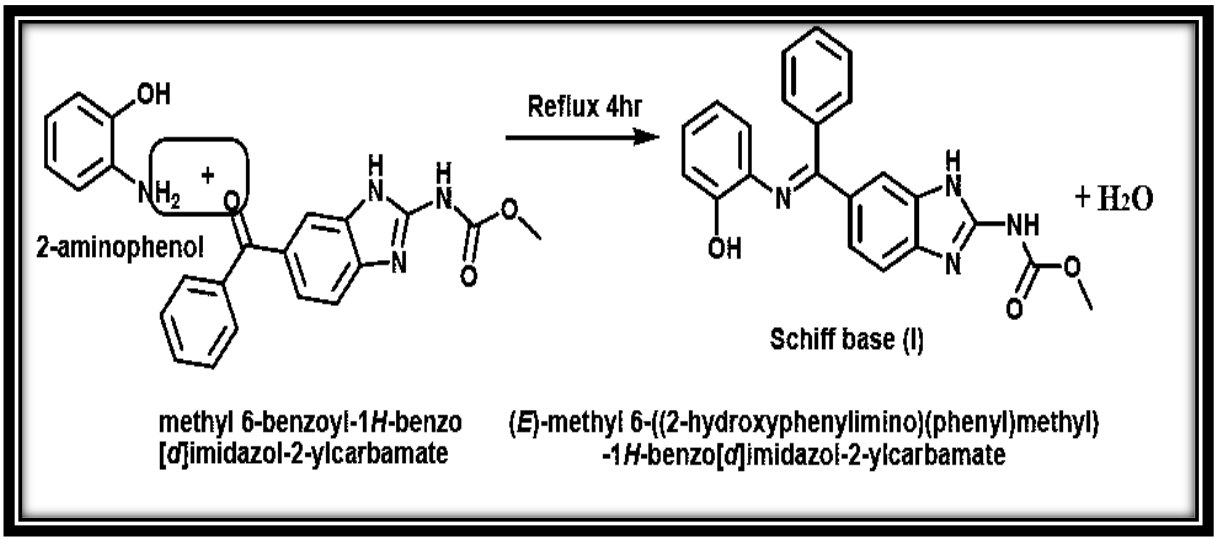

Scheme (1-2): Synthesis of mebendazole Schiff bases(I).

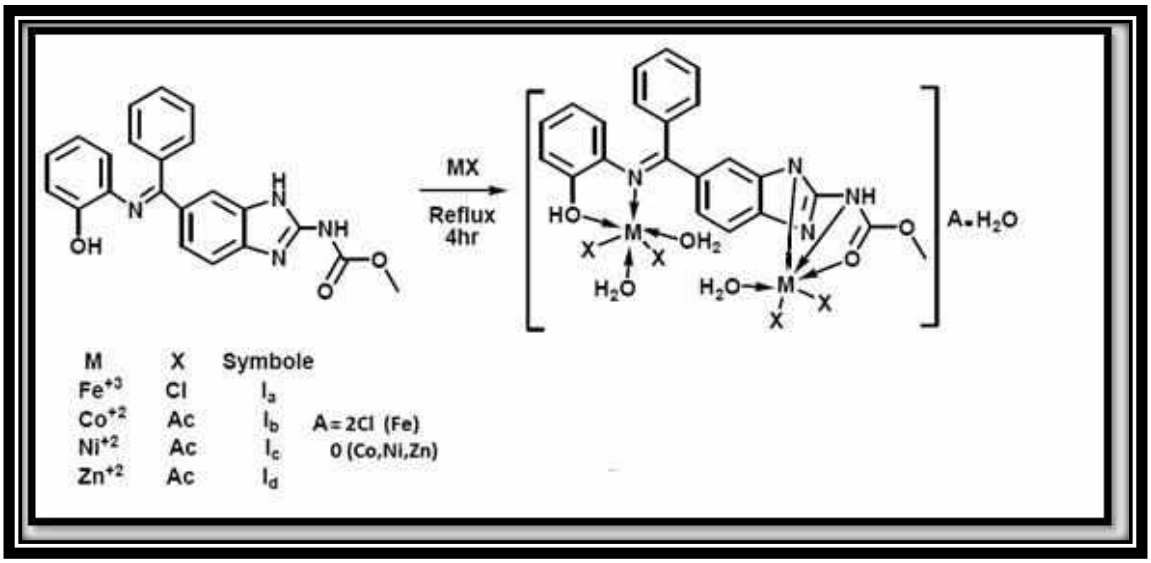

Scheme (1-3): Synthesis of Schiff bases (I) complexes.

In 2013 A. Osowole and co- workers [55] were synthesized Mn(II), Co(II), Ni(II), Cu(II), Zn(II), and Pd(II) complexes of the Schiff base 2-(6-methoxybenzothiazol-2-ylimino) methyl)-4-nitrophenol (HL) derived from condensation of 2-hydroxy-5-nitrobenzaldehyde and 2-amino-6-methoxybenzothiazole. These compounds have been characterized by percentage metal, solubility, infrared and electronic spectra measurements. The *in-vitro* anti-bacterial activities against *Bacillus subtilis, Staphylococcus aureus, Proteus mirabilis, Klebsiella oxytoca, Pseudomonas aeruginosa*, and *Escherichia coli* were also evaluated. The metal complexes formed as $[ML(NO_3)].bH_2O$, where M(II) = Mn, Co, Cu, Zn; b = 0.5 - 4, with the exceptions of the Pd(II) and Ni(II) complexes that analyzed as $[Pd(L)_2].4H_2O$ and $[Ni(L)Cl(H_2O)]$. The infrared spectra confirmed that the coordination was by the Schiff base via the imine nitrogen and phenol oxygen atoms respectively, resulting in a NO chromophore around the metal ion. The electronic spectra measurement was corroborative of 4-coordinate tetrahedral and square planar geometry for the complexes. The complexes mostly exhibit good *in-vitro* antibacterial activities against *S. aureus, E. coli* and *P. mirablilis*. Its

noteworthy that the Pd(II) and Zn(II) complexes had broad spectrum antibacteria activity against the bacteria used with the exception of *B. subtilis* with inhibitory zones range 13.0-22.0 mm and 13.0-27.0 mm respectively. Fig. (1-5) show the chemical structure of complexe $[Pd(L)_2].4H_2O$.

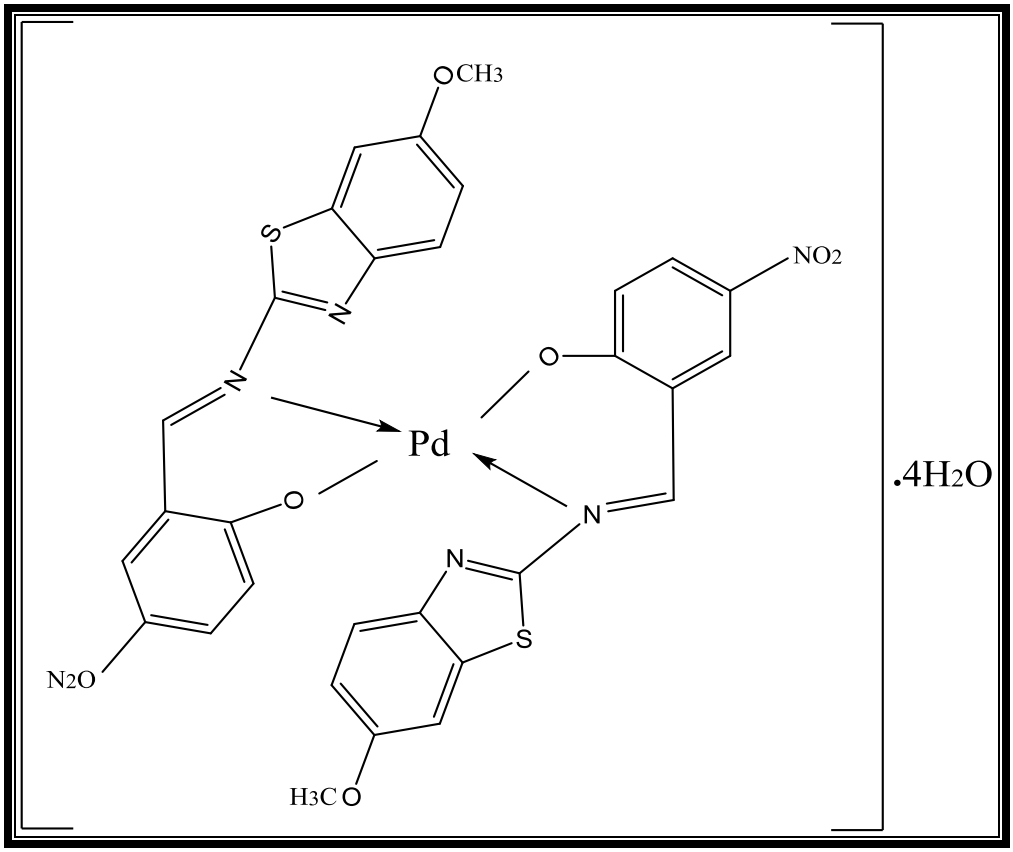

Fig. (1-5): The chemical structure of complex $[Pd(L)_2].4H_2O$.

In 2014 S.M Lateef and H.H. Alkam [56] synthesized Schiff base bidentate ligand (L) type (NO) via condensation of 4−aminoantipyrine and benzil (scheme (1-4)). As well the metal complexes of this Schiff base ligand(L) were synthesized. The ligand is characterized based on melting point, elemental analysis, IR, electronic spectrum, and ^{1}HNMR. While metal complexes are characterized based on melting point, elemental analysis, IR , electronic spectra , magnetic moment , molar conductance ,

^{1}HNMR (for zinc complex only) and chloride content along with mole ratio method . From the elemental analyses and mole ratio method, 1 : 2 metal : ligand for Mn(II) and Cu(II) complexes and 1:1 metal : ligand for Zn(II) and Cd(II) complexes, are found with molecular formula :[Mn $(L)_2Cl_2$]. H_2O, $[Cu(L)_2(H_2O)\ Cl]\ Cl$, $[Zn(L)Cl_2]$. H_2O and [Cd $(L)Cl_2$] .

From the IR results, they suggested that the ligand (L) behaves as bidentate on complexation with metal ions via the azomethine nitrogen and carbonyl oxygen atom of five-member ring of the ligand. The electronic spectral data and magnetic measurements indicate that the complexes exhibited octahedral geometry around Mn(II) and Cu(II) , while tetrahedral geometry around Zn(II) and Cd(II) fig.(1-6). The results of antibacterial activity showed that only Cd(II) complex have a high activity (22mm) for against *Eschirichia coli*.

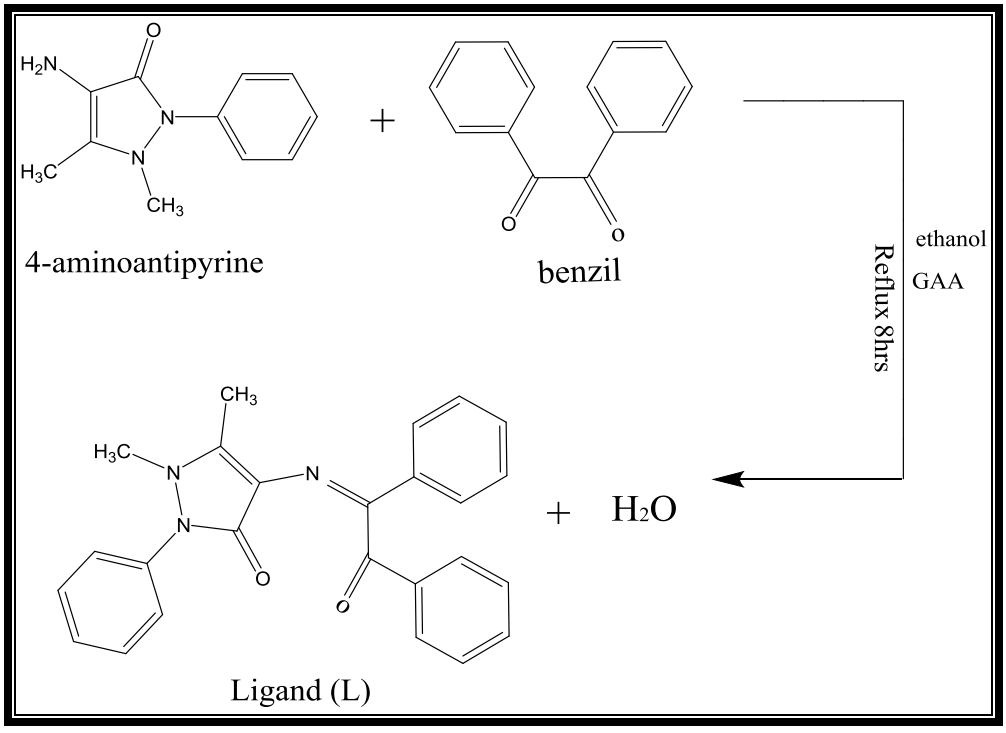

Scheme (1-4) : Synthsis route of ligand(L)

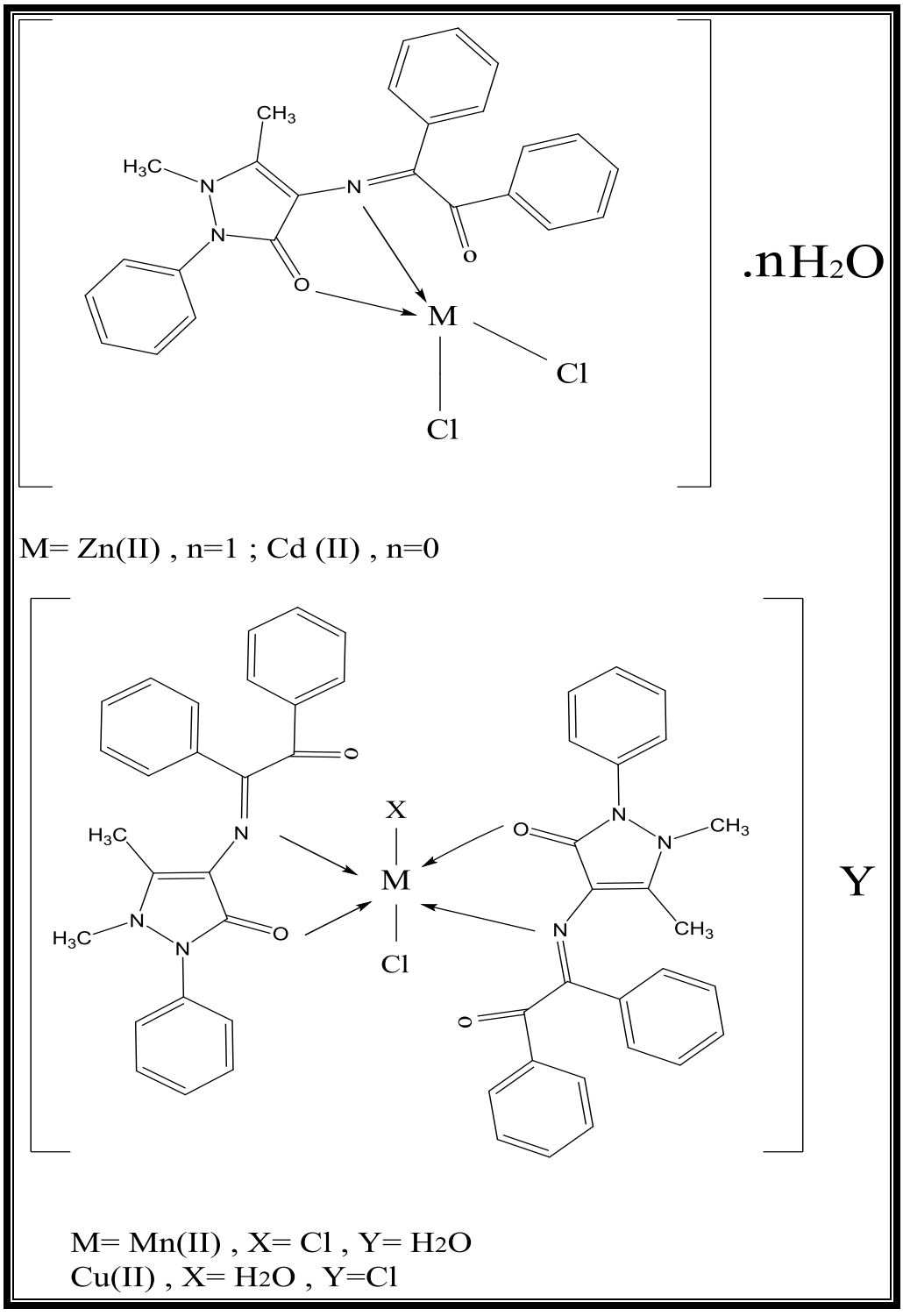

Fig. (1-6): The chemical structure of metal complexes.

In 2014 M.M. Abd-Elzaher and co-workers [57] were reported the synthesis of manganese(II), cobalt(II), nickel(II), copper(II), zinc(II), cadmium(II), mercury(II) and lead(II) complexes of ferrocenyl Schiff base

ligand containing 4-aminoantipyrine were synthesized in good yield. The complexes have been characterised by IR, ^{1}HNMR, UV-Vis., mass spectra, magnetic susceptibility and molar conductivity measurements as well as elemental analysis. The analyses showed that the ligand behaved as neutral tetradentate ligand coordinated to the metal ions via the oxygen atom of carbonyl group and azomethine nitrogen atom forming an octahedral geometry around the metal ions. The biological activity of the ligand and its complexes were carried out against fungal strains of *Aspergillus niger* and bacterial strains of *Bacillus subtilis* (+), *Esherichia coli* (-) using the disk diffusion method. The biological results indicated that the ligand is inactive while its complexes have mild activity. The complexes showed mild antibacterial activity against *Bacillus subtilis* (+), *Esherichia coli* (-) and *Aspergillus niger* (fungi). The biological results are compared with a standard medication, Fig.(1-7) displayed the chemical structure of complexes.

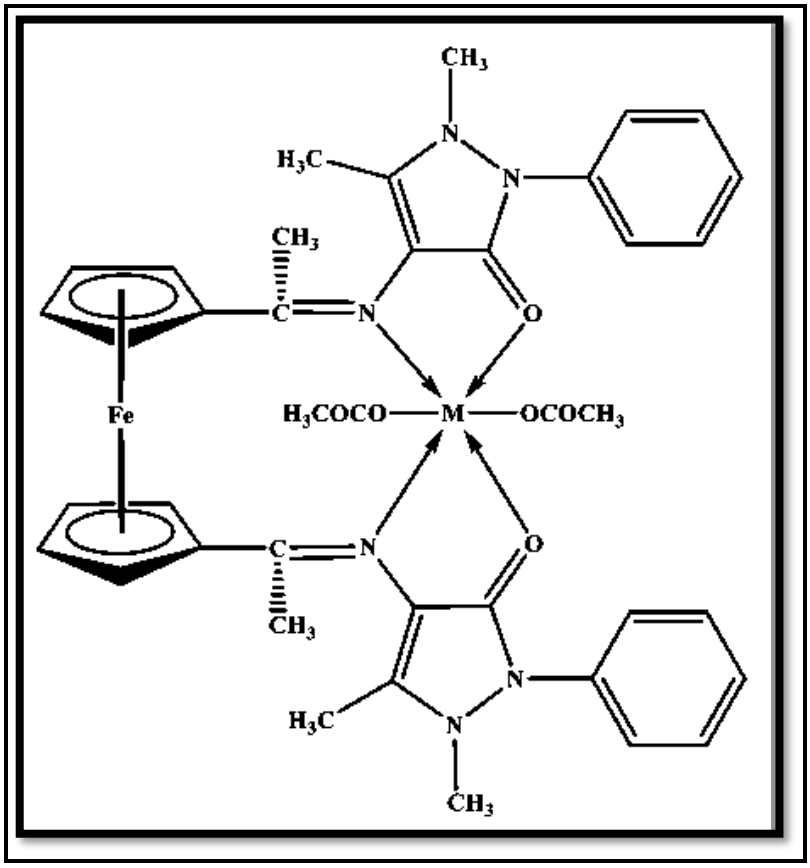

Fig. (1-7): The chemical structure of complexes, M(II)= Mn, Co, Ni, Cu, Zn, Cd, Hg and Pb.

In 2015 J.S.Sultan and co-workers [58] synthesized novel bidentate Schiff base ligand (HL) from condensation reaction of 4-aminoantipyrine (4-AAP) and glyoxylic acid scheme(1-5) . The mixed ligand complexes of (HL) as primary ligand with azide ion (N_3^-) as co-ligand with M(II)=Mn, Co, Ni, Zn, Cd and Hg were synthesized via reaction metal (II) chloride salt with ligand (HL) and sodium azide (NaN_3) using 1:2:2 mole ratio in ethanol solvent, respectively. Spectroscopic methods [FT-IR, UV-Vis, ^{1}H NMR, ^{13}C NMR] and melting point along with elemental microanalysis C.H.N. were used to characterization the new ligand (HL). The complexes of mixed ligand were characterized by melting point, elemental microanalysis (C.H.N), atomic absorption, chloride content, molar conductance, magnetic susceptibility, FTIR and UV-Vis spectral data. The antibacterial activity with four kinds of

bacteria, *Staphylococcus aureus, Bacillus, Escherichia coli* and *Pseudomonas aureus* was studied. The prepared complexes have general molecular formula: $[M(HL)_2(N_3)_2].mH_2O$ where: (M(II) = Co, Cd ; m = 2), (M(II) = Ni, Zn, Hg ; m = 3), except in Mn(II) complex, Schiff base (HL) behaved monodentatc ligand via azomethine nitrogen forming complex with molecular formula $[Mn(HL)_2(N_3)_2]. H_2O$. The antibacterial study showed that the complexes were more toxic to the strain of bacteria taken under study than the Schiff base ligand (HL) . The octahedral geometrical structure was suggested for all prepared complexes based to the characterization data for all technique Fig.(1-8).

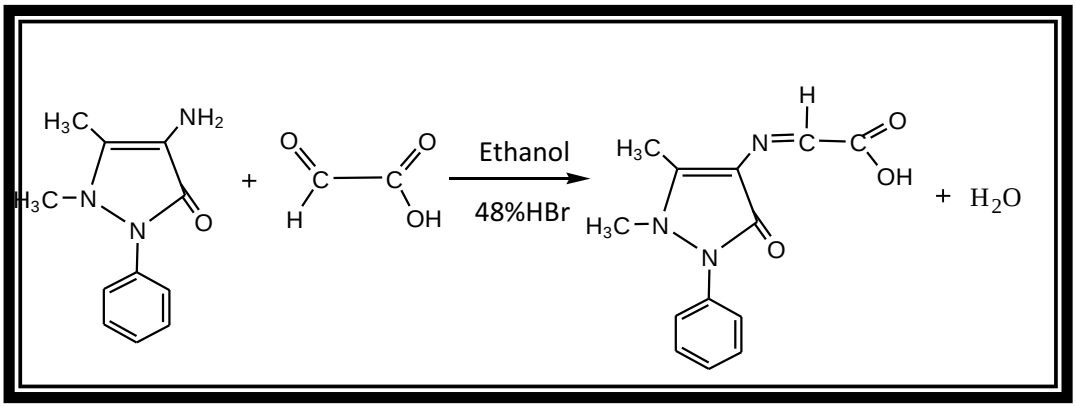

Scheme (1-5): Synthesis route of ligand (HL).

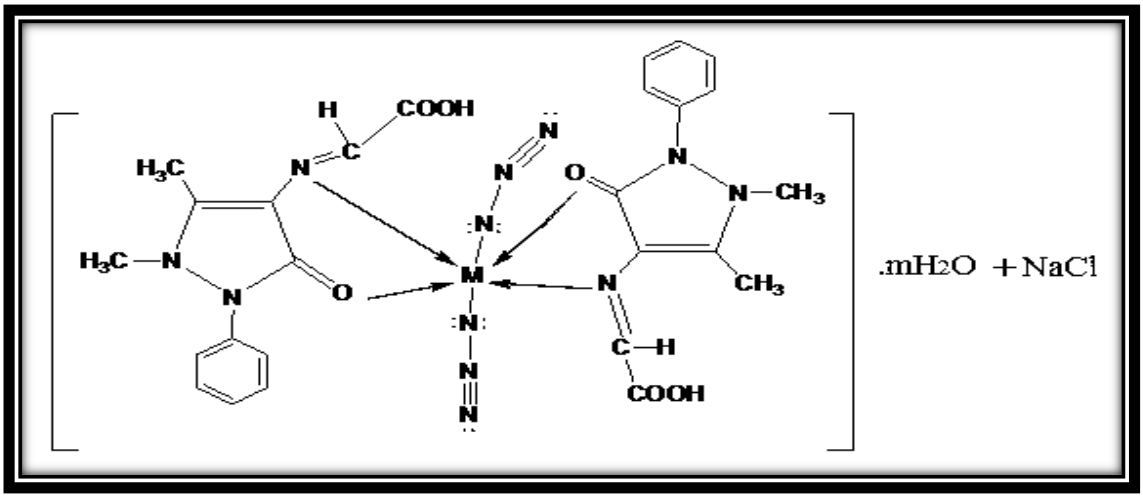

Fig.(1-8):Geometrical structure for prepared complexes , M(II)=Co, Mn ,Cd(m=2) , Zn, Ni , Hg(m=3) .

In 2016 metal complexes of two Schiff base ligands (L^1 and L^2) were synthesized via condensation of 2– Aminobenzothiazole with 2,3-dihydro–1H–indolo–[2,3–b]–phenazin–4(5H)–one (K^1) and with 3–(ethoxymethylene)–2,3–dihydro–1H–indolo–[2,3–b]–phenazin–4(5H)–one (K^2) by Neelima, et al [59]. Complexes of La(III) have been synthesized by reaction of lanthanum(III) salt in 1:2 molar ratio with ligand 2,3–dihydro–1H–indolo–[2,3–b]–phenazin–4(5*H*)–ylidene) benzothiazole–2–amine (L^1) and 3–(ethoxymethylene)–2,3–dihydro–1*H*–indolo[2,3–b]–phenazin–4(5*H*)–ylidene) benzathiazole–2–amine (L^2) in methanol. The ligands and their La(III) complexes were characterized by molar conductance, magnetic susceptibility, elemental analyses, FT–IR, UV–Vis, ^{1}H-^{13}C NMR, thermogravimetric, XRD and SEM analysis. IR spectral data and elemental analyses confirm that Schiff bases are coordinated to the metal ion in a bidentate manner by N, S donor sites of ligands. Thus, with the aid of the infrared spectra, elemental analyses and molar conductance, the proposed configuration is expected to be a capped octahedral, as shown in Scheme (1-6), (1-7).

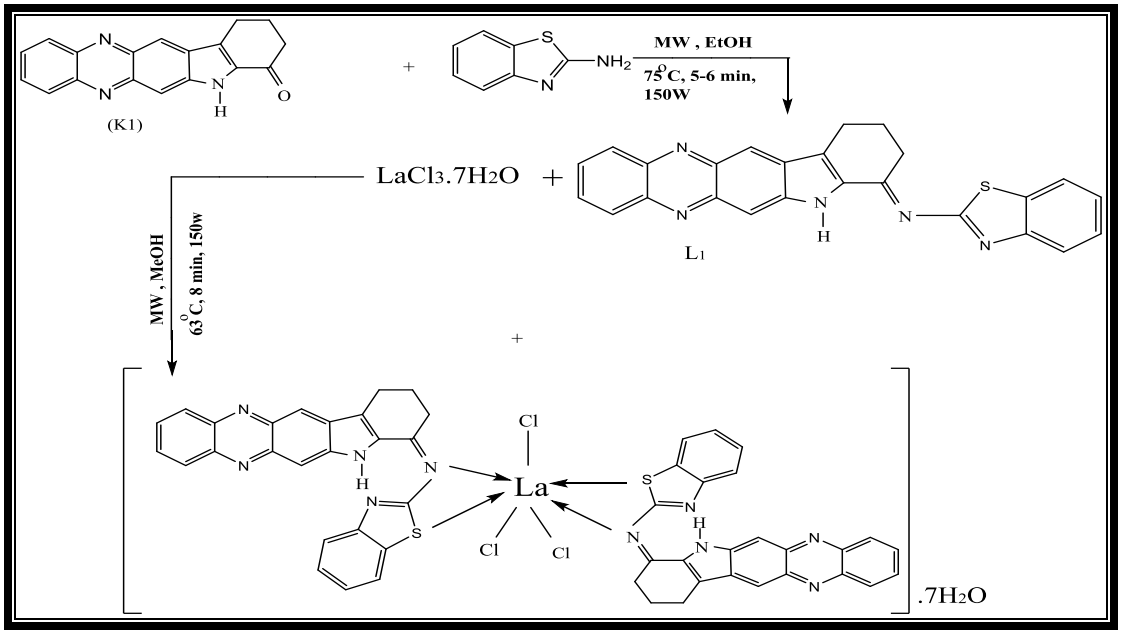

Scheme (1-6): presentation of synthetic route and proposed structure of $[La(L^1)_2Cl_3].7H_2O$.

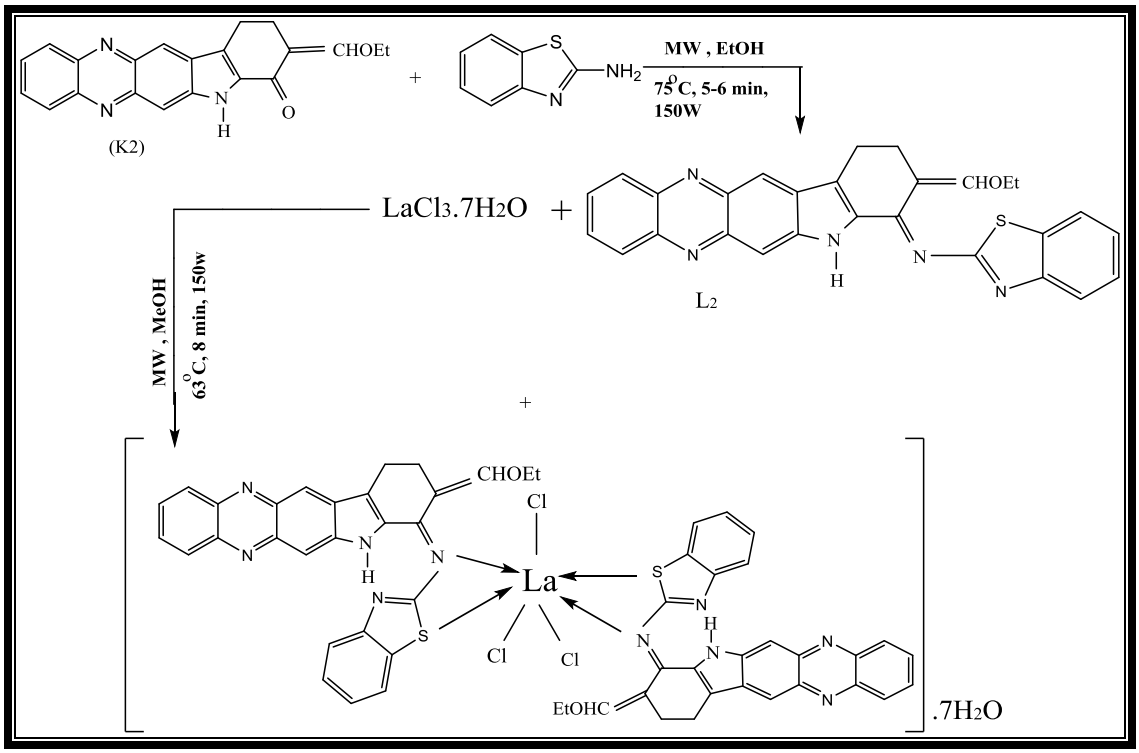

Scheme (1-7): presentation of synthetic route and proposed structure of $[La(L^2)_2Cl_3].7H_2O$.

In 2015 Newly Schiff bases ligand [(E)-3-[(Z)-3-(2- Hydroxy phenylimino)-1,5-dimethyl-2-phenyl-2,3-dihydro-1H-pyrazol-4-ylimino]indolin-2-one](2-DMIAP) was synthesized using two steps by E.K.Kareem and co-workers [60] (Scheme (1-8)).Three chelate complexes have also been synthesized by reaction this ligand (2-DMIAP) with metal ions Co(II), Ni(II) and Cu(II) with molecular formula $[M(2\text{-}DMIAP)_2]Cl_2.H_2O$ .The prepared ligand was characterized by melting point, FT-IR and UV-Vis spectra. The FT-IR spectra of the chelating complexes have been studies. this may indicate that coordination between metal ions and the ligand (2-DMIAP) take place. The UV-Vis spectra of complexes showed bathochromic shift when it compared with that of free ligand (2-DMIAP). The melting points, molar Conductivity, magnetic moment, elemental microanalysis, melting points and the percentage of metal ions were determined. Depending on these results, the suggested

geometrical formula of the synthesized complexes Co(II) , Ni(II) and Cu(II) are octahedral (Fig. (1-9)).

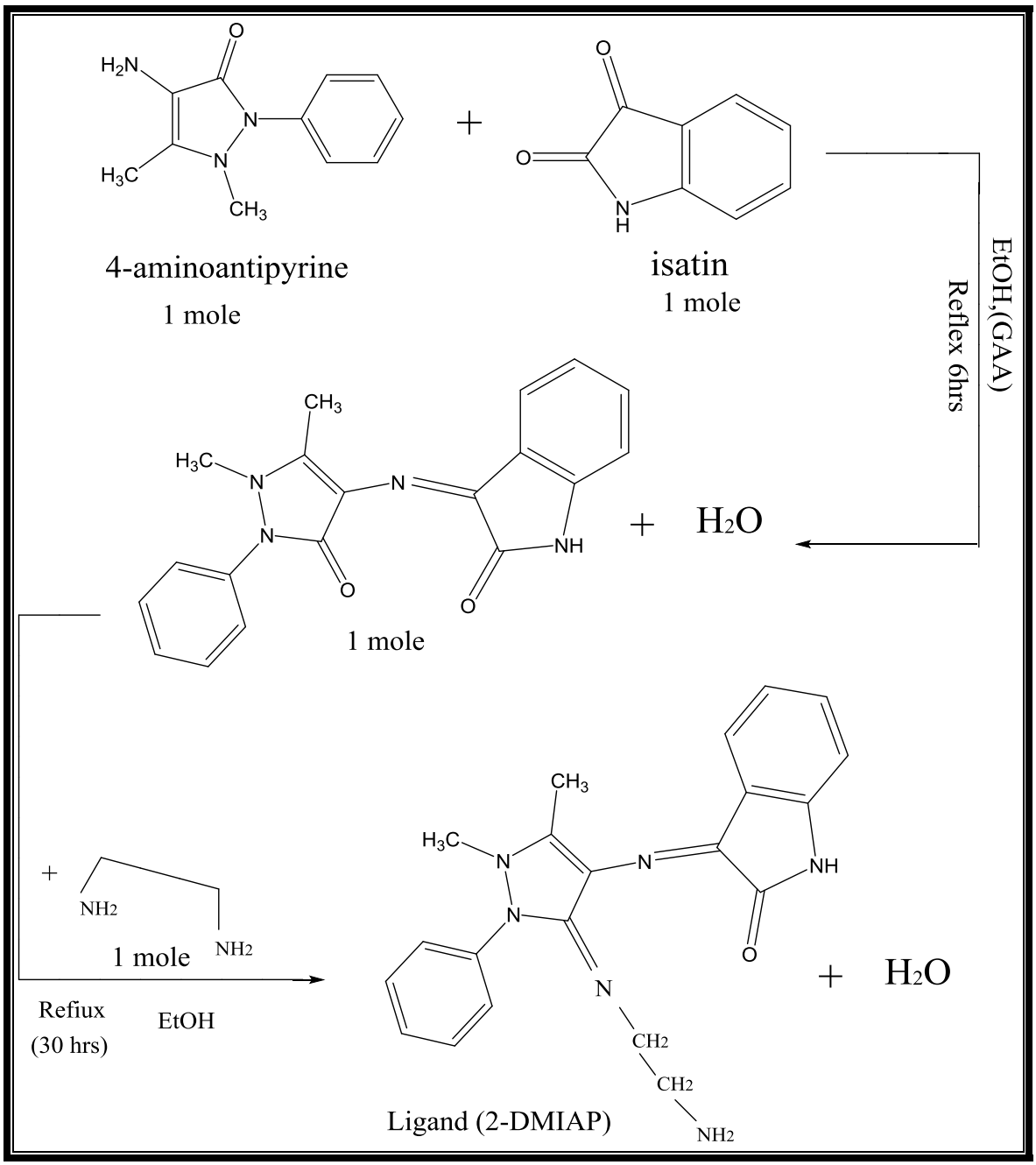

Scheme(1-8) : Synthesis route of ligand (2-DMIAP).

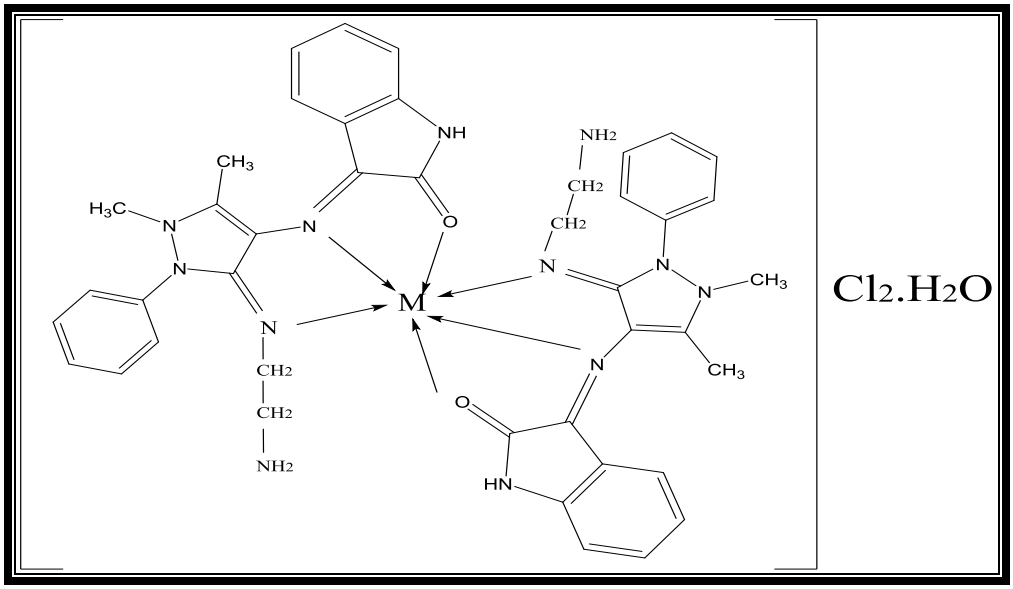

Fig.(1-9): The synthesis geometrical structure of (2-DMIAP) complexes of Co(II), Ni(II) and Cu(II) .

In 2015 S. Ravichandran and C. Marquesan [(61)] were synthesized novel terdentate neutral complexes of Cu(II), Co(II), Ni(II) and Zn(II) by using a Schiff base derived from biologically active 1-phenyl-2,3-dimethyl-4-aminopyrazol-5-one (4-aminoantipyrine) and N-(1-piperidino(4-N,N-dimethylaminobenzyl) acetamide (Mannich base). The structural features of the complexes have been confirmed by microanalytical data, IR, UV-Vis, EPR, Mass, CV and TGA techniques. Electronic absorption spectra of the complexes indicate an octahedral geometry around the metal ion. The neutral nature of the complexes is characterized from their low molar conductance values. The thermal analysis showed the absence of neither coordinated nor lattice water in all the complexes. The antimicrobial activity of the ligand and its complexes has been extensively studied on microorganisms such as *Staphylococcus aureus*, *Bacillus subtilis*, *Escherichia coli* and *Pseudomonas aeruginosa* by well-diffusion technique using DMF as solvent. The values of zone of inhibition were found out at 37^0C for a period of 24 h. It has been found

that all the complexes have higher activity than the free ligand and the standard , as shown in Scheme (1-9) and (1-10).

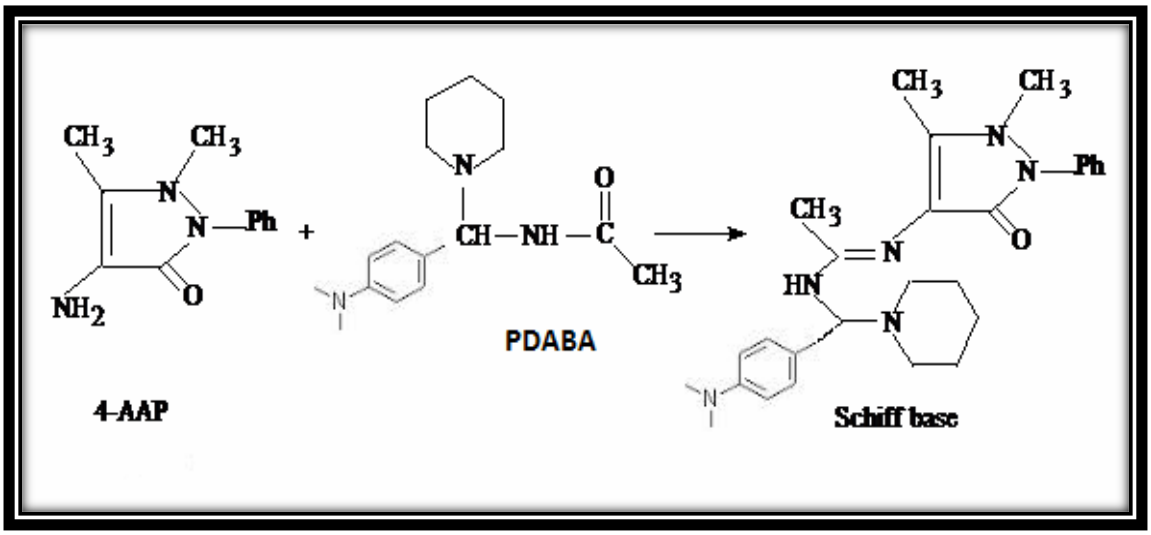

Scheme (1-9): Formation of Schiff base

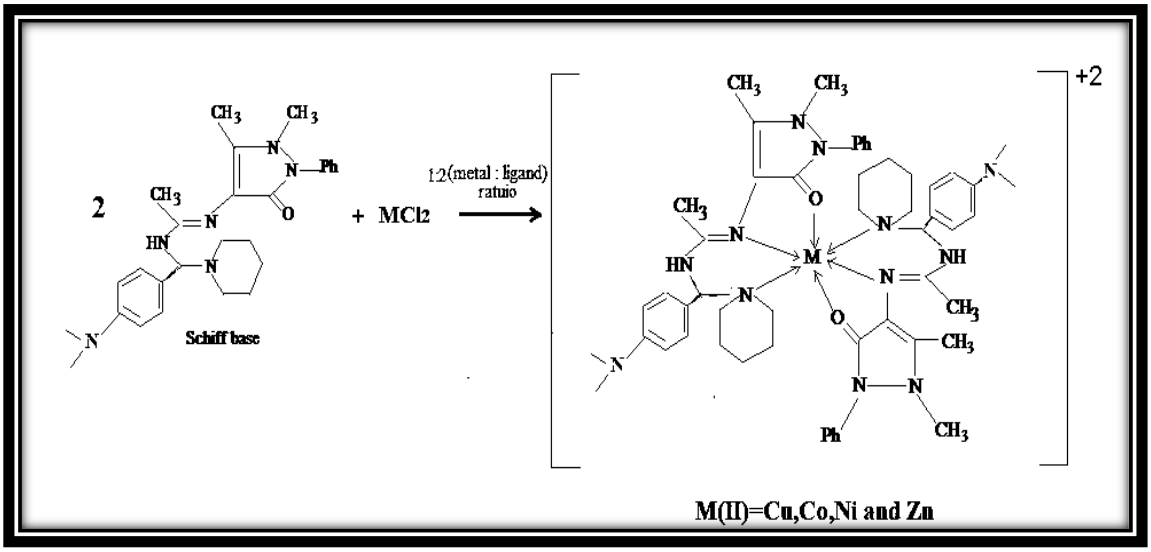

Scheme (1-10): Formation of metal complexes

In 2015 M. Ravi and co-workers [62] were synthesized, character-zation, DNA-interaction, photo-cleavage, radical scavenging, *in-vitro* cytotoxicity, antimicrobial, docking and kinetic studies of Cu (II), Cd (II), Ce (IV) and Zr (IV) metal complexes of an imine derivative, 3 – (1 – (6 – methoxybenzo [d] thiazol – 2 – ylimino) ethyl) – 6 – methyl –

3H – pyran – 2, 4 – dione [3-MBTMPD] . The investigation of metal ligand interactions for the determination of composition of metal complexes, corresponding kinetic studies and antioxidant activity in solution was carried out by spectrophotometric methods. The synthesized metal complexes were characterized by EDX analysis, Mass, IR, ^{1}H-NMR, ^{13}C-NMR and UV–Visible spectra. The geometry of metal complexes of Cu (II), Cd (II), Ce (IV) and Zr (IV) were found to be square planar, tetrahedral, octahedral and square pyramidal respectively, shown in Scheme (1-11).

The antibacterial activity of the synthesized compounds against four bacterial strains viz; *Staphylococcus aureus*, *Bacillus subtilis*, *Escherichia coli* and *Pseudomonas putida*. The order of activity towards gram negative bacteria is: Cd (II)-3-MBTMPD >Ce (IV)-3-MBTMPD> Zr (IV) -3-MBTMPD> Cu (II)-3- MBTMPD > 3-MBTMPD and for gram positive bacteria the order is Cd (II)-3-MBTMPD> Cu (II)-3-MBTMPD> Ce (IV)-3-MBTMPD> Zr (IV)-3-MBTMPD> 3-MBTMPD.

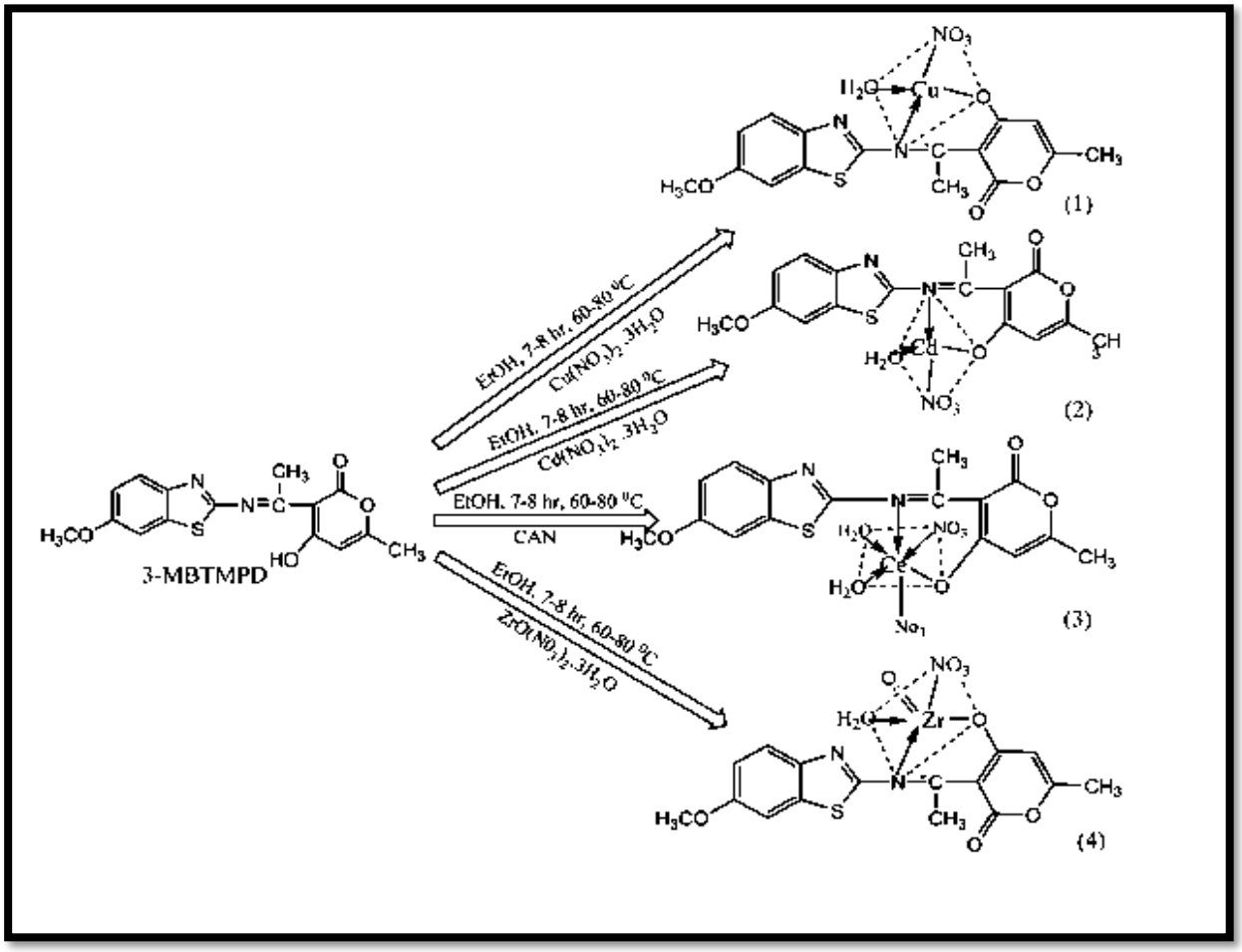

Scheme (1-11): Formation of 3-MBTMPD metal complexes.

In 2015 S. M. Lateef and co-works [63] synthesized new multidentate Schiff base ligand [2-((E)-4-((Z)-2-hydroxy-1,2-diphenylethylidene amino)-1,5-dimethyl-2-phenyl-1H-pyrazol-3(2H)-ylideneamino) propanoic acid] [H_2L] type (NNOO) by two steps (Scheme (1-12)). The ligand was refluxed in ethanol with metal ions [VO(II), Mn(II), Co(II) and Ni(II)] salts to give the complexes of general molecular formula: $[M(H_2L)_2(X)(Y)].B$, where: M=VO(II), X=0, $Y=OSO_3^{-2}$, $B=2H_2O$; M=Mn(II),Ni(II) ,X= H_2O, Y= H_2O, B=2Cl; M=Co(II), X=H_2O, Y=Cl, B=Cl . All complexes were characterized by melting point measurement, atomic absorption (A.A), F.T.I.R., ultraviolet visible(U.V-Vis) spectroscopies (^1H,^{13}C NMR for ligand only), along with conductivity, elemental microanalysis (C.H.N) and chloride content. These studies

revealed an octahedral geometry for VO(II), Mn(II), Co(II) and Ni(II) complexes. The ligand and its complexes exhibited biological activity against the *Staphylococcus aureus* (G+), *E-coli* (G-), *Pseudomonas* (G-) and *Proteus* (G-) except $[Ni(H_2L)_2(H_2O)_2].2Cl$ with *Pseudomonas* has no biological activity.

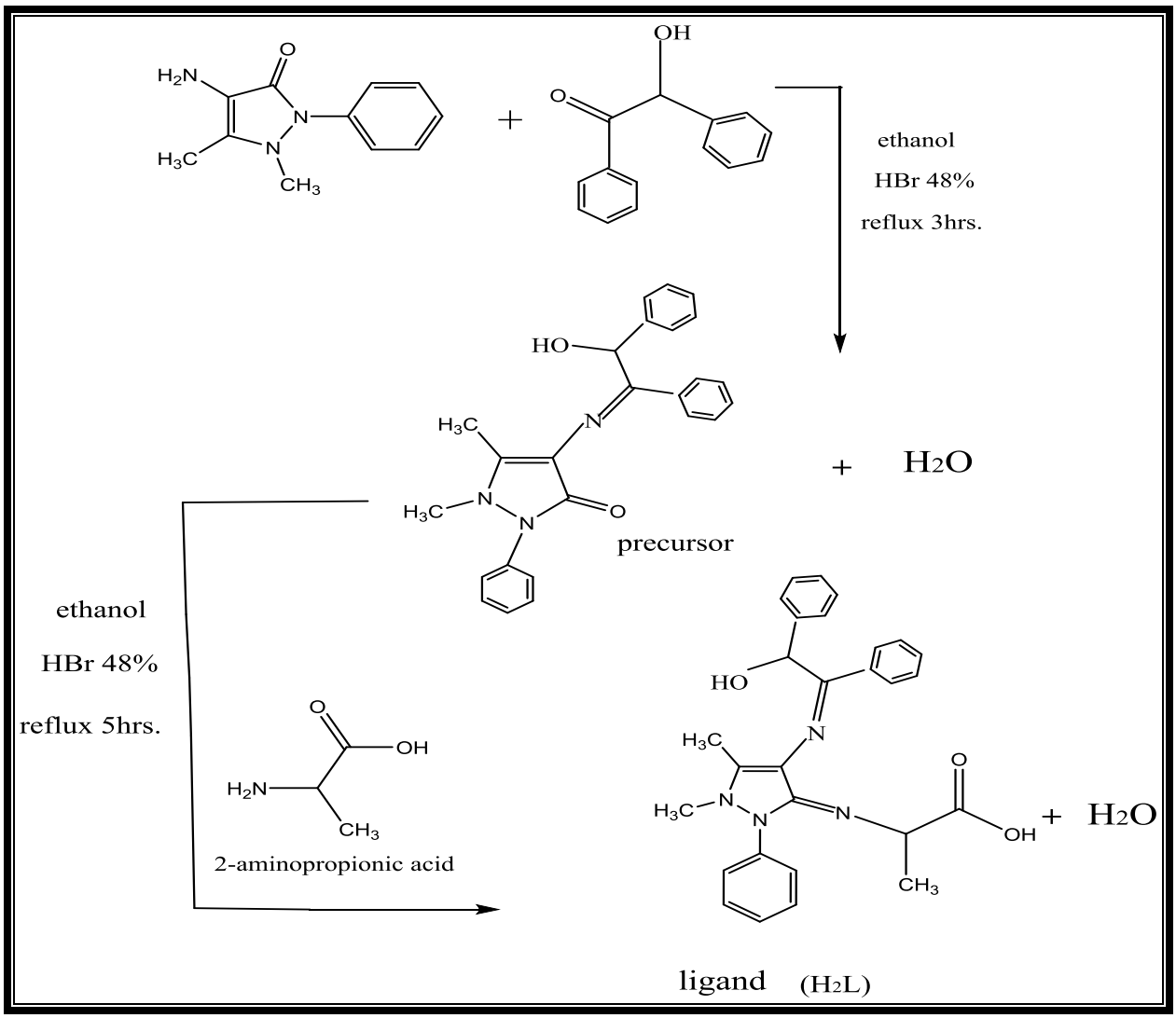

Scheme (1-12): Synthesis route of Schiff base ligand (H_2L)

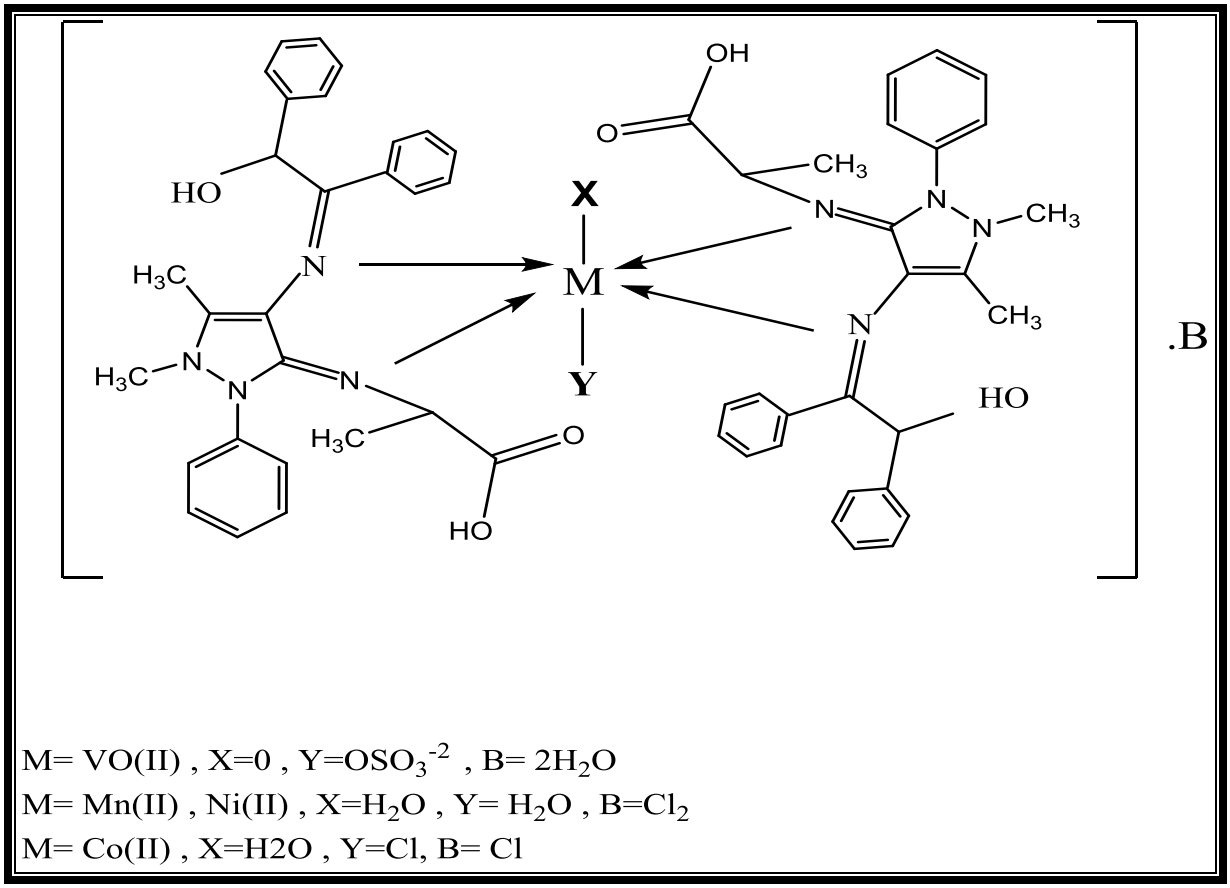

Fig.(1-10): geometrical structure of complexes .

In 2016 J. Jadeja and co-workers [64] prepared N,O,O-donating tridentate ligand by condensed reaction 1,5-dimethyl-2-phenyl-2,3-dihydro-1H-pyrazol-4-amine (4-AAP) with derivative of salicylaldehyde and its metal complexes with Zn, Cd and Hg, which is highly stable at room temperature and characterized by Mass spectrometry, IR, ^{1}H-NMR, ^{13}C-NMR and elemental analysis. Its metal complexes were characterized by ESI-Mass, IR, TGA-DTA and Elemental analysis. All compounds are showing moderate antibacterial and anti-fungal activity compared to standard medication, as shown in Scheme (1-13).

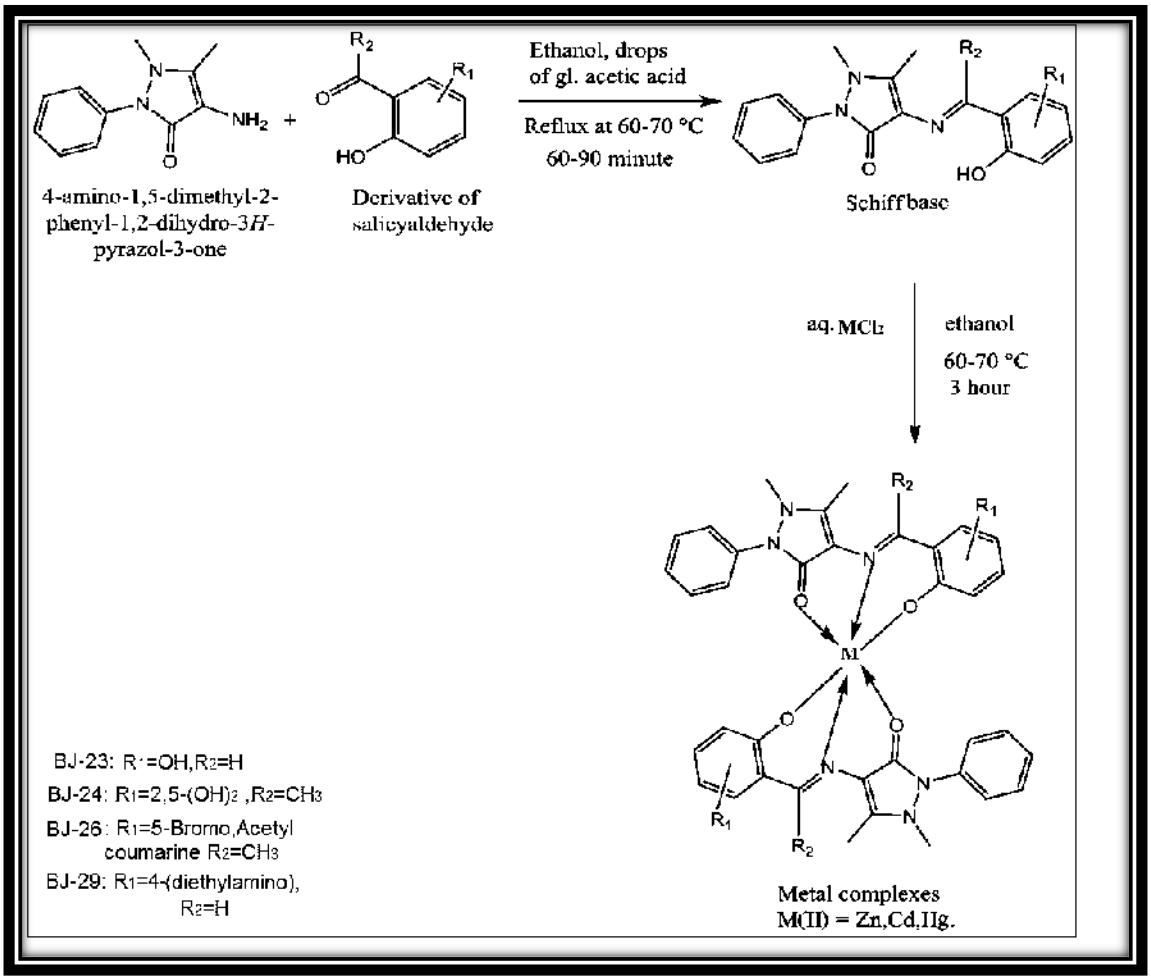

Scheme (1-13): route and proposed structure of ligand and its complexes.

In 2016 J.Joseph and G.Janaki [(65)] synthesized novel copper(II) complexes of Schiff base ligands of 2-aminobenzothiazole derivatives by the condensation of Knoevenagel condensate of acetoacetanilide (obtained from substituted benzaldehydes and acetoacetanilide) and 2-aminobenzothiazole. They were characterized by elemental analysis, IR, ^{1}H-NMR, UV–Vis., molar conductance, thermal denaturation, magnetic susceptibility measurements and electrochemical studies. The metal complexes were prepared following the general procedure. 1:1(L:M)., Square planar geometry has been suggested based on the magnetic moment and electronic spectral data for all the complexes. Antibacterial and antifungal screening of the ligands and their complexes reveal that all the

complexes show higher activities than the ligands. Scheme (1-14) showed the synthesis route of ligands and their complexes.

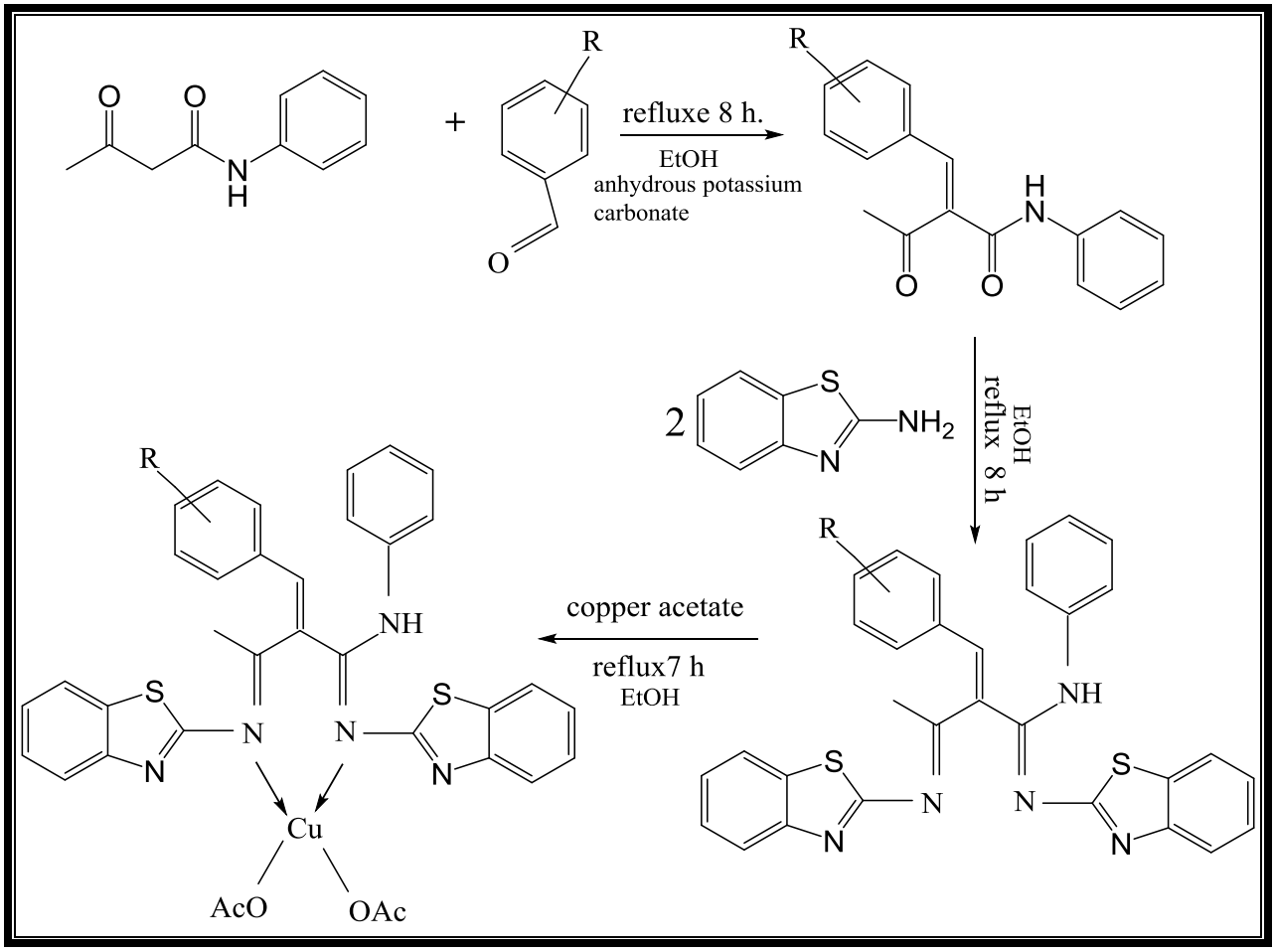

Scheme (1-14): Schematic outline of synthesis of ligands and their Cu(II) complexes.

In 2016 S. M. El-Megharbel and co-workers [66] prepared three new Schiff bases derived from 4-amino antipyrine with 2-furaldehyde, 2-thiophene carboxaldehyde and 2-methoxybenzaldehyde and their Ni(II) complexes. All compounds were characterized based on elemental analyses, IR, electronic spectra, molar conductance, and thermos gravimetric analysis. Infrared spectra proved that three Schiff base chelates are coordinated to the nickel(II) ions as a bidentate fashion with ON and NS for the (2-furaldehyde and 2-methoxybenzaldehyde) and 2-thiophene carboxaldehyde, respectively. The molar conductance data revealed that all

the Ni(II) chelates are non-electrolytes. The general formula of precursors nickel(II) complexes is $[Ni(Ln)_2(Cl)_2]$,(n=1,2,3) with 1:2 (Ni:L) molar ratio . The suggested geometrical formula of Ni(II) complexes are octahedral, as shown in Fig. (1-11) and (1-12).

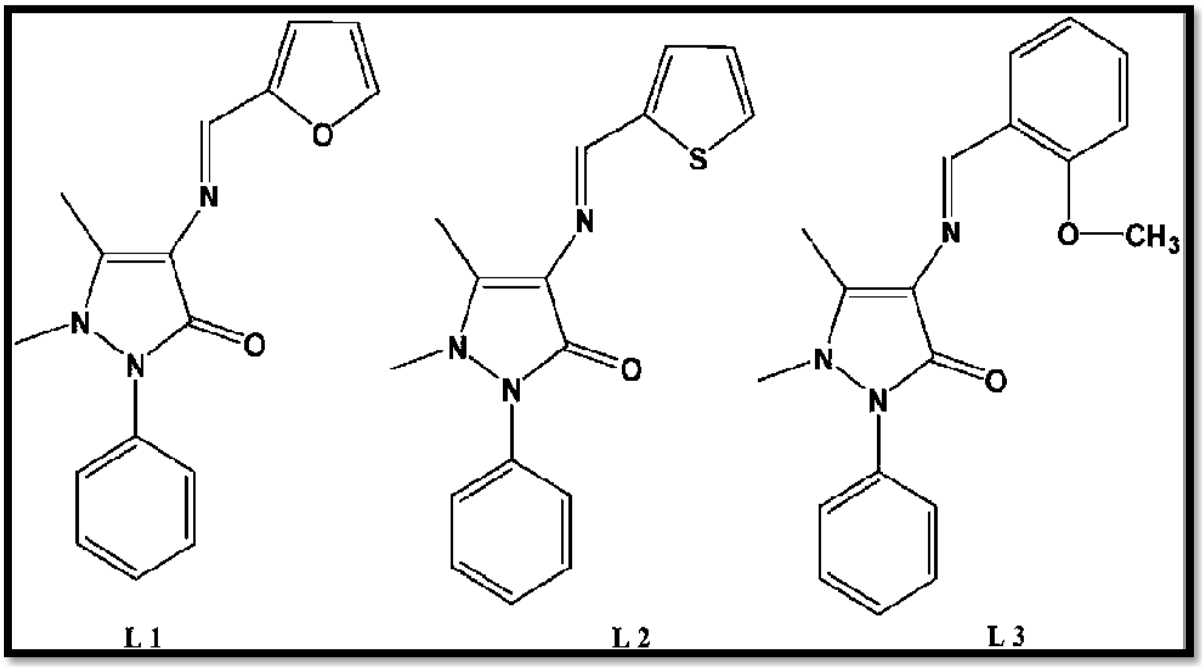

Fig. (1-11): The chemical structures of Schiff bases ligands derived from 4-aminoantipyrine

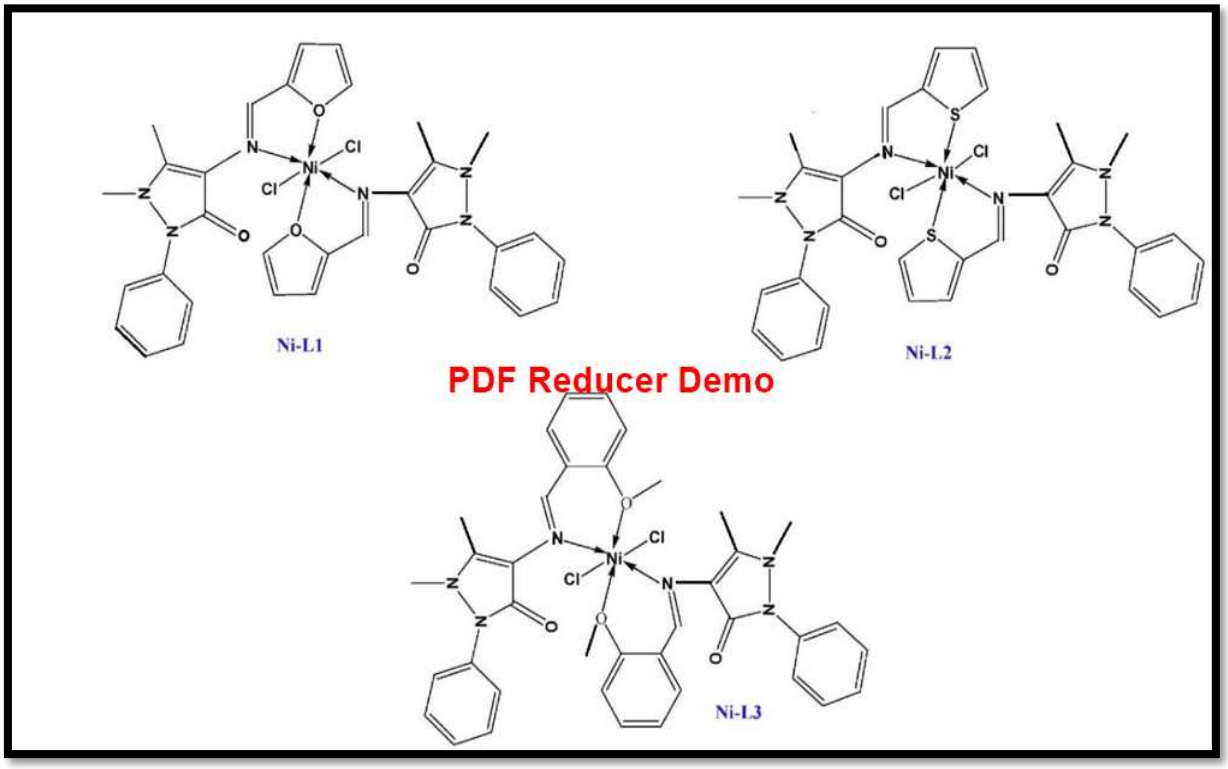

Fig. (1-12): The suggested chemical structure of Ni(II) complexes.

In 2017 W. H. Mahmoud and co-workers [(67)] synthesized novel Schiff base ligand (HL) with the IUPAC name 2-(((1,5-dimethyl-3-oxo-2-phenyl-2,3-dihydro-1H-pyrazol-4-yl)imino)(phenyl)methyl)benzoic acid from condensation o-benzoyl benzoic acid and 4-aminoantipyrine .The synthesized Schiff base ligand and its complexes with metal ions Cr(III), Mn(II), Fe(III), Co(II), Ni(II), Cu(II), Zn(II) and Cd(II)) were characterized by elemental, magnetic susceptibility, molar conductivity, spectroscopic (^{1}HNMR, mass, UV–visible, FTIR, ESR), thermal and X-ray powder diffraction. The diffused reflectance spectra, magnetic susceptibility and ESR spectral data of the complexes confirmed an octahedral geometry around metal ions Fig.(1-13) . The thermal analysis data revealed the decomposition of the complexes in three to five successive decomposition steps within the temperature range of 30–1000^{o}C, and the activation thermodynamic parameters were reported. The *in-vitro* antimicrobial screening of the newly synthesized compounds was tested against different

bacterial and fungal organisms. The results showed that the metal complexes have biologically activity more than the new Schiff base ligand against the tested organisms. The Schiff base ligand and its complexes were also screened for their anticancer activity against breast cancer cell line (MCF7).

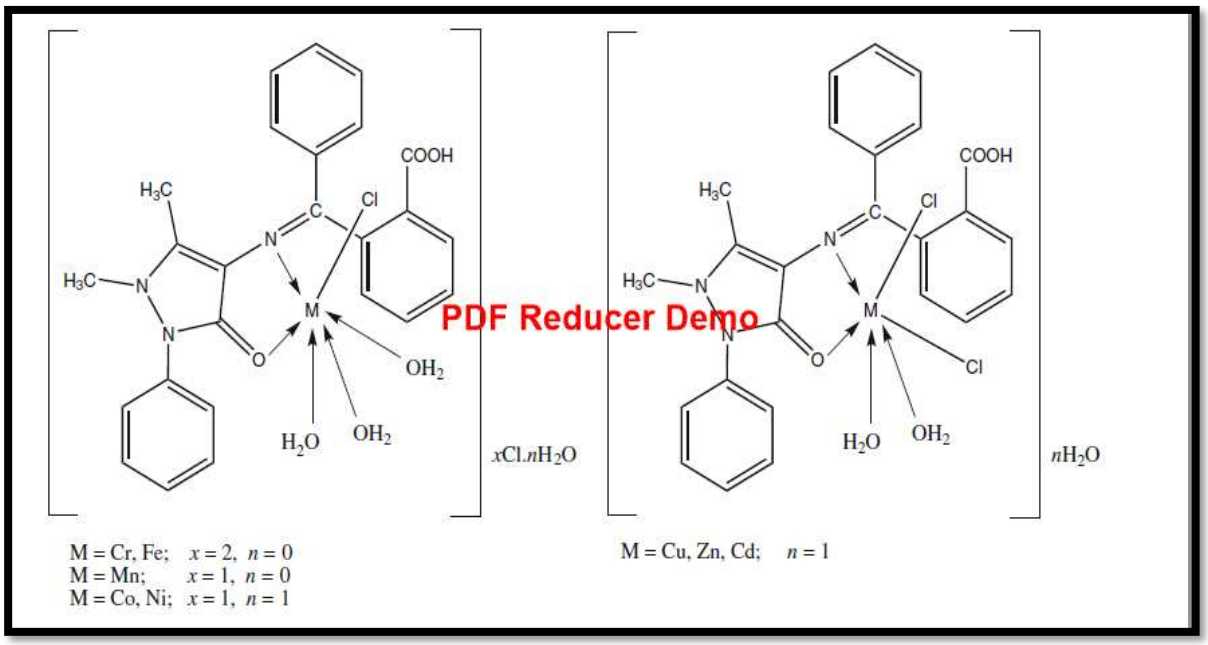

Fig. (1-13): The chemical structure of metal complexes.

In 2017 G.Padole-Gaikwad and co-workers [68] reported the synthesis of novel five transition metal coordination polymers based on maloyl bis-2-aminobenzothiazole (MBAB) , and their structural aspects interpreted on the basis of elemental analysis, infrared spectroscopy, diffuse reflectance spectroscopy, magnetic susceptibility measurement, and thermal techniques. The obtained coordination polymers are formulated as [Mn(II)(MBAB) $(H_2O)_2$] n, {[Co(II)(MBAB)$(H_2O)_2$]H_2O}n, {[Ni(II)(MBAB)$(H_2O)_2$]H_2O}n, [Cu(II)(MBAB)]n and [Zn(II) (MBAB)]n. The detailed thermal study confirms the number and nature of water molecules in coordination polymers. The geometries of coordination polymers were determined on the basis of diffuse reflectance and magnetic susceptibility measurements; octahedral and square planar geometries

were found for Mn(II), Co(II), Ni(II), and Cu(II), Zn(II), respectively. As shown in Fig. (1-14)

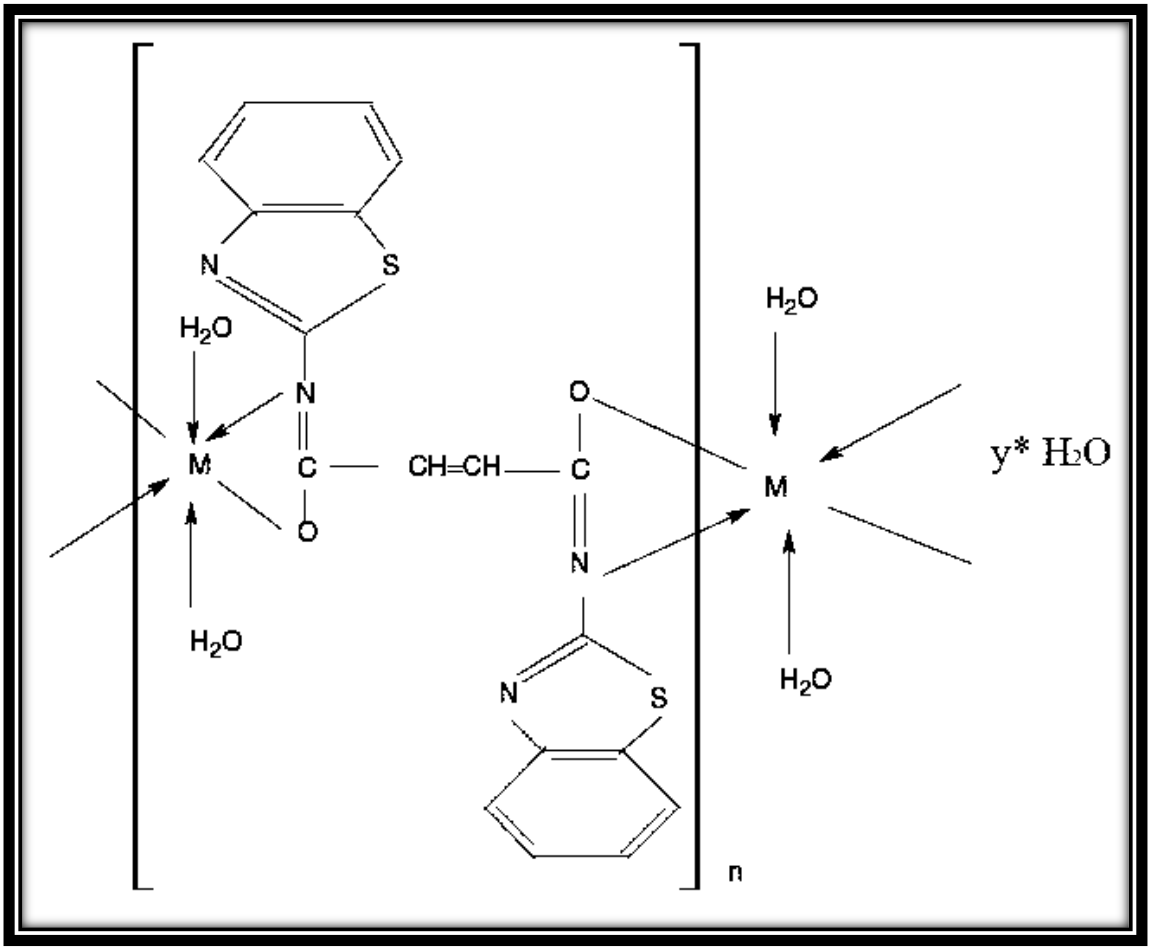

M = metal ion, Mn (II), Co (II), Ni (II), Cu(II) and Zn (II). Y*H_2O is a lattice water. Coordinated-H2O is absent in Cu (II) and Zn (II). y = 1 for Co (II) and Ni (II), and y = 0 for Mn (II) and Zn(II).

Fig. (1-14): The proposed structure of the coordination polymers of maloyl-bis-2-aminobenzothiazole

In 2017 S. H. Kadhim and co-workers [69] synthesized new Schiff base 4-(1-(4-(2-hydroxybenzylideneamino)phenyl) ethylidene amino)-1,5-dimethyl-2-phenyl-1H-pyrazol-3(2H)-one derived from the reaction between Salicylaldehyde, p-amino acetophenone and 4-aminoantipyrine and its complexes with Co(II), Ni(II) and Cu(II). The identification of the ligand and its complexes were carried out by the techniques: UV-visible,

infrared and ^{1}H-NMR spectroscopies, elemental micro analyses of metal ions and (C.H.N), magnetic susceptibility and molar conductivity. The results of this studies show the coordination sites for the ligand with the metal ion were to be through the oxygen of the carbonyl group and nitrogen of the azomethine (C=N) group. According to the observations, the octahedral geometric structure for all synthesized complexes were suggested, as depicted in Fig. (1-15)

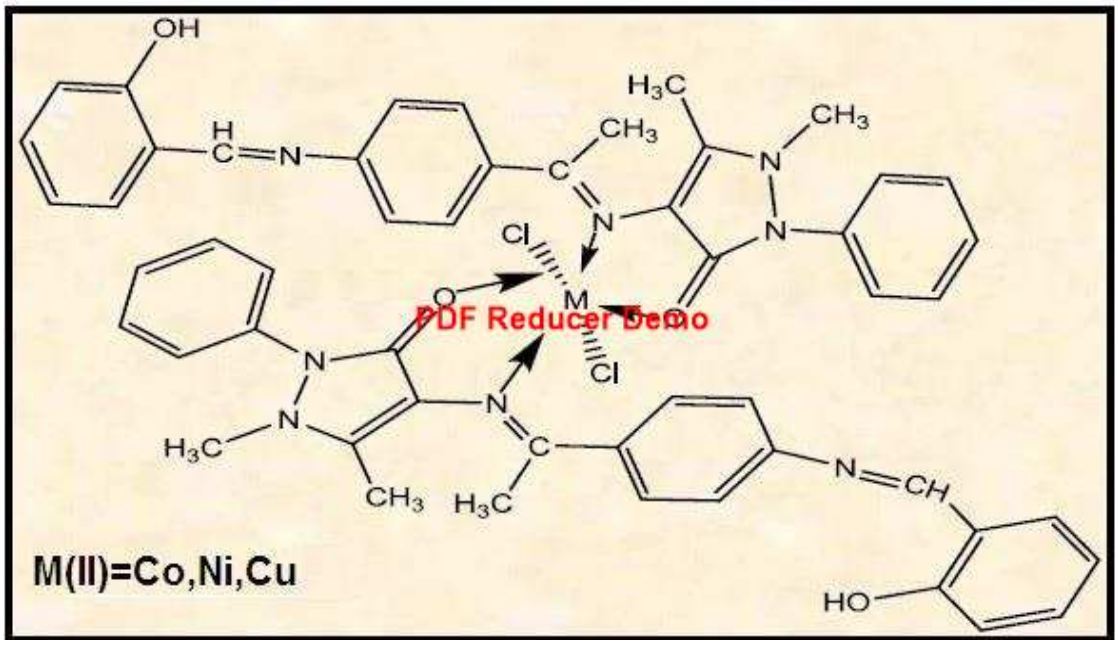

Fig. (1-15): Suggested chemical structure of the octahedral configuration of the Schiff base complexes.

In 2017 A. Ahlawat and co-workers [(70)] synthesized series of organotin(IV) complexes type R_2SnLCl [R = Ph, Bu, Et, Me and L=L_1-L_4] by reaction of diorganotindichloride(IV) with Schiff base ligands, L_1 = (1-[(6-ethoxy-benzothiazol-2-ylimino)-methyl]-naphthalen-2-ol), L_2 = (1-[(6-nitro-benzothiazol-2-ylimino)-methyl]-naphthalen-2-ol), L_3 = (1-[(6-methoxy-benzothiazol-2-ylimino)-methyl]-naphthalen-2-ol) and L_4 = (1-[(6-methyl-benzothiazol-2-ylimino)-methyl]-naphthalen-2-ol) obtained from 2-amino-6-substituted benzothiazole derivatives with 2-hydroxy-1-

naphthaldehyde in 1:1 molar ratio. These organotin(IV) complexes were characterized by various spectroscopic techniques (^{1}H, ^{13}C and ^{119}Sn NMR, FT-IR), and physical techniques (X-ray powder diffraction analysis and elemental analysis). The coordination of the synthesized complexes has been planned as pentacoordinated around the central tin atom during which ligands coordinated to tin atom in bidentate manner acted as N, O donor system producing complexes with distorted trigonal bipyramidal geometry. The ligands and their complexes were screened for antibacterial and antifungal activities against Gram-positive *Bacteria Bacillus cereus, Staphylococcus aureus,* Gram-negative *bacteria Escherichia coli, Pseudomonas aeruginosa* and fungi *Aspergillus niger* and *Aspergillus flavus*. The results of antimicrobial activity indicated that these compounds possess high activity against the tested microorganisms and some compounds were equipotent to the standard drugs particularly against *S. aureus* and *A. niger*. The structures of ligands and their tin complexes were shown in Scheme (1-15).

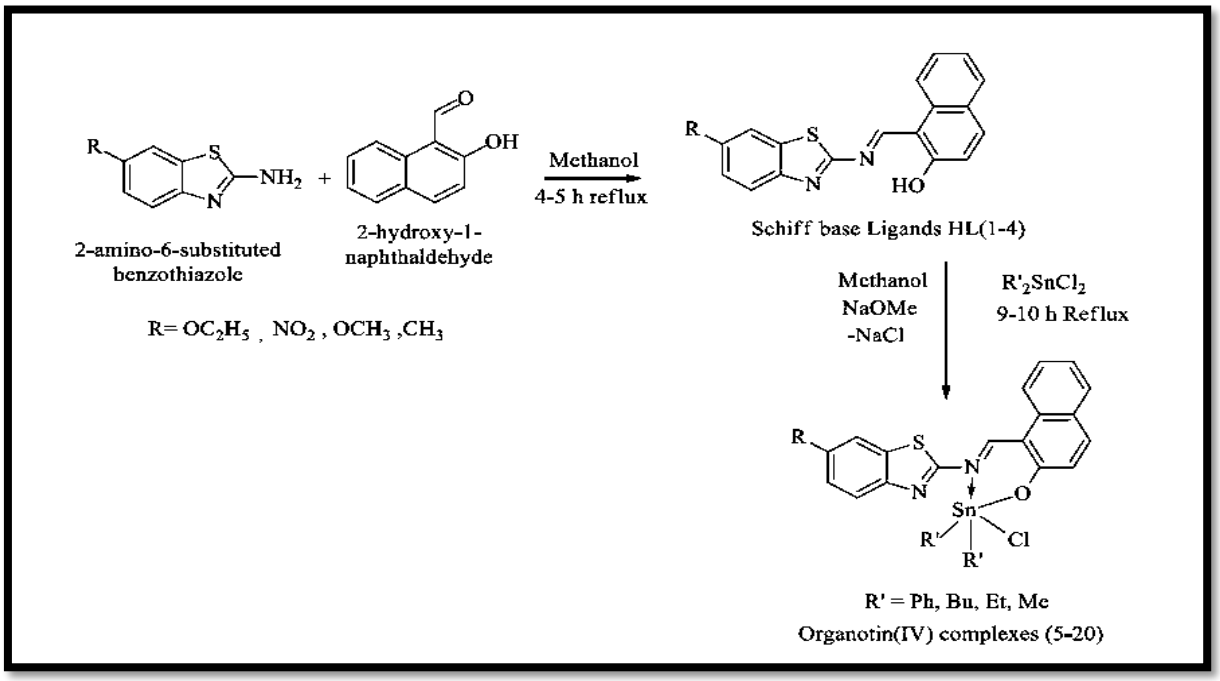

Scheme (1-15): Synthesis route of Schiff base ligands and organotin(IV) complexes.

In 2017 E. Th. Selvi and S. Mahalakshmia [71] were reported synthesis newly heterocyclic Schiff base ligands derived from 4-amino antipyrine, thiophene-2-Carboxaldehyde and 2-amino benzoic acid and their complexes. The Schiff base ligands and their metal complexes of Cu(II), Co (II), Ni (II) and Zn (II) are characterized by UV, FTIR , NMR and Mass studies. All the metal complexes were synthesized following the general procedure. 1:1(L:M). The data of the complexes suggested a square planar geometry for Co, Ni, Cu and tetrahedral for Zn complexes. Based on these data the proposed structure of the complex is shown in Fig. (1-16). Evaluation of antibacterial and antifungal activity of the complexes *against Escherichia coli, Pseudomonas aeruginosa, Staphylococcus aureus, Salmonella typhimurium* and *Candida albicans* exhibited that the complexes have potent biocidal activity than the ligands.

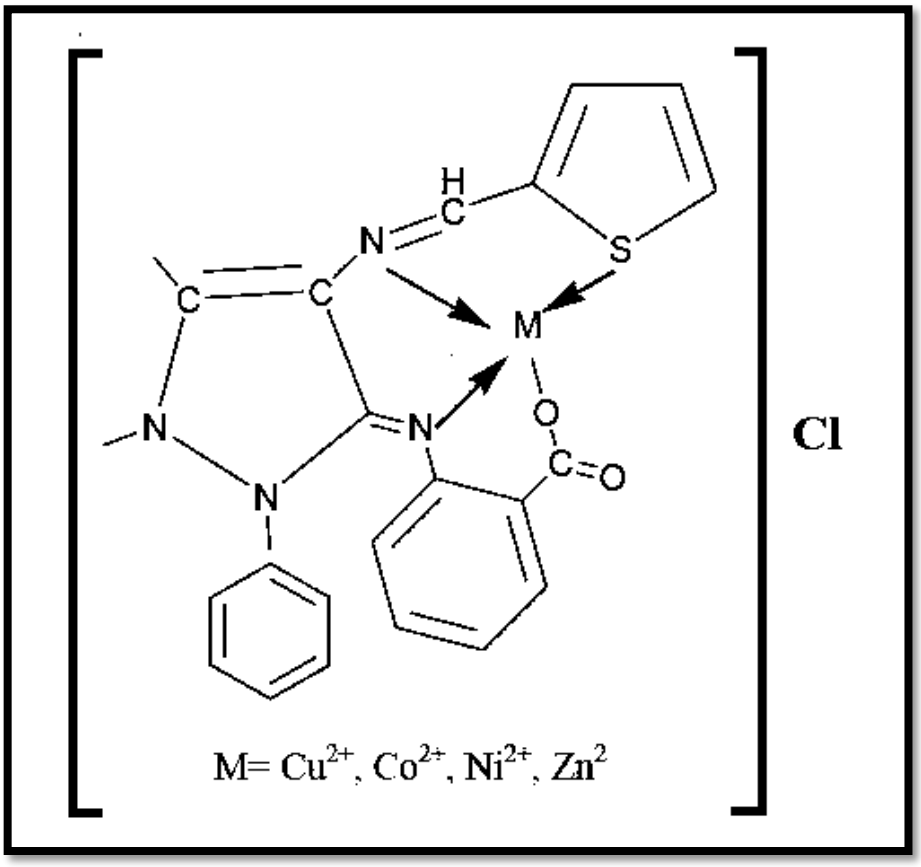

Fig.(1-16): The suggested chemical structure for prepared complexes.

In 2017 Sh.M. Morgan and co-workers [72] synthesized novel series of metal complexes of Cu(II), Co(II), Ni(II), Mn(II) and Cd(II) from Schiff base derived from 4-aminoantipyrine and quinolone -2-carbaldehyde to give 4-((quinolin-2-yl) methyleneamino)-1,2-dihydro-2,3-dimethyl-1-phenylpyrazol-5-one (QMP). The structural features were derived from elemental analysis, mass spectroscopy, X-ray, IR, ^{1}H-NMR, electronic spectra, molar conductance magnetic susceptibility and thermogravimetric studies. According to of these studies the coordination sites were proven to be through oxygen of the ring C=O and nitrogen of the azomethine (HC=N) group. The antimicrobial activity of Schiff base (QMP) and its M(II) complexes were studied and compared with the standard antibacterial and antifungal medications. The geometrical formula for all complexes were octahedral but tetrahedral for Cd(II) complex. See Fig. (1-17).

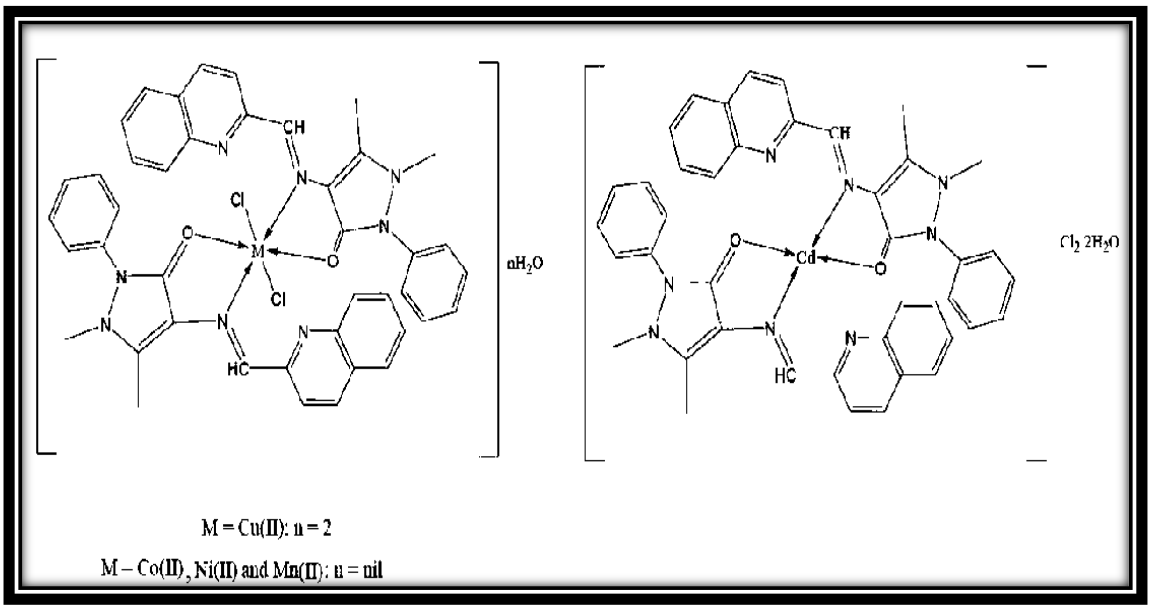

Fig. (1-17): The chemical structure of the metal complexes.

In 2018 N. Raman and co-workers [73] prepared new unique Schiff base ligand, formed by the condensation reaction of 2-aminobenzothiazo-le with curcumin and its Cu(II), Ni(II), Co(II) and Zn(II) complexes incorporating 2,2′-bipyridine as coligand. They were characterized via

analytical and spectroscopic methods. The complexes adopt square planar geometry around Co, Ni and Cu metal ions but tetrahedral geometry for Zn(II) complex shown in Scheme (1-16). It was found that all the complexes are antimicrobial active and show higher activity than the ligand.

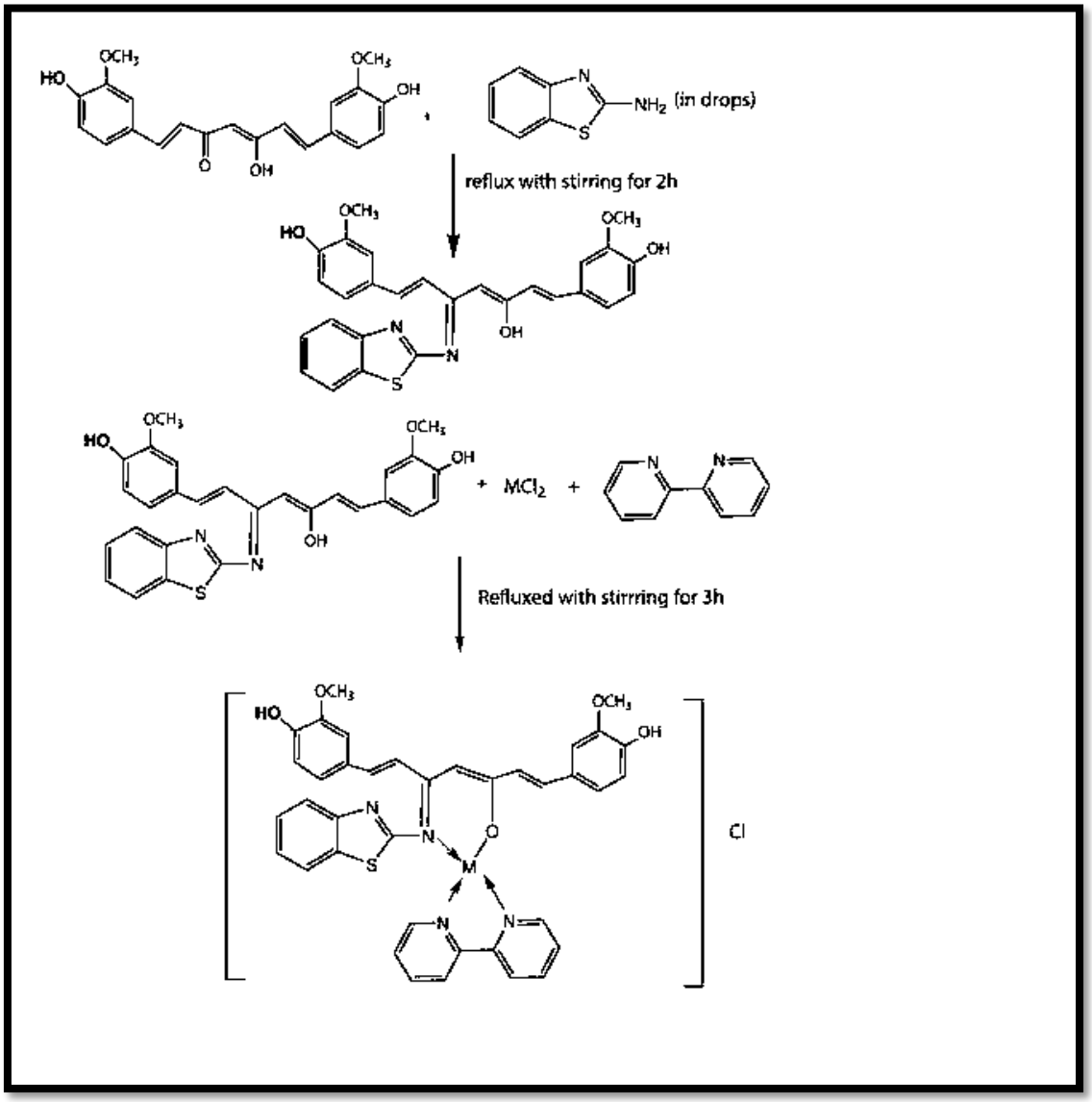

Scheme (1-16): Synthesis route of Schiff base ligand and its metal complexes.

In 2018 Sh. Ibatte and B. More [74] prepared metal complexes of Schiff bases (L) derived from the condensation of 4-aminoantipyrine, 4-chlorobenzaldehyde and acetylacetone. All complexes were characterized by elemental analysis, IR, ^{1}H-NMR, EPR spectroscopy, conductivity, thermal analysis, magnetic measurements and a microbial study. The magnetic measurements and EPR spectral data of the complexes suggested square-planar geometry around the central metal ion for Co, Ni and Cu but tetrahedral geometry for Zn(II) complex see **(**Scheme (1-17)). The molar conductance data revealed that all the complexes were electrolytes in the ratio 1:2 (M:L). The analytical data suggested that the formula of complexes as $[ML_1]X_2$ where M = Co(II), Ni(II), Cu(II), Zn(II) and X = Cl^{-1}, $NO3^{-1}$ and CH_3COO^{-1}. The thermal stability of the complexes were studied by thermogravimetry. The ligands and their metal complexes were screened for antimicrobial activity against *S. typhi, S. aureus, E. coli and B. subtilis*. It is observed that Zn(II) and Cu(II) complexes are more active against the bacterial strains *S. typhi* and *E. coli* as compared to other bacterial strains. Co (II) and Ni(II) complexes were found to be moderately active against all bacterial strains.

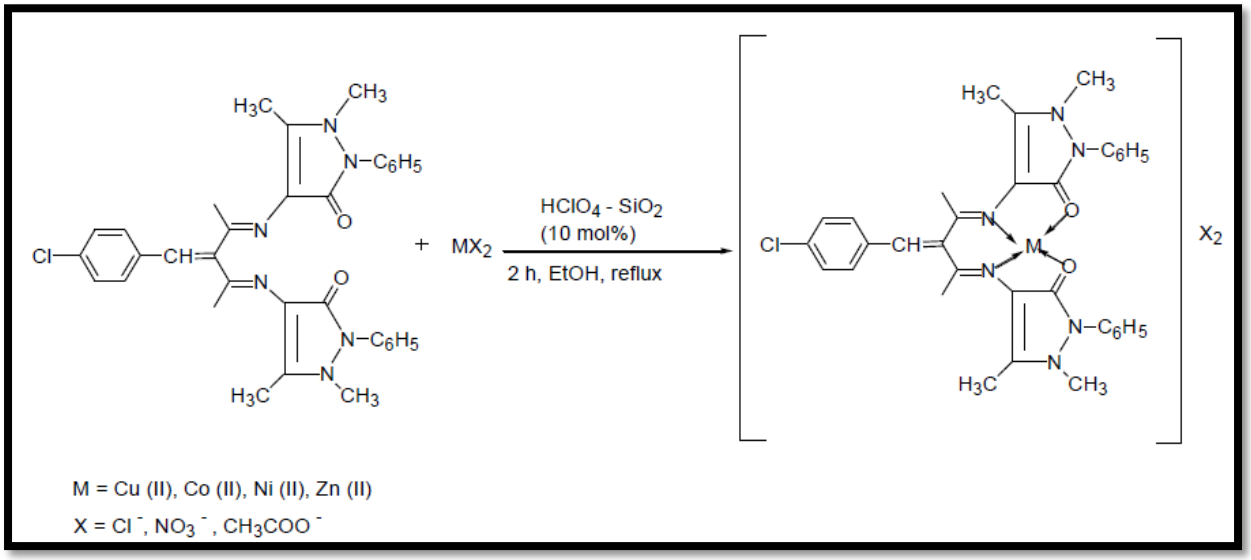

Scheme (1-17): Synthesis route of Schiff base complexes.

In 2018 Neelima and co-workers [75] Synthesized new bioactive metal complexes by reaction Ce(III) salt ($Ce(NO_3)_3.6H_2O$) in 1:2 molar ratio with ligands L^1 and 3-(ethoxymethylene)-2,3-dihydro-*1H*-indolo-[2,3-*b*]-phenazin-4(*5H*)−ylidene)benzathiazole-2-amine (L^2) in methanol. The metal complexes and ligands have been characterized by molar conductance, element analysis, melting point, FT-IR, ^{1}H-NMR, TGA, and XRD analysis, moreover screened the pathogenic organisms *Bacillus subtilis*, *Staplococcusaureus* (as gram positive bacteria), *Escherichia coli* (as gram negative bacteria) and *Candida tropicalis* and *Aspergillusniger* (as fungi species) were compared to known antibiotics amoxicillin. The complexes are more potent than ligands as antimicrobial and antioxidant agent.The Ce(III) have eight coordinated number forming bicapped octahedral geometries. about it each complexes, as shown in Fig. (1-18)

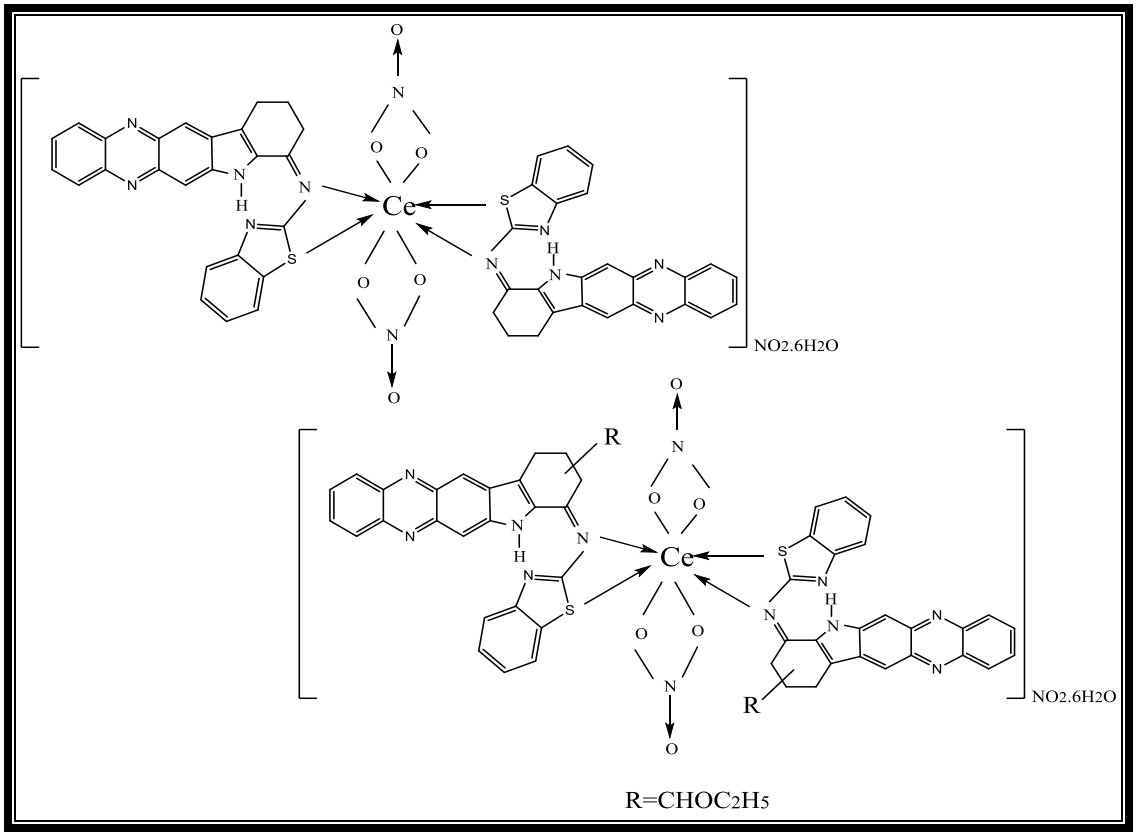

Fig. (1-18): Structure of $[Ce(L^1)_2(NO_3)_2]NO_3.6H_2O$ and $[Ce(L^2)_2(NO_3)_2]NO_3.6H_2O$.

In 2018 A. Palanimurugan and A. Kulandaisamy [76] Synthesized newly Schiff base from salicylalidene-4-imino-2,3-dimethyl-1-phenyl-3-pyrazolin-5-one and 2-aminothiazole and its complexes with VO(II), Co(II), Ni(II), Cu(II), and Zn(II). The prominent structural features of synthesized compounds were studied by elemental analysis, UV-Vis., FTIR, ^{1}H- NMR, ^{13}C-NMR, EPR, Fluorescence emission, Powder XRD, and FAB-Mass spectral measurements. The IR, UV-Vis, spectra and magnetic susceptibility data of the complexes ensured that they are square planar geometry except [VOL]Cl complex which exists in square pyramidal geometry and Zn(II) complex was tetrahedral structure as displayed in Scheme (1-18).

The *in-vitro* antimicrobial activities of the investigated compounds were tested against bacterial and fungal strains by well diffusion method. The minimum inhibitory concentration (MIC) values suggest that metal chelates have higher activity than the free ligand. The Schiff base and its complexes have been tested for the anticancer effect towards the human breast cancer.

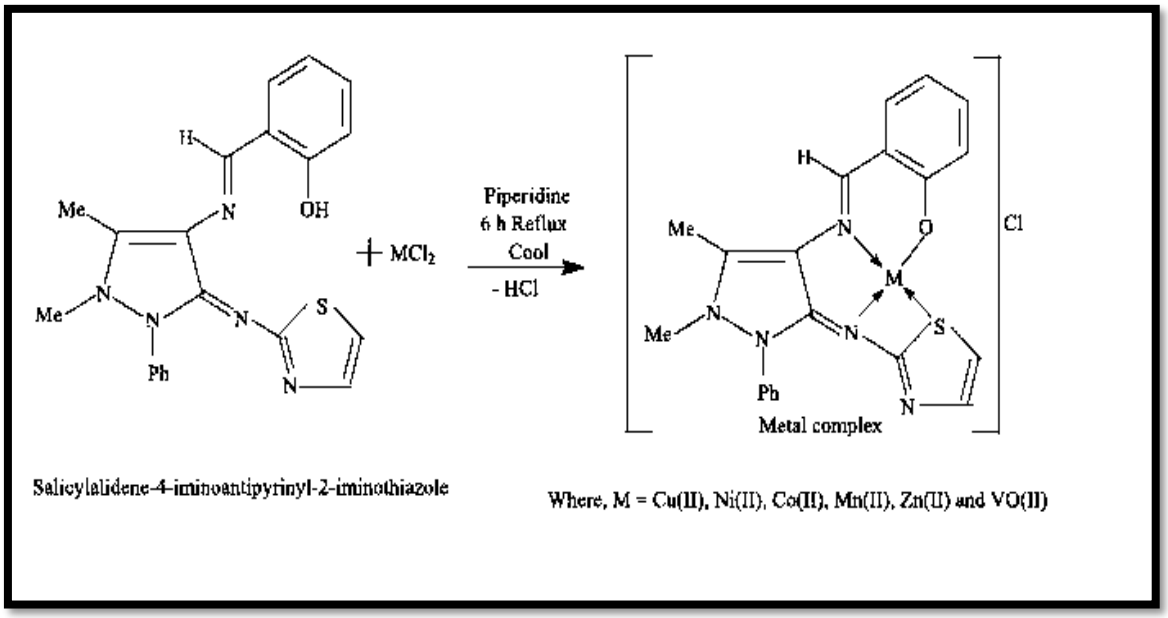

Scheme (1-18): Synthesis route of Cu(II), Co(II), Ni(II), VO(II) and Zn(II) complexes.

(1.9) Uses and applications of (N, O) type ligands and their complexes:

Compounds with (N , O) donor atoms played an important role in many fields like industry , biology and analytical chemistry .

(1.9.1) Applications in industry:

The complexes containing (N,O) donor atoms played an important role in industry, manganese complexes which containing (N,O) used as a catalytic agent in epoxidation of olefins in presence of benzene iodide as oxidation agent[77].

Schiff bases ligands play a major role in the industrial field as rubber accelerators, antioxidant and corrosion inhibitors [78]. The mixture of Schiff bases ligands used with transmission metal as pixie to the gasoline and polymer [79]. 4-aminoantipyrine (4-AAP) was tested as a corrosion inhibitor for mild steel in (2M) HCl solution using different techniques: weight loss, potentiodynamic polarization and electrochemical impedance spectroscopy (EIS). There sults showed that 4-AAP is an inhibitor for mild steel in this medium [80] . In 2012 Acha U. Ezeoke and co-workers [81] reported the study of the inhibitive effect of 4-Aminoantipyrine (4-AAP) on the corrosion of mild steel in (0.5 M) H_2SO_4 solution at (303 – 323) K by weight loss measurement as well as computational techniques. Results obtained showed that 4-aminoantipyrine (4-AAP) is a good inhibitor for the corrosion of mild steel in sulphuric acid solution. In 2014 I. Danaeea and co-workers [82]have been studied the corrosion of Schiff bases containing 2-Aminobenzothiazole in different acid concentrations of H_2SO_4 Solution , inhibitor concentration and temperatures. Corrosion increases with the concentration of acid and the temperature. Inhibition

efficiency (I.E.) of 2-Aminobenzothiazole increases with the concentration of inhibitor and decreases with the increase in concentration of acid. As temperature increases, percentage of inhibition decreases.

(1.9.2) Applications in biochemistry:

Due to the facts that antipyrine derivatives and benzothiazole derivatives, are stable and useful intermediates for the synthesis of the new substrates and precursors of substances with biological activities, interest in studying these compounds has been continued [83,84]. In bio-functional compound aspects, broad properties of this nucleus such as: antimicrobial [85], anticancer [86] analgesliced [87] and optoelectronic material aspects [88]. Schiff bases represent important class of compounds in medical and pharmaceutical and field [89]. Schiff bases transitions metal complexes are one of the most adjustable and totally studied systems, these complexes have applications in clinical field [90]. Some of these complexes play important role in biological oxygen carrier systems [91]. Schiff bases and their metal complexes are of growing importance in coordination chemistry, attributable to recent observations in antibacterial, antifungal and oxygen carrier properties. The investigation of structure and bonding of Schiff base complexes help understand the complexes.

In 2007 Banerjee and co-workers [92] reported the reactivity and the importance of Zn(II) complex with 4-methyl-2,6-bis(((phenyl methyl)imino) methyl)phenol (HL) type (N_2O). The importance of zinc in the biological domain primarily lies in the fact that it is an essential trace element acting as a structural component of proteins and peptide. Its role in the catalytic site of enzymes is also well-known [93]. A topic of substantial current interest, however, stems out of the functionality of zinc in neurobiology [94]. Recent studies shows that a fraction of Zn(II) hase

been found in free or chelatable form in some organs for example: brain [95], pancreas [96] and spermatozoa [97].

(1.9.3) Applications in analytical chemistry:

In analytical chemistry field, Schiff bases have been used in qualitative and quantitative analysis because they form colored complexes with transition metals in most cases [98]. Furthermore, Schiff bases were used as reagent in extraction process of both U(VI) and Th (VI) [99]. In the electric uses field, they used in membrane electrodes industry [100], also in materials of medical imaging and radiation therapy [101]. Besides to control systems and in electrochemical sensitive apparatus, as well as used in various chromatographic methods, which they measure the selectivity and sensitivity [102]. Also Schiff bases and their transition metal complexes have the ability to appear the phases of liquid crystalline which molecules are taking several geometrical structures, these compounds so called metallomesogens[103] . In addition, these compounds give two types of geometrical isomers (cis and trans) as a result for irradiation energy of these materials, which occurs electronic transition, lead to several changes in the structure of the molecule, also Schiff bases used in mineral extraction [104]. Furthermore, complexes of Schiff bases with Cr(III) were synthesized and used as selection catalysts for opening azirdin cycles in organic synthesis. As well, they used as catalysts in the additive reactions (Diels-alder [105].

(1.10) The aim of the work

It's well documented that Schiff base ligands and their complexes have several applications in medicine, industry, biochemistry. Due to these facts. The aim of this work could be summarised:

- Synthesis of three ligands two from type (N , N) and one from type(N , O), including mebendazol, 2-aminobenzothiazole, 2-Amino-6-methoxy benzothiazole and 4-aminoantipyrine.
- Synthesis of metal complexes of these ligands with some metal ions: VO(II), Mn(II), Co(II), Ni(II), Cu(II), Zn(II), Cd(II) and Hg(II).
- Characterization of the structure for all synthesized compounds using melting point and different spectroscopic techniques (FT-IR, UV-Vis, Mass, A.A, ^{1}HNMR and ^{13}CNMR) along with molar conductance, magnetic susceptibility, elemental microanalysis (C.H.N), chloride content and thermogravimetric.
- Study the stereochemistry and the possible structures of the prepared compounds.
- Screened the anti-bacterial activity of the synthesised compounds against two bacterial strains (*Escherichia coli and Staphylococcus aureus*) and Fungi activity against one type of fungi (*Candida albican*s).

Chapter Two

Experimental Part

(2) Experimental:

(2.1) Chemicals:

The Chemicals used in this work and their supplies are tabulated in Table (2-1). All these chemicals were used without further purification.

Table (2-1) Chemicals used in this work and their suppliers.

Materials	Formula	Company source of supply	Purity %
Acetone	C_3H_6O	Merck	99
4-Aminoantipyrine	$C_{11}H_{12}N_3O$	Fluka	99
2-Aminobenzothiazole	$C_7H_6N_2S$	Sigma- Aldrich	98
2-Amino-6-methoxy benzothiazole	$C_8H_8N_2OS$	Sigma- Aldrich	98
Benzene	C_6H_6	Merck	99
Chloroform	$CHCl_3$	Merck	99
Dimethyl formamide (DMF)	C_3H_7NO	Fluka	99
Dimethyl sulfoxide (DMSO)	$(CH_3)_2SO$	Fluka	99
Ethanol	C_2H_5OH	Sigma- Aldrich	99.8
Hydrobromic acide	HBr (48%)	SCR	99
Mebendazole	$C_{16}H_{13}N_3O_3$	Sigma- Aldrich	98
Methanol	CH_3OH	Sigma- Aldrich	98
Cadmium (II) chloride	$CdCl_2$	B.D.H	98
Cobalt (II) chloride hexahydrate	$CoCl_2.6H_2O$	Merck	99
Copper (II) chloride dihydrate	$CuCl_2.2H_2O$	Fluka	99
Manganis(II)chloride tetrahydrate	$MnCl_2.4H_2O$	B.D.H	99
Mercury (II) chloride	$HgCl_2$	B.D.H	99
Nickel (II) chloride hexahydrate	$NiCl_2.6H_2O$	Fluka	99

Vanadyl(II) sulfate monohydrate	$VOSO_4.H_2O$	Riedel-De Haen	98
Zinc (II) chloride	$ZnCl_2$	Fluka	99.9

(2.2) Instruments:

The following measurements were used to characterize synthesized compounds:

(2.2.1) Melting Point Measurements:

An electrothermal apparatus Stuart Melting Point Apparatus were used to measure melting points of starting materials, ligands and their complexes in the college of education for pure sciences, Ibn-Al-Haitham / Baghdad University**.**

(2.2.2) Fourier Transform Infrared Spectra (FT-IR):

Infrared spectra for all compounds were performed using a Shimadzu (FT–IR)–8400S spectrophotometer in the range (4000 – 400 cm^{-1}). Spectra were recoded as potassium bromide discs at Ibn-sina Company and the FT-IR spectra were obtained as KBr discs using a Biotic 600 FT-IR spectrophotometer in the range 4000-400 cm^{-1}. Spectra were recorded as potassium bromide at College of Education for Pure Science (Ibn Al-Haitham), Baghdad University.

(2.2.3) Conductivity Measurements:

Electrical conductivity measurement of the complexes were recorded at (25˚C) for 10^{-3} mole. L^{-1} solution of the samples in dimethylsulphoxide using a Jenway Ltd. 4071 digital conductivity meter in the College of Education for Pure Sciences, Ibn-AL-Haitham / Baghdad University**.**

(2.3.4) Electronicspectra:

The electronic spectra of new ligands and their complexes were obtained using a (UV-Vis.) Spectrophotometer type Shimadzu, (160A) in the range (200-1000) nm, using quartz cell of (1.0) cm length and concentration (10^{-3}) mole. L^{-1} by using the solvent dimethylsulphoxide, at company of Ibn-Sina.

(2.2.5) Mass Spectroscopy:

Mass spectra for new ligands were obtained by Electron Impact (EI) mass spectroscopy using Agilent Technologies Mod.5975C VL MSD. The spectra were recorded at University of Tehran, Islamic Republic of Iran**.**

(2.3.6) ^{1}H and ^{13}C-NMR Spectra:

^{1}H and ^{13}C spectra for new ligands were acquired using a Brucker-400 MHz for ^{1}HNMR and 100 MHz for ^{13}CNMR, respectively. Samples were acquired in DMSO-d_6 using TMS as an internal standard for NMR analysis. The samples were recorded at University of Tehran, Isfahan Universities, Islamic Republic of Iran.

(2.2.7) Elemental Microanalysis:

Elemental micro analysis for the ligands and their complex were performed on a (C.H.N.S.) Euro EA 3000 at College of Education for pure sciences/ Ibn- AL- Haitham, Baghdad, Iraq.

(2.2.8) Metal Analysis :

Metal content for all complexes were measured using a Shimadzu atomic absorption spectrophotometer (F.A.A) 680G in Ibn Sina Company, Ministry of Industry Baghdad, Iraq.

(2.2.9) Chloride Content:

Potentiometric titration method was used to determine chloride content for complexes using a 686-titro processor-665 Dosimat-Metrohm Swiss. Samples were recorded in Ibn Sina Company, Ministry of Industry, Baghdad, Iraq.

(2.2.10) Magnetic Moment Measurement:

Magnetic moments determined with Magnetic Susceptibility Balance Mode (MSB – MKI) and at laboratory temperature, the Faraday Method was used to measure the magnetic sensitivity of the complex. Samples were recorded at College of Science, Al-Mustansiriyah University.

(2.2.11) Thermal Gravimetric Analysis

Thermogravimetric analysis for some complexes was carried out using a STA PT-1000 Linseis company /Germany. The measurement was conducted under argon atmosphere at a heating rate 10 ºC/min. Samples were recorded at College of Education for Pure Science (Ibn Al-Haitham), Baghdad University.

(2.2.12) Proposed molecular structure:

The proposed molecular structure of the complexes were determined using Chem. Office 2016, 3DX Program.

(2.2.13) Biological Activities

The evaluation of starting materials, ligands and their metal complexes against two bacterial strains *(Escherichia coli (G-) and Staphylococcus aureus (G+))* and one fungi species (*Candida albican*s) were performed using agar-well diffusion. In this method, the wells were dug in the media with the help of a sterile metallic borer with centres at least 6 mm. Recommended concentration (100 μL) of the test sample 1 mg/mL in DMSO was introduced in the respective wells. The plates were incubated immediately at 37 ºC for 24h. Activity was evaluated by measuring the diameter of inhibition zones (mm). The samples were recorded at College of Education for Pure Science (Ibn Al-Haitham), Baghdad University.

(2.3) Synthesis of Ligands [L^1 , L^2 , L^3] [106]:

(2.3.1) Synthesis of Ligand [L^1]:

The Schiff base ligand was synthesized by condensation of solution of (2-amino-6-methoxybenzothaiazole) [0.180g ,1mmole] in (10 mL ethanol) with a solution of (mebndazole) [0.295g ,1 mmole] in (10 mL ethanol) and 3drops of HBr 48%. The mixture was refluxed for (30 hrs.) with stirring. The yellow colored solid mass formed during refluxing was cooled to room temperature, filtered and washed with ethanol and recrystallized by (aceton) to get a pure sample. Yield 82%, m.P.: 265-267 ^oC, M.wt : 457.51 g/mol ($C_{24}H_{19}N_5O_3S$) . As displayed in Scheme (2-1).

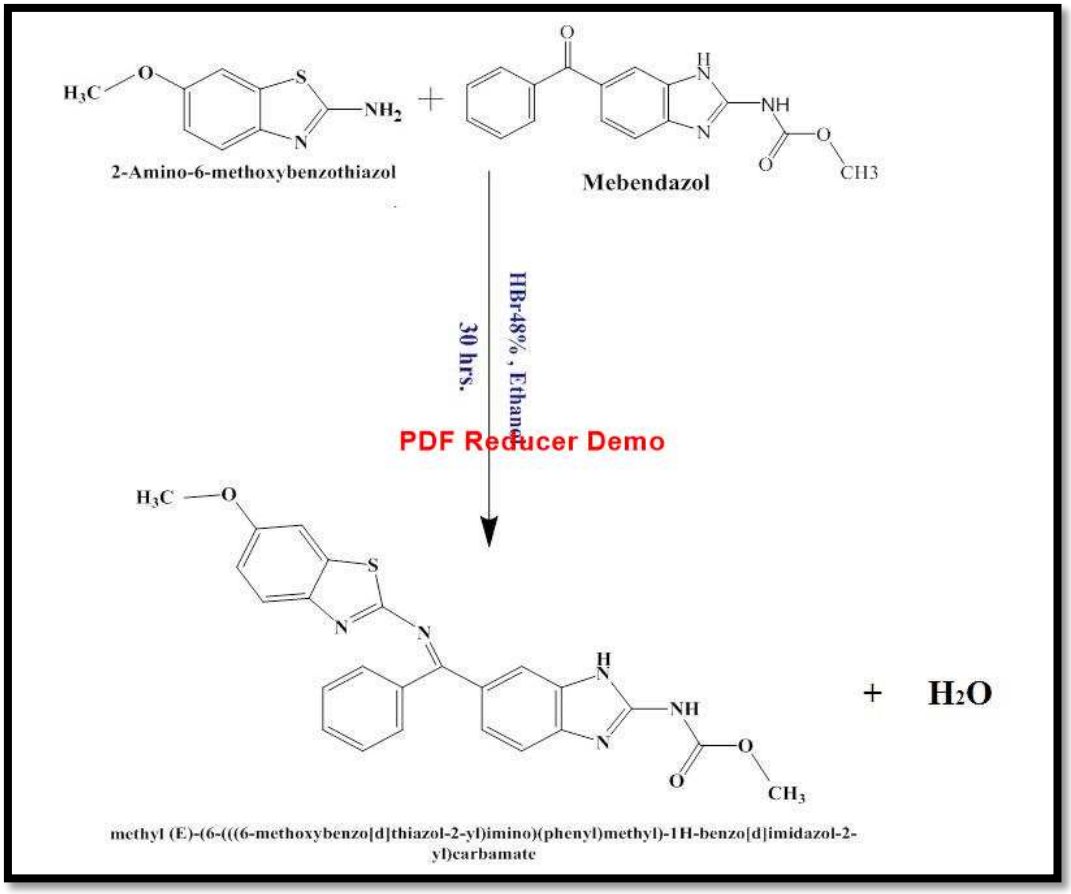

Scheme (2-1): synthesis route of the ligand [L^1].

(2.3.2) Synthesis of ligand [L^2]:

A solution of (2-aminobenzothaiazole) [0.150g ,1mmole] in (10mL ethanol) was added to a solution of (mebndazole) [0.295g ,1 mmole] in (10mL ethanol) and 3drops of HBr 48%. The mixture was refluxed for (30 hrs.) with stirring. The yellow colored solid mass formed during refluxing was cooled to room temperature, filtered and washed by ethanol and recrystallized by (aceton) to get a pure sample. Yield 84%, m.P.: 243-245 ^oC , M.wt : 427.48 g/mol ($C_{23}H_{17}N_5O_2S$) . As depicted in Scheme (2-2).

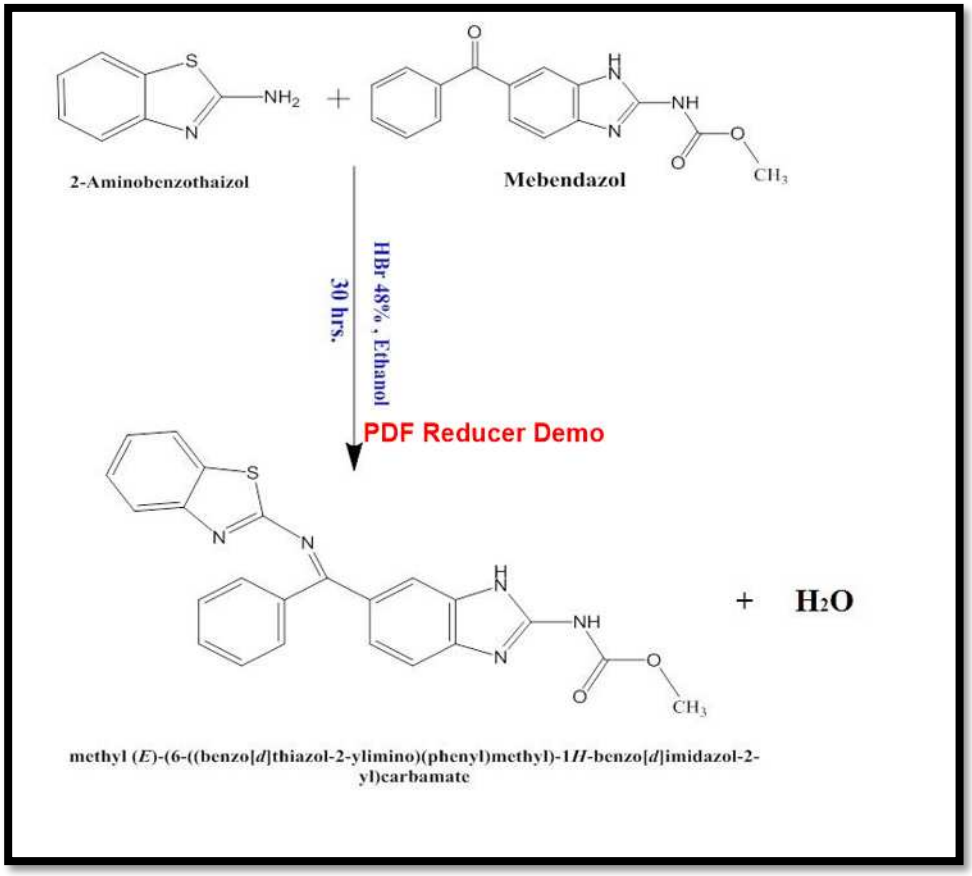

Scheme (2-2): synthesis route of the ligand [L^2]

(2.3.3) Synthesis of ligand (L^3):

A solution of (4-aminoantipyrine) [0.203g ,1mmole] in (10 mL ethanol) was added to a solution of (mebndazole) [0.295g ,1 mmole] in (10 mL ethanol) and 3drops of HBr 48% . The mixture was refluxed for (30 hrs.) with stirring. The orang colored solid mass formed during refluxing was cooled to room temperature, filtered and washed by ethanol and recrystallized by (methanol) to get a pure sample. Yield 79% , m.P. : 237-239 ^oC , M.wt : 480.52 g/mol ($C_{27}H_{24}N_6O_3$) . As shown Scheme (2-3).

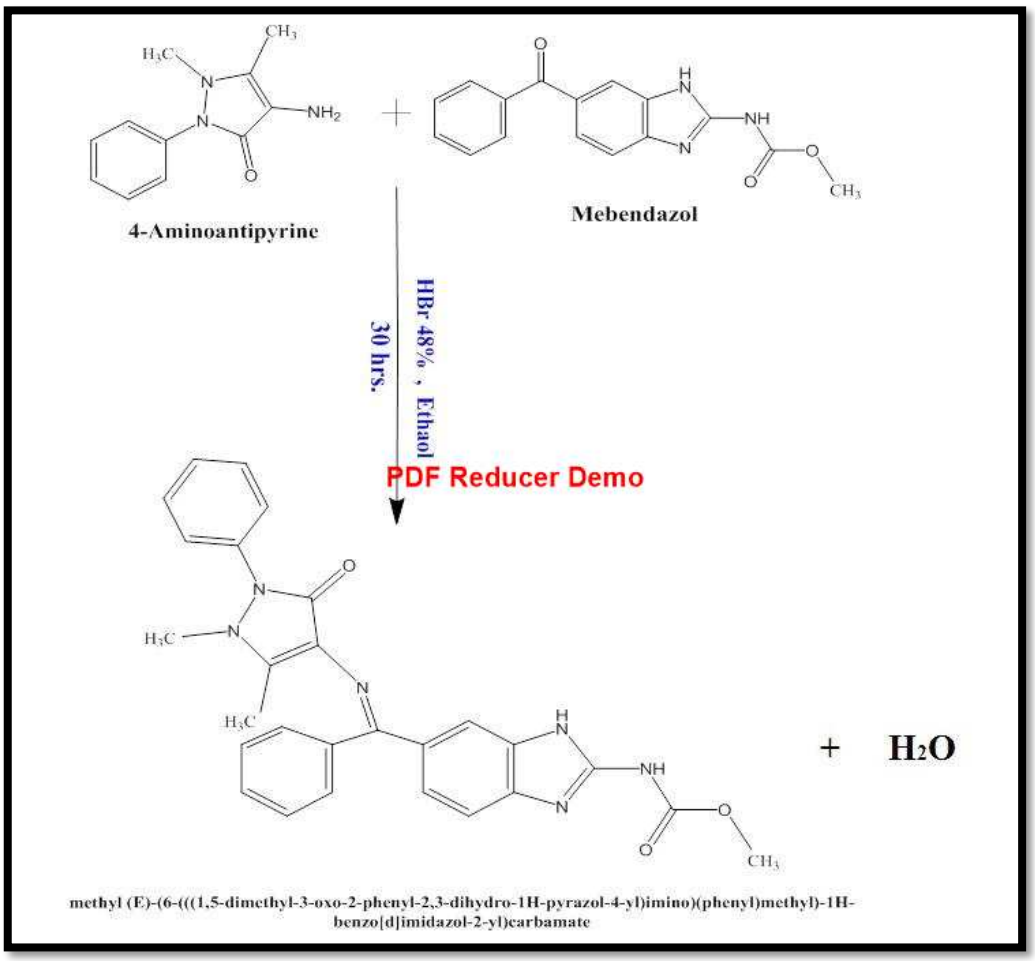

Scheme (2-3): synthesis route of the ligand [L^3].

(2.4) Synthesis of complexes [63] .

(2.4.1) Synthesis of [L^1] complexes.

(2.4.1.1) Synthesis of $[VO(L^1)_2(SO_4)].H_2O$ (1)

A solution of (0.181g, 1mmole) of Vanadyl (II) Sulfate monohydrate dissolved in (10mL) of ethanol was added drop wise to a solution of [L^1] (0.914g, 2mmole) dissolved in (15 mL) aceton. The reaction mixture was allowed to refluxed for (3 hrs.) . A light green precipitate was formed, which filtered off, washed several times with absolute ethanol and dried. Yield (81 %) of the title complex, m.p. : (259-261ºC).

(2.4.1.2) Synthesis of $[Mn(L^1)_2Cl_2].H_2O$(2) , $[Co(L^1)_2Cl_2].H_2O$ (3) ,$[Ni(L^1)_2Cl_2].H_2O$(4) , $[Cu(L^1)_2Cl_2].H_2O$(5) , $[Zn(L^1)_2Cl_2].H_2O$ (6), $[Cd(L^1)_2Cl_2].H_2O$(7) and $[Hg(L^1)_2Cl_2].H_2O$ (8) .

A similar method to that mentioned in [2.4.1.1] in synthesizing of VO(II) complex was used to synthesized the complexes of [L^1] with $MCl_2.nH_2O$ M(II)=[Mn (n=4), Co (n=6), Ni (n=6), Cu (n=2), Zn (n=0), Cd (n=0) and Hg (n=0)] ions. The physical properties of the complexes and their reactant quantity displayed in (Table 2-2).

Table (2-2): Some physical properties of the prepared ligand [L^1] complexes and their reactant quantities.

No.	Empirical Formula	Colour	m.p ºC	Wt of metal salt (1mmol.)	Yield %
1	$[VO(L^1)_2(SO_4)].H_2O$	Light green	259-261	0.181 g	81
2	$[Mn(L^1)_2Cl_2].H_2O$	Light pink	252-254	0.197g	88
3	$[Co(L^1)_2Cl_2].H_2O$	Blue	218-220	0.237 g	78

4	$[Ni(L^1)_2Cl_2].H_2O$	Green	119-121	0.237 g	79
5	$[Cu(L^1)_2Cl_2].H_2O$	Brown	125-127	0.170 g	84
6	$[Zn(L^1)_2Cl_2].H_2O$	Light yellow	219-221	0.136 g	86
7	$[Cd(L^1)_2Cl_2]. H_2O$	Light yellow	220-222	0.183g	85
8	$[Hg(L^1)_2Cl_2].H_2O$	Yellow	180-182	0.271g	87

(2.4.2) Synthesis of ligand [L^2] complexes.

(2.4.2.1) Synthesis of $[VO(L^2)_2(SO_4)]. H_2O$(9) .

A solution of (0.181g, 1mmole) of Vanadyl(II) Sulfate monohydrate dissolved in (10 mL) of ethanol was added drop wise to a solution of [L^2] (0.854g, 2mmole) dissolved in (15 mL) aceton. The reaction mixture was allowed to refluxed for (3hrs.). A green precipitate was formed, which filtered off, washed several times with absolute ethanol and dried. Yield (84 %) of the title complex, m.p.: (256-258 ºC).

(2.4.2.2) Synthesis of $[Mn(L^2)_2Cl_2].H_2O$ (10) , $[Co(L^2)_2Cl_2]$ $.H_2O$ (11) , $[Ni(L^2)_2Cl_2].H_2O$ (12) , $[Cu(L^2)_2Cl_2].H_2O$ (13) , $[Zn(L^2)_2Cl_2]$ $.H_2O$ (14) , $[Cd(L^2)_2Cl_2].H_2O$ (15) and $[Hg(L^2)_2$ $Cl_2].H_2O$ (16) .

A similar method to that mentioned in [2.4.2.1] in syntheszing of VO(II) complex was used to synthesized the complexes of [L^2] with $MCl_2.nH_2O$,M(II)=[Mn (n=4), Co (n=6), Ni (n=6), Cu (n=2), Zn (n=0), Cd (n=0) and Hg (n=0)] ions. The physical properties of the complexes and their reactant quantity displayed in (Table 2-3)

Table (2-3): Some physical properties of the prepared ligand [L^2] complexes and their reactant quantities.

No.	Empirical Formula	Colour	m.p °C	Wt of metal salt (1mmol.)	Yield %
9	$[VO(L^2)_2(SO_4)].H_2O$	Green	256-258	0.181 g	90
10	$[Mn(L^2)_2Cl_2].H_2O$	Light yellow	212-214	0.197g	87
11	$[Co(L^2)_2Cl_2].H_2O$	Blue	180-182	0.237 g	75
12	$[Ni(L^2)_2Cl_2].H_2O$	Dark green	204-206	0.237 g	81
13	$[Cu(L^2)_2Cl_2].H_2O$	Dark brown	191-193	0.170 g	89
14	$[Zn(L^2)_2Cl_2].H_2O$	Light yellow	223-225	0.136 g	78
15	$[Cd(L^2)_2Cl_2].H_2O$	Light yellow	248-250	0.183g	84
16	$[Hg(L^2)_2Cl_2].H_2O$	Yellow	203-205	0.271g	74

(2.4.3) Synthesis of ligand [L^3] complexes.

(2.4.3.1) Synthesis of $[VO(L^3)_2(SO_4)].H_2O$ (17) .

A solution of (0.181g, 1mmole) of Vanadyl(II) Sulfate monohydrate dissolved in (10 mL) of ethanol was added drop wise to a solution of [L^3] (0.960g, 2mmole) dissolved in (15 mL) methanol. The reaction mixture was allowed to reflux for (3hrs.) . A green precipitate was formed, which filtered off, washed several times with absolute ethanol and dried. Yield (79 %) of the title complex, m.p.: (198 – 200 ºC).

(2.4.3.2) Synthesis of $[Mn(L^3)(H_2O)Cl]Cl.H_2O$(18) , $[Co(L^3)_2(H_2O)Cl]Cl.H_2O$(19) , $[Ni(L^3)_2Cl]Cl.H_2O$(20) , $[Cu(L^3)_2Cl_2].H_2O$(21) , $[Zn(L^3)_2Cl_2].H_2O$(22) , $[Cd(L^3)_2Cl_2].H_2O$(23) and $[Hg(L^3)_2Cl_2].H_2O$(24) .

A similar method to that mentioned in [2.4.3.1] in synthesizing of VO(II) complex was used to synthesized the complexes of [L^3] with $MCl_2.nH_2O$ M(II)=[Mn(n=4), Co (n=6), Ni (n=6), Cu (n=2), Zn (n=0), Cd (n=0) and Hg (n=0)] ions. The physical properties of the complexes and their reactant quantity tabutated in (Table 2-4) .

Table (2-4): Some physical properties of the prepared ligand [L^3] complexes and their reactant quantities.

No.	Empirical Formula	colour	m.p °C	Wt of metal salt (1mmol.)	Yield %
17	$[VO(L^3)_2(SO_4)].H_2O$	Green	198-200	0.181 g	83
18	$[Mn(L^3)_2(H_2O)Cl]Cl.H_2O$	Light yellow	208-210	0.197g	86
19	$[Co(L^3)_2(H_2O)Cl]Cl.H_2O$	Dark green	212-214	0.237 g	78
20	$[Ni(L^3)_2Cl]Cl.H_2O$	Yellow	199-201	0.237 g	80
21	$[Cu(L^3)_2Cl_2].H_2O$	Dark brown	152-154	0.170 g	83
22	$[Zn(L^3)_2Cl_2].H_2O$	Light yellow	199-201	0.136 g	87
23	$[Cd(L^3)_2Cl_2].H_2O$	Yellow	202-204	0.183g	89
24	$[Hg(L^3)_2Cl_2].H_2O$	Yellow	246-248	0.271g	90

Chapter Three

Results&Discussion

(3) Results and discussion:

(3.1) Characterization of ligands [L^1, L^2 and L^3]:

In this study three newly Schiff base ligands were synthesized and characterization by spectroscopic methods [FT-IR , U.V-Vis, Mass spectrum ,^{1}H-NMR and ^{13}C-NMR] besides to melting point and elemental microanalysis .

(3.1.1) Solubility

The solubility of prepared ligands were tested in different solvents. the results were tabulated in Table (3-1).

Table (3-1): Solubility of prepared ligands in different solvents.

Compounds	H_2O	C_2H_5OH	CH_3OH	C_3H_6O	DMSO	DMF	C_6H_6	$CHCl_3$
[L^1]	-	÷	÷	+	+	+	-	÷
[L^2]	-	÷	÷	+	+	+	-	÷
[L^3]	-	÷	+	+	+	+	-	-

(+) soluble, (-) insoluble, (÷) sparingly

(3.1.2) Elemental microanalyses and some physical Properties:

Some physical properties of new ligands were listed in Table (3-2). Elemental microanalysis (C.H.N.S.) was in a good agreement with calculated values.

Table (3-2): Elemental microanalysis results and some physical properties for prepared ligands.

Compounds	Molecular formula	M.wt g/mol	yield %	m.p. °C	Color	found/(calc.)%			
						C	H	N	S
$[L^1]$	$C_{24}H_{19}N_5O_3S$	457.51	82	265-267	Yellow	62.79	4.10	15.12	6.80
						(62.95)	(4.15)	(15.30)	(6.99)
$[L^2]$	$C_{23}H_{17}N_5O_2S$	427.48	84	243-245	Yellow	64.48	3.73	16.00	7.20
						(64.56)	(3.98)	(16.38)	(7.49)
$[L^3]$	$C_{27}H_{24}N_6O_3$	480.52	79	237-239	Orang	66.89	4.80	17.11	-
						(67.43)	(4.99)	(17.48)	-

Calc.: calculated

(3.1.3) FT-IR spectra of ligands [L^1, L^2 and L^3] and their starting materials.

(3.1.3.1) FT-IR spectrum for Mebendazol (MBZ):

The FT-IR spectrum for (Mebendazole) was shown in Fig. (3-1) , which showed two band at wave numbers (3402) cm^{-1} and (3367) which returns to the frequency of (N-H) groups . The band at (1716)cm^{-1} refers to υ(C=O ester) and a band at the wave number (1647) cm^{-1} refers to (C=O ketonic) [54].The two bands at the wave numbers (1593) and (1523) cm^{-1} refers to υ(C=N) and υ(C=C) respectively and the band at (1091) was assigned to υ(C-O) . The band assigned at (1481) cm^{-1} refer to υ(C-N) [107]. The assignment of characteristic bands were summarised in table (3-3).

(3.1.3.2) FT-IR spectrum for 2-Amino-6-methoxy benzothaizol (AMBT):

The FT-IR spectrum for (AMBT), Fig. (3-2), exhibits two sharp bands at (3390) cm^{-1} and (3294) cm^{-1} ,which due to the $\upsilon_{asy}.NH_2$ and $\upsilon_{sy}.NH_2$ respectively . The band at (1643) cm^{-1} can be refer to δ(N-H) bending and a strong band at (1604) cm^{-1} indicates stretching frequency of (C=N) [108]. The band at (1546) cm^{-1} refers to υ (C=C)aromatic and the two bands located at (1373) cm^{-1} and (709) cm^{-1} where assigned to υ(C-N) and υ(C-S-C) respectively [109].The assignment of characteristic bands were summarised in table (3-3).

(3.1.3.3) FT-IR spectrum for ligand [L^1]:

The FT-IR spectrum for (L^1), Fig (3-3), showed a strong band at (3367) cm^{-1} attributed to υN-H frequency. The spectrum showed new band at (1633) cm^{-1} related to stretching frequency of imine group (C=N) and a band at (1611) cm^{-1} can be ascribed to the stretching of υ(C=N) group in the benzothiazole ring[110]. On the other hand a band at (1593) cm^{-1} can be refer to υ(C=N) stretching of MBZ ring[107] .The two bands at (1357) cm^{-1} and (709) cm^{-1} may be refer to υ(C-N) and υ(C-S-C) respectively[111]. The appearance of iminic band and the disappearance of carbonyl(C=O) band of MBZ in the ligand spectrum and disappearance of two bands for $\upsilon_{asy}.$ and $\upsilon_{sy}.$ of NH_2 in the ligand, confirms the formation of Schiff base ligand. The characteristic bands are summarised in table (3-3).

(3.1.3.4) FT-IR spectrum for 2-Aminobenzothaizol:

The FT-IR spectrum for (ABT), Fig. (3-4), exhibits two sharp bands at (3398) cm^{-1} and (3271) cm^{-1} due to the $\upsilon_{asy}.NH_2$ and $\upsilon_{sy}.NH_2$ respectively . The band at (1643) cm^{-1} and a strong band at (1589) refers to υ(N-H)

bending and υ(C=N) respectively [112]. The band at (1546) cm^{-1} refers to υ (C=C)aromatic, moreover, the two bands located at (1365) cm^{-1} and (717) cm^{-1} assigned to υ(C-N) and υ(C-S-C) respectively [109]. The assignment of characteristic bands is summarised in table (3-3).

(3.1.3.5) FT-IR spectrum for ligand [L^2]:

The FT-IR spectrum for (L^2),Fig (3-5), showed a band at (3367)cm^{-1}, which attributed to υNH frequency and the new band located at (1639) cm^{-1} assigned to stretching frequency of imine(C=N) .The band at (1604) which refers to υ(C=N thaizole) rings . [113]. The band at (1593) cm^{-1} can be refer to υ(C=N) stretching of MBZ[107]. The two bands at (1350) cm^{-1} and (705) cm^{-1} may be refer to υ(C-N) and υ(C-S-C) respectively [114].The appearance of iminic υ(C=N) band and the disappearance of carbonyl(C=O) band of MBZ in the ligand spectrum and disappearance of two bands for $\upsilon_{asy.}$ and $\upsilon_{sy.}$ for (NH_2) band in the ligand band in the ligand, confirms the formation of Schiff base ligand. The characteristic bands are summarised in table (3-3).

(3.1.3.6) FT-IR spectrum for 4-aminoantipyrine:

The FT-IR spectrum for (4-AAP), Fig. (3-6), exhibits two sharp bands at (3433) cm^{-1} and (3325) cm^{-1} due to the $\upsilon_{asy.}NH_2$ and $\upsilon_{sy.}NH_2$ respectively. The two bands located at (2985) cm^{-1} and (2912) cm^{-1} were assigned to υ(C-H) aro. and υ (C-H) ali. stretching frequency respectively. The strong band at (1647) cm^{-1} indicates stretching frequency of carbonyl group υ(C=O) of 4-AAP ring[8,115]. The band located at (1589) where assigned to υ (C=C). The band at (1354) cm^{-1} were assigned to υ (C-N) and the stretching frequency of υ(N-N) of five member ring appeared at (1078)

cm^{-1} [116,117]. The assignment of characteristic bands is summarised in table (3-3)

(3.1.3.7) FT-IR spectrum for ligand [L^3]:

The FT-IR spectrum for (L^3), Fig. (3-7), exhibits the strong band at (1645) cm^{-1} indicates stretching frequency of carbonyl group υ(C=O) of 4-AAP ring [118]. On the other hand, a new band at (1635) cm^1 related to stretching frequency of imine (C=N). The band at (1597) can be refer to υ(C=N) stretching of MBZ and a band at (1357) cm^{-1} was assigned to υ(C-N). The stretching frequency of υ(N-N) of five member ring appeared at (1082) [119].The appearance of iminic band and the disappearance of carbonyl(C=O) band of MBZ in the ligand spectrum and disappearance of two bands for $\upsilon_{asy.}$ and $\upsilon_{sy.}$ of NH_2 in the ligand, confirms the formation of Schiff base ligand [104]. The characteristic bands are summarised in table (3-3).

Table (3–3): FT-IR data (cm^{-1}) for the starting materials and the ligands

Compounds	$\nu_{asy}(NH_2)$ $\nu_{sy}(NH_2)$	ν(N-H) groups	ν(C-H) aro. ν(C-H) ali.	ν(C=O)	ν(C=N) imin	ν(C=N) in plane	ν(C=C) arom.
MBZ	-	3367 (w) 3402 (s)	3070 (w) 2921 (w)	1647 (s)	-	1593 (s)	1523, 1481
AMBT	3390 3294 (s)	-	3097 (w) 2978 (w)	-	-	1604 (s)	1546, 1465
ABT	3398 3271 (s)	-	3055 (w) 2904 (w)	-	-	1589 (s)	1546, 1527
4-AAP	3433 3325 (s)	-	2985 (w) 2912 (w)	1647 (s)	-	-	1589, 1492
[L^1]	-	3367 (s)	3047 (w) 2947 (w)	-	1633 (m)	1611 1593 (m)	1562, 1525
[L^2]	-	3367 (s)	3055 (w) 3020 (w)	-	1639 (m)	1604 1593 (s)	1573, 1526
[L^3]	-	3367 (s)	3032 (w) 2958 (w)	1645 (m)	1635 (m)	1597 (S)	1568, 1523

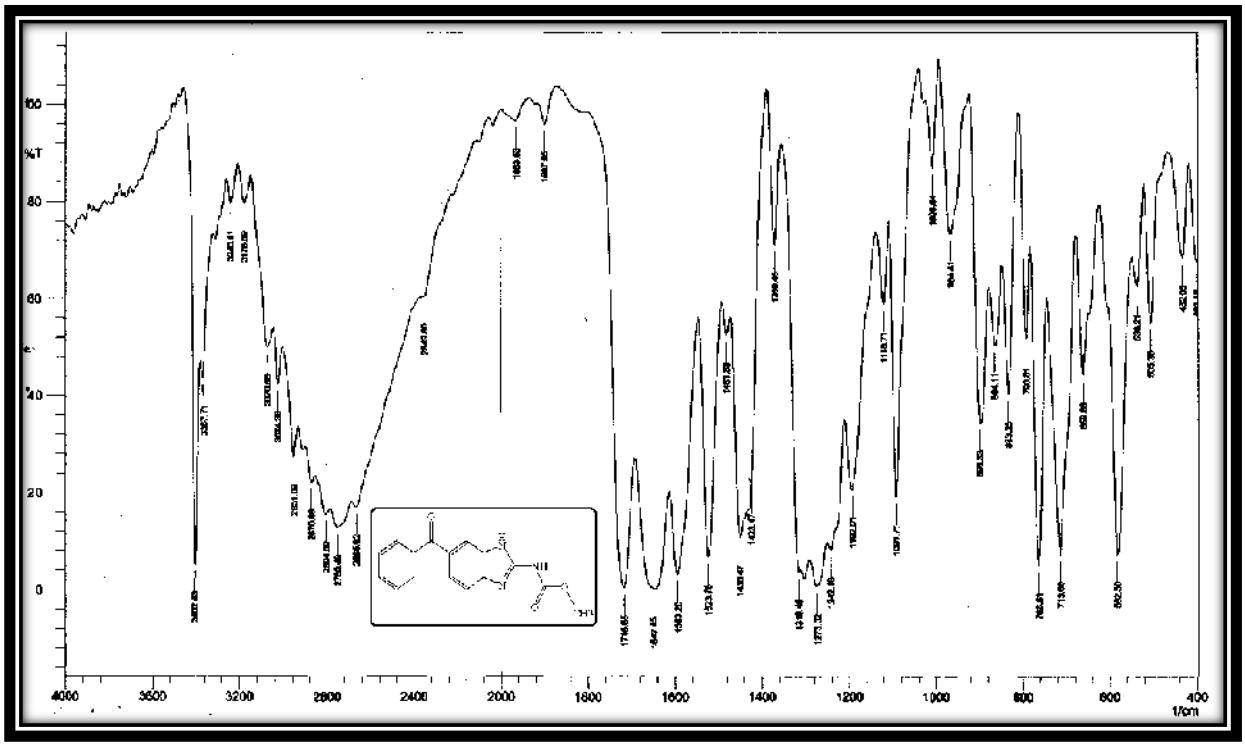

Fig. (3-1) FT-IR spectrum of the Mebendazol.

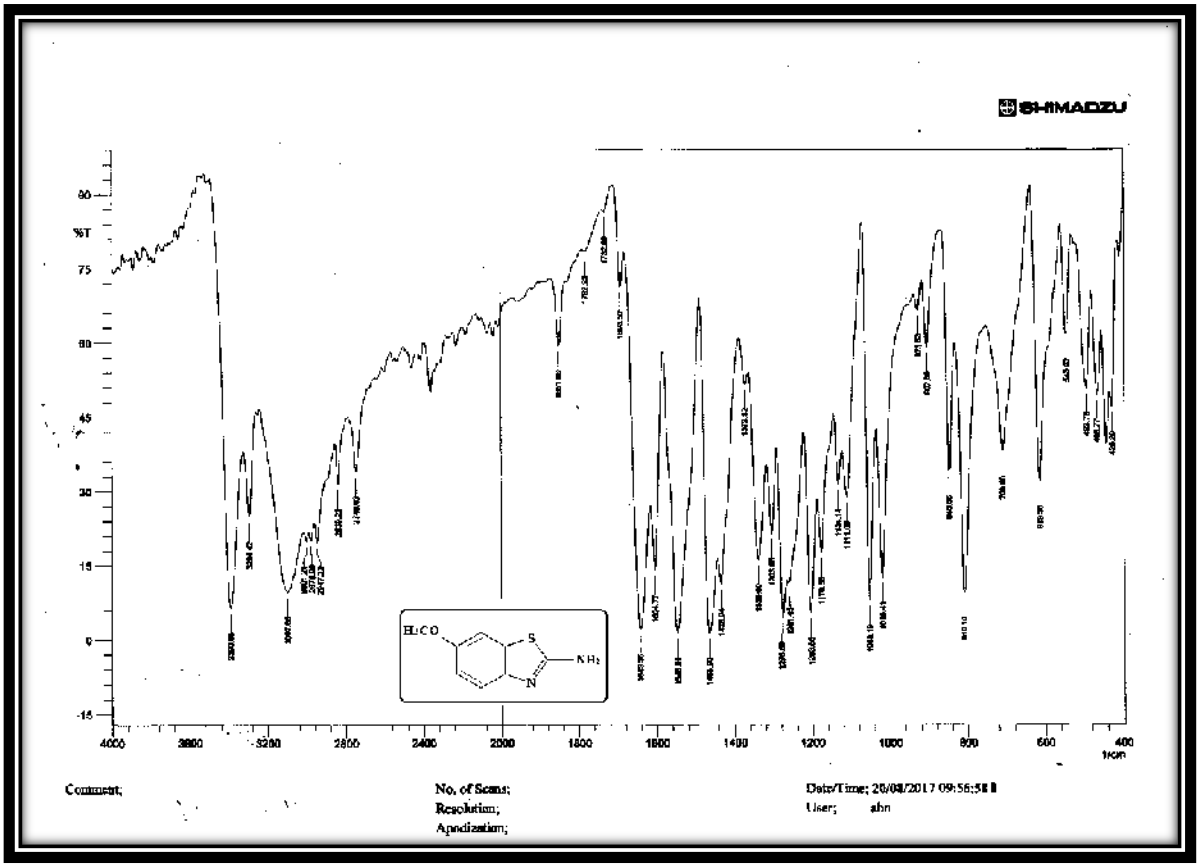

Fig. (3-2) FT-IR spectrum of the 2-amin-6-methoxyobenzothaizol.

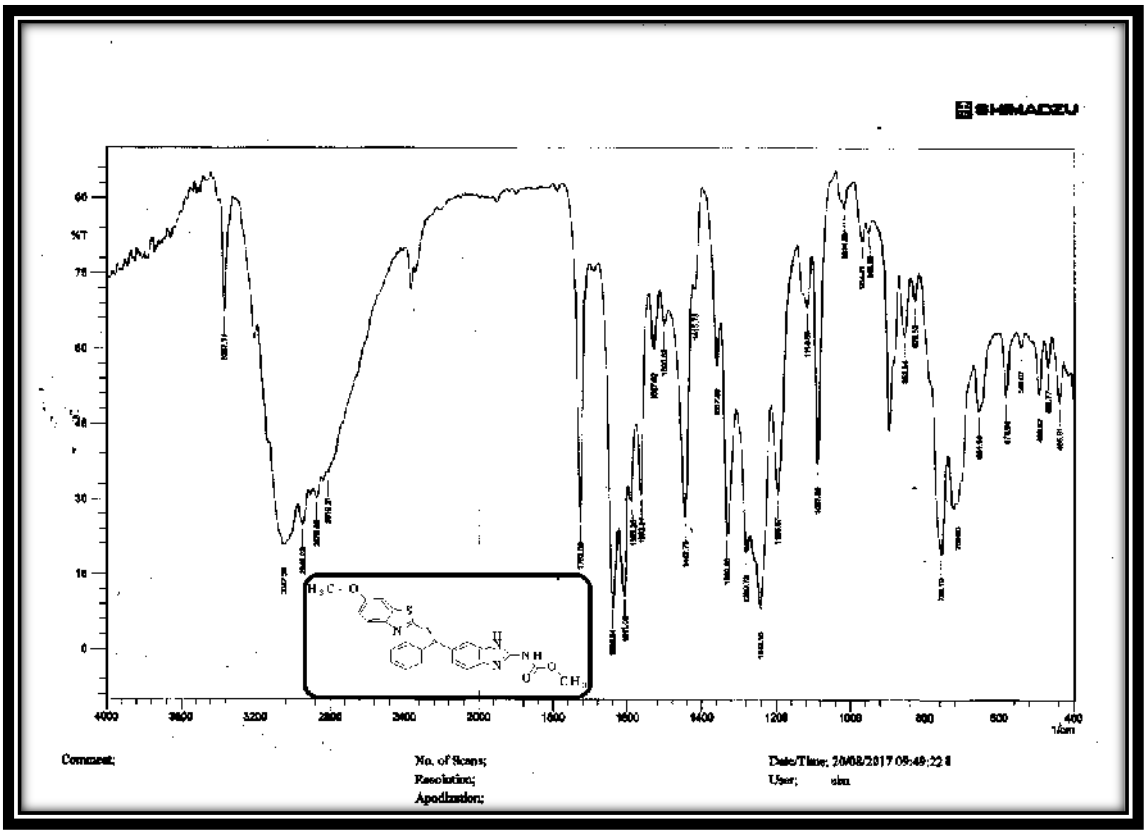

Fig. (3-3) FT-IR spectrum of the ligand [L^1].

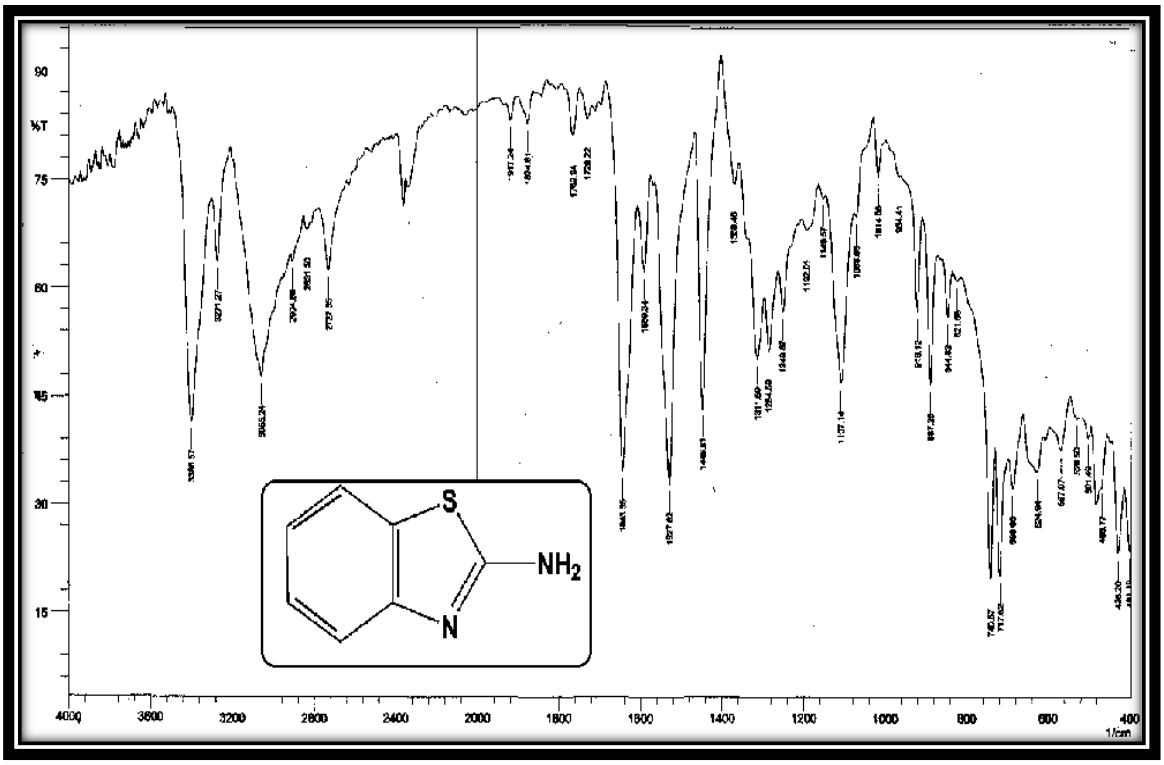

Fig. (3-4) FT-IR spectrum of the 2-aminobenzothaizol.

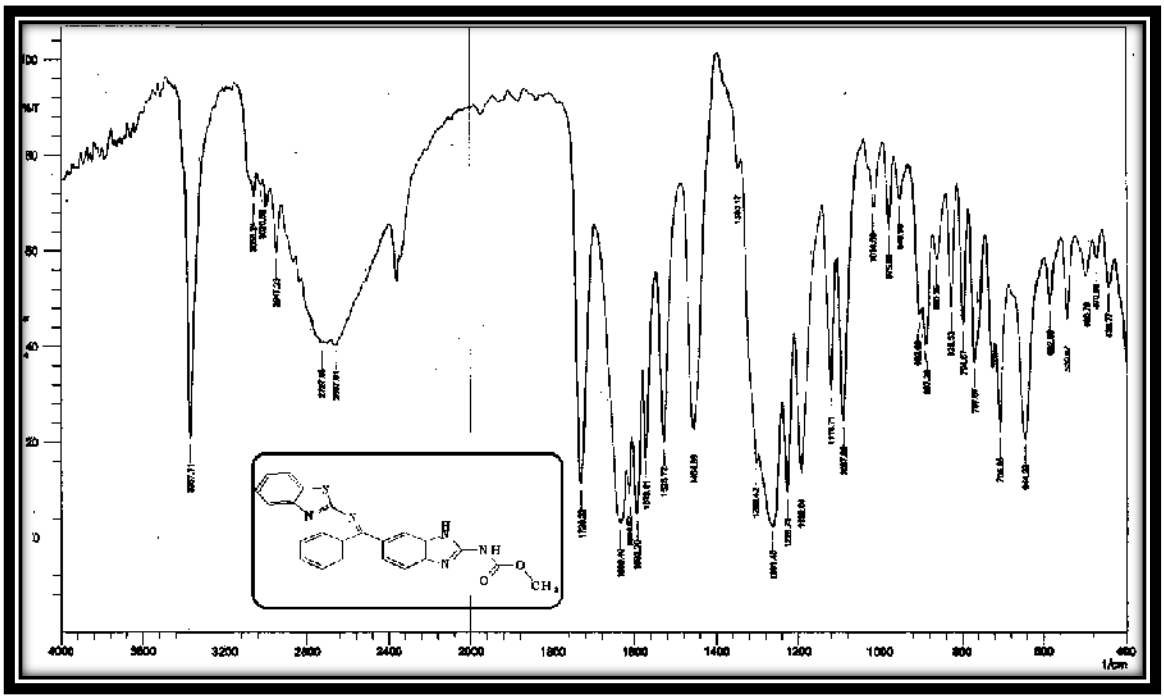

Fig. (3-5) FT-IR spectrum of the ligand [L^2].

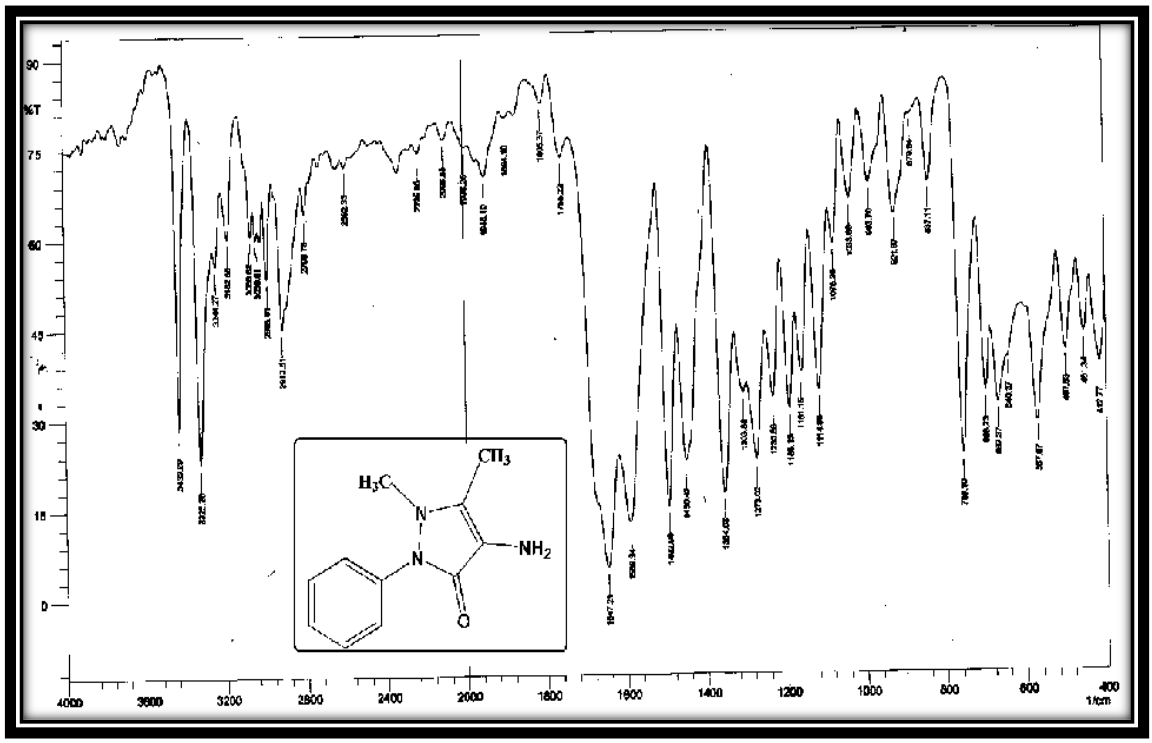

Fig. (3-6) FT-IR spectrum of the 4-aminoantipyrine.

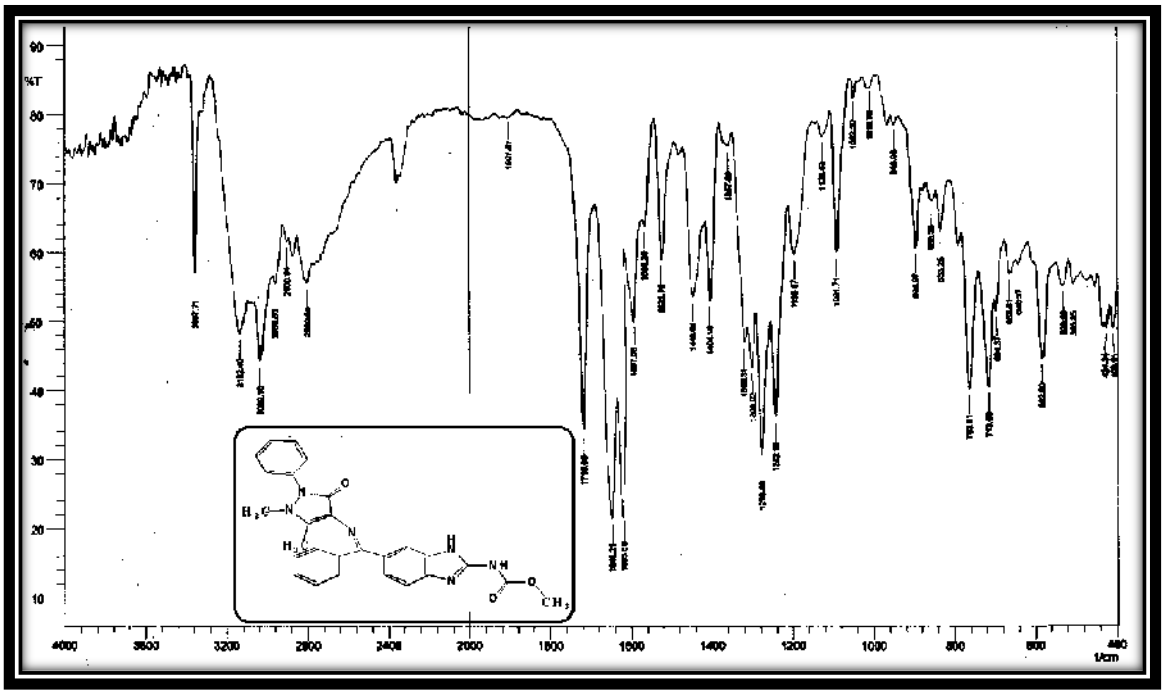

Fig. (3-7) FT-IR spectrum of the ligand [L^3].

(3.1.4) (UV. -Vis.) spectra of ligands [L^1, L^2 and L^3].

(3.1.4.1) (UV. -Vis.) spectrum of ligand [L^1].

The (UV. -Vis.) spectrum for (L^1) (Fig.(3-8)) exhibits an intense absorption peak at (267)nm (37453) cm^{-1} assigned to ($\pi \rightarrow \pi^*$) electronic transition and peak at (305) nm (32787)cm^{-1} assigned to ($\pi \rightarrow \pi^*$) electronic transition [120]. The absorption spectral data of the ligand tabulated in Table (3-4) .

(3.1.4.2) (UV. -Vis.) spectrum of ligand [L^2].

The (UV. -Vis.) spectrum for (L^2) (Fig. (3-9)) exhibits an intense absorption peak at (270) nm (37037) cm^{-1} assigned to ($\pi \rightarrow \pi^*$) electronic transition and peak at (316) nm (31646) cm^{-1} assigned to ($\pi \rightarrow \pi^*$) electronic transition [121]. The absorption spectral data of the ligand tabulated in Table (3-4).

(3.1.4.3) (UV. -Vis.) spectrum of ligand [L^3].

The (UV. -Vis.) spectrum for (L^3) Fig. (3-10) exhibits an intense absorption peak at (263) nm (38023) cm^{-1} assigned to ($\pi \rightarrow \pi^*$) electronic transition and peak at (319) nm (31348) cm^{-1} assigned to ($\pi \rightarrow \pi^*$) electronic transition [122]. The absorption spectral data of the ligand tabulated in Table (3-4).

Table (3-4): Electronic spectral data of the ligands.

Compounds	λ (nm)	υ^- (cm^{-1})	ε_{max} $molar^{-1}cm^{-1}$	Assignments
[L^1]	267	37453	3064	$\pi \rightarrow \pi^*$
	305	32787	4516	$\pi \rightarrow \pi^*$
[L^2]	270	37037	2738	$\pi \rightarrow \pi^*$
	316	31646	3592	$\pi \rightarrow \pi^*$
[L^3]	263	38023	3075	$\pi \rightarrow \pi^*$
	319	31348	3320	$\pi \rightarrow \pi^*$

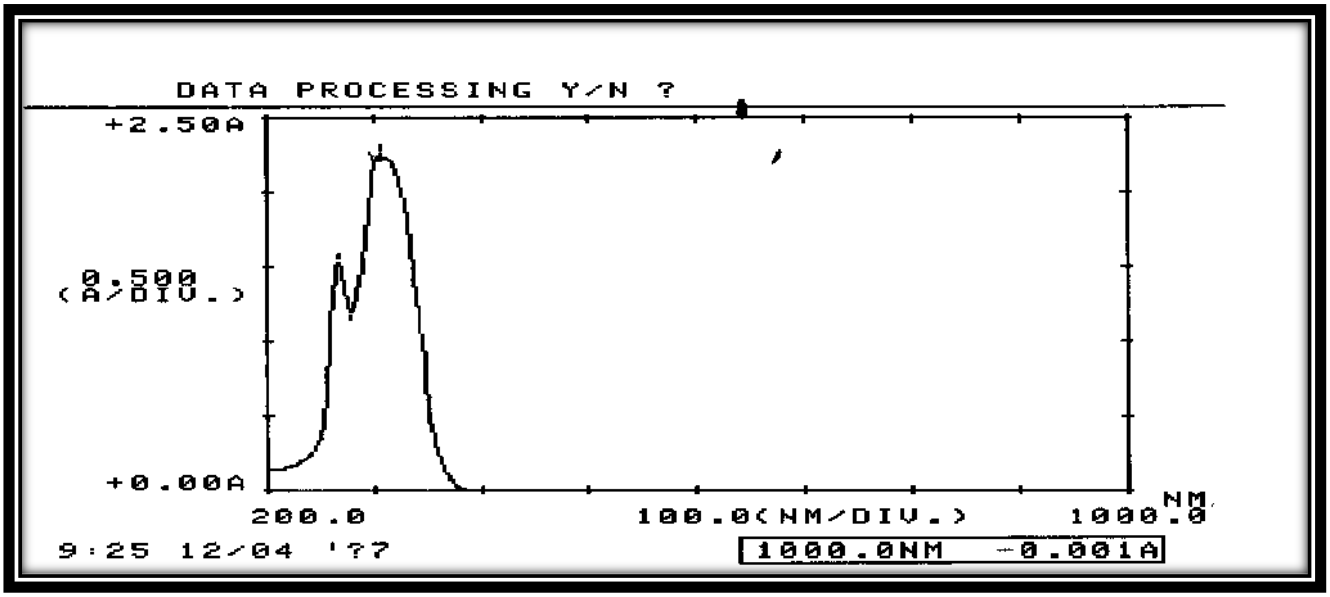

Fig.(3-8): Electronic spectrum of ligand [L^1].

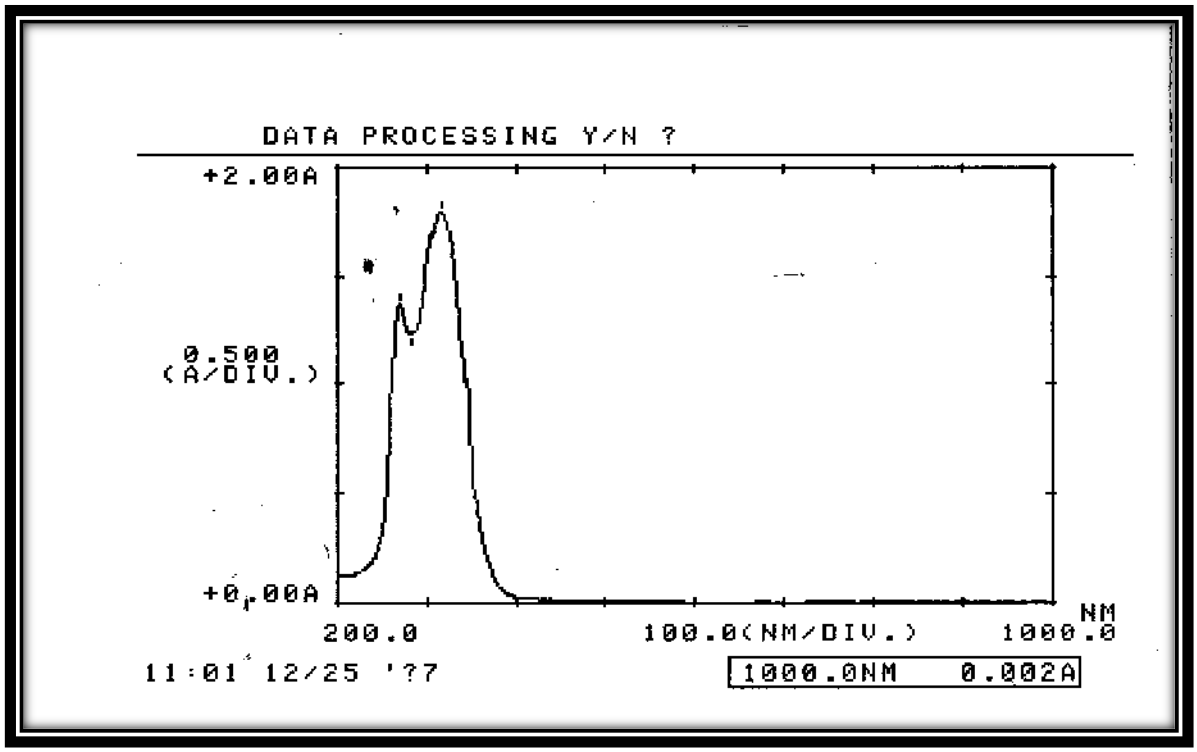

Fig. (3-9): Electronic spectrum of ligand [L^2].

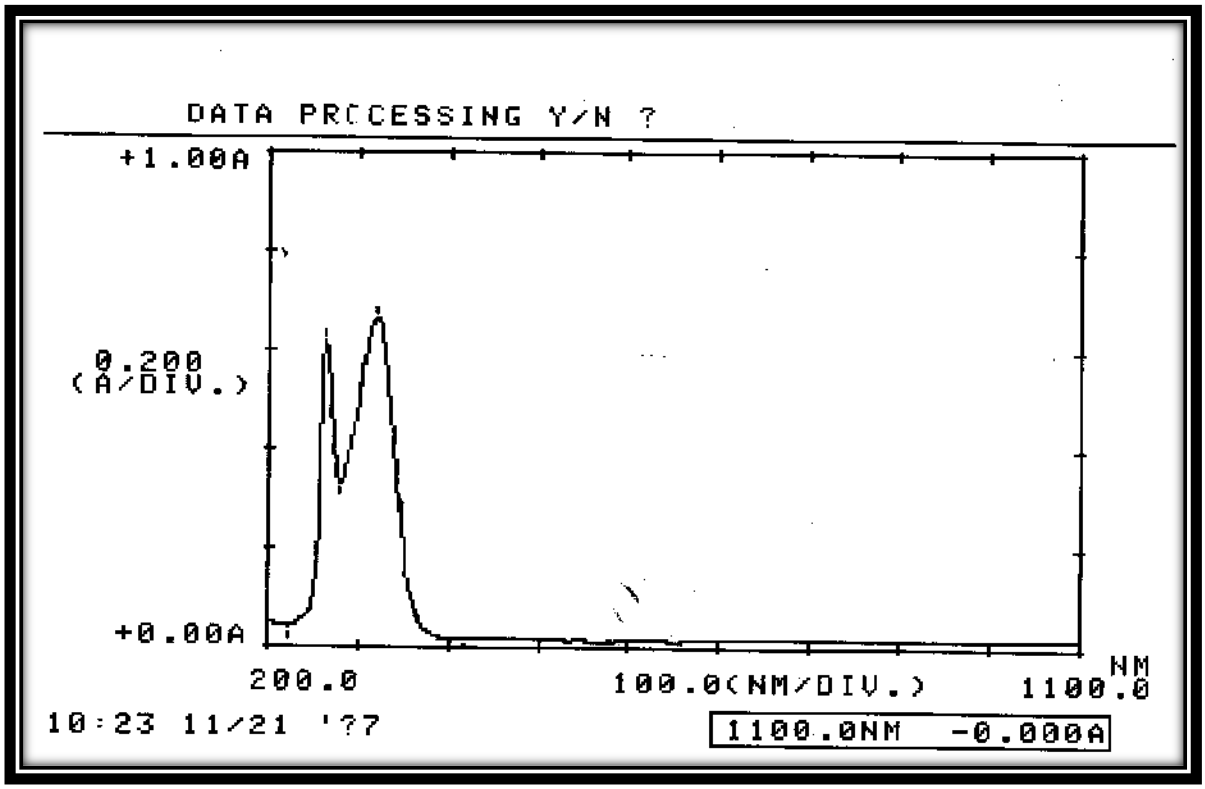

Fig. (3-10): Electronic spectrum of ligand [L^3].

(3.1.5) ^{1}H-NMR and ^{13}C-NMR spectra for ligands [L^1, L^2 and L^3].

The ^{1}H and ^{13}C correlated NMR analysis were used to characterise the ligands [L^1, L^2 and L^3]. The spectra were recorded in DMSO–d6 as a solvent.

(3.1.5.1) ^{1}H-NMR spectrum for the ligand [L^1].

In solution, it is clear that an occurs of hydrogen bonding between the hydrogen of the N-H groups and the oxygen of the Solvent. This phenomenon has been confirmed by the ^{1}H-NMR spectrum about this ligand and other ligands.

^{1}H-NMR spectrum for (L^1), (Fig. (3-11)) displayed the broad signal at (δ_H =11.73-12.45ppm, 2H) is due to the hydrogen bonding process occurred between the protons of the (N-H) groups [117] and the lon pairs of oxygen atom of solvent. The broadness of these signals could be related to hydrogen bonding (N–H…...O) [117]. The resonances at chemical shift (δ_H = 7.58 - 7.92 ppm) are assignable to protons of aromatic ring (Ar–CH) [59]. The appearances of these protons as a multi are due to mutual coupling. The signal at chemical shift (δ_H = 3.84 ppm) was attributed to protons of (OCH_3). The signal at chemical shift (δ_H =3.70 ppm) assigned to protons group (CO_2CH_3). The spectrum displayed chemical shifts at (δ_H = 2.57 ppm and 3.38 ppm) referred to DMSO, and the presence of water molecules in the solvent respectively [123]. The results are summarised in table (3-5).

Table (3-5): ^{1}H-NMR data for [L^{1}] measured in DMSO-d6 and chemical shift in ppm (δ)

Compound	Functional groups	δ (ppm)
[L^{1}]	N-H groups	(11.73-12.45)(2H,br)
	-Ar-CH	(7.58 -7.92) (11H,m)
	-OCH_3	3.84 (3H,s)
	-CO_2CH_3	3.70 (3H,s)
	HDO	3.38
	DMSO-d6 solvent	2.57

s= Singlet m=multi br= broad

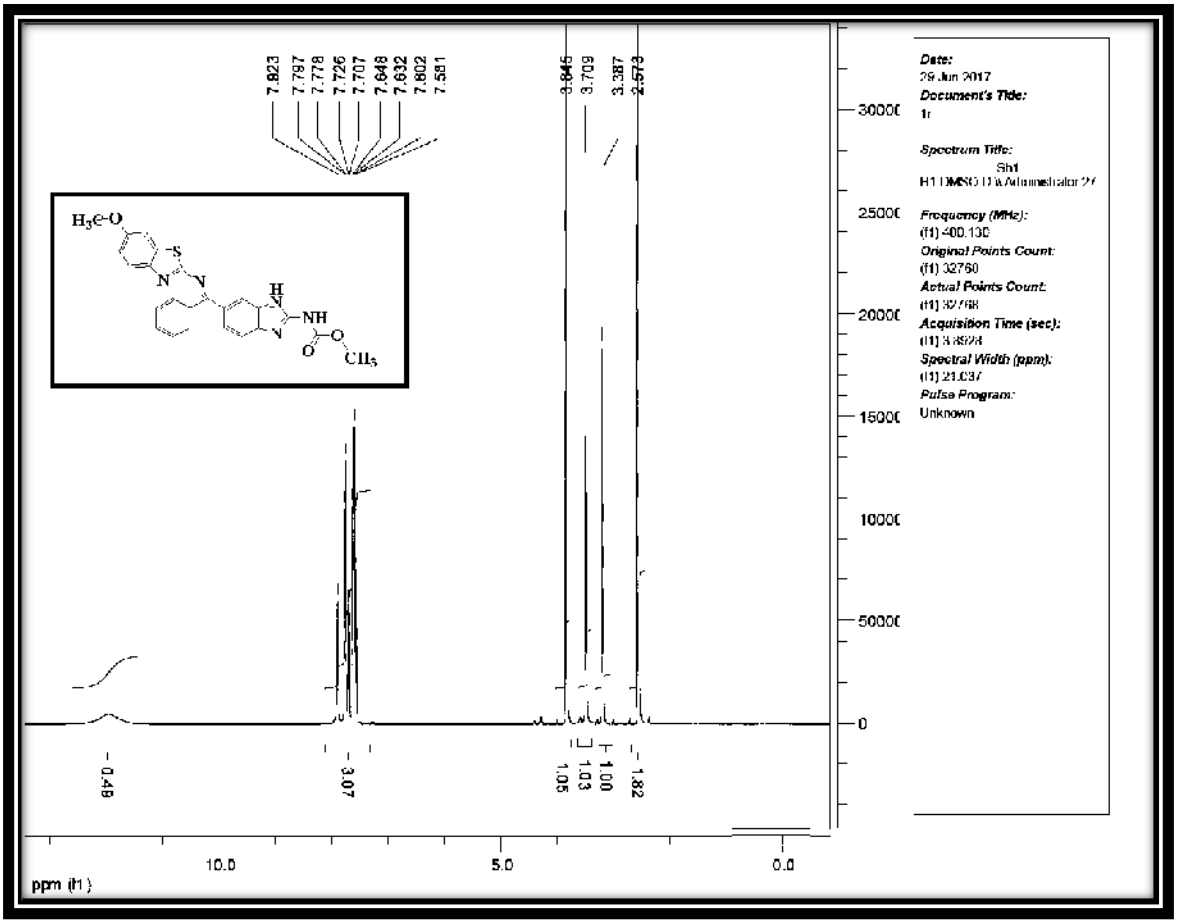

Fig. (3-11): ^{1}HNMR spectrum for [L^{1}] in DMSO-d6.

(3.1.5.2) ^{13}C-NMR spectrum for the ligand [L^1]:

The ^{13}C-NMR spectrum of (L^1), (Fig. (3-12)) solvent shows chemical shift at range (δ= 120.32-156.39 ppm) assigned to aromatic carbon atoms. The chemical shifts at (δ=179.54 ppm) attributed to the carbonyl carbon atom (C_2), while the chemical shift at (δ=153.39 ppm) attributed to the imine carbon atom (C_{10}) and carbon (C_{17}) [124]. The chemical shift at (δ=149.38ppm) attributed to the (C_3), while the chemical shifts at (δ=55.64 ppm and 52.62 ppm) assigned to methoxy group carbon atoms ($C_{24,\ 1}$) respectively [125]. The results are listed in table (3-6).

Table (3-6):^{13}C-NMR data for [L^1] measured in DMSO-d6 and chemical shift in ppm (δ)

Compound	Functional groups	δ_c (ppm)
[L^1]	Ar–C	(120.32-156.39)
	C_2	(179.57)
	$C_{10,17}$	(153.39)
	C_3	(149.38)
	$C_{24,1}$	(55.64)(52.62)

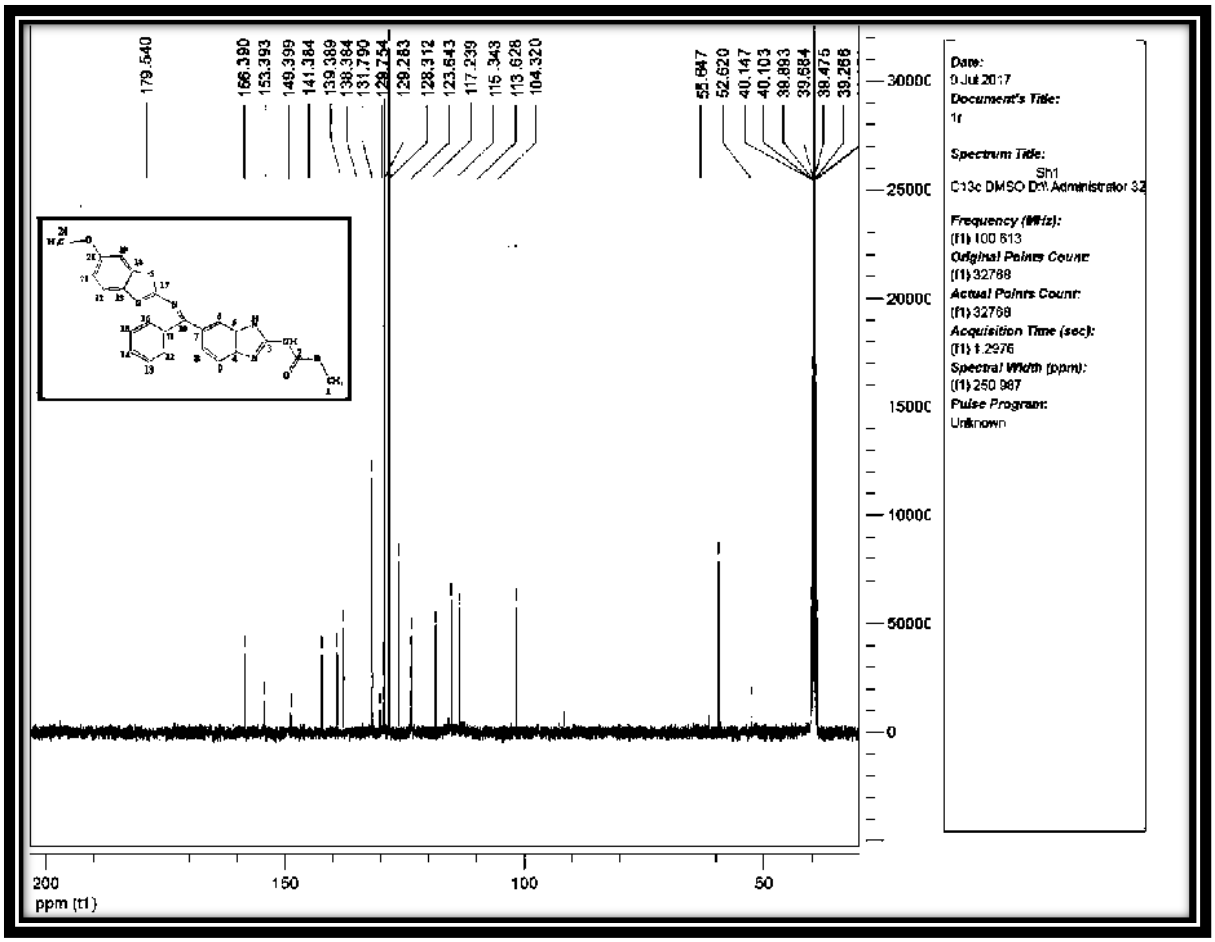

Fig.(3-12): ^{13}C-NMR spectrum for [L^1] in DMSO-d6.

(3.1.5.3) ^{1}H-NMR spectrum for the ligand [L^2]:

^{1}H-NMR spectrum for (L^2), (Fig. (3-13)) displayed broad signal at (δ_H =11.65-12.55ppm,2H) due to hydrogen bonding between the protons of the (N-H) groups [117] and the lon pairs of oxygen atoms of solvent facilities. The broadness of these signals could be related to hydrogen bonding (N–H…...O) [117]. The resonances at chemical shift (δ_H = 7.57 - 7.91ppm) (Ar–CH) are assignable to protons of aromatic ring [72]. The appearances of these protons as a multi are due to mutual coupling. Signal at chemical shift (δ_H =3.70 ppm) returns to protons group (CO_2CH_3) [126]. The spectrum displayed chemical shifts at (δ_H = 2.56 ppm and 3.39 ppm)

referred to the DMSO mentioned earlier. The results are summarised in table (3-7).

Table (3-7):^{1}H-NMR data for [L^2] measured in DMSO-d6 and chemical shift in ppm (δ)

Compound	Functional groups	δ (ppm)
[L^2]	N-H groups	(11.65-12.55) (2H,br)
	-Ar-CH	(7.57-7.91) (12H,m)
	$-CO_2CH_3$	3.70 (3H,s)
	HDO	3.39
	DMSO-d6 solvent	2.56

s= Singlet m=multi br= broad

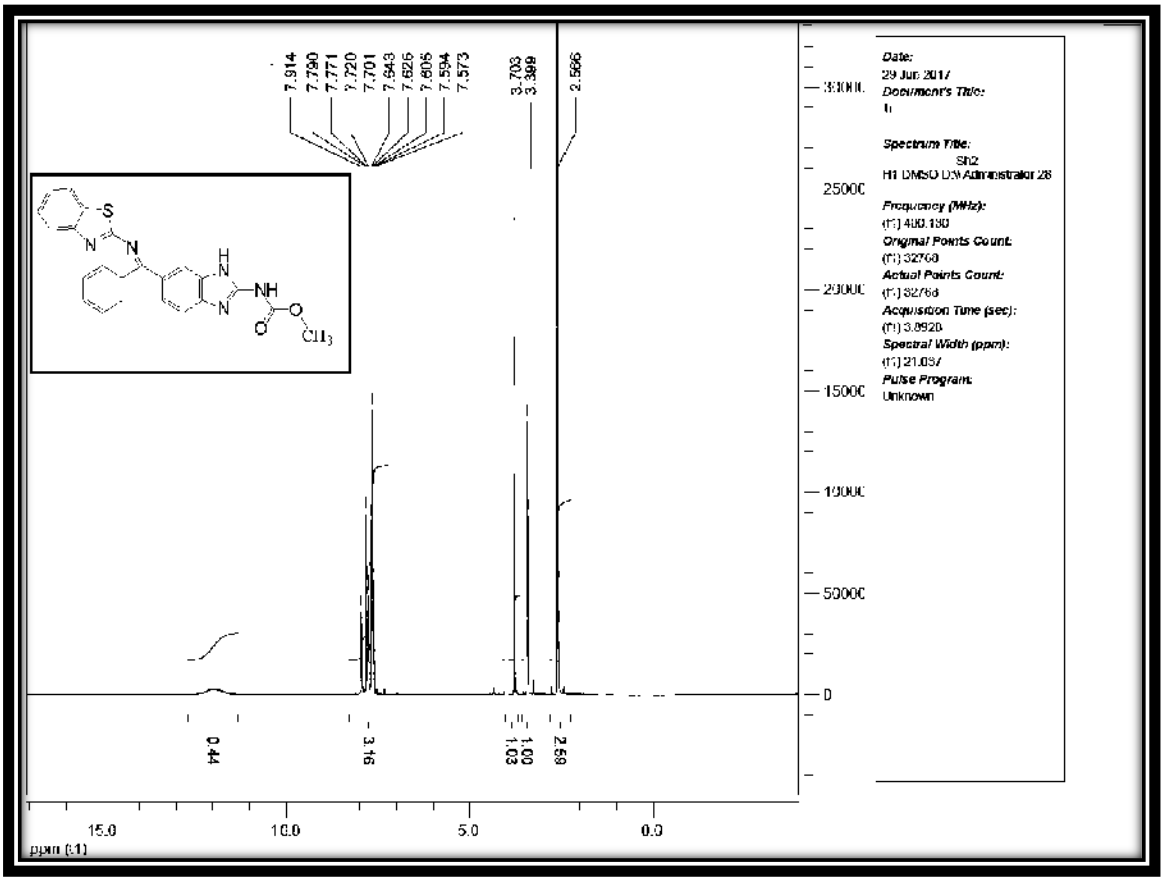

Fig.(3-13): ^{1}H-NMR spectrum for [L^2] in DMSO-d6.

(3.1.5.4) ^{13}C-NMR spectrum for the ligand [L^2]:

The ^{13}C-NMR spectrum of (L^2), (Fig.(3-14)) solvent shows chemical shift at range (δ= 115.65-149.39 ppm) assigned to aromatic carbon atoms [62]. The chemical shifts at (δ=174.57 ppm) attributed to the carbonyl carbon atom (C_2), while the chemical shift at (δ=154.40 ppm) attributed to the imine carbon atom (C_{10}) and carbon (C_{17}). The chemical shift at (δ=147.32 ppm) attributed to the (C_3), while the chemical shifts at (δ= 52.62 ppm) assigned to methoxy group carbon atom (C_1) [127]. The results are listed in table (3-8).

Table (3-8):^{13}C-NMR data for [L^2] measured in DMSO-d6 and chemical shift in ppm (δ)

Compound	Functional groups	δ_c (ppm)
[L^2]	Ar–C	(115.65-149.39)
	C_2	(174.57)
	$C_{10,17}$	(154.40)
	C_3	(147.32)
	C_1	(52.62)

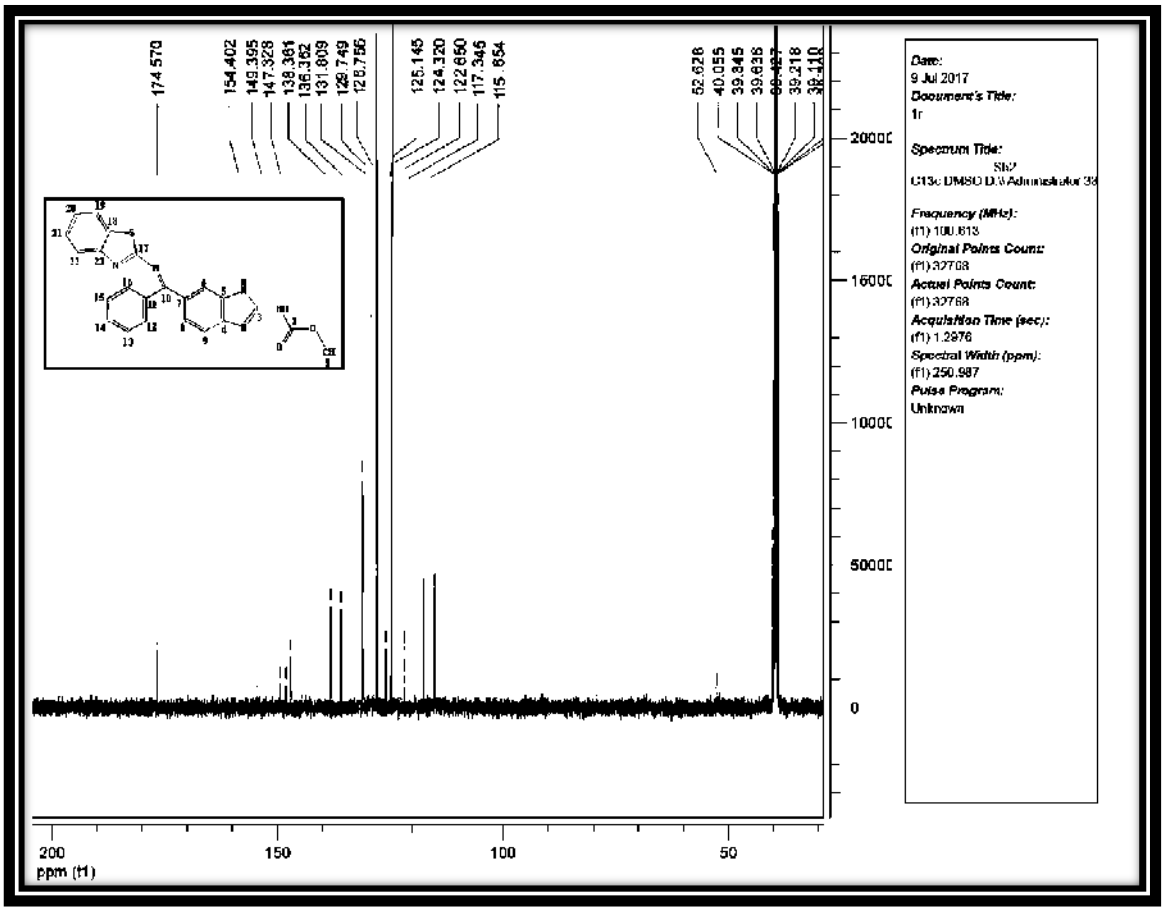

Fig.(3-14): ^{13}C-NMR spectrum for [L^2] in DMSO-d6.

(3.1.5.5) ^{1}H-NMR spectrum for the ligand [L^3]:

^{1}HNMR spectrum for (L^3) , (Fig.(3-15)) displayed signal at (δ_H =12.34 ppm, 2H) which due to the inter hydrogen bonding process occurred between the protons of the (N-H) groups [117] and the lon pairs of oxygen atoms of solvent facilities. The broadness of these signals could be related to hydrogen bonding (N–H…..O) [117]. The resonances at chemical shift (δ_H = 7.49 - 7.73ppm) (Ar–H) are assignable to protons of aromatic ring [128]. The appearances of these protons as a multi are due to mutual coupling. Signal at chemical shift (δ_H =3.72 ppm) returns to protons group (CO_2CH_3). The sharp singlet signals at (δ_H = 3.18 and 2.49 ppm) equivalent to three protons (3H, S) is attributed to the protons of methyl group [129]. The spectrum displayed chemical shifts at (δ_H = 2.56 ppm and

3.39 ppm) referred to the DMSO mentioned earlier. The results are summarised in table (3-9).

Table (3-9):^{1}H-NMR data for [L^3] measured in DMSO-d6 and chemical shift in ppm (δ)

Compound	Functional groups	δ (ppm)
[L^3]	N-H groups	(12.34) (2H,s)
	-Ar-CH	(7.49 - 7.73) (13H,m)
	$-CO_2CH_3$	3.72 (3H,s)
	CH_3-N.	(3.18) (3H,s)
	$-CH_3$	(2.49) (3H,s)
	HDO	3.38
	DMSO-d6 solvent	2.51

s= Singlet m=multi br= broad

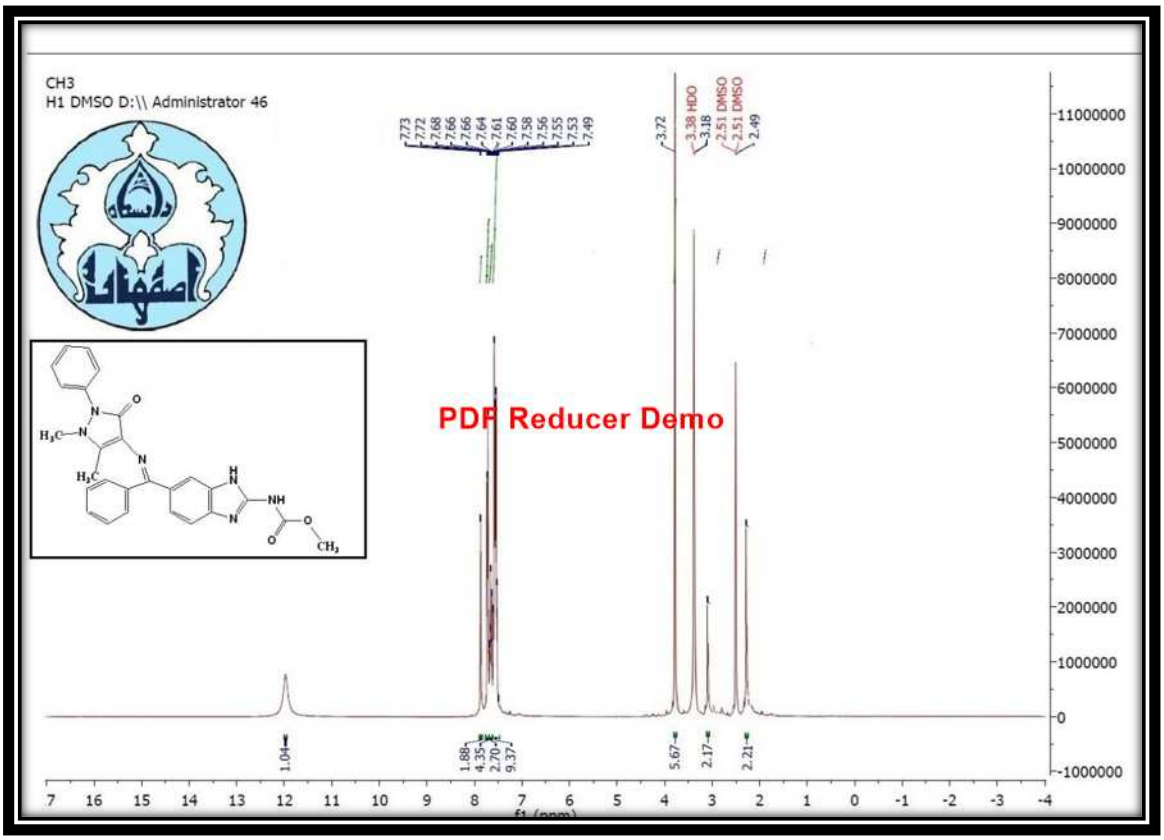

Fig.(3-15): ^{1}H-NMR spectrum for [L^3] in DMSO-d6.

(3.1.5.6) ^{13}C-NMR spectrum for the ligand [L^3]:

The ^{13}CNMR spectrum of (L^3), (Fig. (3-16)) in DMSO-d6 solvent shows chemical shift at range (δ= 114.05-138.38 ppm) assigned to aromatic carbon atoms. The chemical shifts at (δ=167.55 ppm) attributed to the carbonyl carbon atom (C_{18}). The chemical shift at (δ=160.39 ppm) attributed to the imine carbon atom (C_2) [130]. The chemical shift at (δ=154.33 ppm) attributed to the carbonyl carbon atom (C_{10}). The chemical shift at (δ=150.37ppm) attributed to the (C_{19}), while the chemical shift at (δ=149.37ppm) attributed to the (C_3) .The chemical shift at (δ=110.78ppm) attributed to the (C_{17}) . The chemical shift at (δ= 52.62 ppm) assigned to methoxy group carbon atom (C_1). The chemical shifts at (δ=33.05 ppm and 14.29 ppm) assigned to methyl group carbon atoms ($C_{21, 20}$) respectively [131]. The results are listed in table (3-10).

Table (3-10):^{13}C-NMR data for [L^3] measured in DMSO-d6 and chemical shift in ppm (δ)

Compound	Functional groups	δ_c (ppm)
[L^3]	Ar–C	(114.05-138.38)
	$C_{18, 2}$	(167.55) (160.39)
	$C_{10,19}$	(154.33)(150.37)
	$C_{3,17}$	(149.37)(110.78)
	C_1	(52.62)
	$C_{21,20}$	(33.05) (14.29)

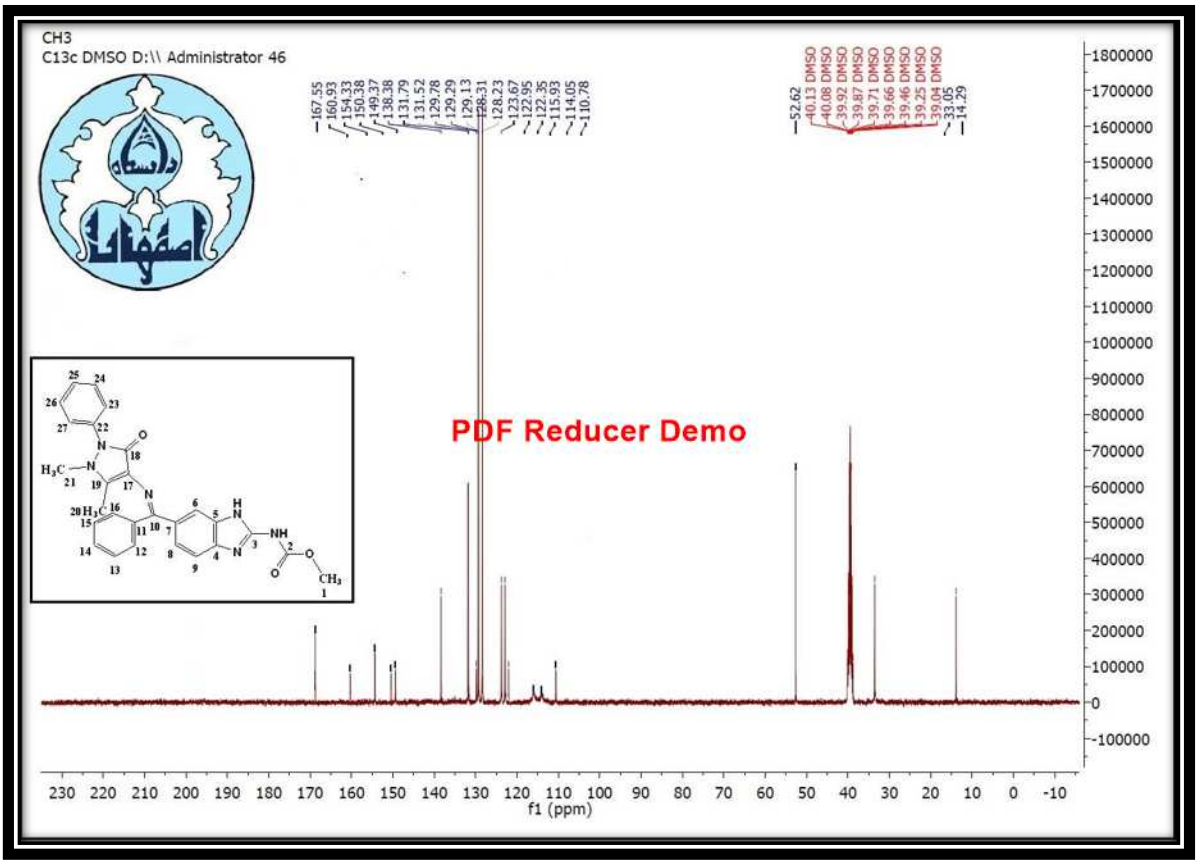

Fig. (3-16): ^{13}CNMR spectrum for [L^3] in DMSO-d6.

(3.1.6) Mass Spectra of Ligands [L^1, L^2 and L^3]:

(3.1.6.1) Mass Spectrum of [L^1]:

The mass spectrum of (L^1) is depicted in Figure (3.17). The molecular ion peak for the ligand is observed at m/z^+ = 457.2 $[M]^+$ for $C_{24}H_{19}N_5O_3S$; requires = 457.51[132]. The other peaks detected at m/ z^+ = 426.2-77.1 correspond to $[C_{23}H_{16}N_5O_2S]^+$- $[C_6H_5]^+$. The fragmentation pattern of (L^1) tabulated in Table (3-11). The suggested mass fragmentation of (L^1) is shown in Scheme (3-1).

Table (3-11): The fragmentation pattern of [L^1]

Fragment	Mass/charge (m/z^+)	Relative abundance %
$[M]^+ = [\ C_{24}H_{19}N_5O_3S\ ]^+$	457.2	51
$[C_{23}H_{16}N_5\ O_2S\ ]^+$	426.2	23
$[C_{22}H_{16}\ N_5OS]^+$	398.1	27.5
$[C_{21}H_{14}\ N_5S\ ]^+$	368.2	17
$[C_{20}H_{14}\ N_3S\ ]^+$	328.1	59
$[C_{18}H_{13}\ N_2S\ ]^+$	289.3	9
$[C_{16}H_{13}\ N_2S\ ]^+$	266.2	100
$[C_{14}H_{13}\ N_2\ ]^+$	208.1	19
$[C_{13}H_{10}N]^+$	180.0	61.5
$[C_{11}H_{10}N]^+$	156.3	12.5
$[C_7H_6N]^+$	104.2	14
$[C_6H_5]^+$	77.1	65

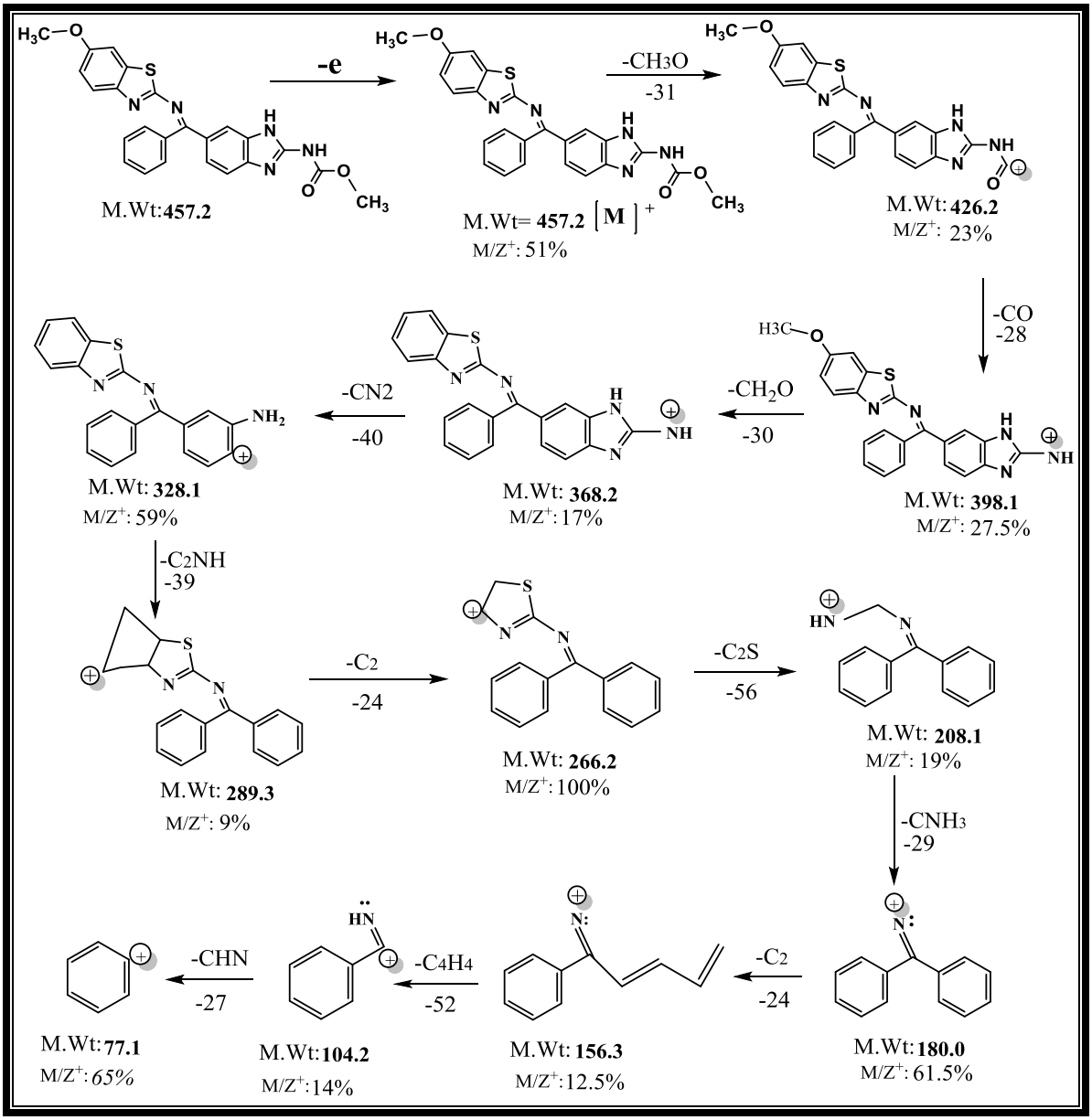

Scheme (3-1): Suggested mass fragmentation of Schiff base [L^1].

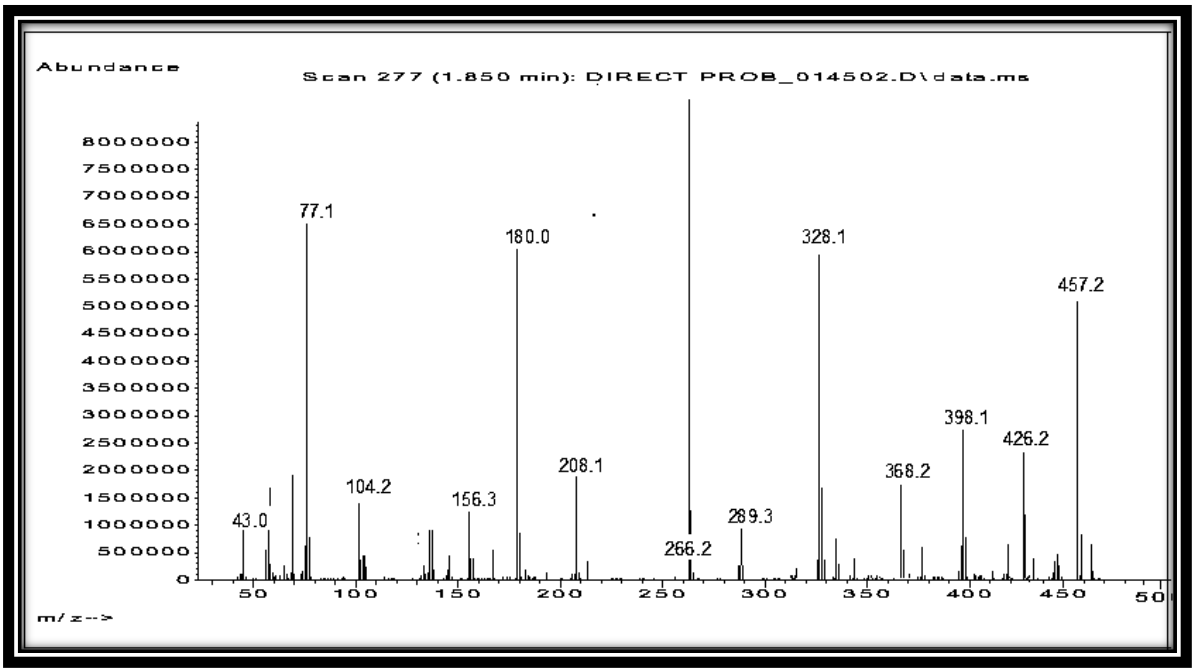

Fig. (3-17): Mass spectrum of [L^1].

(3.1.6.2) Mass Spectrum of [L^2]:

The mass spectrum of (L^2) is depicted in Figure (3.18). The molecular ion peak for the ligand is observed at $m/z^+ = 427.1$ $[M]^+$ for $C_{23}H_{17}N_5O_2S$; requires = 427.48 [133]. The other peaks detected at $m/z^+ =$ 382.1-77.3 correspond to $[C_{22}H_{16}N_5S]^+$- $[C_6H_5]^+$. The fragmentation pattern of (L^2) tabulated in Tabel (3-12). The Suggested mass fragmentation of (L^2) is shown in Scheme (3-2).

Table (3-12): The fragmentation pattern of [L^2]

Fragment	Mass/charge (m/z^+)	Relative abundance %
$[M]^+ = [C_{23}H_{17}N_5O_2S]^+$	427.1	49.5
$[C_{22}H_{16}N_5S]^+$	382.1	20
$[C_{21}H_{13}N_4S]^+$	353.2	33
$[C_{20}H_{13}N_2S]^+$	313.2	63

$[C_{16}H_{13}N_2S\ ]^+$	265.3	11
$[C_{14}H_{12}NS\ ]^+$	226.4	100
$[C_{13}H_{10}N\ ]^+$	180.1	60.5
$[C_8H_8N]^+$	118.2	14.5
$[C_6H_5]^+$	77.3	65

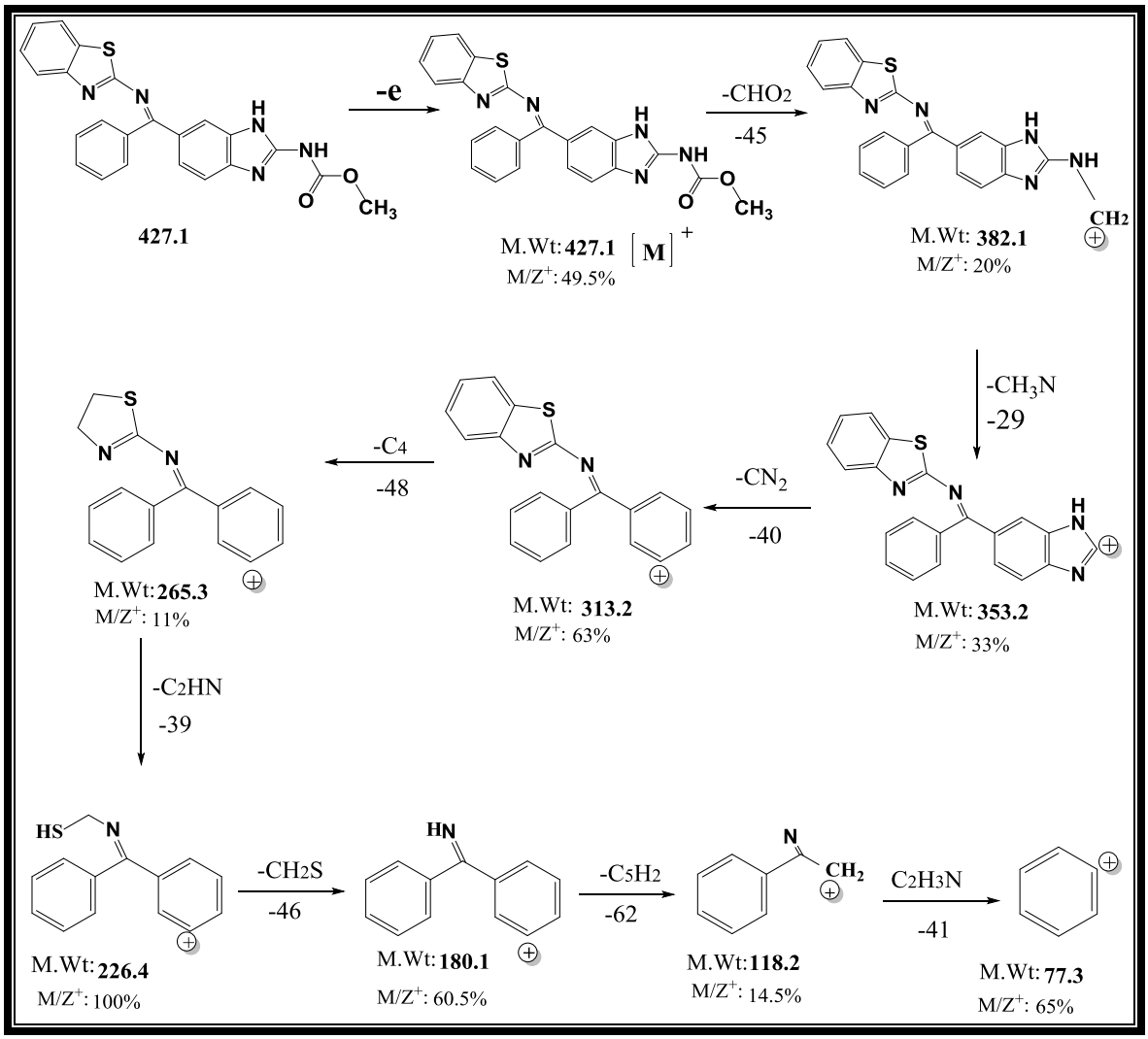

Scheme (3-2): Suggested mass fragmentation of Schiff base [L^2].

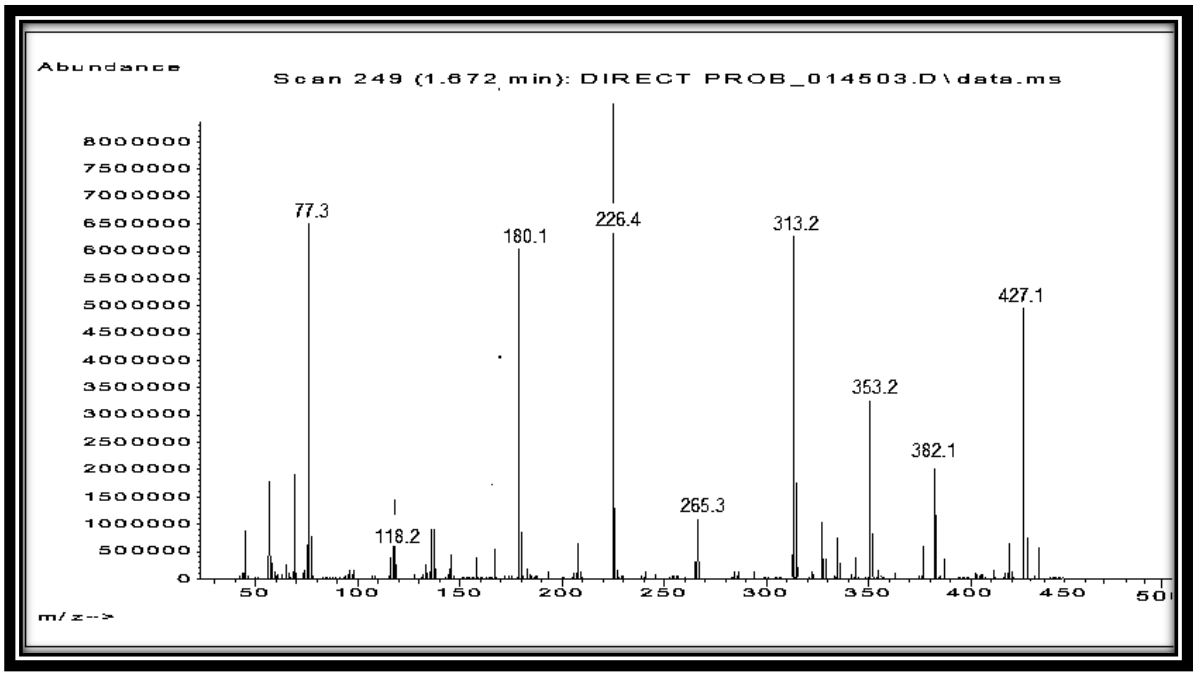

Fig. (3-18): Mass spectrum of [L^2].

(3.1.6.3) Mass Spectrum of [L^3]:

The mass spectrum of (L^3) is depicted in Figure (3.19). The molecular ion peak for the ligand is observed at $m/z^+ = 480.4$ $[M]^+$ for $C_{27}H_{19}N_5O_3S$; requires = 480.52 [134]. The other peaks detected at m/z^+ = 494.1-77.1 correspond to $[C_{26}H_{21}N_6O_2]^+$- $[C_6H_5]^+$. The fragmentation pattern of L^3 tabulated in Tabel (3-13) .The Suggested mass fragmentation of (L^3) is shown in Scheme (3-3).

Table (3-13): The fragmentation pattern of [L^3]

Fragment	Mass/charge (m/z^+)	Relative abundance %
$[M]^+ = [C_{27}H_{24}N_6O_3]^+$	480.4	72
$[C_{26}H_{21}N_6O_2]^+$	449.1	17
$[C_{25}H_{20}N_5O]^+$	406.2	83
$[C_{22}H_{20}N_5O]^+$	370.1	12
$[C_{19}H_{16}N_5O]^+$	330.1	18
$[C_{18}H_{16}N_3O]^+$	290.1	100
$[C_{17}H_{14}NO]^+$	248.3	60
$[C_{16}H_{14}N]^+$	220.1	9
$[C_{13}H_{10}N]^+$	180.0	54
$[C_{10}H_{10}N]^+$	144.2	21
$[C_7H_6N]^+$	104.2	32
$[C_6H_5]^+$	77.2	49

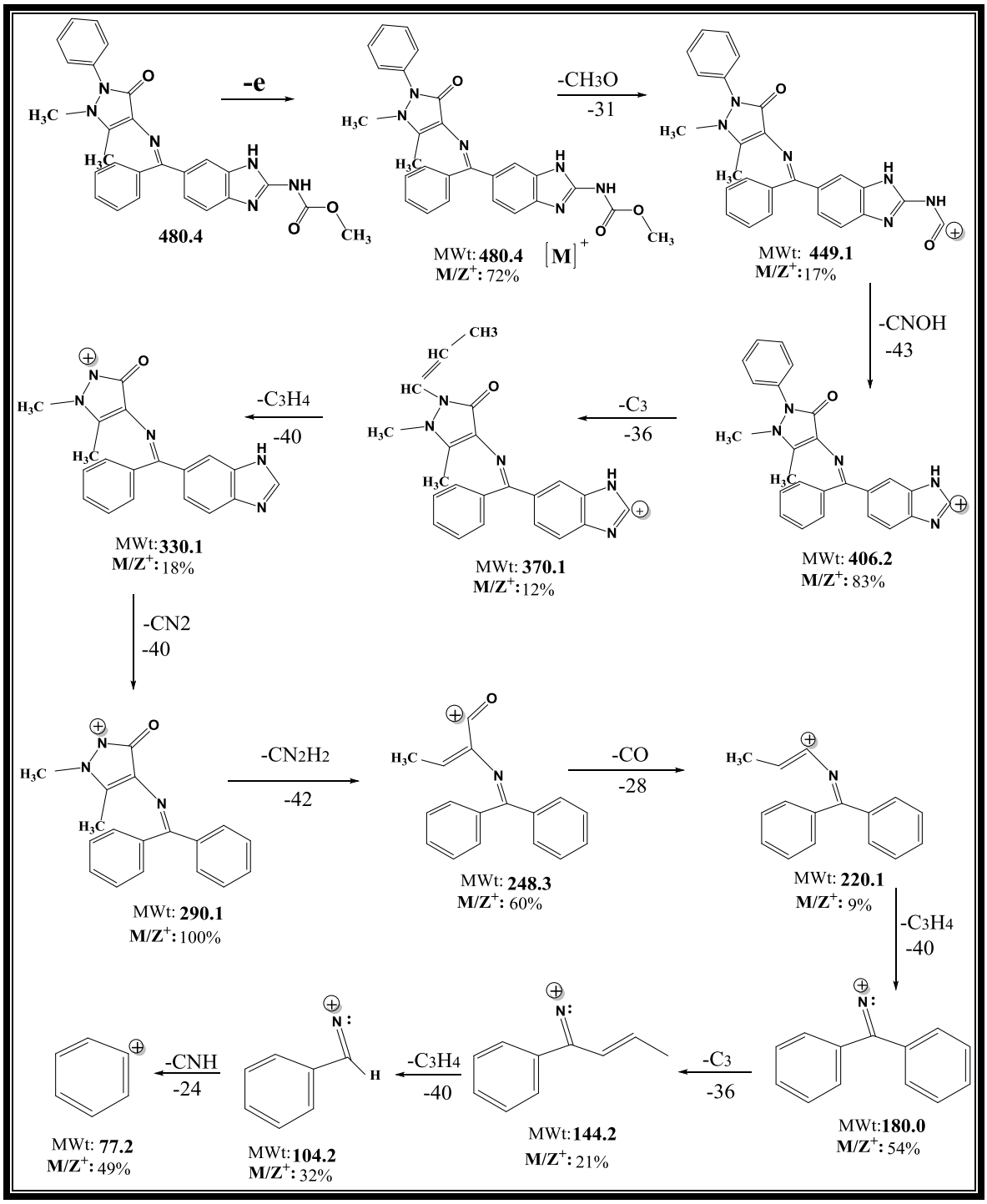

Scheme (3-3): Suggested mass fragmentation of Schiff base [L^3].

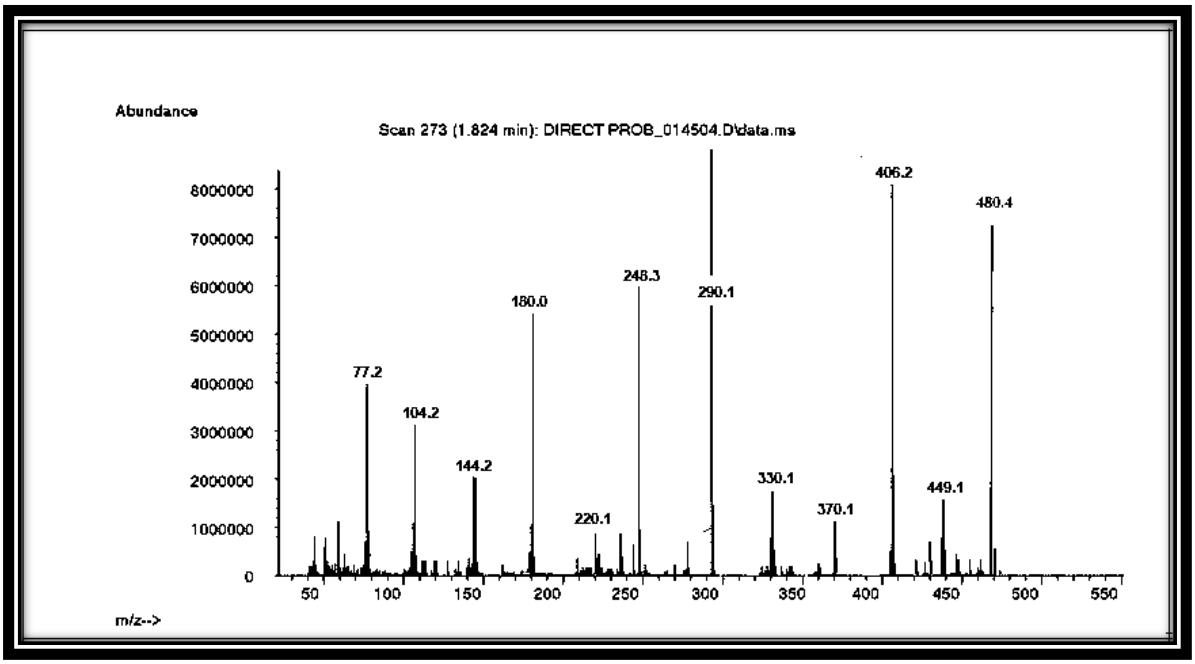

Fig. (3-19): Mass spectrum of [L^3].

(3.1.7) The suggested structural formula of ligands [L^1, L^2 and L^3]

According to the results obtained from FT- IR, U.V-Vis, Mass spectra ,^{1}H-NMR and ^{13}C-NMR spectra, the suggested structural formula of ligands (L^1, L^2 and L^3) were shown in figs. (3-20), (3-21) and (3-22) respectively as 3D drawing by using Ultra chem. Office program, 3Dx (2016).

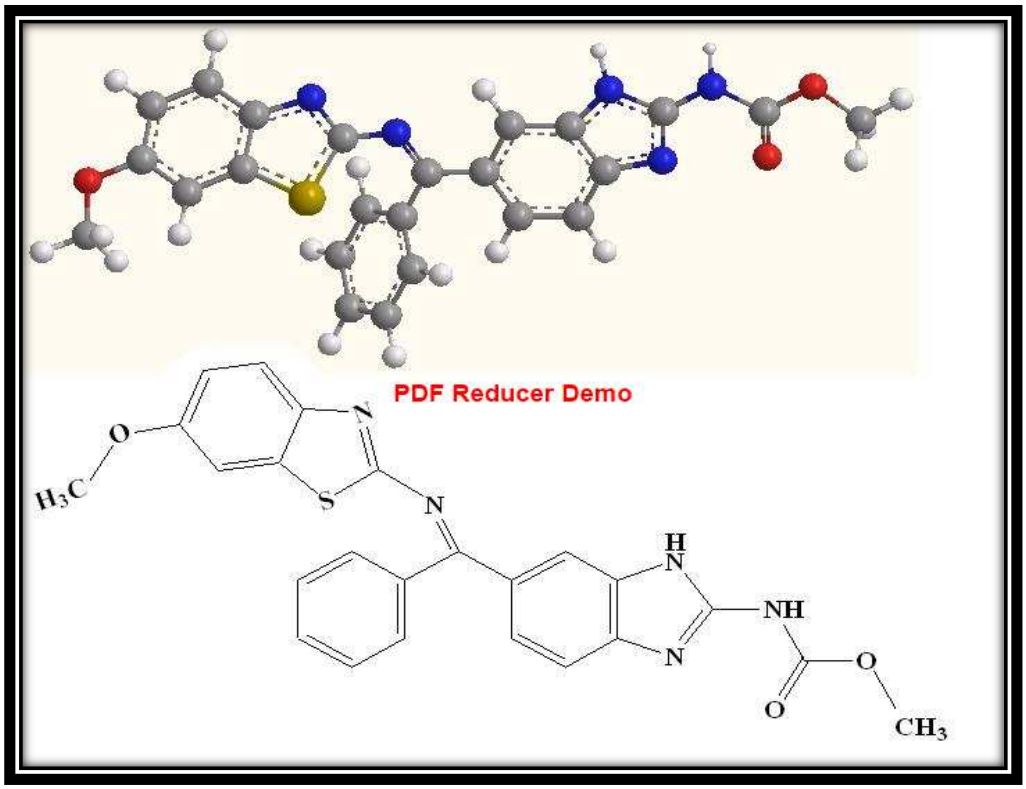

Fig. (3-20): The suggested structural formula of ligand [L^1].

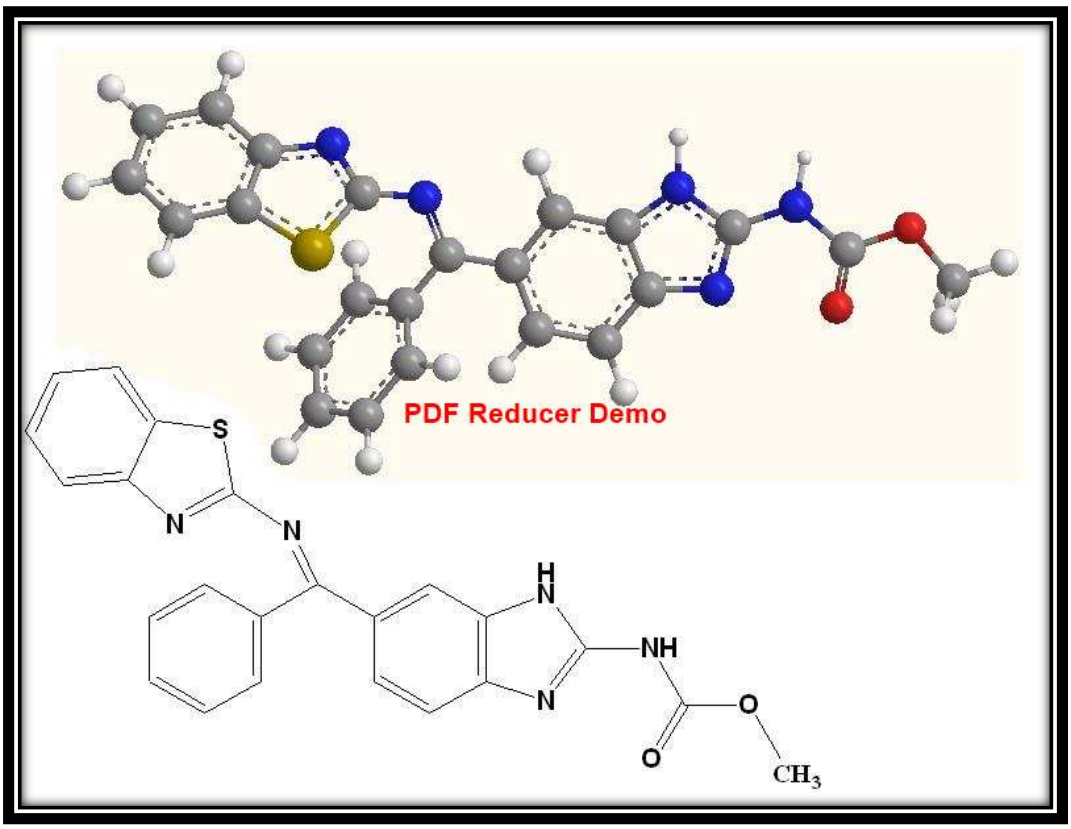

Fig. (3-21):The suggested structural formula of ligand [L^2].

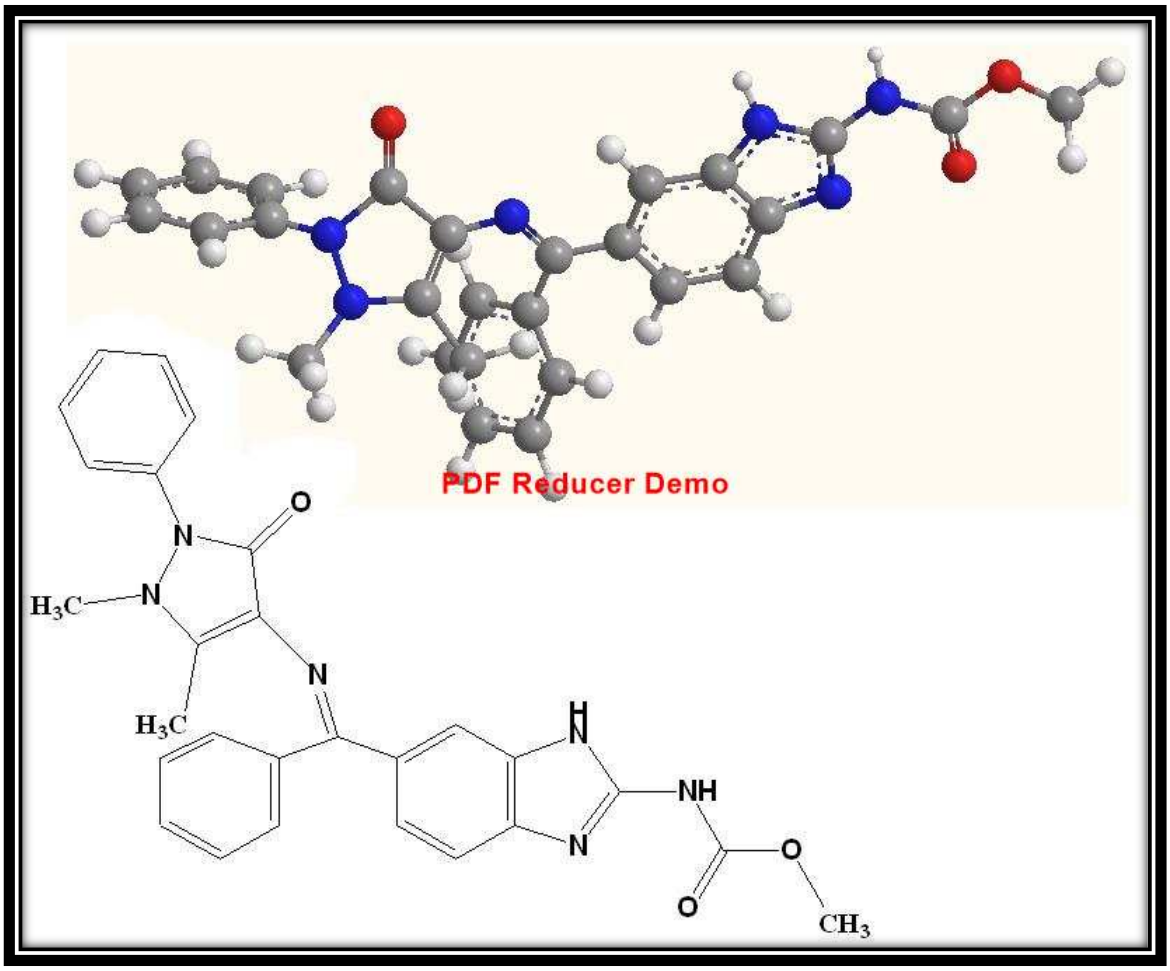

Fig. (3-22) :The suggested structural formula of ligand [L^3].

(3.1.8) Nomenclature of ligands [L^1, L^2 and L^3].

Nomenclature (IUPAC) of prepared ligands (L^1, L^2 and L^3) were:

1. [L^1]….. Methyl (E)-(6-(((6-methoxybenzo[d]thiazol-2-yl)imino) (phenyl) methyl)-1H-benzo[d]imidazol-2-yl) carbamate.
2. [L^2]….. Methyl (E)-(6-((benzo[d]thiazol-2-ylimino) (phenyl) methyl)- 1H-benzo[d]imidazol-2-yl) carbamate.
3. [L^3]…..Methyl (E)-(6-(((1,5-dimethyl-3-oxo-2-phenyl-2,3-dihydro-1H-pyrazol-4-yl)imino)(phenyl)methyl)-1H-benzo[d]imidazol-2-yl)carbamate.

(3.2) Characteriasation of ligand's [L^1, L^2 and L^3] complexes [(1)-(24)].

All complexes were prepared by similar method shown in schemes (3-3) and (3-4) of (L^1), (3-5) and (3-6) of (L^2) and in schemes (3-7) and (3-8) of (L^3) .The complexes were prepared from metal (II) chloride salt but VO(II) complex by $VOSO_4.H_2O$, in 1:2 [M:L] ratio reflux in (aceton or methanol), the pure complexes were formed .

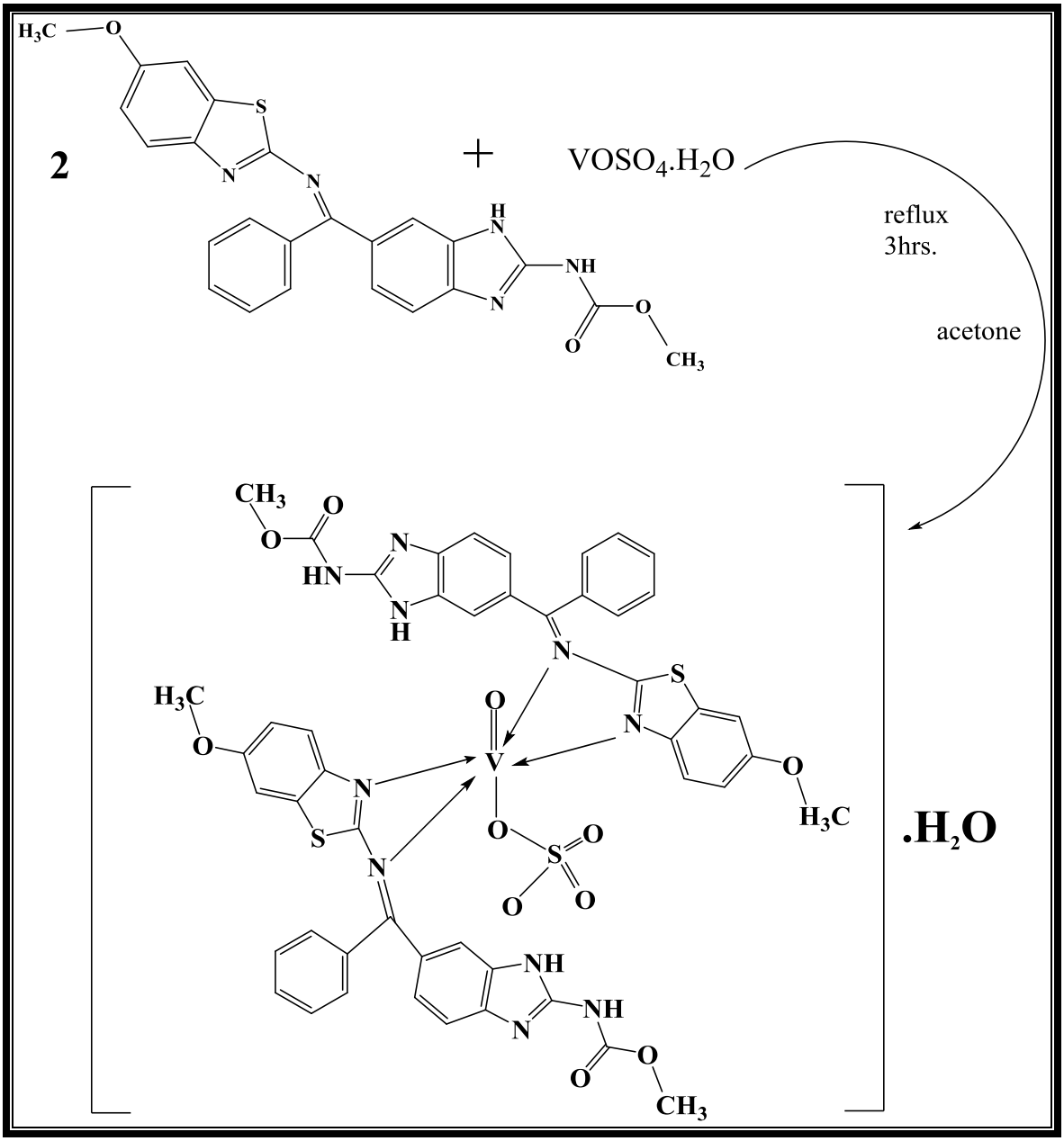

Scheme (3-4): Synthesis route of $[VO(L^1)_2(SO_4)].H_2O$

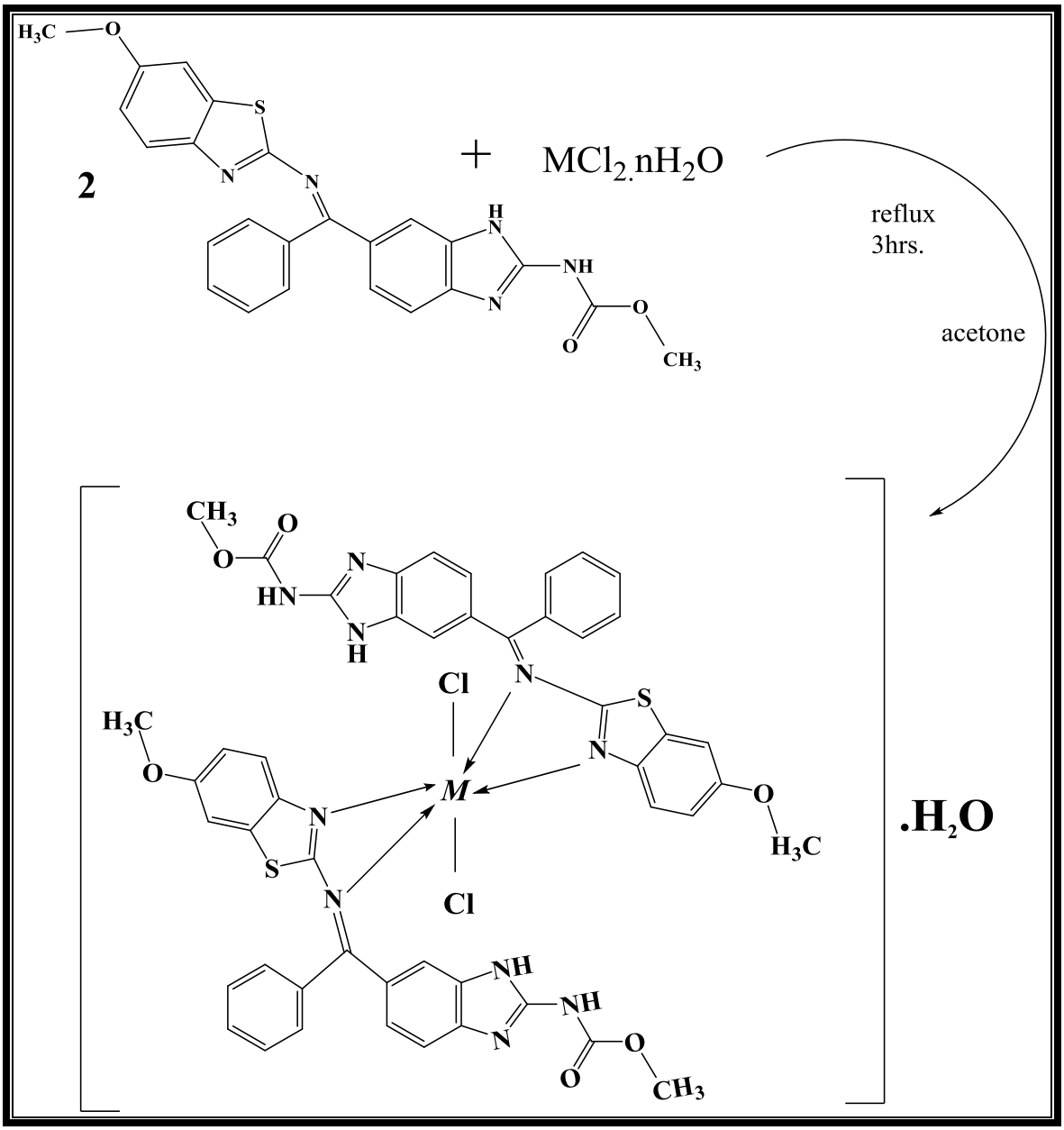

M(II) = Mn , Co, Ni , Cu , Zn , Cd , Hg , n= 4(Mn) , 6(Co, Ni) , 2(Cu) , 0(Zn, Cd , Hg),

Scheme (3-5): Synthesis route of ligand [L^1] complexes.

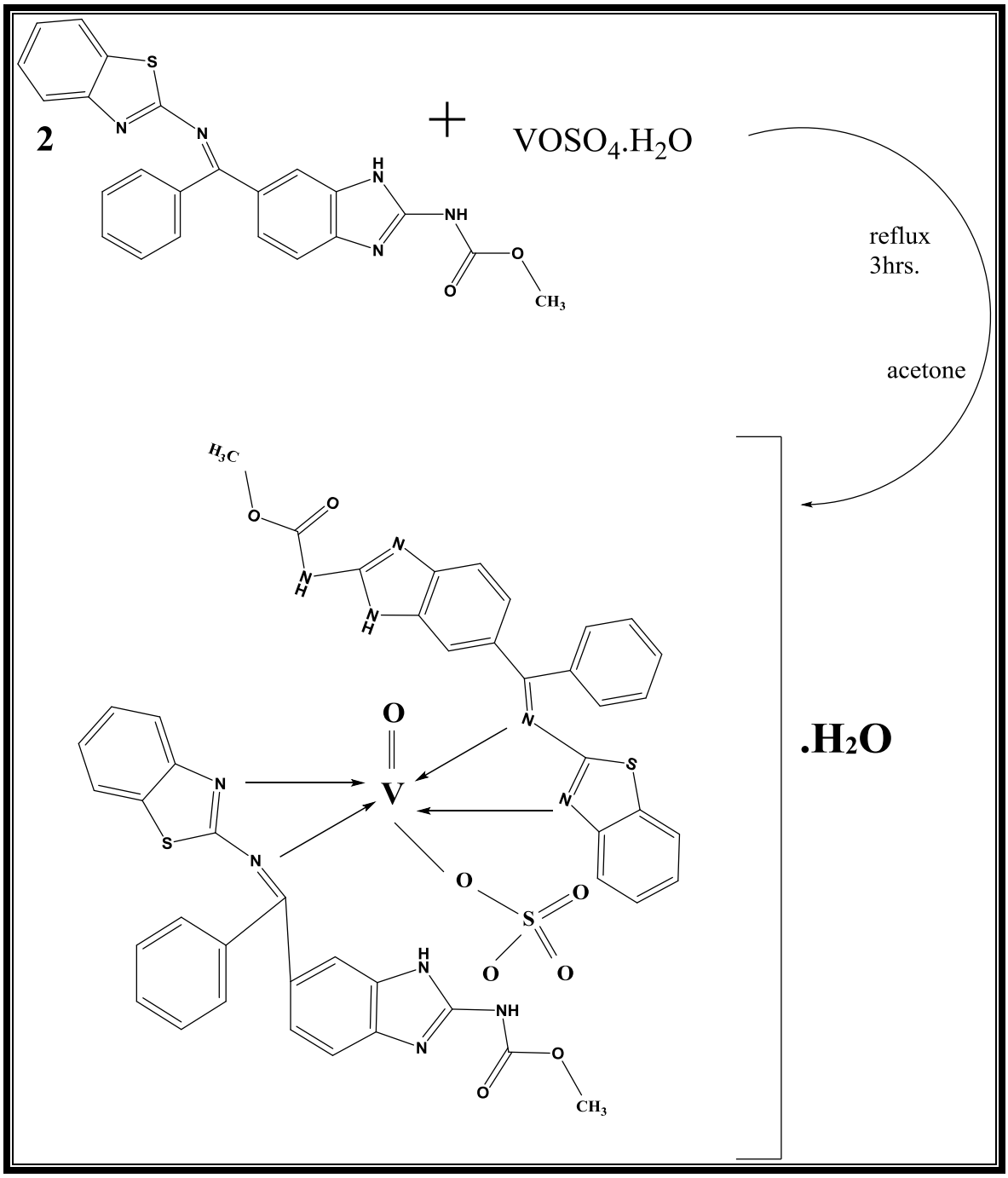

Scheme (3-6): Synthesis route of $[VO(L^2)_2(SO_4)]. H_2O$

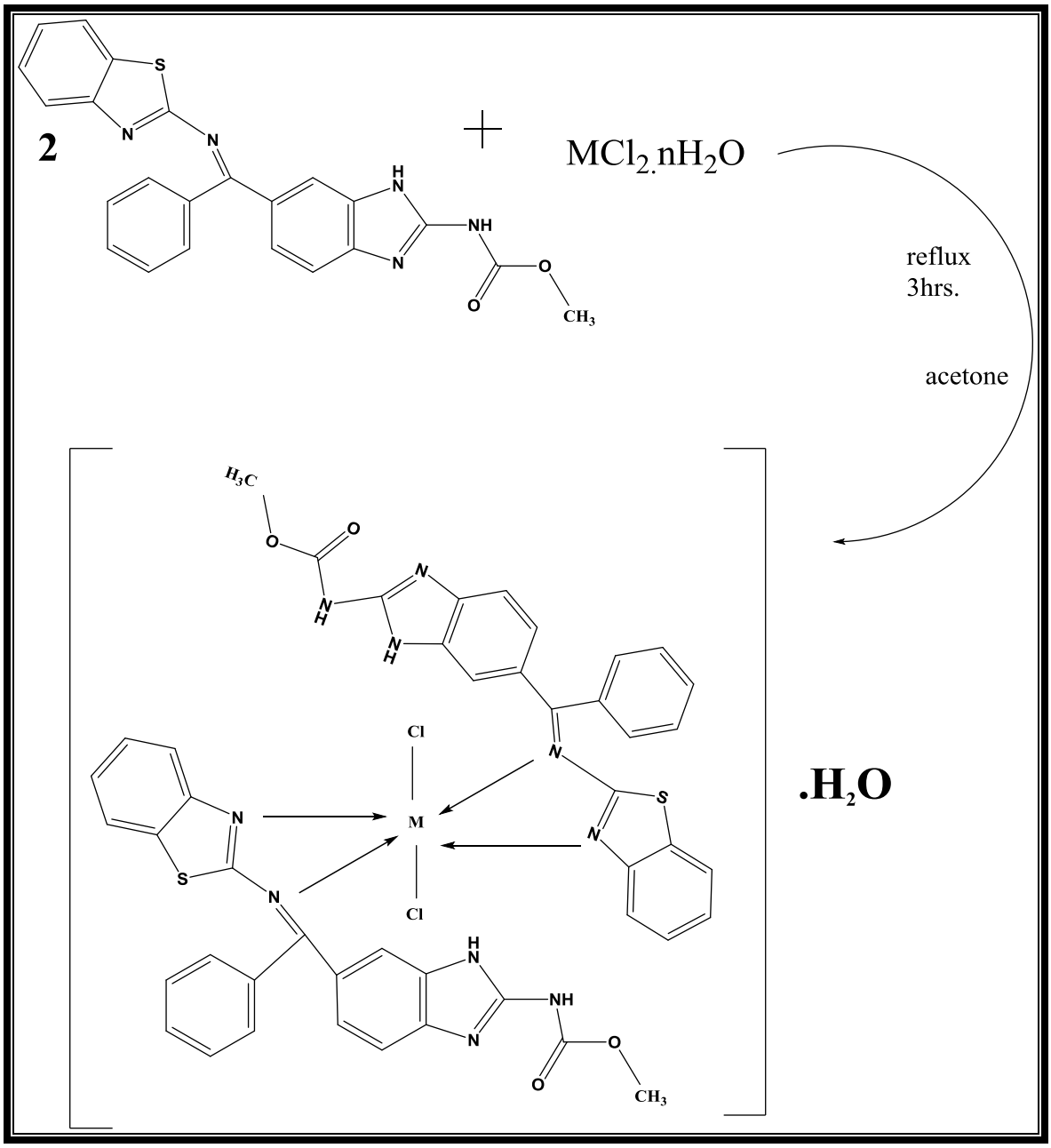

M(II)= Mn , Co, Ni , Cu , Zn , Cd , Hg , n= 4(Mn) , 6(Co, Ni) , 2(Cu) , 0(Zn, Cd , Hg),

Scheme (3-7): Synthesis route of ligand [L^2] complexes.

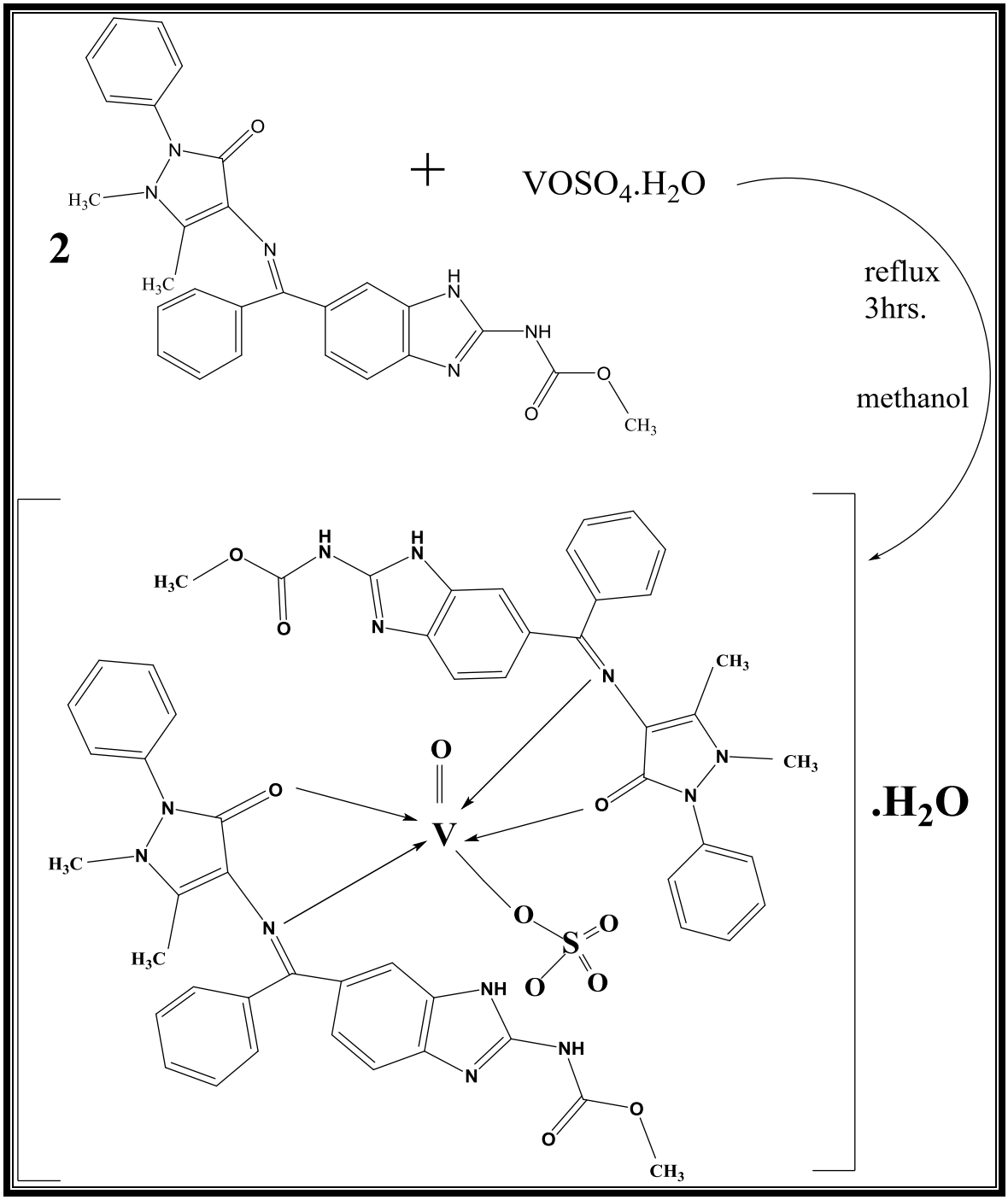

Scheme (3-8): Synthesis route of $[VO(L^3)_2(SO_4)]. H_2O$

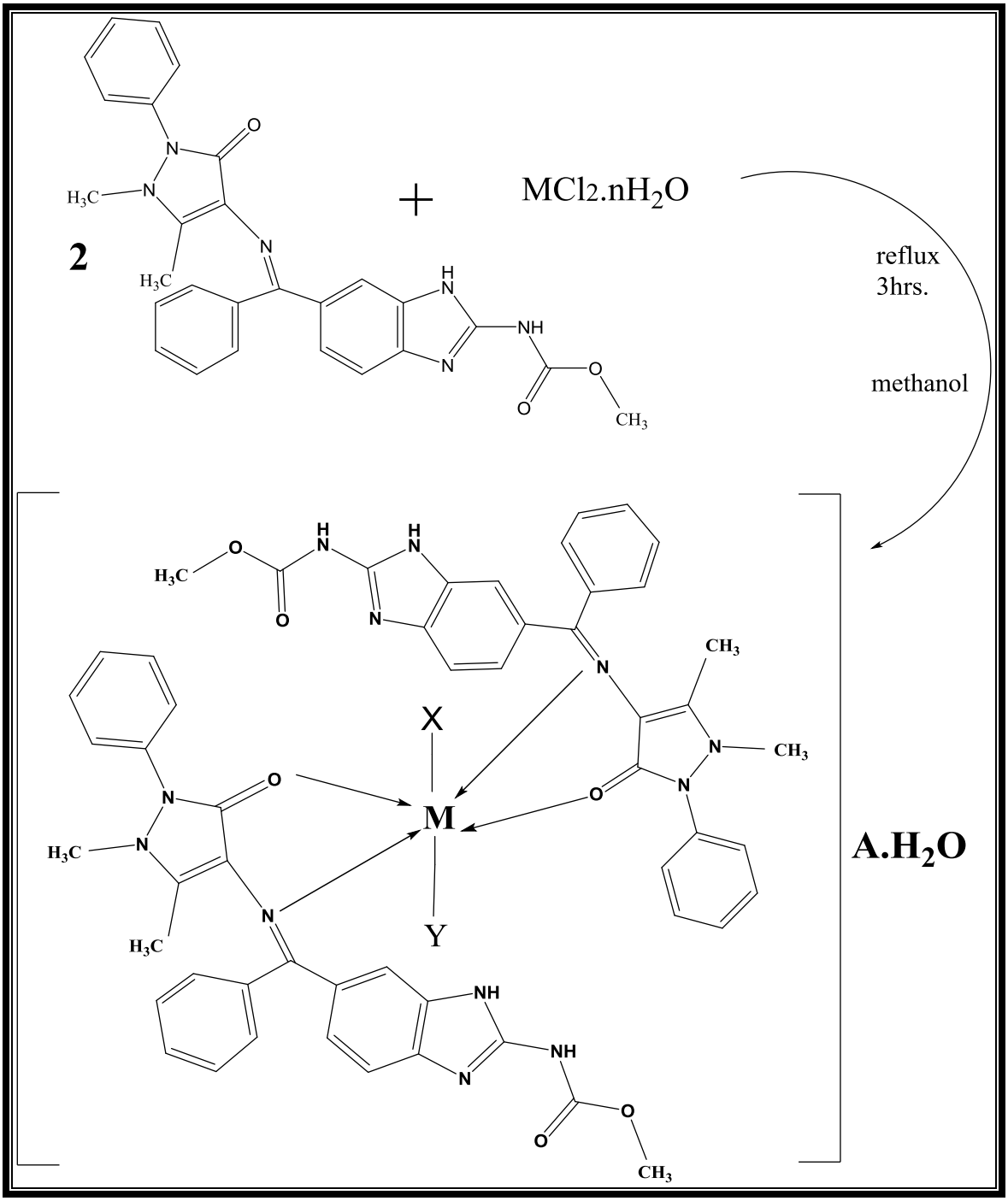

M(II) = Mn , Co, Ni , Cu , Zn , Cd , Hg , n= 4(Mn) , 6(Co, Ni) , 2(Cu) , 0(Zn, Cd , Hg)

Mn,Co (X=Cl , Y= H_2O , A=Cl)

Ni (X=Cl ,Y=0 , A=Cl)

Cu , Zn , Cd , Hg (X=Cl , Y=Cl , A=0)

Scheme (3-9): Synthesis route of ligand [L^3] complexes.

Spectroscopic methods [FT- IR, U.V-Vis and A.A] along with molar conductivity, elemental microanalysis C.H.N.S, chloride content, magnetic susceptibility and thermal analysis were used to characterized the prepared complexes.

(3.2.1) Solubility:

Solubility of all prepared complexes (1-24) was tested in different solvents. The results were listed in tables (3-14), (3-15) and (3-16).

Table (3-14): Solubility of the [L^1] complexes in different solvents.

No.	Compounds	H_2O	C_2H_5OH	CH_3OH	C_3H_6O	DMSO	DMF	C_6H_6	$CHCl_3$
1	$[VO(L^1)_2(SO_4)].H_2O$	-	+	+	+	+	+	-	-
2	$[Mn(L^1)_2Cl_2].H_2O$	-	+	+	+	+	+	-	-
3	$[Co(L^1)_2Cl_2].H_2O$	-	+	+	+	+	+	-	-
4	$[Ni(L^1)_2Cl_2].H_2O$	-	+	+	+	+	+	-	-
5	$[Cu(L^1)_2Cl_2].H_2O$	-	+	+	+	+	+	-	-
6	$[Zn(L^1)_2Cl_2].H_2O$	-	+	+	+	+	+	-	-
7	$[Cd(L^1)_2Cl_2].H_2O$	-	+	+	+	+	+	-	-
8	$[Hg(L^1)_2Cl_2].H_2O$	-	+	+	+	+	+	-	-

Table (3-15): Solubility of the [L^2] complexes in different solvents.

No.	Compounds	H_2O	C_2H_5OH	CH_3OH	C_3H_6O	DMSO	DMF	C_6H_6	$CHCl_3$
9	$[VO(L^2)_2(SO_4)].H_2O$	-	+	+	+	+	+	-	-
10	$[Mn(L^2)_2Cl_2].H_2O$	-	+	+	+	+	+	-	-
11	$[Co(L^2)_2Cl_2].H_2O$	-	+	+	+	+	+	-	-
12	$[Ni(L^2)_2Cl_2].H_2O$	-	+	+	+	+	+	-	-
13	$[Cu(L^2)_2Cl_2].H_2O$	-	+	+	+	+	+	-	-
14	$[Zn(L^2)_2Cl_2].H_2O$	-	+	+	+	+	+	-	-
15	$[Cd(L^2)_2Cl_2].H_2O$	-	+	+	+	+	+	-	-
16	$[Hg(L^2)_2Cl_2].H_2O$	-	+	+	+	+	+	-	-

Table (3-16): Solubility of the [L^3] complexes in different solvents.

No.	Compounds	H_2O	C_2H_5OH	CH_3OH	C_3H_6O	DMSO	DMF	C_6H_6	$CHCl_3$
17	$[VO(L^3)_2(SO_4)].H_2O$	-	+	+	+	+	+	-	-
18	$[Mn(L^3)_2(H_2O)Cl]Cl.H_2O$	-	+	+	+	+	+	-	-
19	$[Co(L^3)_2(H_2O)Cl]Cl.H_2O$	-	+	+	+	+	+	-	-
20	$[Ni(L^3)_2Cl]Cl.H_2O$	-	+	+	+	+	+	-	-
21	$[Cu(L^3)_2Cl_2].H_2O$	-	+	+	+	+	+	-	-
22	$[Zn(L^3)_2\ Cl_2].H_2O$	-	+	+	+	+	+	-	-
23	$[Cd(L^3)_2Cl_2].H_2O$	-	+	+	+	+	+	-	-
24	$[Hg(L^3)_2Cl_2].H_2O$	-	+	+	+	+	+	-	-

(3.2.2) Elemental microanalysis and some physical properties of complexes [1-24]

Some physical properties, elemental microanalysis (C.H.N.S), metal and chloride analysis for all prepared complexes (1-24) are in agreement with calculated values, were listed in tables (3-17), (3-18) and (3-19).

Table (3-17): Elemental microanalysis results and some physical properties of ligand [L^1] complexes.

	Empirical formula	M.wt g/mol.	Yield %	Colour	m.p. °C	Microanalysis found, (Calc.) %					
						C	H	N	S	metal	Cl
1	$[VO^{II}C_{48}H_{38}N_{10}O_6S_2SO_4].H_2O$	1096	81	Light green	259-261	52.20	3.61	12.49	8.60	4.57	-
						(52.55)	(3.65)	(12.77)	(8.76)	(4.66)	-
2	$[Mn^{II}C_{48}H_{38}N_{10}O_6\ S_2Cl_2].H_2O$	1058	88	Light pink	252-254	54.20	3.63	13.10	5.98	5.06	6.60
						(54.44)	(3.78)	(13.23)	(6.05)	(5.20)	(6.71)
3	$[Co^{II}C_{48}\ H_{38}N_{10}O_6S_2Cl_2].H_2O$	1062	78	Blue	218-220	54.11	3.68	13.02	5.95	5.45	6.54
						(54.24)	(3.77)	(13.18)	(6.02)	(5.56)	(6.68)
4	$[Ni^{II}C_{48}\ H_{38}N_{10}O_6S_2Cl_2].H_2O$	1062	79	Green	119-121	54.09	3.60	13.01	5.80	5.40	6.57
						(54.24)	(3.77)	(13.18)	(6.03)	(5.56)	(6.68)
5	$[Cu^{II}C_{48}\ H_{38}N_{10}O_6S_2Cl_2].H_2O$	1067	84	Brown	125-127	53.78	3.59	13.03	5.72	5.77	6.56
						(53.98)	(3.75)	(13.12)	(6.00)	(6.00)	(6.65)
6	$[Zn^{II}C_{48}\ H_{38}N_{10}O_6S_2Cl_2].H_2O$	1069	86	Light yellow	219-221	53.62	3.67	12.90	5.87	5.97	6.54
						(53.88)	(3.74)	(13.10)	(5.99)	(6.08)	(6.64)
7	$[Cd^{II}C_{48}\ H_{38}N_{10}O_6S_2Cl_2].H_2O$	1116	85	Light yellow	220-222	51.40	3.52	12.39	5.65	9.90	6.22
						(51.61)	(3.58)	(12.54)	(5.73)	(10.04)	(6.36)
8	$[Hg^{II}C_{48}\ H_{38}N_{10}O_6S_2Cl_2].H_2O$	1204	87	Yellow	180-182	47.61	3.07	11.41	5.20	16.56	5.74
						(47.84)	(3.32)	(11.63)	(5.32)	(16.69)	(5.90)

Calc.: Calculated

Table (3-18): Elemental microanalysis results and some physical properties of ligand [L^2] complexes.

	Empirical formula	M.wt g/mol.	yield %	Colour	m.p. °C	Microanalysis found, (Calc.) %					
						C	H	N	S	Metal	Cl
9	$[VO^{II}C_{46}H_{34}N_{10}O_4S_2SO_4].H_2O$	1035	90	Green	256-258	53.17	3.34	13.38	9..14	4.81	-
						(53.33)	(3.48)	(13.53)	(9.28)	(4.93)	-
10	$[Mn^{II}C_{46}H_{34}N_{10}O_4S_2Cl_2].H_2O$	998	87	Light yellow	212-214	55.10	3.48	13.87	6.30	5.41	7.00
						(55.31)	(3.61)	(14.03)	(6.41)	(5.51)	(7.11)
11	$[Co^{II}C_{46}H_{34}N_{10}O_4S_2Cl_2].H_2O$	1002	75	Blue	180-182	54.86	3.39	13.81	6.25	5.78	7.02
						(55.09)	(3.59)	(13.97)	(6.39)	(5.89)	(7.09)
12	$[Ni^{II}C_{46}H_{34}N_{10}O_4S_2Cl_2].H_2O$	1002	81	Dark green	204-206	54.89	3.42	13.62	6.25	5.80	6.89
						(55.09)	(3.59)	(13.97)	(6.39)	(5.89)	(7.09)
13	$[Cu^{II}C_{46}H_{34}N_{10}O_4S_2Cl_2].H_2O$	1007	89	Dark brown	191-193	54.60	3.47	13.64	6.29	6.25	6.89
						(54.82)	(3.57)	(13.90)	(6.36)	(6.36)	(7.05)
14	$[Zn^{II}C_{46}H_{34}N_{10}O_4S_2Cl_2].H_2O$	1009	78	Light yellow	223-225	54.47	3.43	13.68	6.28	6.32	6.86
						(54.71)	(3.57)	(13.88)	(6.35)	(6.44)	(7.04)
15	$[Cd^{II}C_{46}H_{34}N_{10}O_4S_2Cl_2].H_2O$	1056	84	Light yellow	248-250	51.91	3.26	13.00	5.95	10.51	6.58
						(52.27)	(3.41)	(13.26)	(6.06)	(10.61)	(6.72)
16	$[Hg^{II}C_{46}H_{34}N_{10}O_4S_2Cl_2].H_2O$	1144	74	Yellow	203-205	47.90	2.92	12.00	5.30	17.29	6.04
						(48.25)	(3.15)	(12.24)	(5.59)	(17.57)	(6.21)

Calc.: Calculated

Table (3-19): Elemental microanalysis results and some physical properties of ligand [L^3] complexes.

	Empirical formula	M.wt g/mol.	Yield %	Colour	m.p. °C	Microanalysis found, (Calc.) %				
						C	H	N	Metal	Cl
17	$[VO^{II}C_{54}H_{48}N_{12}O_6SO_4].H_2O$	1142	83	Green	198-200	56.59	4.14	14.59	4.21	-
						(56.74)	(4.38)	(14.71)	(4.47)	-
18	$[Mn^{II}C_{54}H_{48}N_{12}O_6H_2OCl]Cl.H_2O$	1122	86	Light yellow	208-210	57.49	4.46	14.81	4.88	6.26
						(57.75)	(4.63)	(14.97)	(4.91)	(6.33)
19	$[Co^{II}C_{54}H_{48}N_{12}O_6H_2OCl]Cl.H_2O$	1126	78	Dark green	212-214	57.37	4.34	14.75	5.01	6.25
						(57.55)	(4.62)	(14.92)	(5.24)	(6.31)
20	$[Ni^{II}C_{54}H_{48}N_{12}O_6Cl]Cl.H_2O$	1108	80	Yellow	199-201	58.28	4.24	15.01	5.13	6.25
						(58.48)	(4.51)	(15.16)	(5.32)	(6.41)
21	$[Cu^{II}C_{54}H_{48}N_{12}O_6Cl_2].H_2O$	1113	83	Dark brown	152-154	58.02	4.20	14.88	5.66	6.19
						(58.22)	(4.49)	(15.09)	(5.75)	(6.38)
22	$[Zn^{II}C_{54}H_{48}N_{12}O_6Cl_2].H_2O$	1115	87	Light yellow	199-201	58.02	4.21	14.87	5.66	6.28
						(58.17)	(4.49)	(15.08)	(5.83)	(6.37)
23	$[Cd^{II}C_{54}H_{48}N_{12}O_6Cl_2].H_2O$	1162	89	Yellow	202-204	55.66	4.21	14.09	9.10	5.74
						(55.81)	(4.31)	(14.47)	(9.65)	(6.11)
24	$[Hg^{II}C_{54}H_{48}N_{12}O_6Cl_2].H_2O$	1250	90	Yellow	246-248	51.53	3.28	13.17	16.02	5.50
						(51.84)	(4.00)	(13.44)	(16.08)	(5.68)

Calc.: Calculated

(3.2.3) Molar conductance of metal complexes with L^1 , L^2 and L^3 [(1)-(24)] .

The conductivity measurement for compounds are used to determine the conductance of the compound (electrolyt or non electrolyt)[135]

The molar conductance of the prepared complexes (1-24) in DMSO solvent in 10^{-3}M solution at room temperature are tabulated in table (3-20). The conductance of complexes (1→17 and 21→24) lie in the range (1.62-22.20) $S.cm^2.mole^{-1}$, indicating their non-electrolytic behavior. The molar conductance of complexes (18, 19 and 20) lie in the (30.70, 32.92, 34.80) $S.cm^2.mole^{-1}$,indicating the 1:1 electrolyte natures[136].

(3.2.4) Magnetic susceptibility of ligand's [L^1, L^2 and L^3] complexes [(1)-(24)].

The effective magnetic moments (μ_{eff} B.M) of metal complexes were measured in the solid state by following Faraday's method[137,138]. The magnetic properties of these complexes should provide a way of counting the number of unpaired electrons [139,140]. This should help in predicting the bonding nature between metal ion and ligand as well as electronic structure and geometry of complexes. The magnetic susceptibility was measured at (298 K) and the effective magnetic moment (μeff.) values for complexes were listed in table (3-20). The values of μeff. for some prepared complexes V(IV) , Mn(II) , Co(II) and Cu(II) showed paramagnetic nature ,which corresponded to high spin octahedral geometry around central metal ion .The value of μeff = 0.00 for Ni(II) with (L^3) showed diamagnetic nature , suggesting low-spin complex [141,142] , while Zn(II), Cd(II) and Hg(II) complexes are diamagnetic nature because of (d^{10}) system .

The values of (μeff B.M) were calculated from the following relationships

$X_M = X_g \times M_{wt}$ ……...… (1)

$X_A = X_M - D$ ……..... (2)

$$\mu_{eff}\ M = 2.828\ \sqrt{X_A . T}\quad \text{B.M} \ldots\ldots\ldots (3)$$

Where:

X_M = Molar susceptibility

X_g = Gramic susceptibility

M = Molecular weight of complex

X_A = Atomic susceptibility

T = Temperature (K)

D = Diamagnetic correction Factor, by using Pascal's constant for ligand atoms and metal ions, we can calculate the value of this factor.

The results obtained from Faraday's method were compared with those calculated from spin only (μ_s), magnetic moment values obtained from the following equation:

$$\mu s = 2\sqrt{S(S+1)}\ \text{B.M} \quad \ldots\ldots\ldots (4)$$

Where S = n/2 (n = no. of unpaired electrons).

$$\mu s = \sqrt{n\ (n+2)}\ \text{B.M}$$

The X_M, X_A, and μ_{eff} of the complex were calculated using the X_g value obtained and theoretically calculated D. Three models of magnetic sensitivity calculations were selected to illustrate the extraction mechanism μ_{eff} for complexes.

$[VO(L^1)_2Cl_2].H_2O$, $[Ni(L^2)_2Cl_2].H_2O$, $[Co(L^3)_2(H_2O)Cl_2].H_2O$

$[VO(L^1)_2Cl_2].H_2O$ (1)

$X_M = Xg \times M.wt$

$= 0.95 \times 10^{-6} \times 1096$

$= 1041.2 \times 10^{-6}$

$X_A = X_M - (-D)$

$= 1041.2 \times 10^{-6} + 262.1 \times 10^{-6}$

$= 1303.3 \times 10^{-6}$

$\mu eff = 2.828\sqrt{XA.T}$

$\mu_{eff} = 2.828\sqrt{(1303.3 \times 10^{-6})298}$

$= 1.76$ B.M

$[Ni(L^2)_2Cl_2].H_2O$ (12)

$X_M = Xg \times M.wt$

$= 3.12 \times 10^{-6} \times 1002$

$= 3126.24 \times 10^{-6}$

$X_A = X_M - (-D)$

$= 3126.24 \times 10^{-6} + 250.3 \times 10^{-6}$

$= 3376.54 \times 10^{-6}$

$\mu eff = 2.828\sqrt{XA.T}$

$\mu_{eff} = 2.828\sqrt{(3376.54 \times 10^{-6})298}$

$= 2.84$ B.M

$[Co(L^3)_2(H_2O)Cl_2].H_2O$ (19)

$X_M = Xg \times M.wt$

$= 7.9 \times 10^{-6} \times 1126$

$= 8895.4 \times 10^{-6}$

$X_A = X_M - (-D)$

$= 8895.4 \times 10^{-6} + 422.2 \times 10^{-6}$

$= 9317.4 \times 10^{-6}$

$\mu eff = 2.828\sqrt{XA.T}$

$\mu_{eff} = 2.828\sqrt{(9317.4 \times 10^{-6})298}$

$= 4.71$ B.M

Table (3-20): The molar conductivity and magnetic moment of the complexes.

No.	Compounds	$X_g \times 10^{-6}$	$X_M \times 10^{-6}$	$X_A \times 10^{-6}$	μ_{eff} (B.M)	Λ_m S.cm^2.mole^{-1}
1	$[VO(L^1)_2(SO_4)].H_2O$	0.95	1041.5	1303.3	1.76	2.70
2	$[Mn(L^1)_2Cl_2].H_2O$	12.92	13669.36	13929.36	5.76	8.74
3	$[Co(L^1)_2Cl_2].H_2O$	8.93	9483.66	9713.66	4.81	9.79
4	$[Ni(L^1)_2Cl_2].H_2O$	2.93	3111.66	3371.66	2.83	11.77
5	$[Cu(L^1)_2Cl_2].H_2O$	0.9	960.3	1270.3	1.74	3.96
6	$[Zn(L^1)_2Cl_2].H_2O$	---	---	---	0.00	2.06
7	$[Cd(L^1)_2Cl_2].H_2O$	---	---	---	0.00	5.42
8	$[Hg(L^1)_2Cl_2].H_2O$	---	---	---	0.00	1.62
9	$[VO(L^2)_2(SO_4)].H_2O$	1.00	1305.0	1290.1	1.75	7.60
10	$[Mn(L^2)_2Cl_2].H_2O$	13.3	13273.4	13523.4	5.68	6.54
11	$[Co(L^2)_2Cl_2].H_2O$	9.51	9529.02	9779.02	4.83	16.80
12	$[Ni(L^2)_2Cl_2].H_2O$	3.13	3136.26	3386.26	2.84	22.20
13	$[Cu(L^2)_2Cl_2].H_2O$	1.00	1007	1257	1.73	10.48
14	$[Zn(L^2)_2Cl_2].H_2O$	---	---	---	0.00	2.53
15	$[Cd(L^2)_2Cl_2].H_2O$	---	---	---	0.00	4.61
16	$[Hg(L^2)_2Cl_2].H_2O$	---	---	---	0.00	1.73
17	$[VO(L^3)_2(SO_4)].H_2O$	0.8	913.6	1345.6	1.79	14.91
18	$[Mn(L^3)_2(H_2O)Cl]Cl.H_2O$	12.13	13609.86	14031.86	5.78	30.70
19	$[Co(L^3)_2(H_2O)Cl]Cl.H_2O$	7.9	8895.4	9317.4	4.71	32.92
20	$[Ni(L^3)_2Cl]Cl.H_2O$	---	---	---	Dia	34.80
21	$[Cu(L^3)_2Cl_2].H_2O$	0.98	1090.74	1306.74	1.76	21.60
22	$[Zn(L^3)_2Cl_2].H_2O$	---	---	---	0.00	14.82
23	$[Cd(L^3)_2Cl_2].H_2O$	---	---	---	0.00	14.90
24	$[Hg(L^3)_2Cl_2].H_2O$	---	---	---	0.00	17.62

(3.2.5) FT-IR spectra of ligand's [L^1, L^2 and L^3] complexes [(1)-(24)].

(3.2.5.1) FT-IR spectra of ligand's [L^1] complexes [(1)-(8)].

The FT- IR spectra of synthesized complexes (1-8) are shown in Fig. (3-23) - (3-30) respectively. The assignment of the characteristic bands are summarized in table (3-21). The IR spectra of these prepared complexes were compared with that of free ligand (L^1) to determine the coordination sites involved in chelation, and that means the position of some guide bands in the spectrum of free ligand were expected to change upon chelation [143].

The detected band at (1633) cm^{-1} assigned to the stretching frequency of azomethine group (υC=N) of the free ligand . This band was shifted to higher frequency at range (1652-1639) cm^{-1} in spectra of all prepared complexes, this shift to higher frequency may be due to involved nitrogen atom of azomethine group in coordination with metal ions [70].

The band at (1611) cm^{-1} stretching vibration which refers to υC=N for thaizol ring of free ligand was shifted to higher frequency at range (1628-1611) cm^{-1} in the spectra of all complexes, showed that the coordination between nitrogen atom of this group (C=N) and metal ions was happened[144]. The weak band at (709) cm^{-1} assigned to υ(C-S-C) in IR spectrum of free ligand appeared in range (705-709) cm^{-1} in IR spectra of all complexes. Slightly or no change of this band indicating noninvolvement of S atom of thaizol ring in coordination [145]. The new band in the IR spectrum of VO(II) complex at (975) cm^{-1} was attributed to υV=O group [146]. Also new other bands in the spectrum of VO(II) complex, at (1049, 891) cm^{-1} and at (644, 424) cm^{-1} which refer to υ(SO_4^{-2}) and δ(SO_4^{-2}) respectively indicates that the SO_4^{-2} involved in the coordination with VO(II) ion as monodentate ligand [116, 147]. At the lower frequency region, the IR spectra of all synthesized complexes showed new bands ,which are

not present in the spectrum of the free ligand, these bands are located at (588– 509) cm^{-1} attributed to υ(M-N) [65,148].The band at (3376, 3370) cm^{-1} in spectra of all complexes was attributed to ν(N-H) overlap with band of H_2O hydrate [149] excepting Mn(II) and Co(II) complexes the band of H_2O hydrate appeared at (3452 , 3458) respectively.

These observation in the IR spectra of the ligand (L^1) and it's complexes indicate that the ligand coordinates with metal ions: VO(II), Mn(II), Co(II), Ni(II), Cu(II), Zn(II), Cd(II), and Hg(II) via nitrogen atom of (C=N) group of thaizol ring and nitrogen atom of azomethine group, behaving bidentate ligand toward these metal ions.

Table (3-21): Infrared spectral data (cm^{-1}) of the ligand [L^1] and its metal complexes.

No.	compounds	ν(N-H) group	ν(C=N) imin	ν(C=N) inplane	C-S-C	M-N	Additional bands
	$[L^1]$	3367 (m)	1633 (m)	1611 (m)	709 (w)	-	$\nu(CH_{Ar.})3055_{(w)}$,$\nu(CH_{alph.})2947_{(w)}$, $\nu(CH_3O_{asy})1280_{(w)}$,$\nu(CH_3O_{sy})1067_{(m)}$ $\delta(CH_3O)$in plane $540_{(w)}$,
1	$[VO(L^1)_2(SO_4)].H_2O$	3367 (m)	1644 (s)	1619 (m)	709 (w)	582 (w)	$\nu(CH_{Ar.})3055_{w)}$, $\nu(CH_{alph.})2951_{(w)}$, $\nu(CH_3O_{asy})1273_{(w)}$,$\nu(CH_3O_{sy})1091_{(m)}$ $\delta(CH_3O)$in plane $543_{(w)}$,V=O)$975_{(m)}$, ν(OSO)1049,891 , δ(OSO)644,424
2	$[Mn(L^1)_2Cl_2].H_2O$	3367 (m)	1645 (m)	1621 (s)	705 (w)	509 (w)	$\nu(CH_{Ar.})2997_{(w)}$,$\nu(CH_{alph.})2947_{(w)}$, $\nu(CH_3O_{asy})1273_{(s)}$,$\nu(CH_3O_{sy})1091_{(m)}$, $\delta(CH_3O)$in plane $536_{(w)}$, hydrate (H_2O) 3452
3	$[Co(L^1)_2Cl_2].H_2O$	3367 (m)	1650 (s)	1615 (s)	705 (w)	586 (w)	$\nu(CH_{Ar.})3059_{(w)}$,$\nu(CH_{alph.})2951_{(w)}$, $\nu(CH_3O_{asy})1276_{(s)}$,$\nu(CH_3O_{sy})1095_{(m)}$ $\delta(CH_3O)$in plane $543_{(w)}$, hydrate (H_2O) 3458
4	$[Ni(L^1)_2Cl_2].H_2O$	3370 (m)	1652 (m)	1618 (s)	709 (w)	586 (w)	$\nu(CH_{Ar.})3062_{(w)}$,$\nu(CH_{alph.})2958_{(w)}$, $\nu(CH_3O_{asy})1280_{(s)}$,$\nu(CH_3O_{sy})1111_{(m)}$ $\delta(CH_3O)$in plane $540_{(w)}$
5	$[Cu(L^1)_2Cl_2].H_2O$	3367 (m)	1639 (s)	1620 (s)	707 (w)	588 (w)	$\nu(CH_{Ar.})3059_{(w)}$,$\nu(CH_{alf.})2954_{(w)}$, $\nu(CH_3O_{asy})1276_{(s)}$,$\nu(CH_3O_{sy})1091_{(m)}$ $\delta(CH_3O)$in plane $536_{(w)}$

6	$[Zn(L^1)_2Cl_2].H_2O$	3367 (m)	1640 (m)	1628 (s)	705 (w)	588 (w)	$\nu(CH_{Ar.})3059_{(w)}$,$\nu(CH_{alf.})2947_{(w)}$, $\nu(CH_3O_{asy})1261_{(s)}$,$\nu(CH_3O_{sy})1091_{(m)}$ $\delta(CH_3O)$in plane $540_{(w)}$
7	$[Cd(L^1)_2Cl_2].H_2O$	3367 (m)	1642 (m)	1626 (s)	705 (w)	588 (w)	$\nu(CH_{Ar.})3020_{(w)}$,$\nu(CH_{alph.})2947_{(w)}$ $\nu(CH_3O_{asy})1261_{(s)}$,$\nu(CH_3O_{sy})1091_{(m)}$ $\delta(CH_3O)$in plane $540_{(w)}$
8	$[Hg(L^1)_2Cl_2].H_2O$	3367 (m)	1639 (s)	1615 (s)	705 (w)	582 (w)	$\nu(CH_{aro.})2997_{(w)}$,$\nu(CH_{alf.})2947_{(w)}$, $\nu(CH_3O_{asy})1261_{(s)}$,$\nu(CH_3O_{sy})1097_{(m)}$ $\delta(CH_3O)$in plane $540_{(w)}$

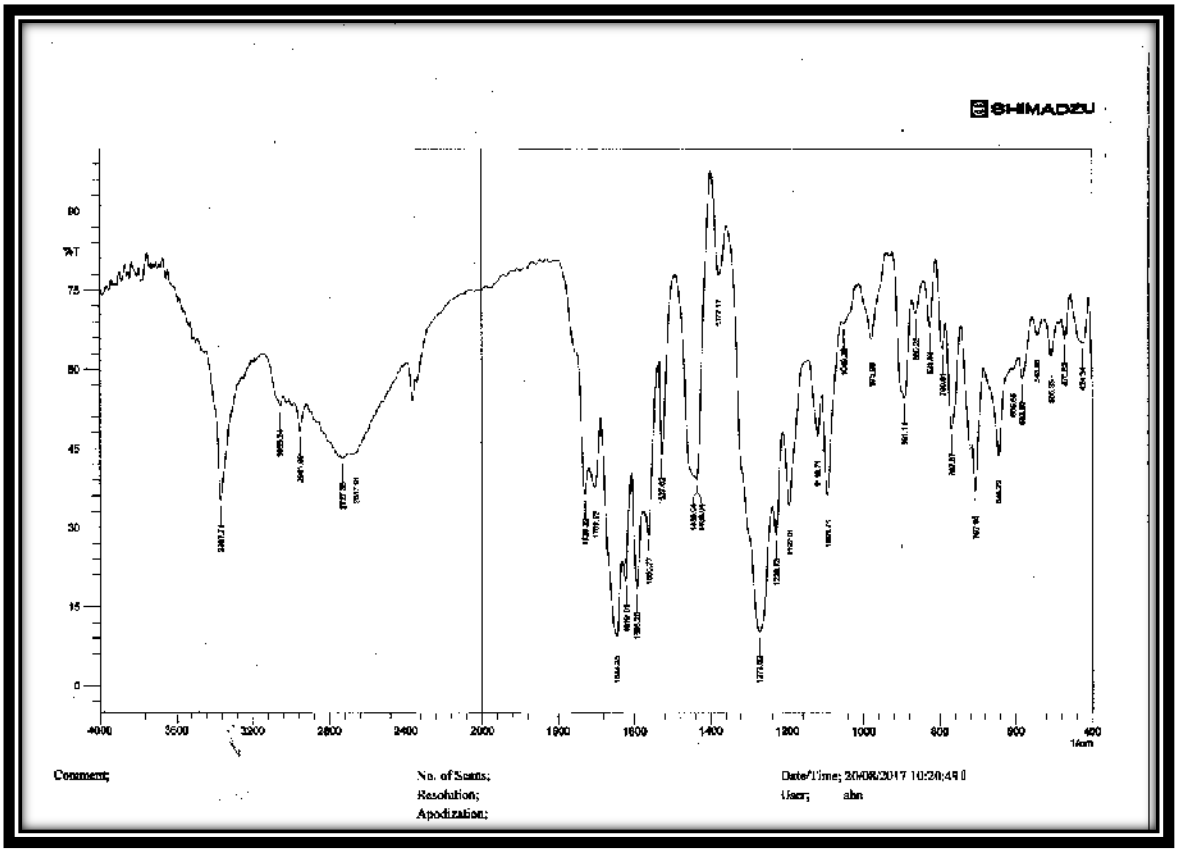

Fig. (3-23) FT-IR spectrum of $[VO(L^1)_2(SO_4)].H_2O$ (1).

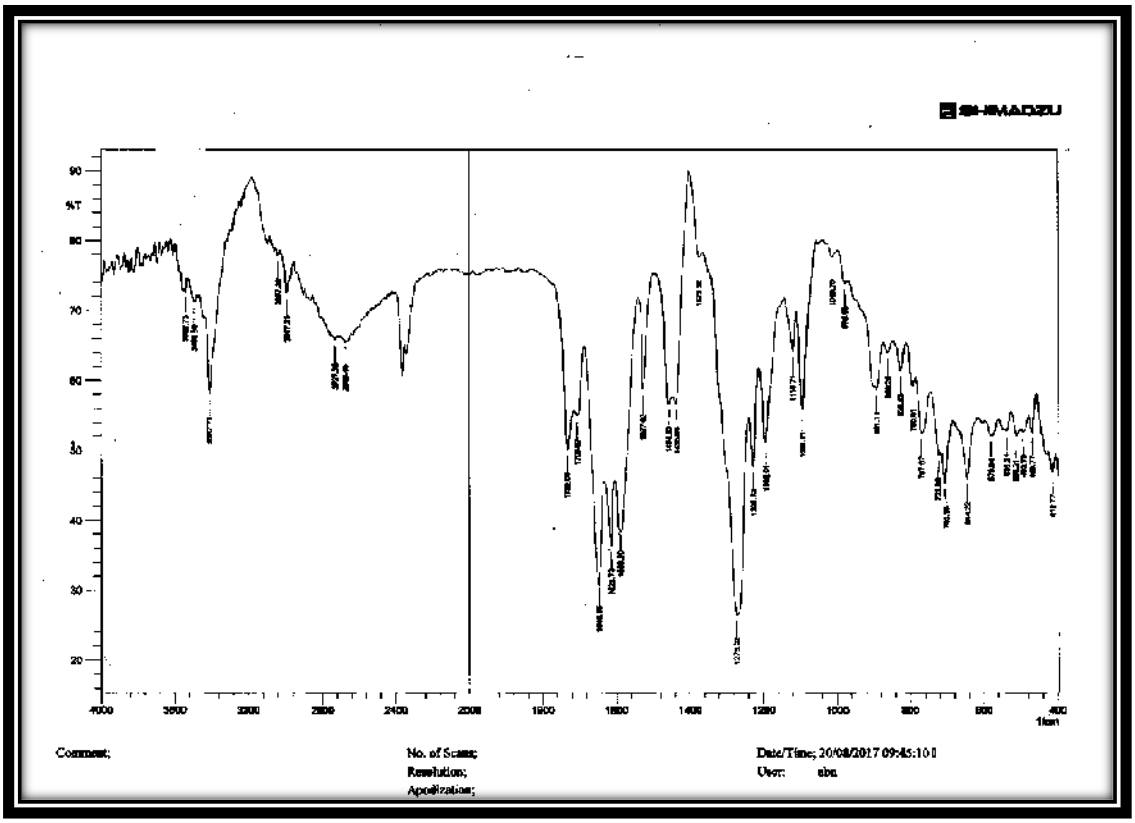

Fig. (3-24): FT- IR Spectrum of $[Mn(L^1)_2Cl_2].H_2O$ (2)

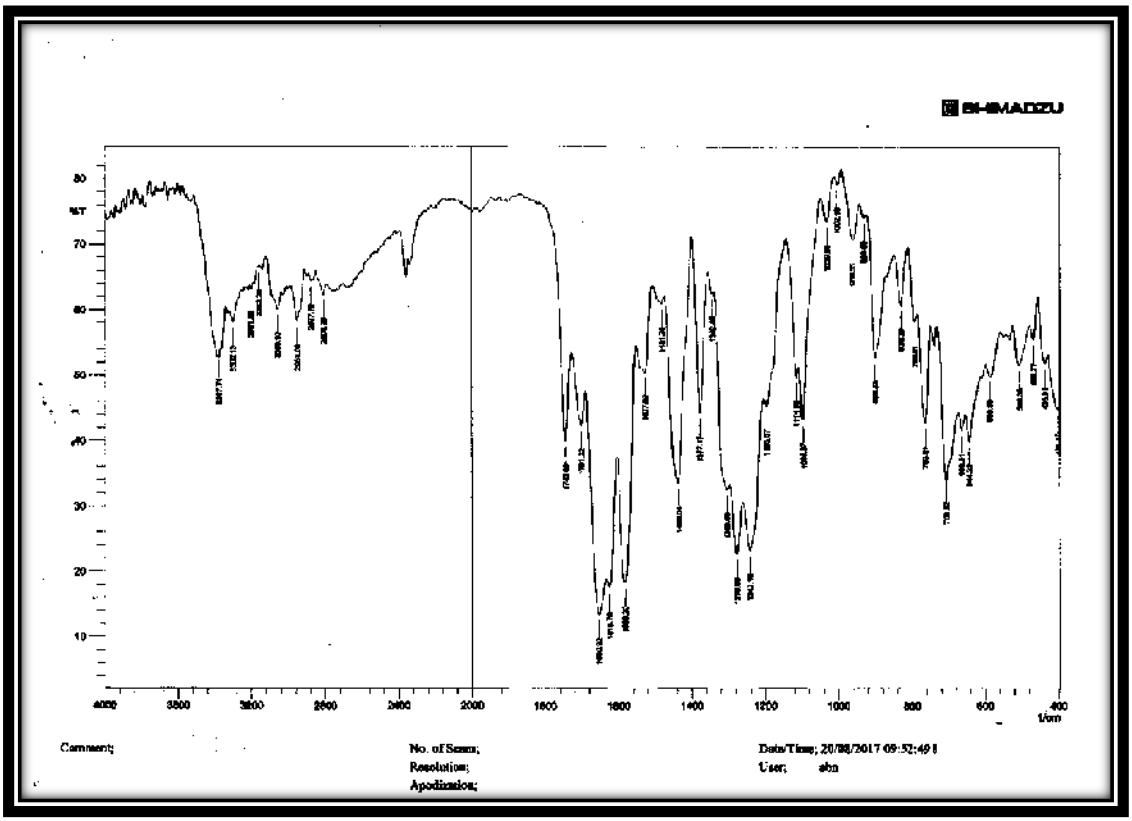

Fig. (3-25):FT-IR spectrum of $[Co\ (L^1)_2Cl_2].H_2O$ (3).

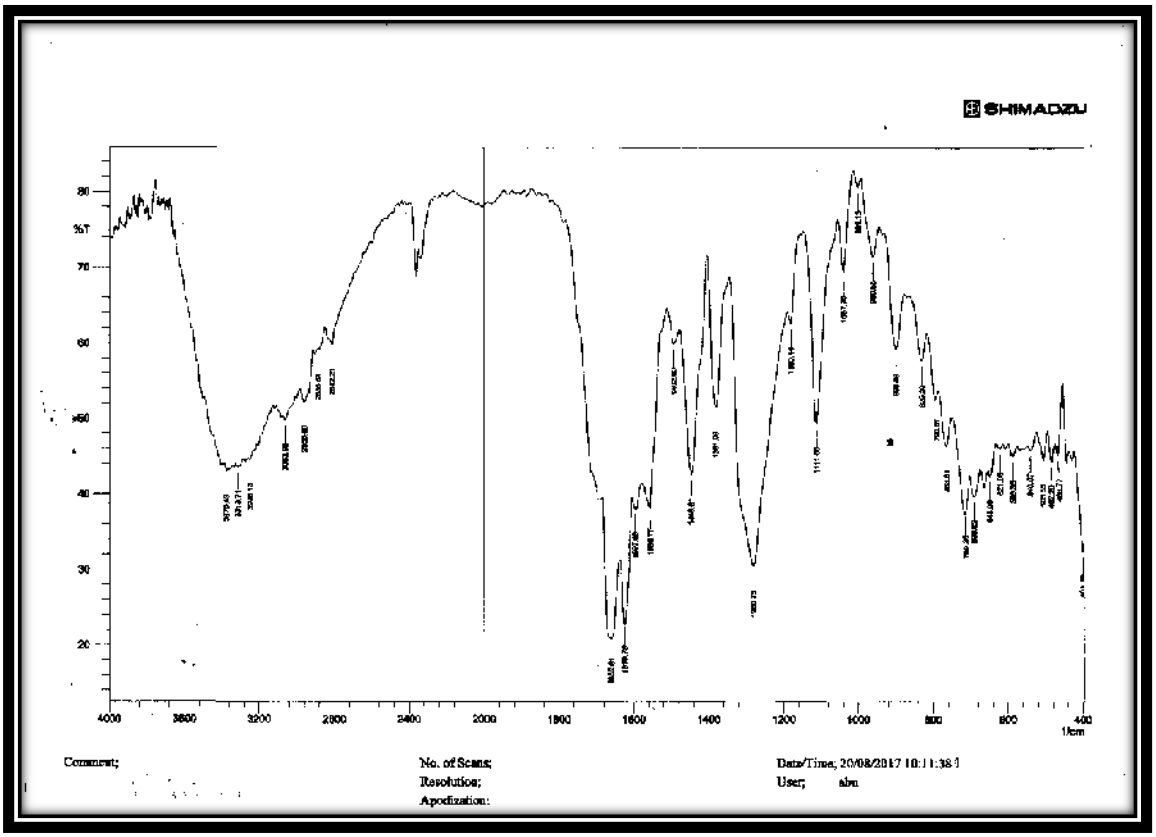

Fig. (3-26):FT-IR spectrum of [Ni $(L^1)_2Cl_2$].H_2O (4).

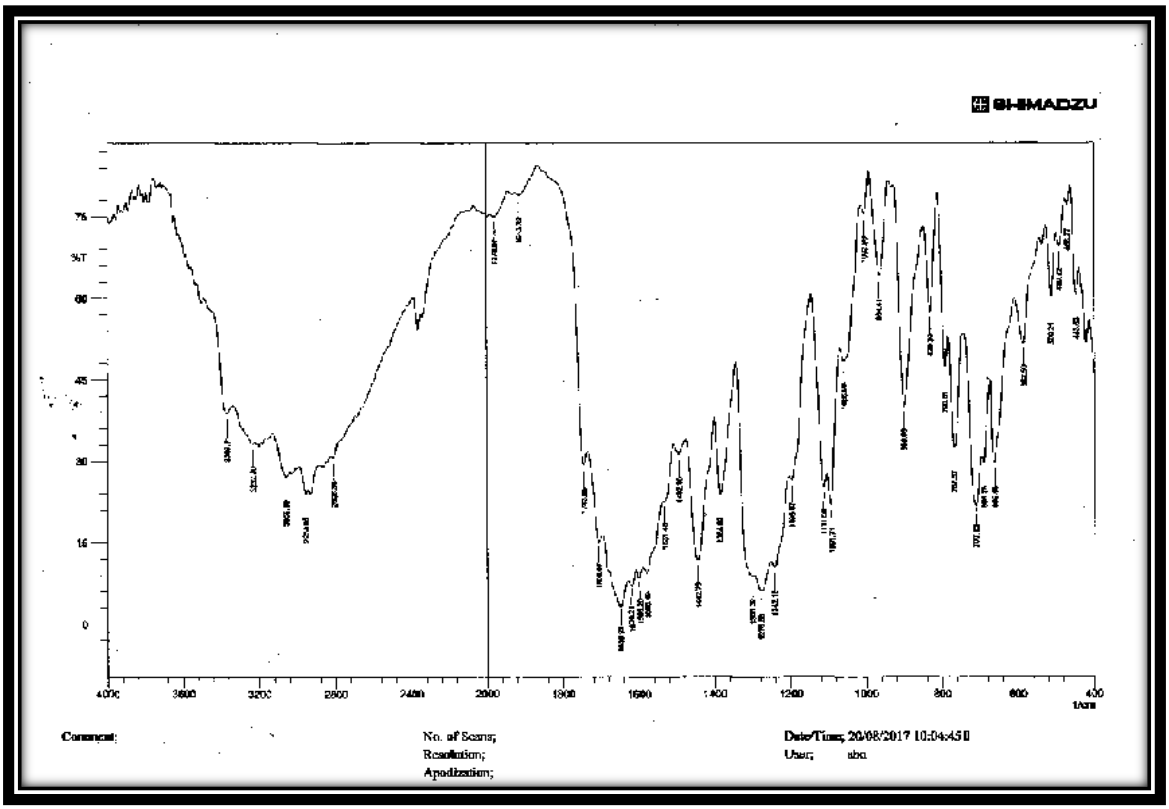

Fig. (3-27): FT-IR spectrum of [Cu $(L^1)_2Cl_2$].H_2O (5).

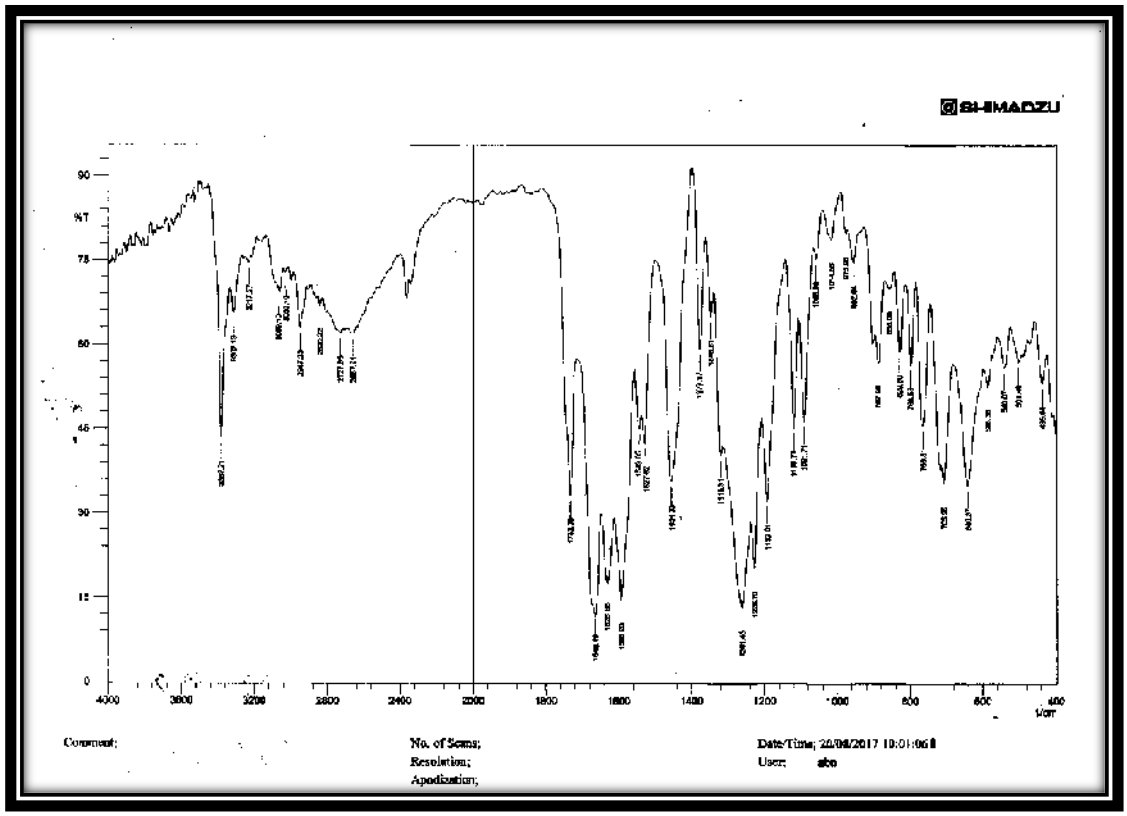

Fig. (3-28): FT-IR spectrum of $[Zn(L^1)_2Cl_2].H_2O$ (6).

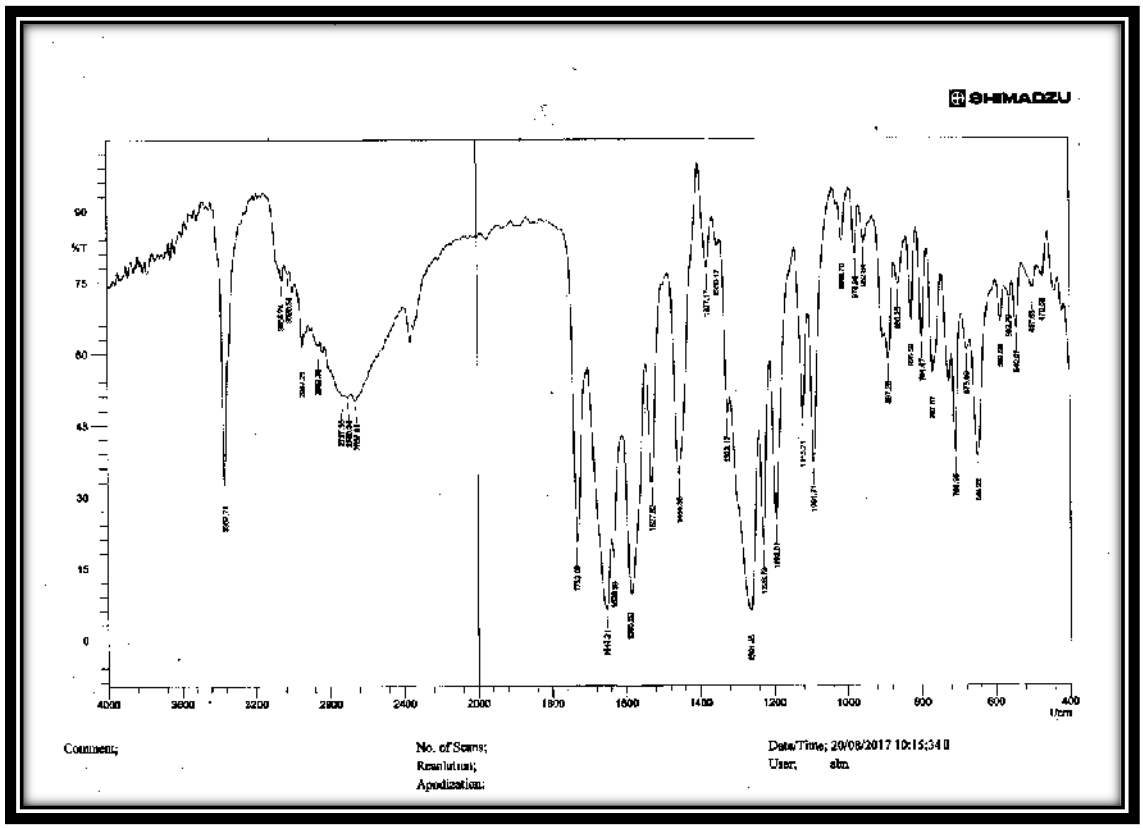

Fig. (3-29): FT-IR spectrum of $[Cd\ (L^1)_2Cl_2].H_2O$ (7).

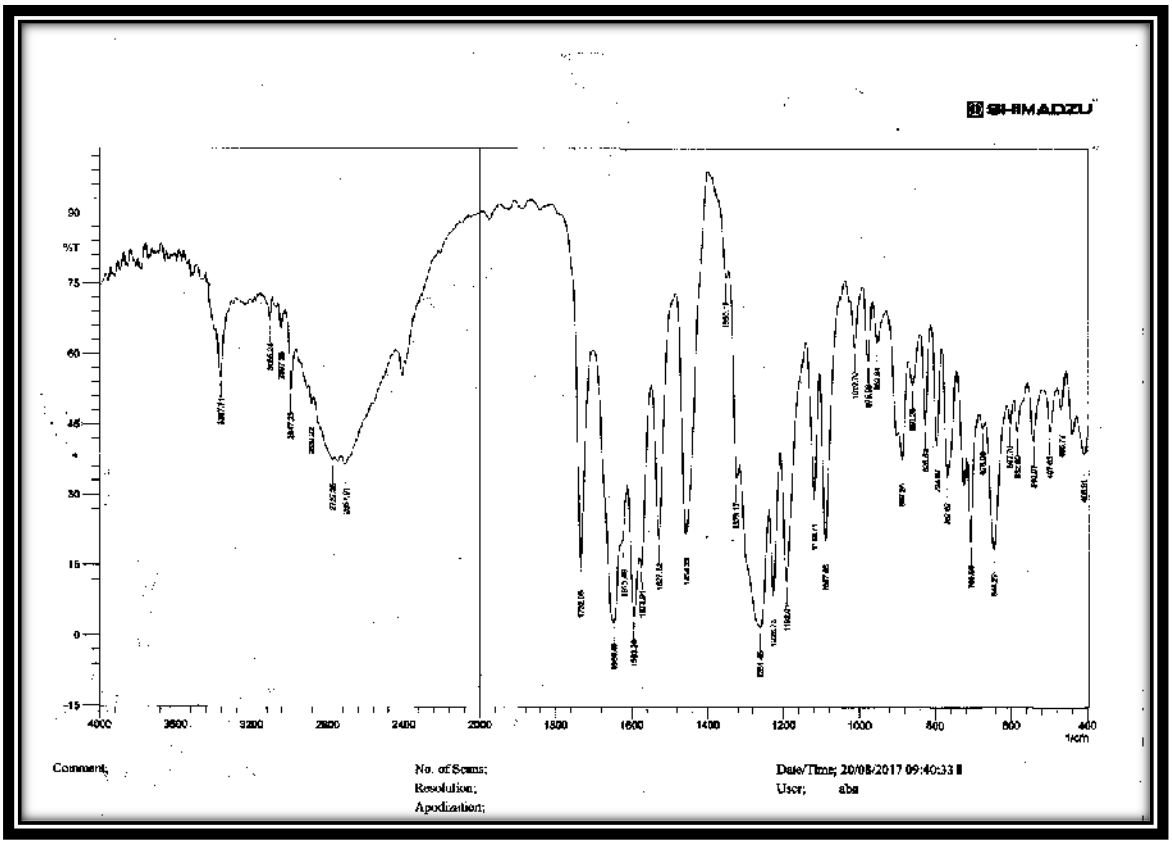

Fig. (3-30): FT-IR spectrum of [Hg $(L^1)_2Cl_2$].H_2O (8).

(3.2.5.2) FT-IR spectra of ligand's [L^2] complexes [(9)-(16)].

The FT- IR spectra for prepared complexes (9-16): are shown in Fig. (3-31) - (3-38) respectively. The assignment of the characteristic bands are summarized in table (3-22). The band at (1639) cm^{-1} assigned to the stretching frequency of azomethine group (υC=N) of the free ligand. This band was shifted to higher frequency at range (1651-1644) cm^{-1} in spectra of these prepared complexes. This shift to higher frequency may be due to involved nitrogen atom of azomethine group in coordination with metal ions(67).

On the other hand, the band at (1604) cm^{-1} stretching vibration which refers to υC=N for thaizol ring of free ligand, was shifted to higher frequency at range (1629-1617) cm^{-1} in the spectra of all complexes, showing that the coordination between nitrogen atom of this group (C=N)

and metal ions was happened[150]. The weak band at (709) cm^{-1} which is assigned for υ(C-S-C) in IR spectrum of free ligand appeared in range (705-709) cm^{-1} in IR spectra of all complexes. Slightly or no change of this band indicating noninvolvement of S atom of thaizol ring in coordination[145]. The new band in the IR spectrum of VO(II) complex at (952) cm^{-1} was attributed to υV=O group[146]. Also new other bands in the spectrum of VO(II) complex, at (1041, 990) cm^{-1} and at (644,489) cm^{-1} which refer to υ(SO_4^{-2}) and δ(SO_4^{-2}) respectively indicates that the SO_4^{-2} involved in the coordination with VO(II) ion as monodentate ligand[116,147]. At the lower frequency region, the IR spectra of all prepared complexes showed new bands which are not present in the spectrum of the free ligand, these bands are located at (598−509) cm^{-1}which are attributed to υ(M-N) [151]. The band at (3458 , 3471 , 3485) cm^{-1} was attributed to H_2O hydrate in spectra of Co(II), Cu(II), Cd(II) complexes respectively while the band at (3420, 3367) cm^{-1} in spectra of some complexes was attributed to ν(N-H) overlap with band of H_2O hydrate [149].

These observations in the IR spectra of the ligand (L^2) and it's complexes indicate that the ligand coordinates with metal ions: VO(II), Mn(II), Co(II), Ni(II), Cu(II), Zn(II), Cd(II), and Hg(II) via nitrogen atom of (C=N) group of thaizol ring and nitrogen atom of azomethine group, behaving bidentate ligand toward these metal ions.

Table (3-22): Infrared spectral data (cm^{-1}) of the ligand [L^2] and its metal complexes.

No.	compounds	ν(N-H) group	ν(C=N) imin	ν(C=N) inplane	C-S-C	M-N	Additional bands
	[L^2]	3367 (m)	1639 (m)	1604 (s)	705 (w)	-	$\nu(CH_{Ar.})3055_{(w)}$,$\nu(CH_{alph.})2947_{(w)}$
9	$[VO(L^2)_2(SO_4)].H_2O$	3367 (m)	1645 (m)	1626 (m)	705 (w)	570 (w)	$\nu(CH_{Ar.})3055_{w)}$,$\nu(CH_{alph.})2951_{(w)}$, $\nu(V=O)952_{(m)}$, ν(OSO)1041,990 , δ(OSO)644,489
10	$[Mn(L^2)_2Cl_2].\ H_2O$	3367 (m)	1645 (m)	1617 (s)	705 (w)	525 (w)	$\nu(CH_{Ar})2997_{(w)}$,$\nu(CH_{alph.})2947_{(w)}$,
11	$[Co(L^2)_2Cl_2].H_2O$	3402 (b)	1650 (s)	1624 (s)	709 (w)	596 (w)	$\nu(CH_{Ar.})3059_{(w)}$ $\nu(CH_{alph.})2951_{(w)}$, hydrate ($H_2O$) 3458
12	$[Ni(L^2)_2Cl_2].H_2O$	3402 (b)	1644 (s)	1619 (s)	705 (w)	598 (w)	$\nu(CH_{Aro.})3062_{(w)}$,$\nu(CH_{alph.})2958_{(w)}$,
13	$[Cu(L^2)_2Cl_2].H_2O$	3405 (m)	1651 (s)	1629 (m)	709 (m)	509 (w)	$\nu(CH_{Ar.})3059_{(w)}$,$\nu(CH_{alph.})2954_{(w)}$ hydrate (H_2O) 3471
14	$[Zn(L^2)_2Cl_2].H_2O$	3420 (m)	1648 (m)	1619 (s)	705 (m)	532 (w)	$\nu(CH_{Ar.})3059_{(w)}$,$\nu(CH_{alph.})2947_{(w)}$,
15	$[Cd(L^2)_2Cl_2].H_2O$	3367 (m)	1644 (m)	1627 (s)	705 (m)	535 (w)	$\nu(CH_{Ar.})3020_{(w)}$,$\nu(CH_{alph.})2947_{(w)}$ hydrate (H_2O) 3485
16	$[Hg(L^2)_2Cl_2].H_2O$	3367 (m)	1646 (s)	1623 (s)	705 (m)	593 (w)	$\nu(CH_{Ar.})2997_{(w)}$,$\nu(CH_{alf.})2947_{(w)}$

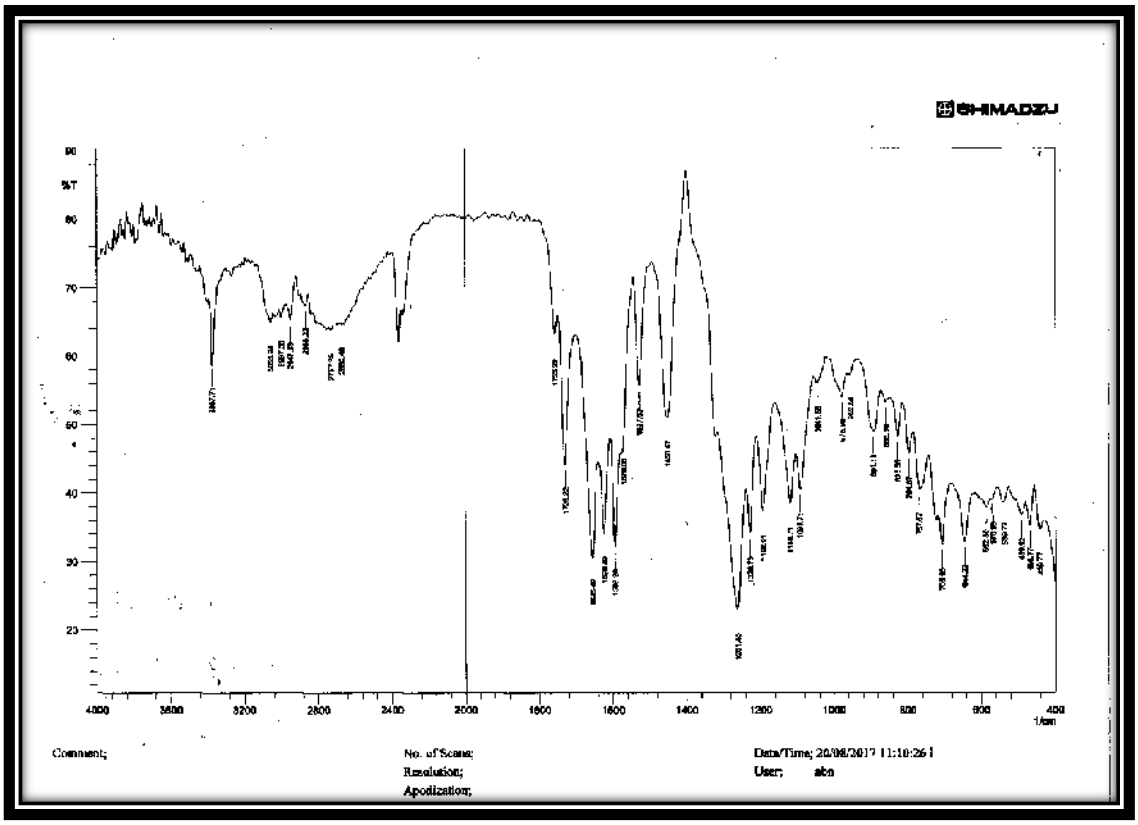

Fig.(3-31): FT-IR spectrum of $[VO(L^2)_2(SO_4)].H_2O$(9).

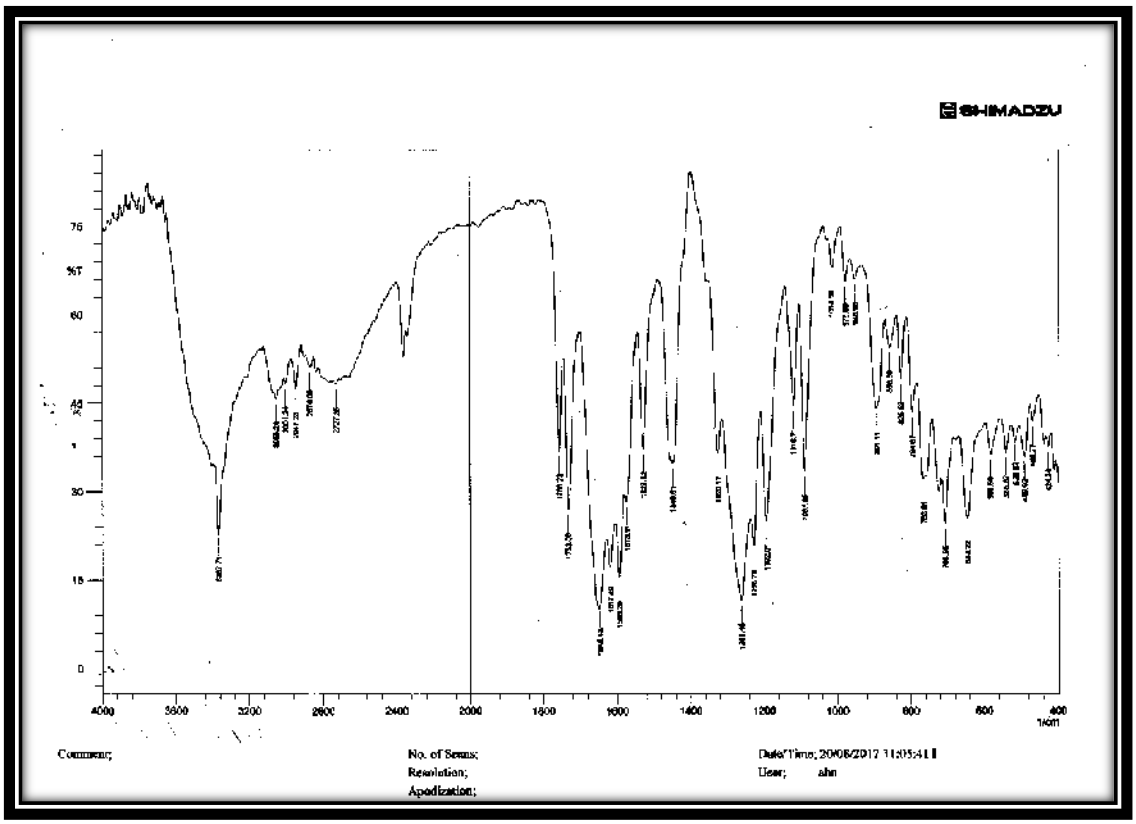

Fig.(3-32): FT-IR spectrum of $[Mn(L^2)_2Cl_2]$(10).

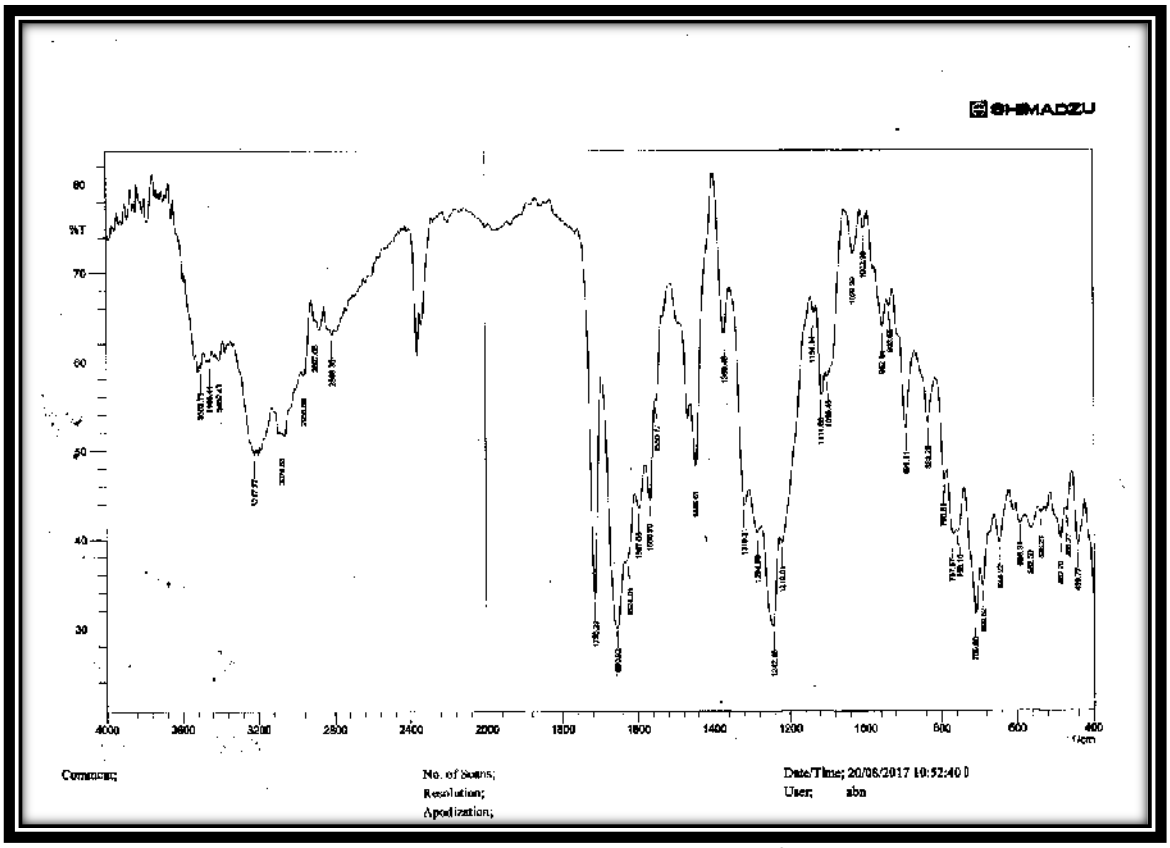

Fig.(3-33): FT-IR spectrum of $[Co(L^2)_2Cl_2].H_2O$(11).

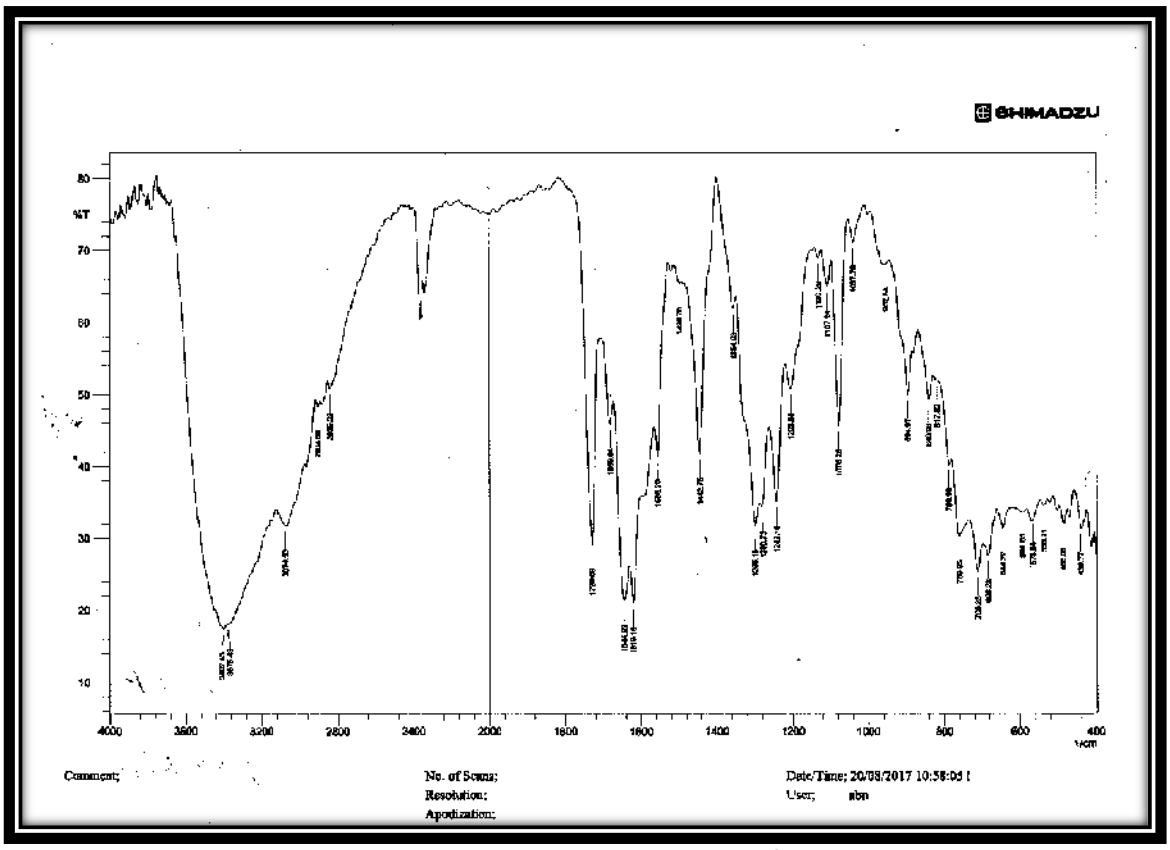

Fig.(3-34): FT-IR spectrum of $[Ni(L^2)_2Cl_2].H_2O$(12).

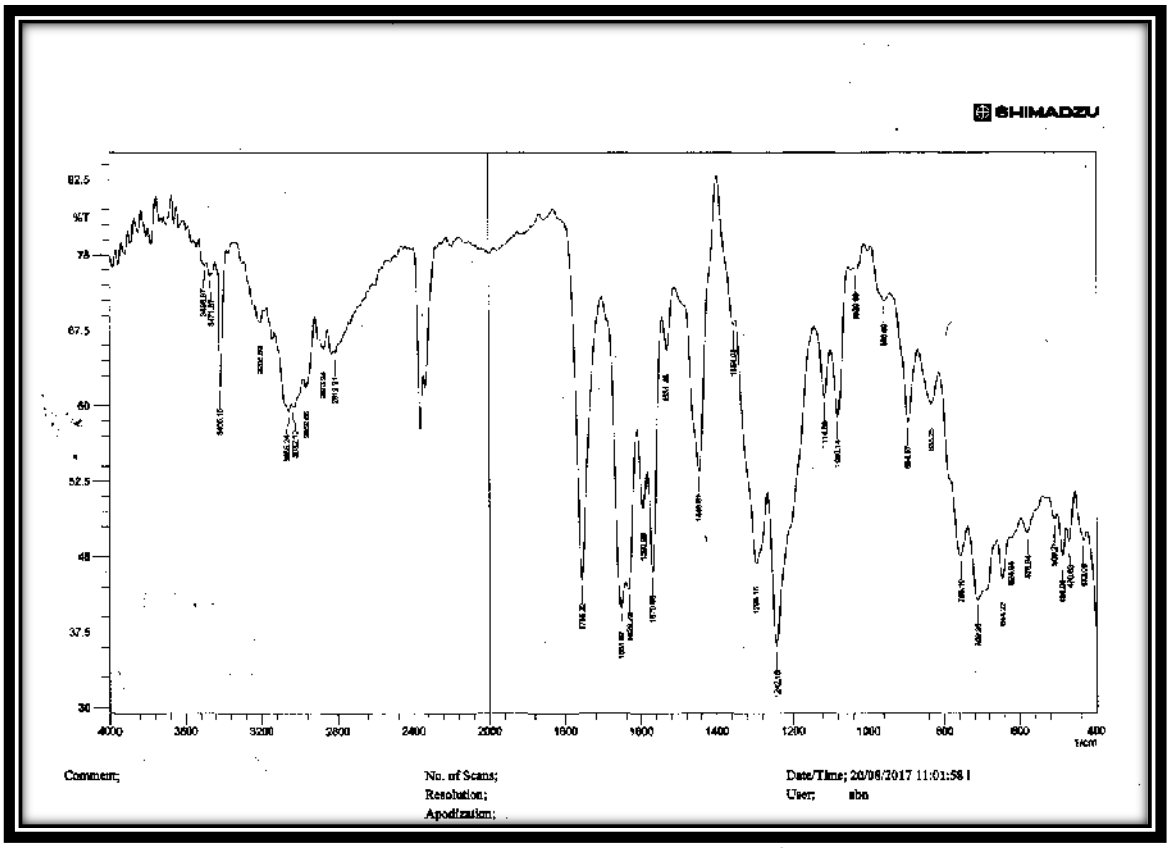

Fig.(3-35): FT-IR spectrum of $[Cu(L^2)_2Cl_2].H_2O$(13).

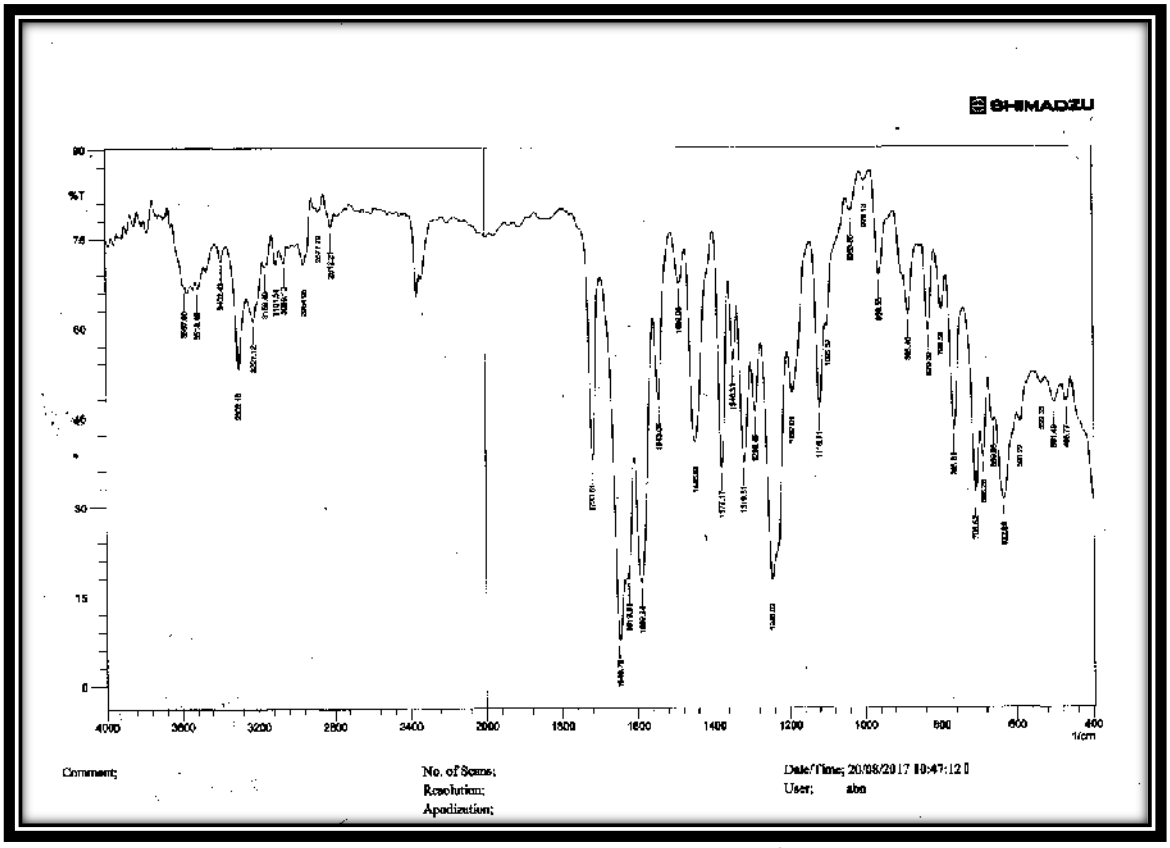

Fig.(3-36): FT-IR spectrum of $[Zn(L^2)_2Cl_2].H_2O$(14).

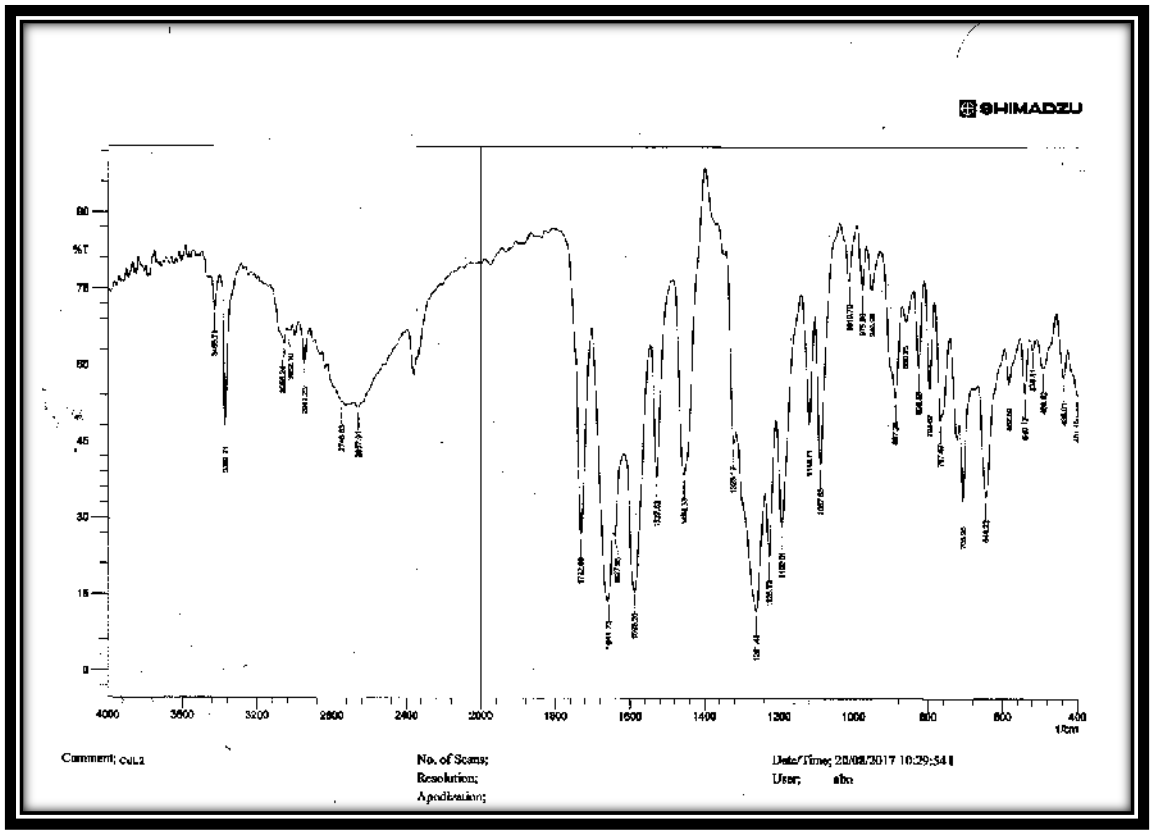

Fig.(3-37): FT-IR spectrum of $[Cd(L^2)_2Cl_2].H_2O$(15).

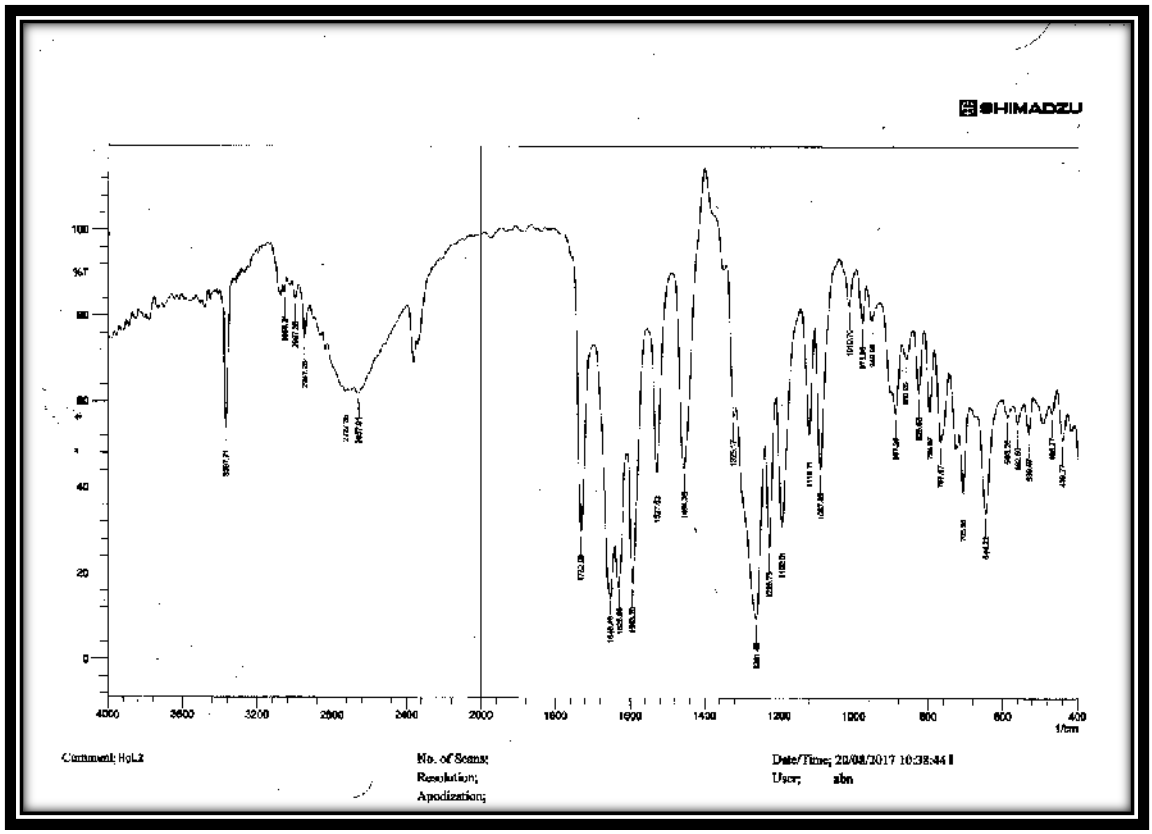

Fig.(3-38): FT-IR spectrum of $[Hg(L^2)_2Cl_2].H_2O$ (16).

(3.2.5.3) FT-IR spectra of ligand's [L^3] complexes [(17)-(24)].

The FT- IR spectra for prepared complexes (17-24) are shown in Fig. (3-39) to Fig. (3-46) respectively. The assignment of the characteristic bands are summarized in table (3-23). The detected band at (1635) cm^{-1} which was assigned to the stretching frequency of azomethine group υ(N=C) of the free ligand, this band was shifted to lower frequency at range (1629-1620) cm^{-1} in spectra of all synthesized complexes. This shift to lower frequency may be due to involved nitrogen atom of azomethine group in coordination with metal ions [152].

The band at (1645) cm^{-1} stretching vibration which refers to υC=O for 4-AAP ring of free ligand, was shifted to higher frequency at range (1660-1650) cm^{-1} in the spectra of all complexes, showing that the coordination between oxygen atom of this group (C=O) and metal ions was happened [153,154].

The IR spectra of all prepared complexes exhibited broad band at range (3446-3342) cm^{-1}, that may be attributed to υ(O-H) of hydrated water molecules in molecular formula of complexes [155] . Furthermore, band at (3420) cm^{-1} in spectra of Mn(II) and Co(II) complexes was attributed to ν(N-H) overlap with band of H_2O hydrate and the spectra of these complexes revealed new bands at (875 and 840) attributed to coordinated H_2O molecule (aqua) [156]. The new band in the IR spectrum of VO(II) complex at (995) cm^{-1} was attributed to υV=O group[146]. Also new other bands in the spectrum of VO(II) complex at (1033, 960) cm^{-1} and at (644 , 439) cm^{-1} which refer to $\upsilon(SO_4^{-2})$ and $\delta(SO_4^{-2})$ respectively indicates that the SO_4^{-2} involved in the coordination with VO(II) ion as monodentate ligand. [116,147] At the lower frequency region, the IR spectra of all prepared complexes showed new bands which are not present in the spectrum of the

free ligand. These bands are located at (559−516) cm^{-1} and at (455−493) cm^{-1} attributed to υ(M-N) and υ(M-O) respectively[157,158].

These observations in the IR spectra of the ligand (L^3) and it's complexes indicate that the ligand coordinates with metal ions: VO(II), Mn(II), Co(II), Ni(II), Cu(II), Zn(II), Cd(II), and Hg(II) via oxygen atom of (C=O) group of 4-AAP ring.

Table (3-23): Infrared spectral data (cm^{-1}) of the ligand [L^3] and its metal complexes.

No.	compounds	ν(N-H) group	ν(C=O)	ν(C=N) imin	M-N	M-O	Additional bands
	$[L^3]$	3367 (m)	1645 (s)	1635 (s)	-	-	$\nu(CH_{Ar.})3032_{(w)}$,$\nu(CH_{alph.})2958_{(w)}$,
17	$[VO(L^3)_2(SO_4)].H_2O$	3402 (b)	1653 (m)	1629 (s)	540 (m)	486 (m)	$\nu(CH_{Ar.})3055_{w)}$,$\nu(CH_{alph.})295_{w}$ $\nu(V=O)995_{(m)}$,ν(OSO)1033,960, δ(OSO)644,439, hydrated(H_2O)3483
18	$[Mn(L^3)_2(H_2O)Cl]Cl.H_2O$	3402 (b)	1651 (s)	1630 (s)	536 (m)	466 (w)	$\nu(CH_{Ar.})3070_{w)}$,$\nu(CH_{alph.})2962_{(w)}$, coordinated ($H_2O$)$875_{(w}$
19	$[Co(L^3)_2(H_2O)Cl]Cl.H_2O$	3406 (b)	1650 (m)	1630 (s)	516 (m)	439 (m)	$\nu(CH_{Ar.})3059_{(w)}$, $\nu(CH_{alph.})2945_{(w)}$, coordinated (H_2O)840
20	$[Ni(L^3)_2Cl]Cl.H_2O$	3402 (b)	1660 (m)	1624 (s)	559 (m)	486 (m)	$\nu(CH_{Ar.})3062_{(w)}$,$\nu(CH_{alph.})2904_{(w)}$, hydrated($H_2O$)3450
21	$[Cu(L^3)_2Cl_2].H_2O$	3402 (b)	1655 (m)	1640 (s)	547 (m)	482 (w)	$\nu(CH_{Ar.})3059_{(w)}$, $\nu(CH_{alph.})2954_{(w)}$,hydrated($H_2O$)3483
22	$[Zn(L^3)_2Cl_2].H_2O$	3403 (b)	1652 (m)	1630 (s)	551 (m)	455 (m)	$\nu(CH_{Ar.})3062_{(w)}$,$\nu(CH_{alf.})2958_{(w)}$ hydrated(H_2O)3533
23	$[Cd(L^3)_2Cl_2].H_2O$	3367 (b)	1655 (s)	1620 (s)	540 (m)	482 (m)	$\nu(CH_{Ar.})3062_{(w)}$,$\nu(CH_{alph.})2954_{(w)}$ hydrated(H_2O) 3483
24	$[Hg(L^3)_2Cl_2].H_2O$	3367 (m)	1659 (s)	1631 (s)	540 (m)	486 (m)	$\nu(CH_{Ar.})3059_{(w)}$,$\nu(CH_{alph.})2954_{(w)}$, hydrated($H_2O$)3445

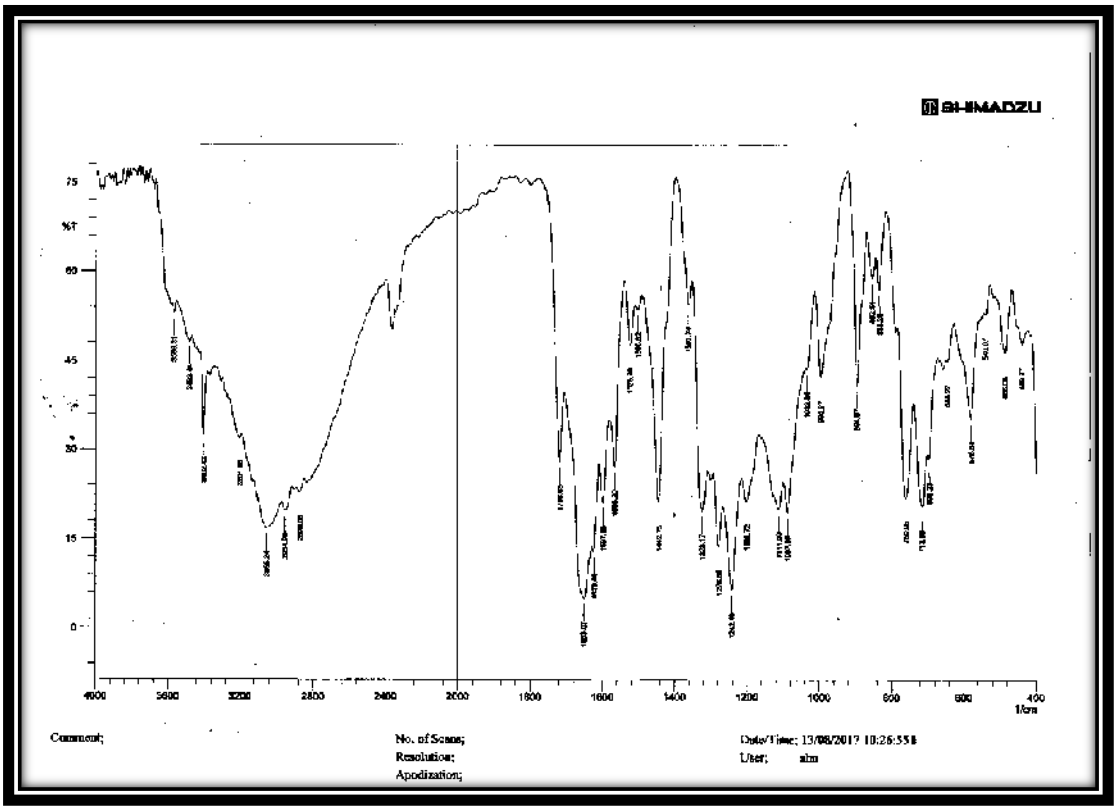

Fig.(3-39): FT-IR spectrum of $[VO(L^3)_2(SO_4)].H_2O$(17).

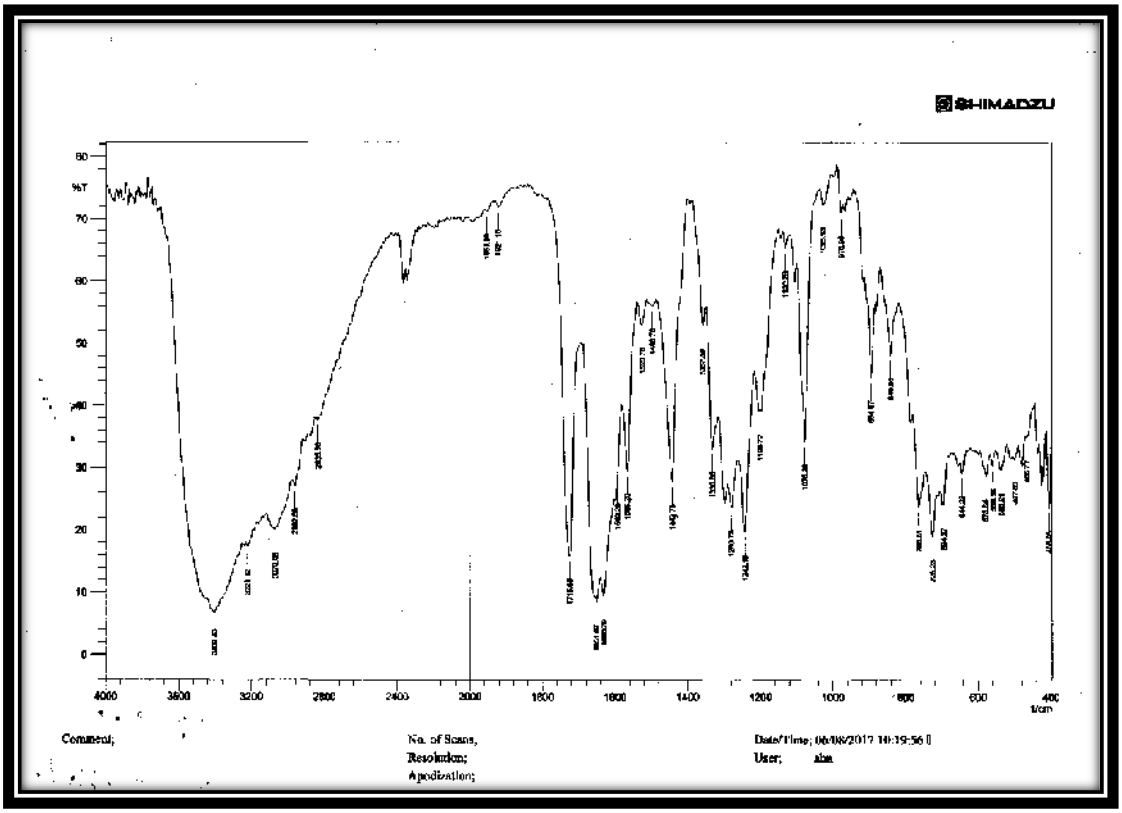

Fig.(3-40): FT-IR spectrum of $[Mn(L^3)_2(H_2O)Cl].H_2O$(18).

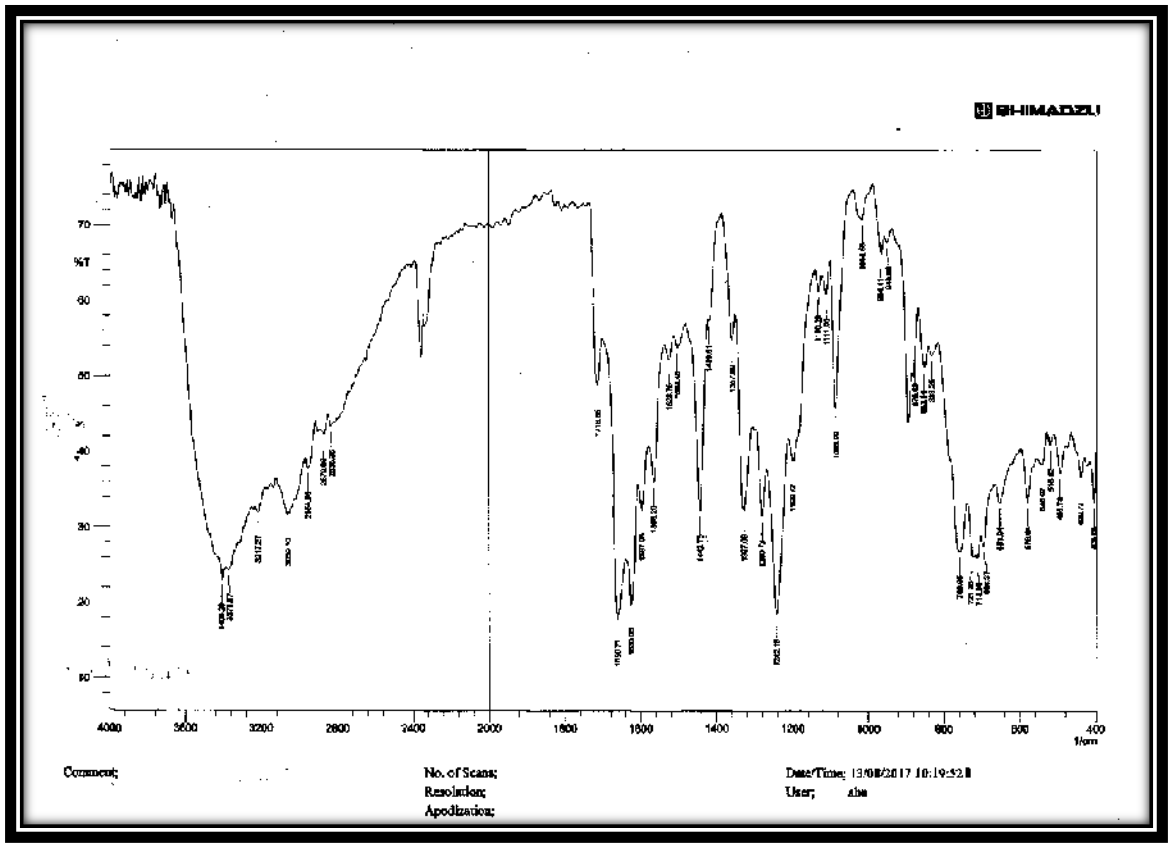

Fig.(3-41): FT-IR spectrum of $[Co(L^3)_2(H_2O)Cl].H_2O$(19).

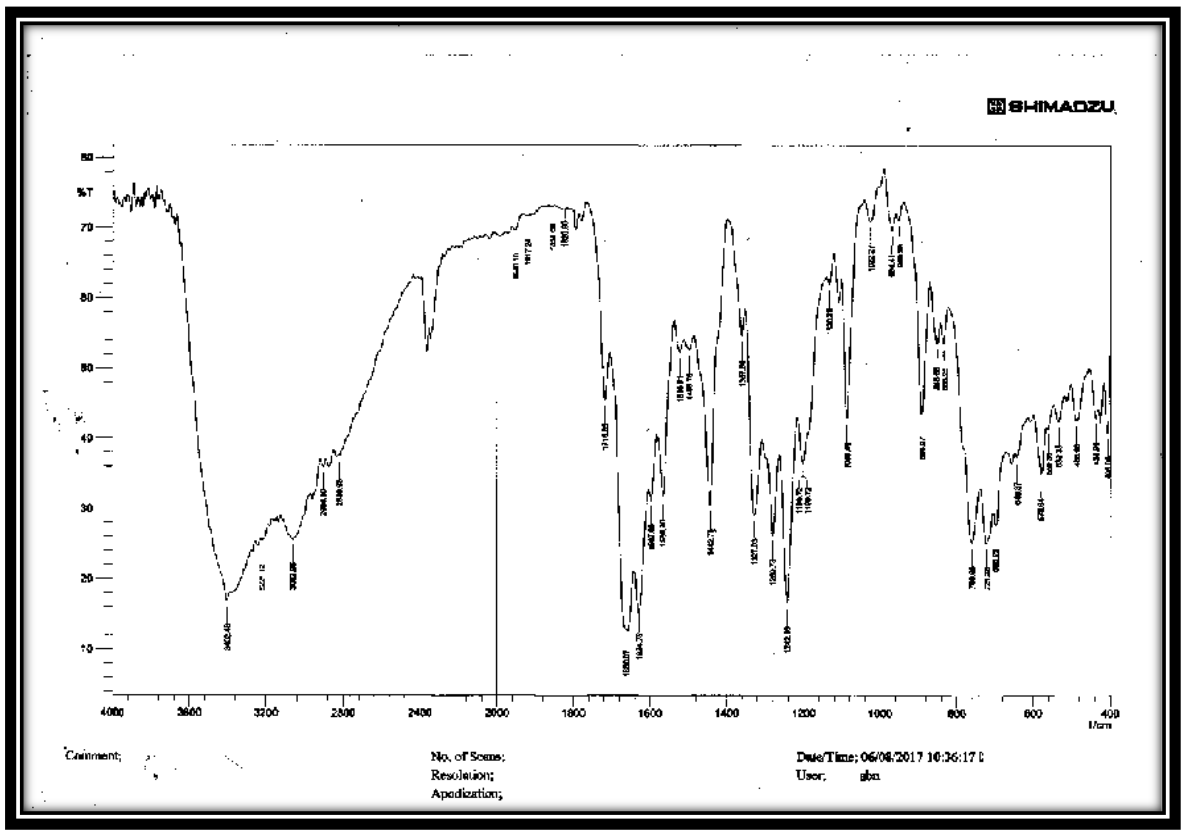

Fig.(3-42): FT-IR spectrum of $[Ni(L^3)_2Cl]Cl.H_2O$(20).

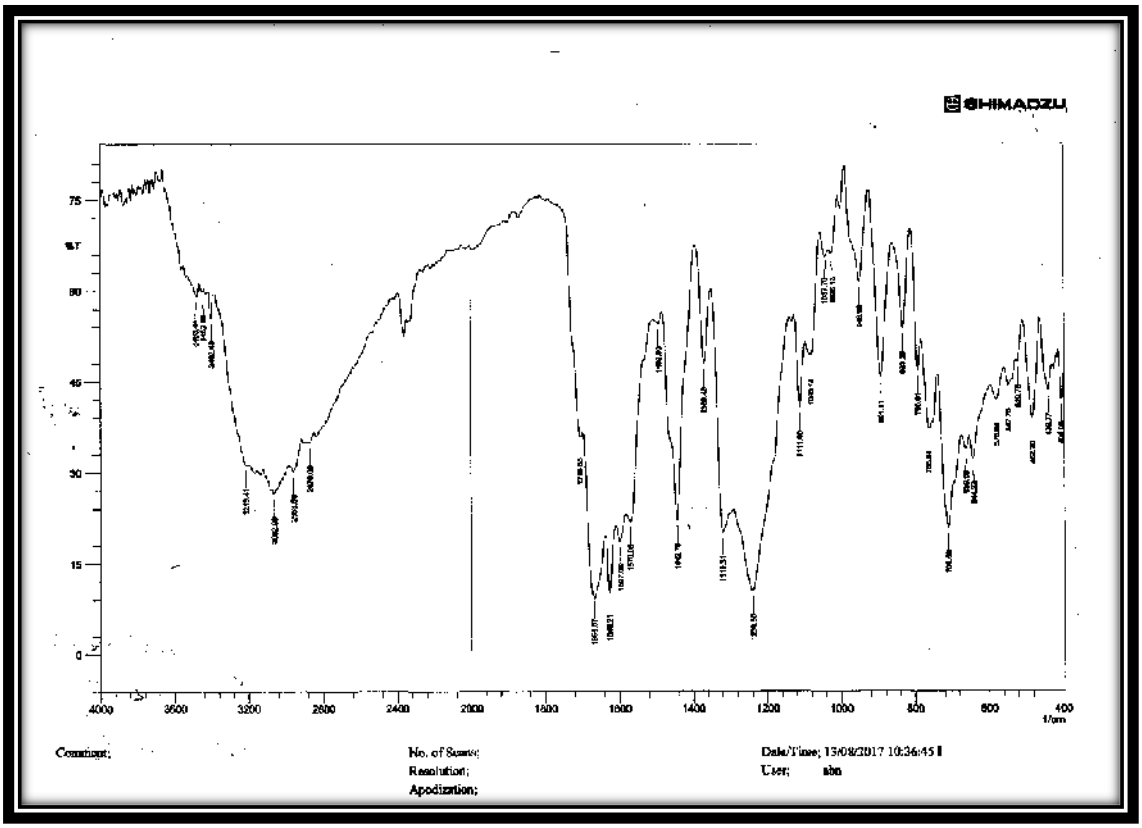

Fig.(3-43): FT-IR spectrum of $[Cu(L^3)_2Cl_2].H_2O$(21).

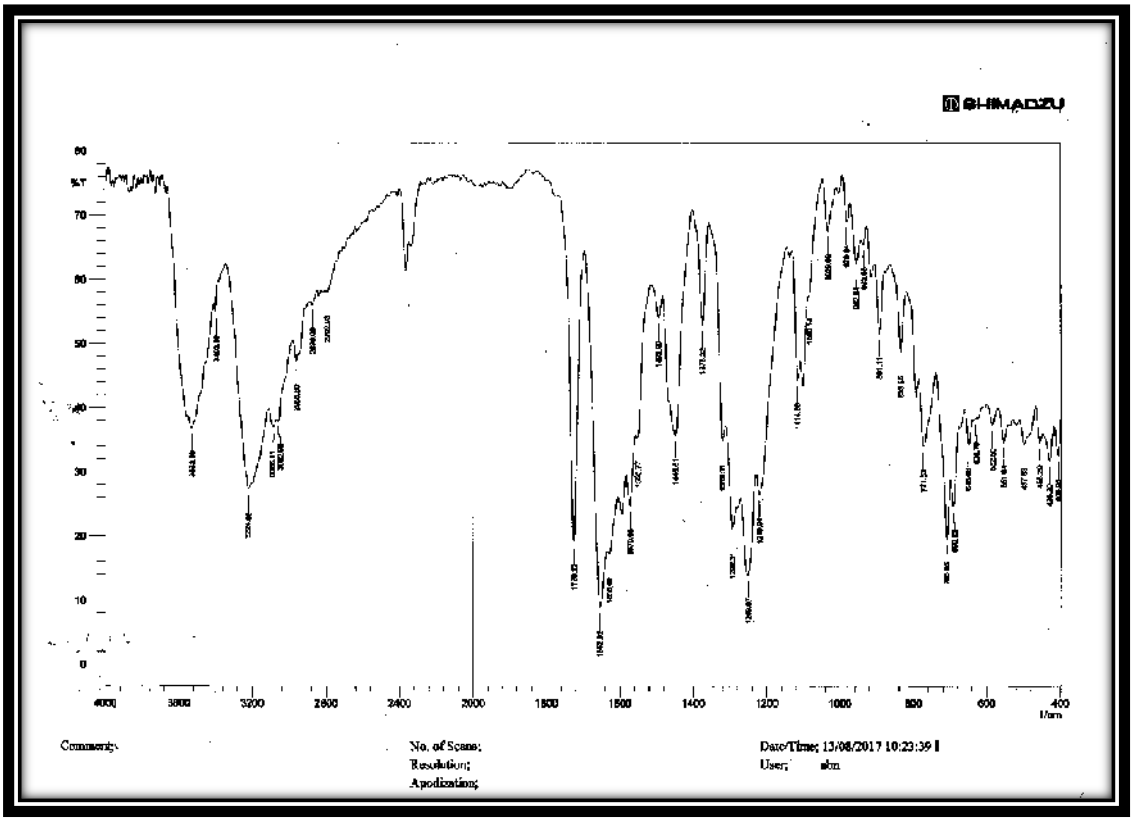

Fig.(3-44): FT-IR spectrum of $[Zn(L^3)_2Cl_2].H_2O$(22).

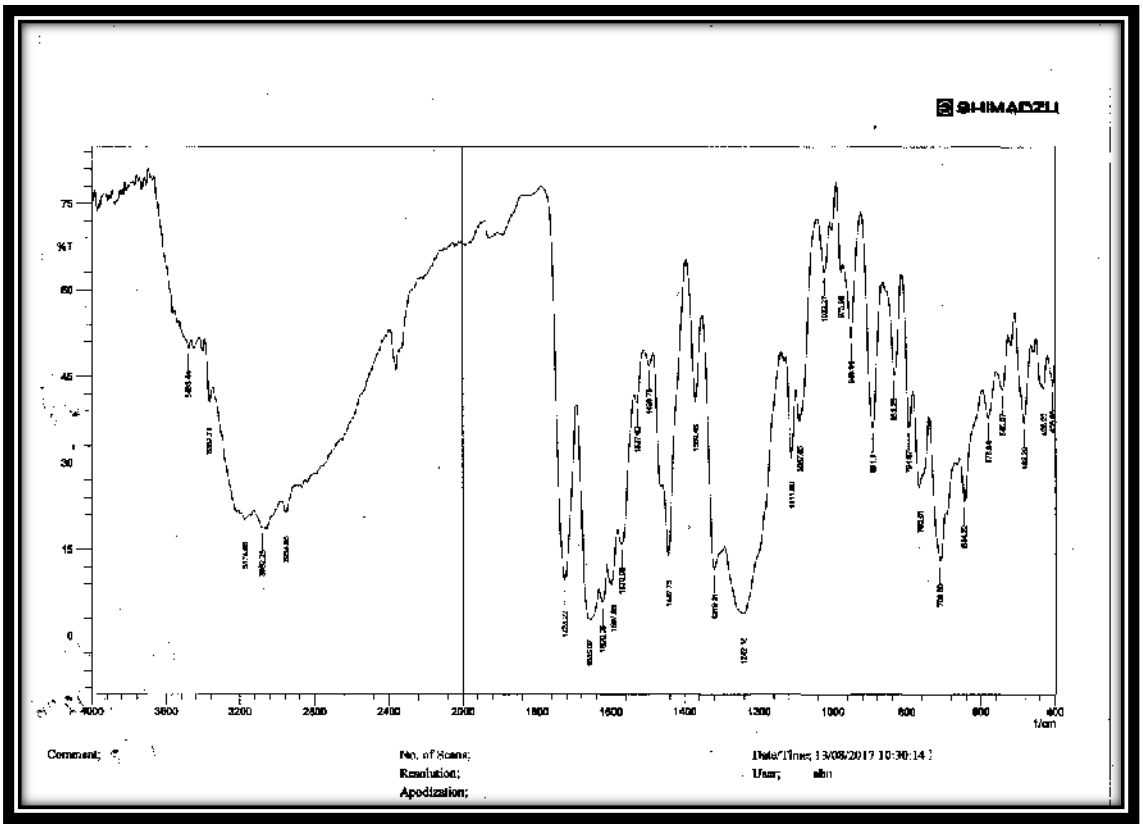

Fig.(3-45): FT-IR spectrum of $[Cd(L^3)_2Cl_2].H_2O$(23).

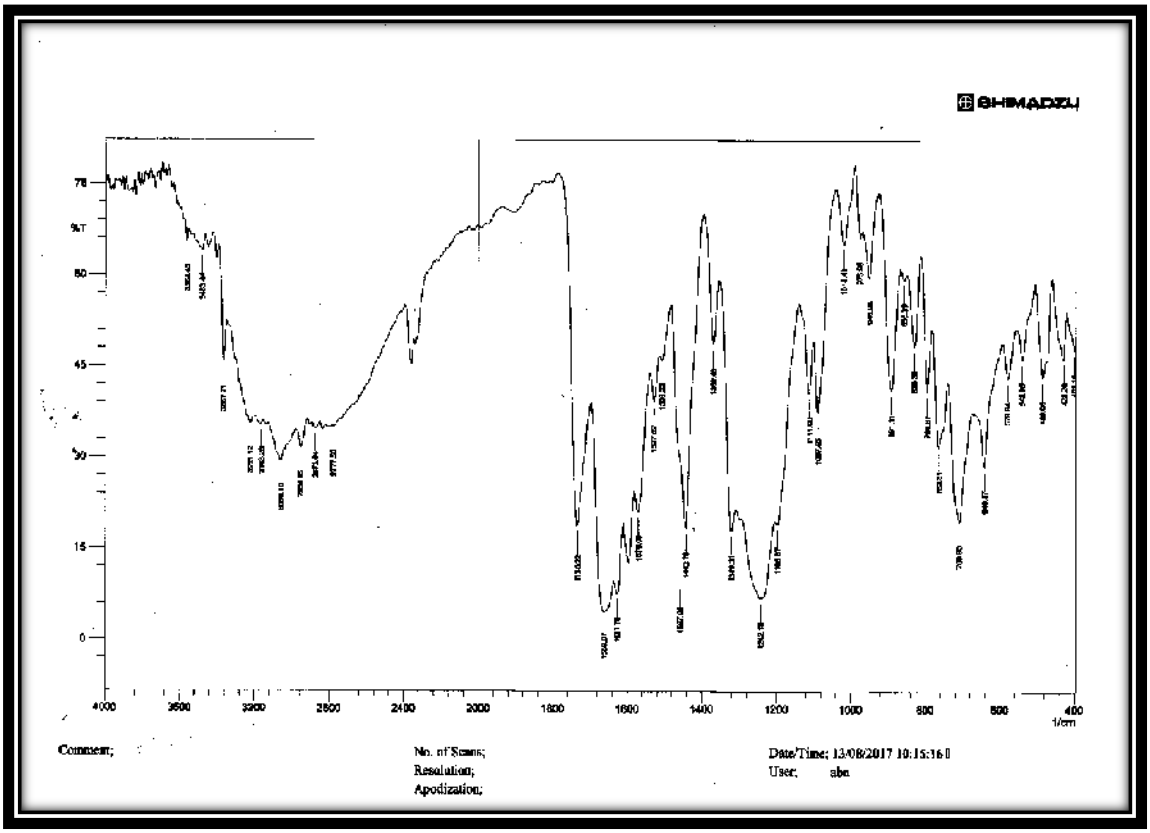

Fig.(3-46): FT-IR spectrum of $[Hg(L^3)_2Cl_2].H_2O$(24).

(3.2.6) (UV.-Vis.) spectra of ligand's [L^1, L^2 and L^3] complexes [(1)-(24)].

(3.2.6.1) (UV.-Vis.) spectra of ligand's [L^1] complexes [(1)-(8)].

The electronic spectral data for prepared complexes (1-8) were summarized in Table (3-24) together with electronic transitions and suggested geometrical formula. The electronic spectra for all synthesized complexes displayed three absorption peaks in the ultraviolet region. The first peak at range (266 –269) nm (37594 –37175) cm^{-1}, the second peak at range (301-346) nm (33222-28902) cm^{-1}. Besides to the third peak at range (359-379) nm (27855– 26385) cm^{-1} . The first two peaks were attributed to the intra-ligand $\pi \rightarrow \pi^*$, which exhibited bathochromic shift or hypsochromic shift when it comparison with that of free ligand . This confirming the coordination of the ligand to the central metal ion[159] , while the third peak was related to charge transfer electronic transition type (M→ L) [55].

$[VO(L^1)_2(SO_4)].H_2O$

The electronic spectrum of VO(II) complex Fig.(3-47) and (3-48) displayed three additional peaks. The first peak at (526) nm (19011) cm^{-1} and the second peak at (638) nm (15674) cm^{-1} besides to the third peak at (858) nm (11655) cm^{-1} , were attributed to (d-d) spin-allowed electronic transitions type $^2B_2g \rightarrow {}^2A_1g$, $^2B_2g \rightarrow {}^2B_1g$ and $^2B_2g \rightarrow {}^2Eg$ respectively, suggesting octahedral geometry about VO(II) ion[160].

$[Mn(L^1)_2Cl_2].H_2O$

The UV-Vis spectrum of Mn (II) complex, Fig. (3-49) and (3-50) showed three new peaks. The first peak at (466) nm (21459) cm^{-1} and the second peak at (575) nm (17391) cm^{-1} besides to the third peak at (682) nm (14663) cm^{-1} , were attributed to (d-d) spin-forbidden electronic transitions

type $^6A_1g \rightarrow {}^4T_2g_{(G)}$, $^6A_1g \rightarrow {}^4T_1g_{(G)}$ and $^6A_1g \rightarrow {}^4Eg_{(D)}$ respectively, indicating octahedral geometry around Mn(II) ion [161].

$[Co(L^1)_2Cl_2].H_2O$

The electronic spectrum of Co(II) complex showed three additional absorption peaks, Fig. (3-51) and (3-52). The first peak at (608) nm (16447) cm^{-1}, the second peak at (679) nm (14925) cm^{-1}, and the third peak at (977) nm (10235) cm^{-1} were attributed to (d-d) spin-allowed electronic transitions type $^4T_1g_{(F)} \rightarrow {}^4T_1g_{(P)}\upsilon_3$, $^4T_1g_{(F)} \rightarrow {}^4A_2g_{(F)}\upsilon_2$ and $^4T_1g_{(F)} \rightarrow {}^4T_2g_{(F)}\upsilon_1$ respectively, characteristic octahedral geometry around Co(II) ion [162].

$[Ni(L^1)_2Cl_2].H_2O$

The electronic spectrum of Ni(II) complex, Fig. (3-53) and (3-54) displayed three new absorption peaks. The first peak at (515) nm (19417) cm^{-1}, the second peak at (767) nm (13038) cm^{-1}, and the third peak at (831) nm (12034) cm^{-1} due to (d-d) spin-allowed electronic transitions type $^3A_2g_{(F)} \rightarrow {}^3T_1g_{(P)}\upsilon_3$, $^3A_2g_{(F)} \rightarrow {}^3T_1g_{(F)}\upsilon_2$ and $^3A_2g_{(F)} \rightarrow {}^3T_2g_{(F)}\upsilon_1$ which are a good evidence for octahedral geometry of Ni(II) complexes [163].

$[Cu(L^1)_2Cl_2].H_2O$

The UV-Vis spectrum of Cu(II) complex, Fig. (3-55) and (3-56) showed additional absorption peak at (862) nm (11601) cm^{-1} was attributed to (d-d) spin-allowed electronic transitions type $^2Eg \rightarrow {}^2T_2g$ confirming distorted octahedral geometry about Cu(II) ion[164].

$[Zn(L^1)_2Cl_2].H_2O$, $[Cd(L^1)_2Cl_2].H_2O$, and $[Hg(L^1)_2Cl_2].H_2O$

The electronic spectra of Zn(II), Cd(II), and Hg(II) complexes, Fig. [(3-57)- (3-62)] respectively, exhibit no peak in the visible region because of (d^{10}-system) of metal (II) ion. This means no (d-d) electronic transition happened [165].

Table (3-24): Electronic spectral data for [L^1] complexes.

No.	Compounds	λ (nm)	υ⁻ (cm^{-1})	εmax (molar^{-1} cm^{-1})	Assignment	Suggested Structure
	[L^1]	267	37453	3064	($\pi \rightarrow \pi^*$)	-
		305	32787	4516	($\pi \rightarrow \pi^*$)	
1	**[$VO(L^1)_2(SO_4)].H_2O$**	266	37594	2960	Intra-ligand	Oh
		313	31949	4152	Intra-ligand	
		364	27473	1446	LMC.T	
		526	19011	16	($^2B_2g \rightarrow {}^2A_1g$)	
		638	15674	22	($^2B_2g \rightarrow {}^2B_1g$)	
		858	11655	33	($^2B_2g \rightarrow {}^2Eg$)	
2	**[$Mn(L^1)_2Cl_2].H_2O$**	267	37453	2658	Intra-ligand	Oh
		301	33223	3955	Intra-ligand	
		362	27624	1396	MLC.T	
		466	21459	3	($^6A_1g \rightarrow {}^4T_2g_{(G)}$)	
		575	17391	4	($^6A_1g \rightarrow {}^4T_1g_{(G)}$)	
		682	14663	6	($^6A_1g \rightarrow {}^4Eg_{(D)}$)	
3	**[$Co(L^1)_2Cl_2].H_2O$**	266	37594	2594	Intra-ligand	Oh
		312	32051	3647	Intra-ligand	
		361	27701	1391	MLC.T	
		608	16447	96	($^4T_1g_{(F)} \rightarrow {}^4T_1g_{(P)}$)	
		679	14925	159	($^4T_1g_{(F)} \rightarrow {}^4A_2g_{(F)}$)	
		977	10235	20	($^4T_1g_{(F)} \rightarrow {}^4T_2g_{(F)}$)	

No.	Compounds	λ (nm)	υ⁻ (cm^{-1})	ε_{max} (molar^{-1} cm^{-1})	Assignment	Suggested Structure
4	$[Ni(L^1)_2Cl_2].H_2O$	268	37313	2720	Intra-ligand	Oh
		346	28902	2589	Intra-ligand	
		379	26385	1665	MLCT	
		515	19417	3	$(^3A_2g_{(F)} \rightarrow {}^3T_1g_{(P)})$	
		767	13038	13	$(^3A_2g_{(F)} \rightarrow {}^3T_1g_{(F)})$	
		831	12034	11	$(^3A_2g_{(F)} \rightarrow {}^3T_2g_{(F)})$	
5	$[Cu(L^1)_2Cl_2].H_2O$	269	37175	2995	Intra-ligand	Distorted Oh
		315	31746	3475	Intra-ligand	
		368	27174	1564	MLCT	
		862	11601	98	$(^2Eg \rightarrow {}^2T_2g)$	
6	$[Zn(L^1)_2Cl_2].H_2O$	266	37594	2438	Intra-ligand	Oh
		313	31949	3453	Intra-ligand	
		367	27248	1454	MLCT	
7	$[Cd(L^1)_2Cl_2].H_2O$	267	37453	2641	Intra-ligand	Oh
		314	31847	3293	Intra-ligand	
		359	27855	1353	MLCT	
8	$[Hg(L^1)_2Cl_2].H_2O$	268	37313	2098	Intra-ligand	Oh
		312	32051	2558	Intra-ligand	
		370	27027	1208	MLCT	

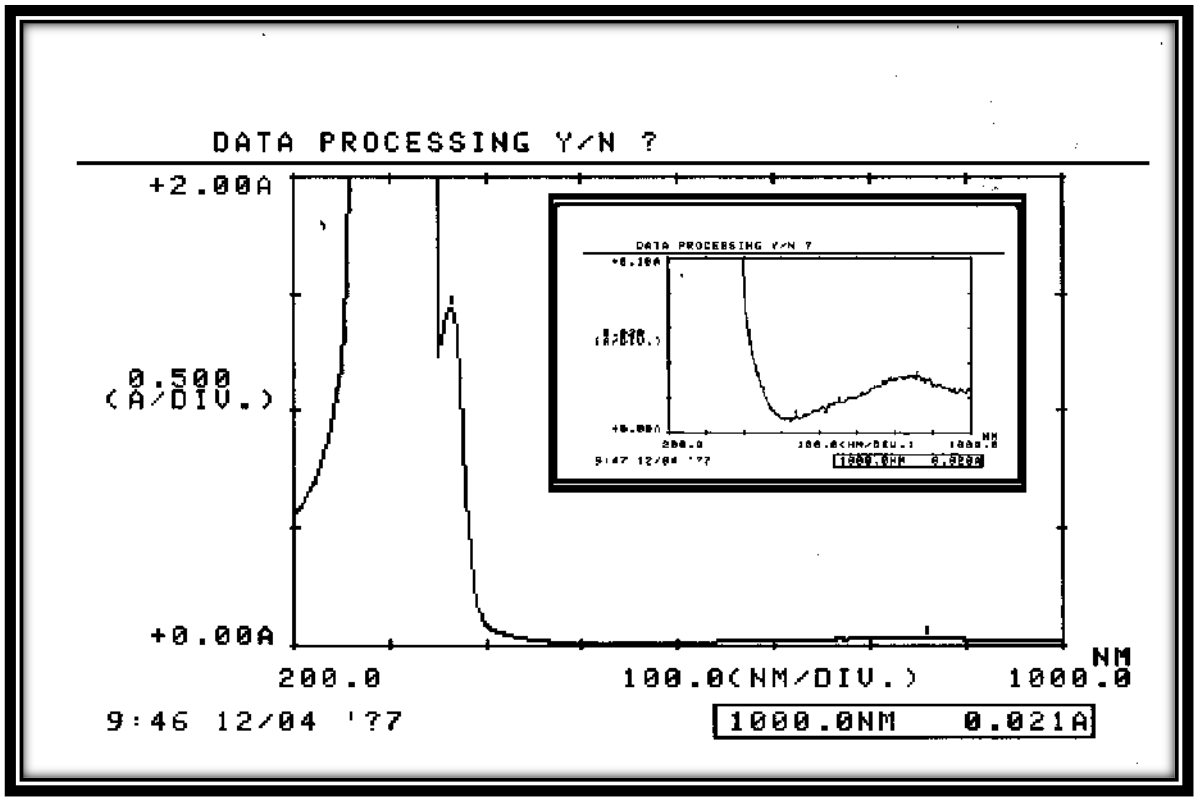

Fig.(3-47): Electronic spectrum of $[VO(L^1)_2(SO_4)].H_2O$ (1) in 10^{-3}M.

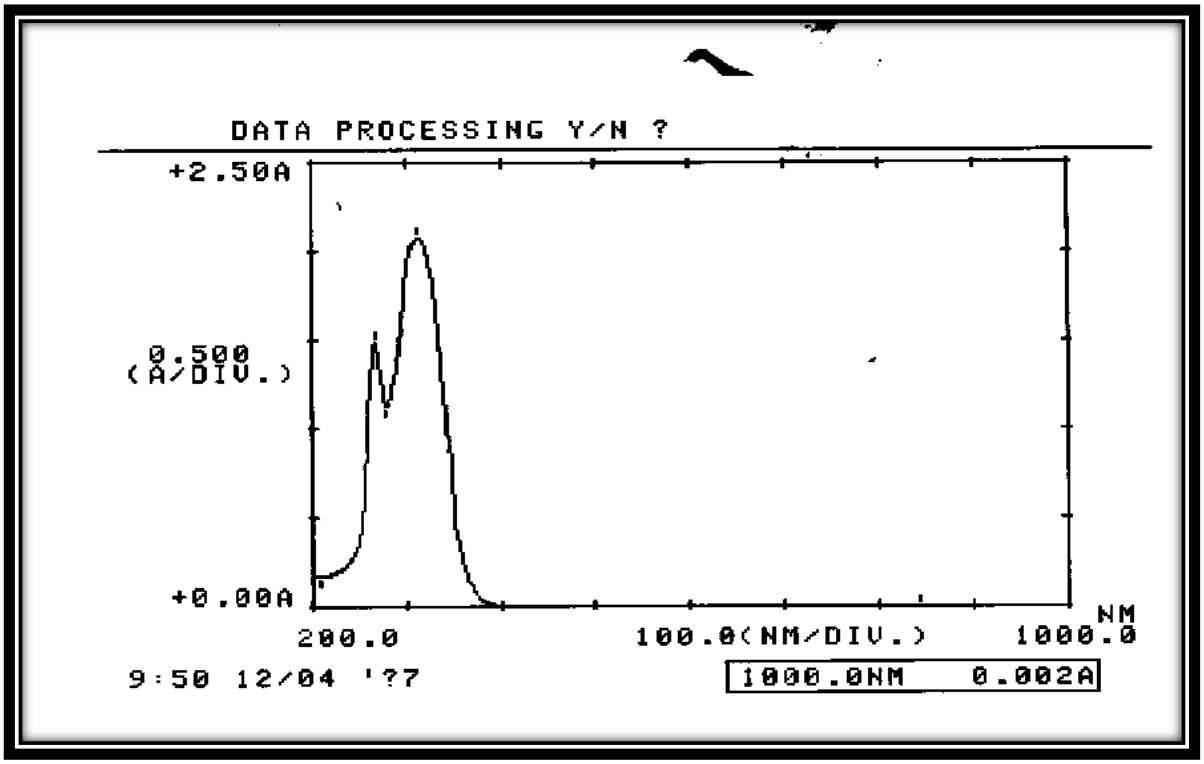

Fig. (3-48): Electronic spectrum of $[VO(L^1)_2(SO_4)].H_2O$ (1) in $5X10^{-4}$M

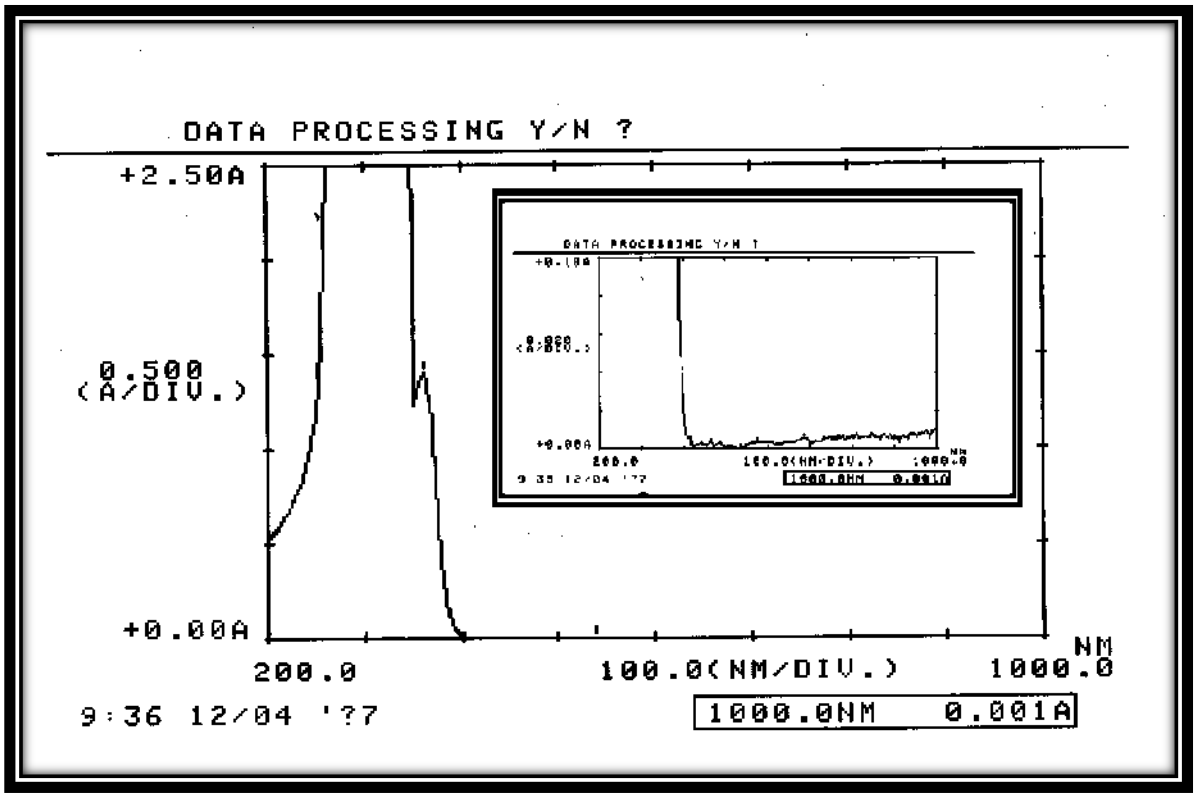

Fig.(3-49): Electronic spectrum of [Mn $(L^1)_2Cl_2$].H_2O (2) in 10^{-3}M.

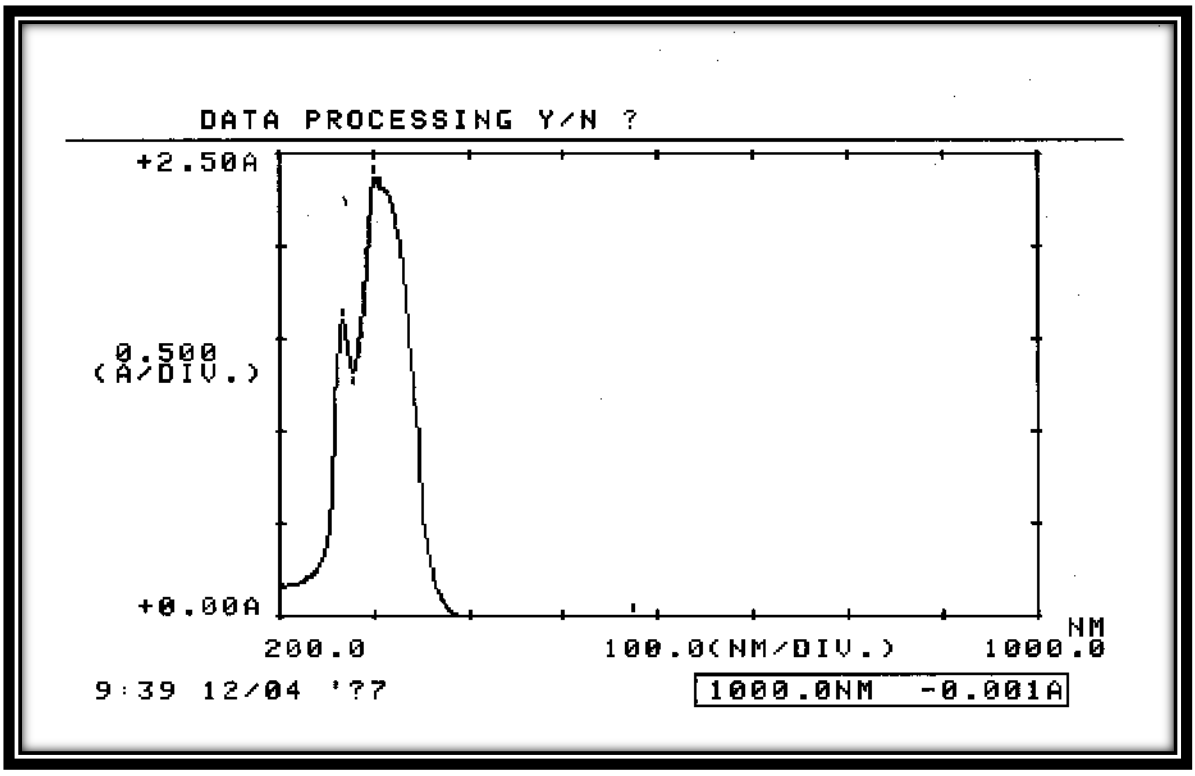

Fig. (3-50): Electronic spectrum of [Mn $(L^1)_2Cl_2$].H_2O (2) in $6x10^{-4}$M.

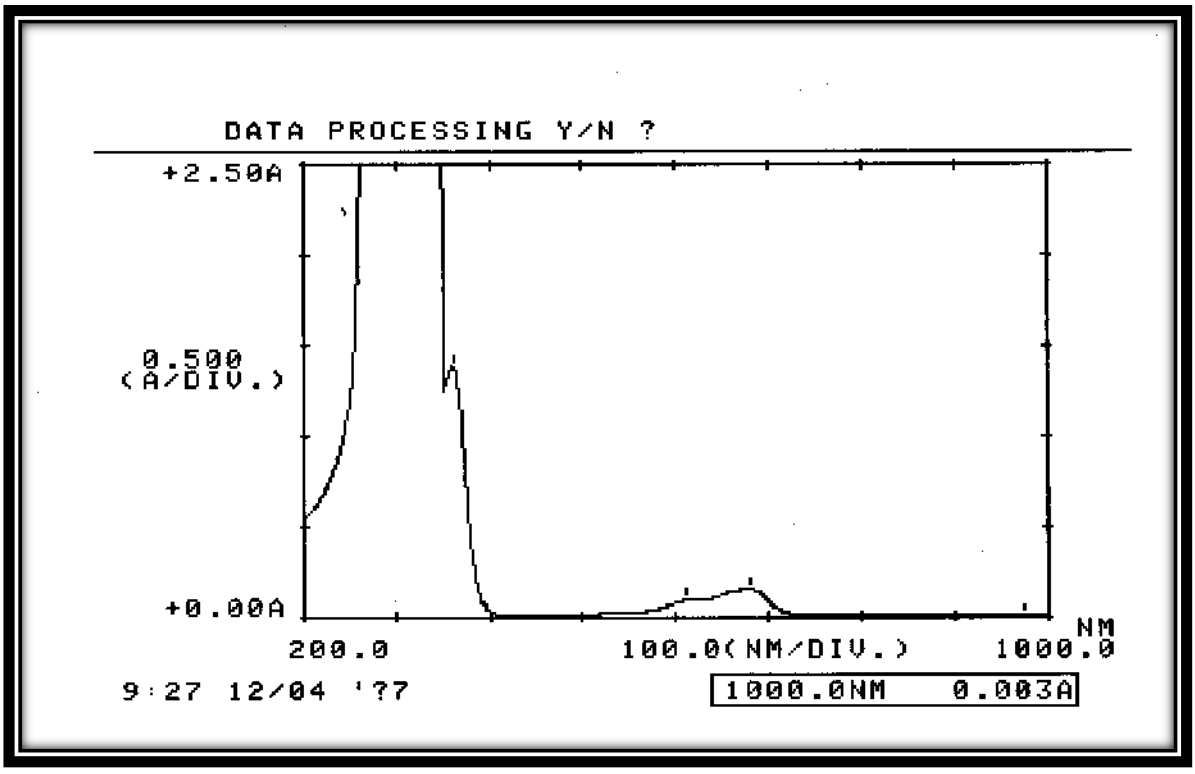

Fig.(3-51): Electronic spectrum of [Co $(L^1)_2Cl_2$].H_2O (3) in 10^{-3}M.

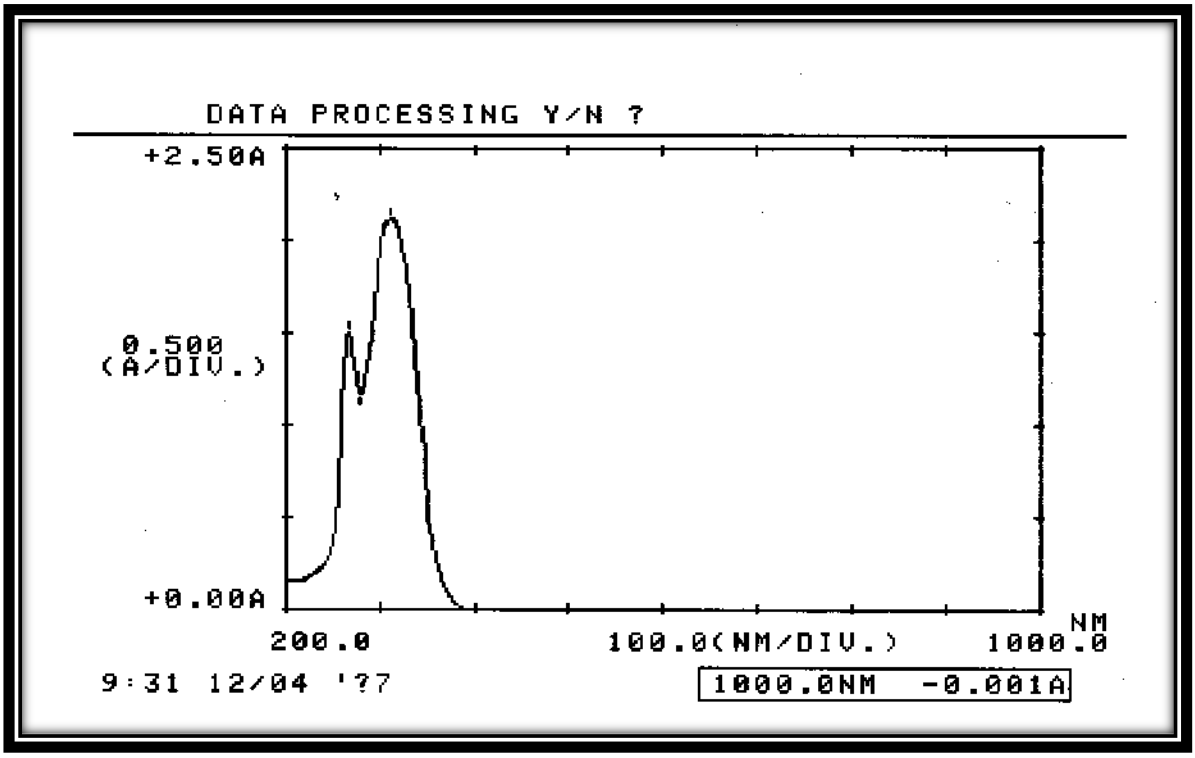

Fig.(3-52): Electronic spectrum of [Co $(L^1)_2Cl_2$].H_2O (3) in $5.8x10^{-4}$M.

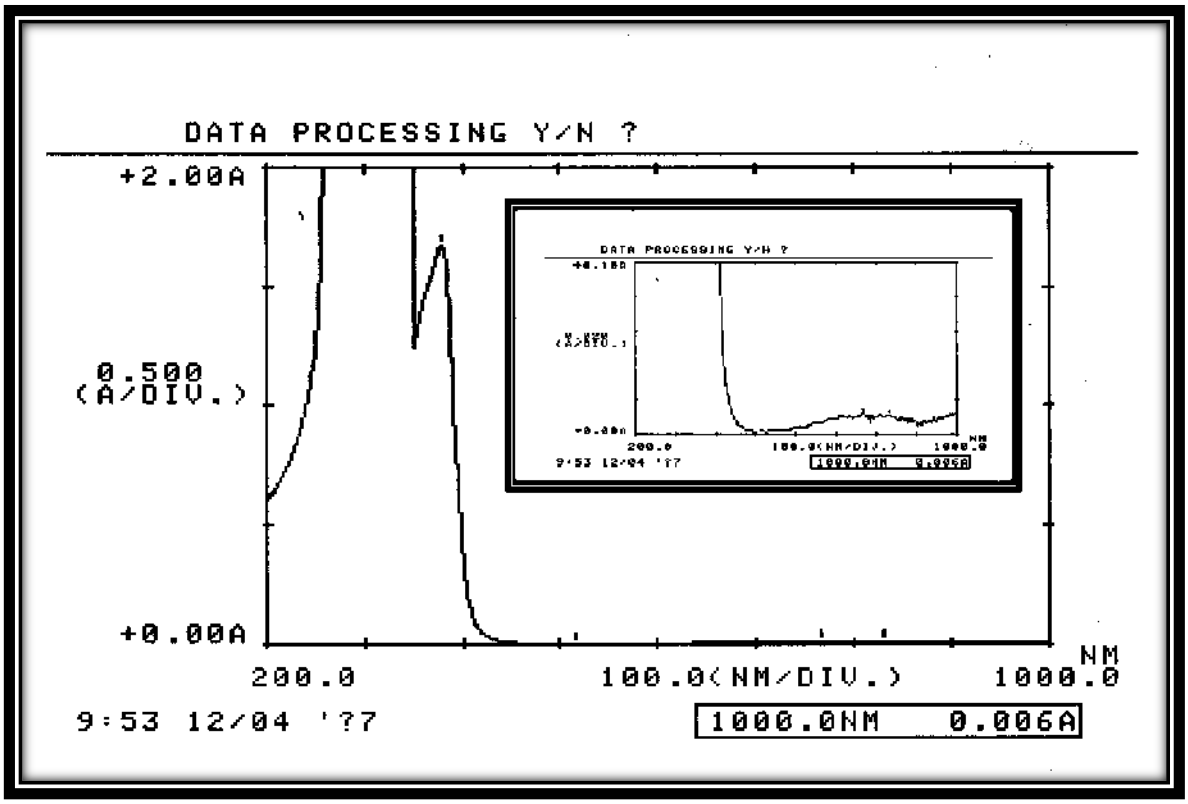

Fig.(3-53): Electronic spectrum of [Ni $(L^1)_2Cl_2$].H_2O (4) in 10^{-3}M.

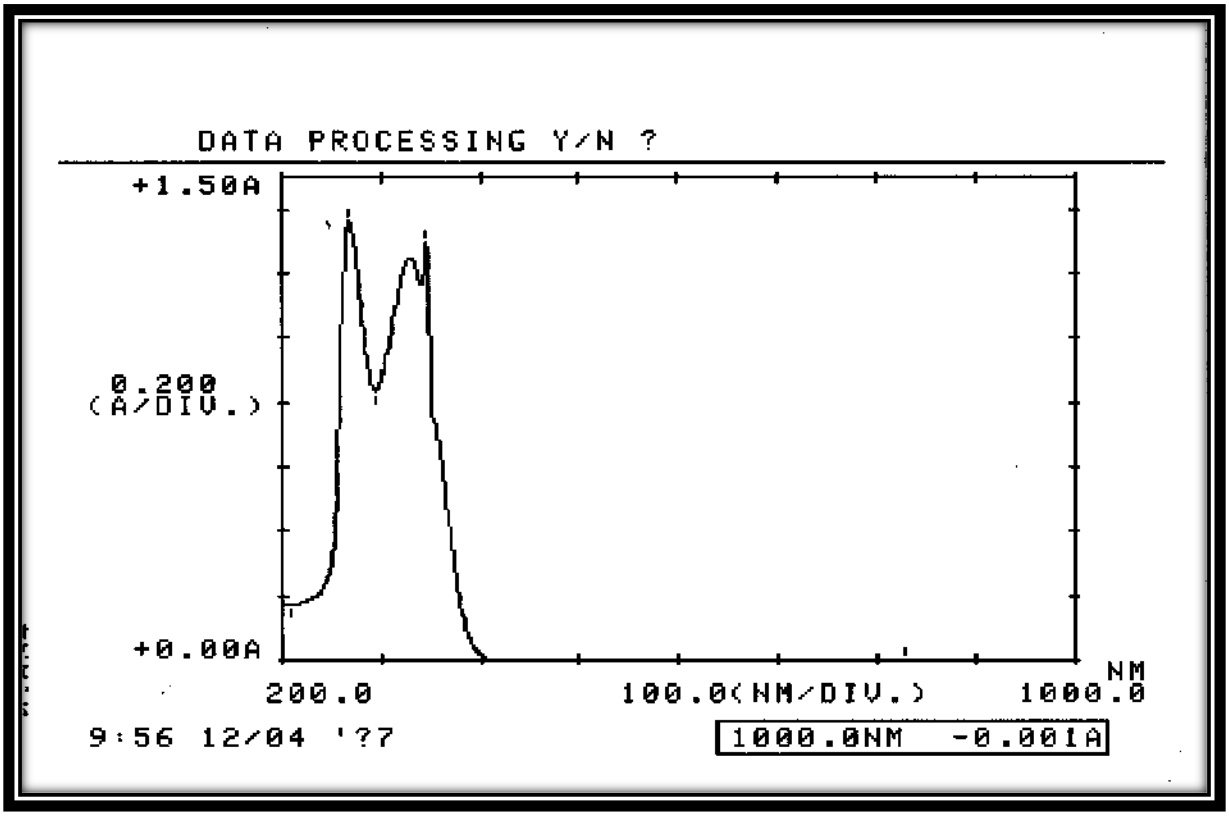

Fig.(3-54): Electronic spectrum of [Ni$(L^1)_2Cl_2$].H_2O (4) in $5x10^{-4}$M.

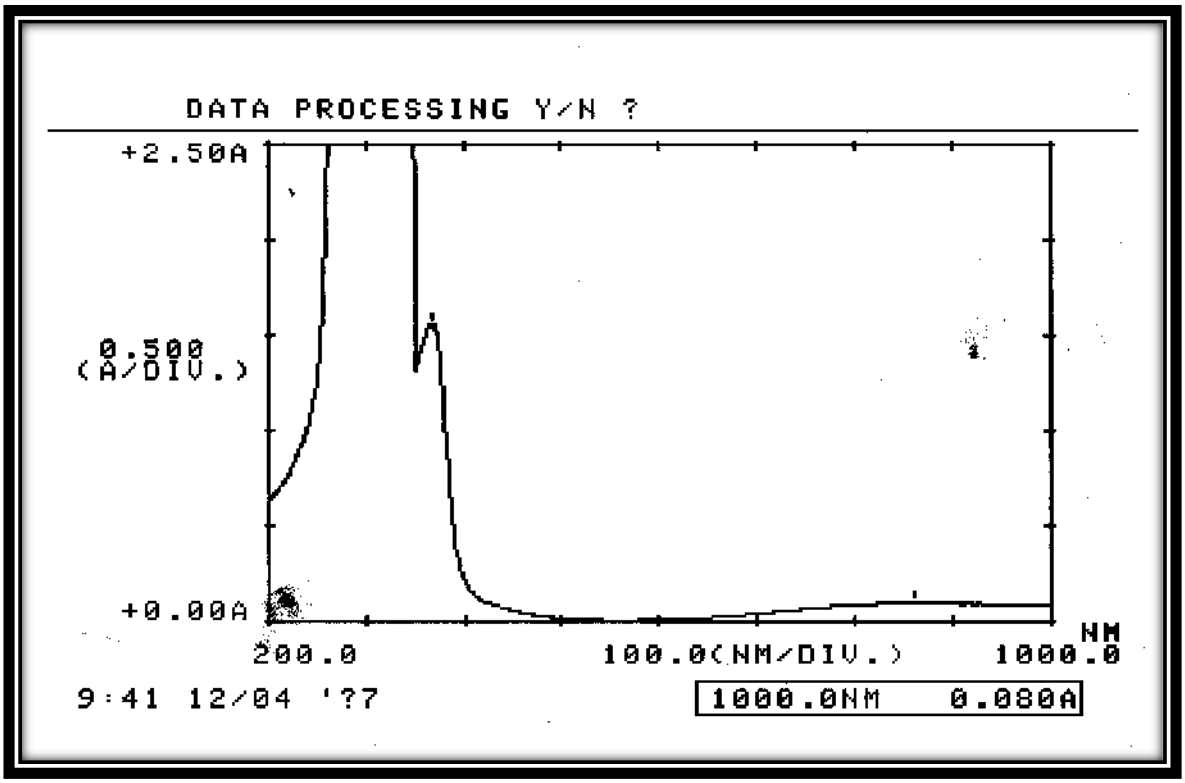

Fig.(3-55): Electronic spectrum of $[Cu(L^1)_2Cl_2].H_2O$ (5) in 10^{-3}M.

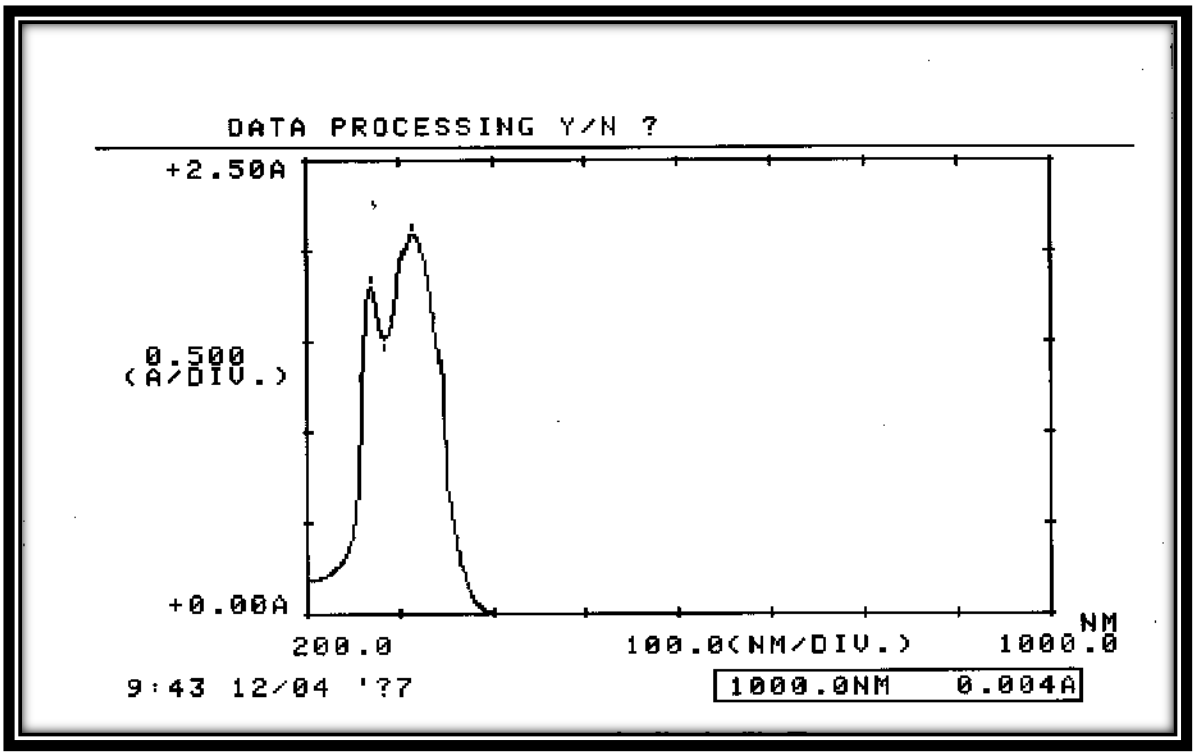

Fig.(3-56): Electronic spectrum of $[Cu(L^1)_2Cl_2].H_2O$ (5) in $6x10^{-4}$M.

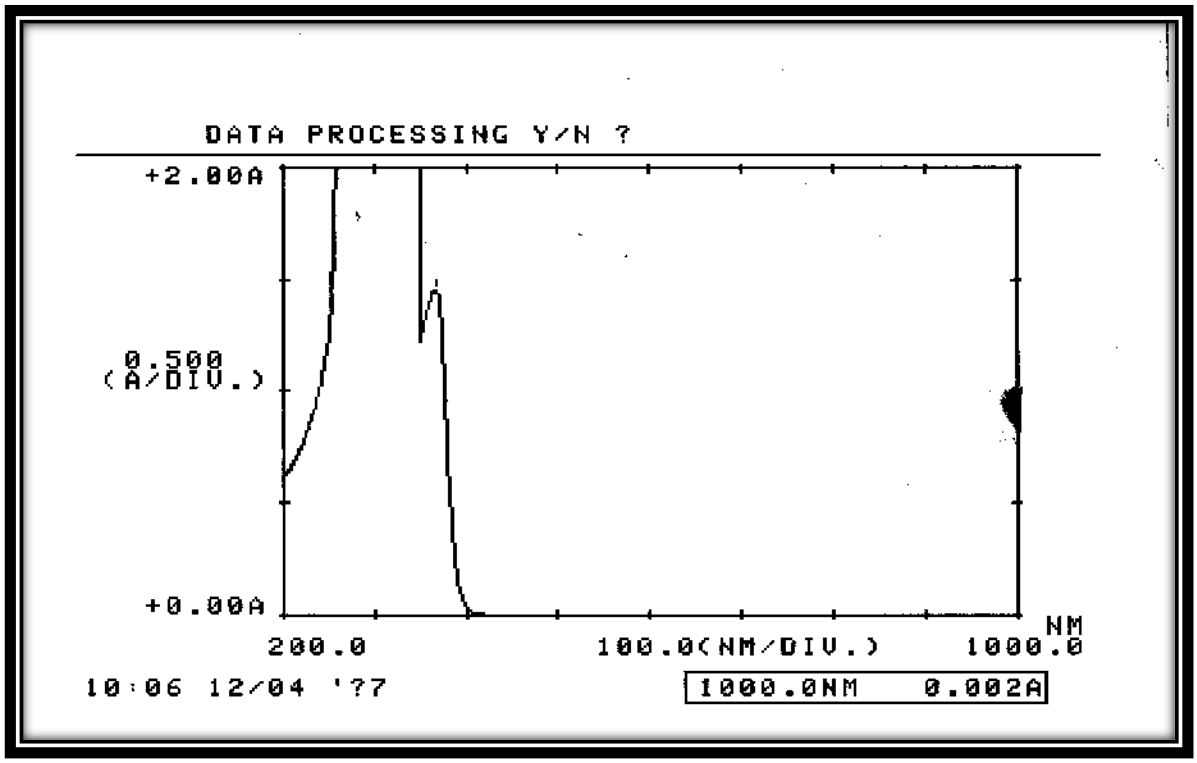

Fig.(3-57): Electronic spectrum of $[Zn(L^1)_2Cl_2].H_2O$ (6) in 10^{-3}M.

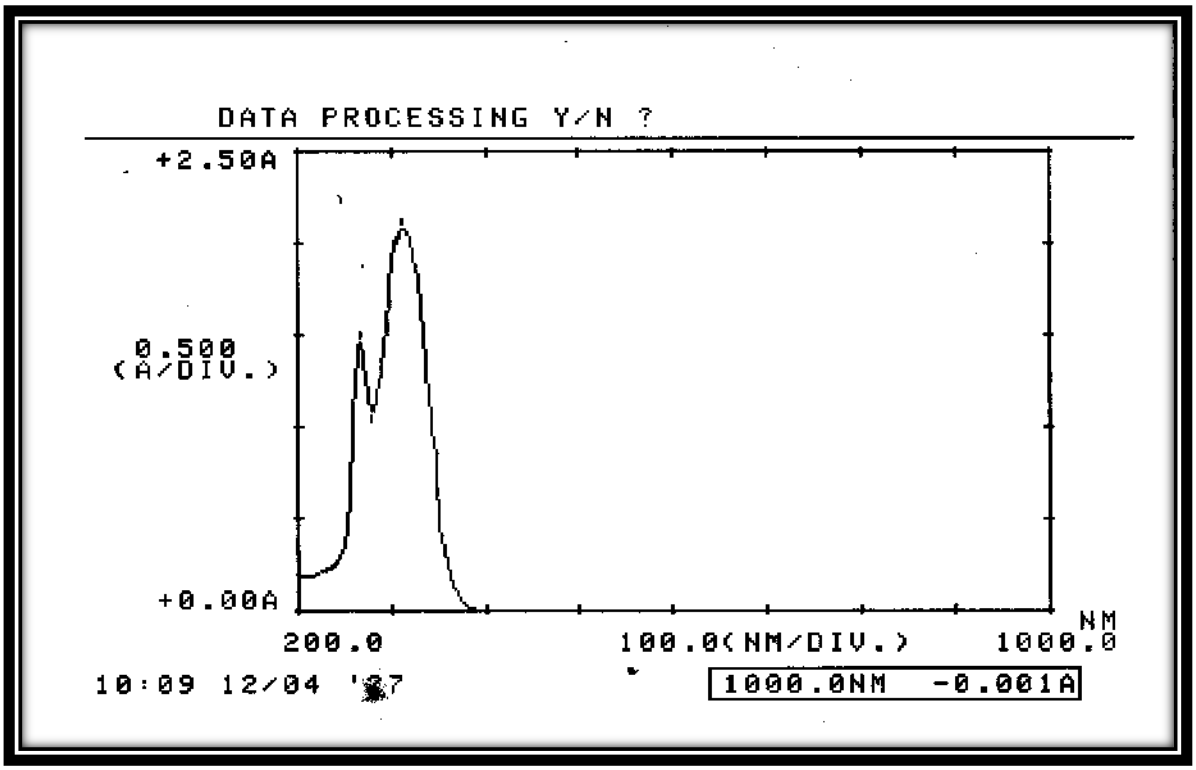

Fig.(3-58): Electronic spectrum of $[Zn(L^1)_2Cl_2].H_2O$ (6) in $6x10^{-4}$M.

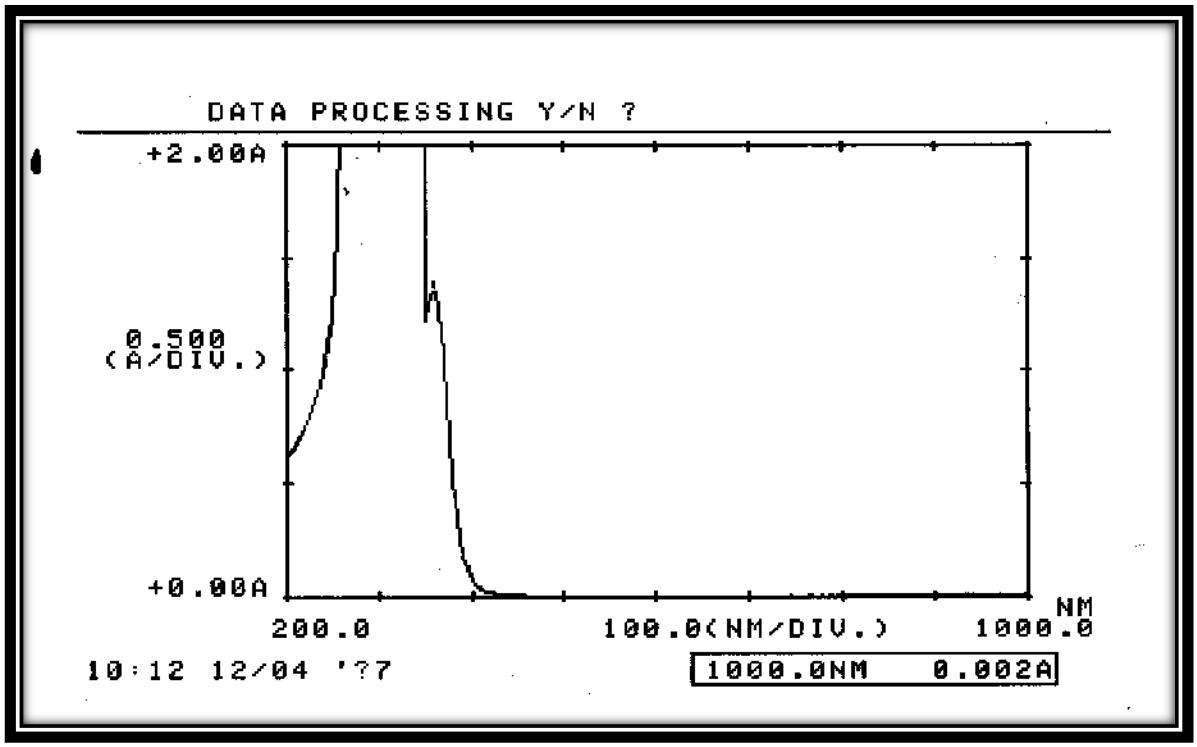

Fig.(3-59): Electronic spectrum of $[Cd(L^1)_2Cl_2].H_2O$ (7) in 10^{-3}M.

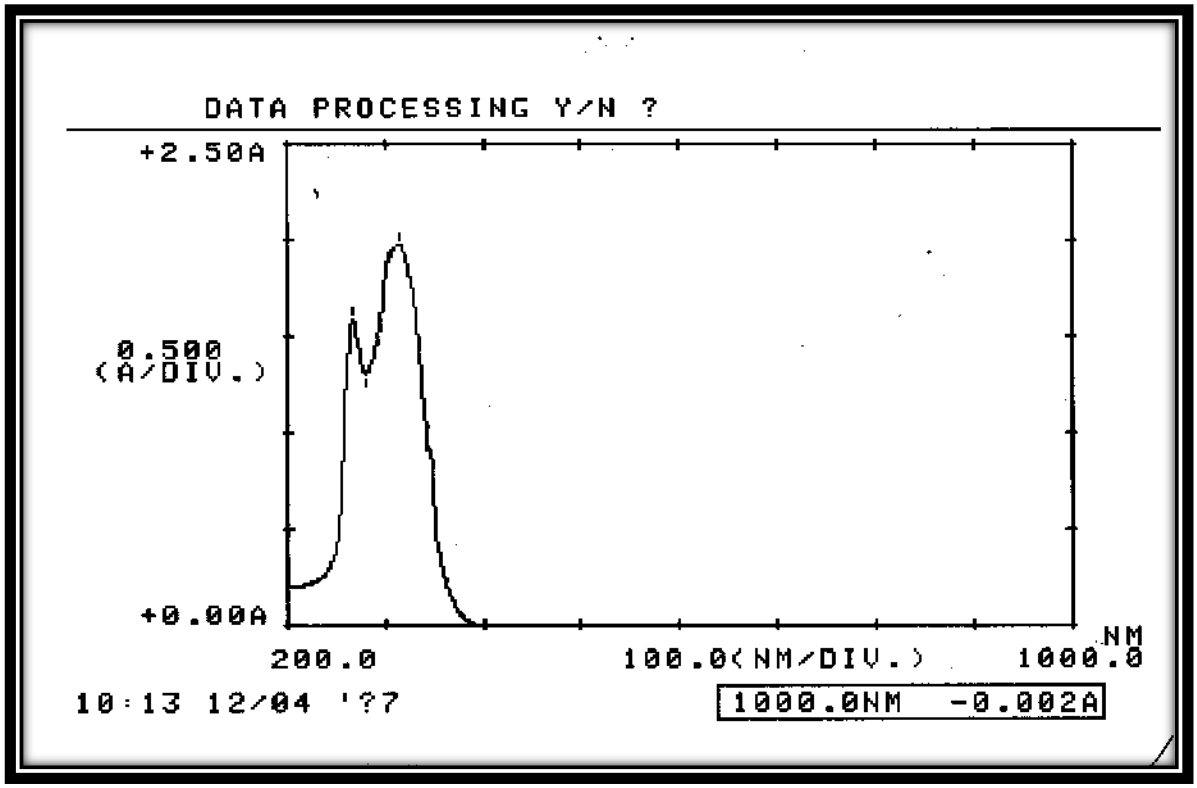

Fig.(3-60): Electronic spectrum of $[Cd(L^1)_2Cl_2].H_2O$ (7) in $6x10^{-4}$M.

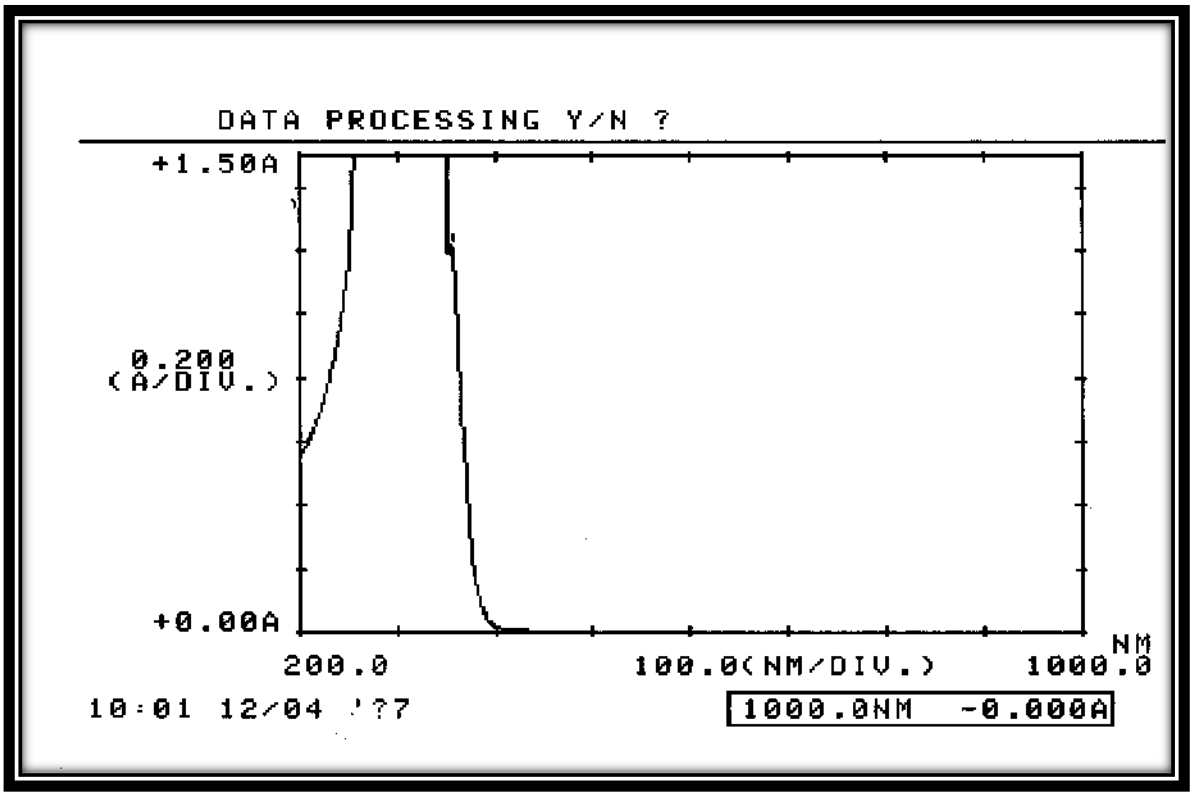

Fig.(3-61): Electronic spectrum of $[Hg(L^1)_2Cl_2].H_2O$ (8) in 10^{-3}M.

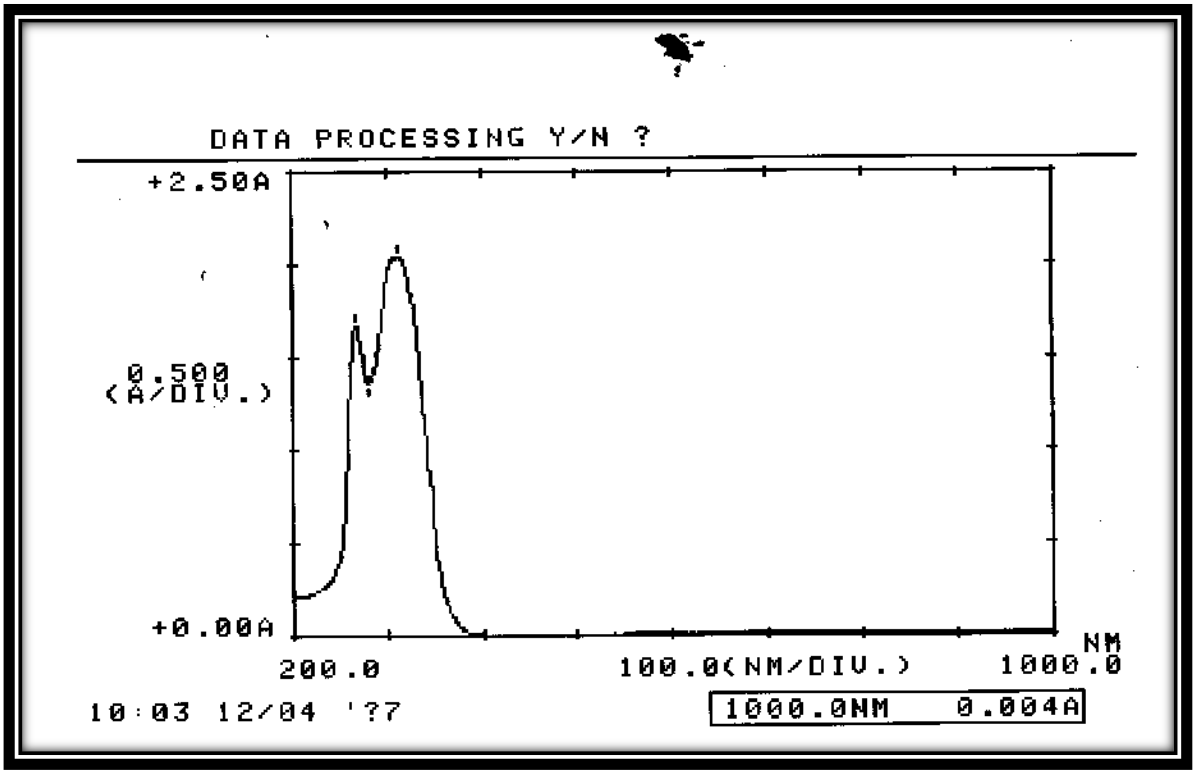

Fig.(3-62): Electronic spectrum of $[Hg(L^1)_2Cl_2].H_2O$ (8) in $8x10^{-4}$M.

(3.2.6.2) (UV.-Vis.) spectra of ligand's [L^2] complexes [(9)-(16)].

The electronic spectral data for prepared complexes (9-16) were summarized in Table (3-25) together with electronic transitions and suggested geometrical formula. The electronic spectra for all synthesized complexes displayed three absorption peaks in the ultraviolet region. The first peak at range (268 –270) nm (37313 –37037) cm^{-1} , the second peak at range (301-318) nm (33222-31447) cm^{-1} , and the third peak at range (358-362) nm (27933– 27624) cm^{-1} . The first two peaks were attributed to the intra-ligand $\pi \rightarrow \pi^*$, which exhibited bathochromic shift or hypsochromic shift when it comparison with that of free ligand this confirming the coordination of the ligand to the central metal ion[159] . While, the third peak was related to charge transfer electronic transition type (M→L) [55].

$[VO(L^2)_2(SO_4)]. H_2O$

The electronic spectrum of VO(II) complex, Fig. (3-63) and (3-64) displayed three additional peaks, the first peak at (497) nm (20121) cm^{-1}, the second peak at (682) nm (14663) cm^{-1} and the third peak at (813) nm (12300) cm^{-1} were attributed to (d-d) spin-allowed electronic transitions type $^2B_2g \rightarrow {}^2A_1g$, $^2B_2g \rightarrow {}^2B_1g$ and $^2B_2g \rightarrow {}^2Eg$ respectively suggesting octahedral geometry about VO(II) ion[166].

$[Mn(L^2)_2Cl_2]. H_2O$

The UV-Vis spectrum of Mn(II) complex, Fig. (3-65) and (3-66) showed five new peaks. The first peak at (420) nm (23809) cm^{-1}, the second peak at (484) nm (20661) cm^{-1}, the third peak at (534) nm (18727) cm^{-1}, the fourth peak at (736) nm(13587) cm^{-1} and the fifth peak at (811) nm (12330) cm^{-1} were attributed to (d-d) spin-forbidden electronic transitions type $^6A_1g \rightarrow {}^4A_1g, {}^4Eg_{(G)}$, $^6A_1g \rightarrow {}^4T_1g_{(P)}$, $^6A_1g \rightarrow {}^4T_2g_{(G)}$, $^6A_1g \rightarrow {}^4T_1g_{(G)}$ besides to

$^6A_1g \rightarrow {}^4Eg_{(D)}$, respectively indicating octahedral geometry around Mn(II) ion[167].

$[Co(L^2)_2Cl_2]. H_2O$

The electronic spectrum of Co(II) complex showed three additional absorption peaks, Fig. (3-67) and (3-68). The first peak at (523) nm (19120) cm^{-1}, the second peak at (678) nm (14749) cm^{-1} and the third peak at (889) nm (11248) cm^{-1} were attributed to (d-d) spin-allowed electronic transitions type $^4T_1g \rightarrow {}^4T_1g_{(P)}$ υ_3 , $^4T_1g \rightarrow {}^4A_2g_{(F)}$ υ_2 and $^4T_1g \rightarrow {}^4T_2g_{(F)}$ υ_1 respectively, characteristic octahedral geometry around Co(II) ion [168].

$[Ni(L^2)_2Cl_2]. H_2O$

The electronic spectrum of Ni(II) complex, Fig. (3-69) and (3-70) displayed three new absorption peaks. The first peak at (428) nm (23364) cm^{-1}, the second peak at (570) nm (17544) cm^{-1}, and the third peak at (811) nm (12330) cm^{-1} due to (d-d) spin-allowed electronic transitions type $^3A_2g_{(F)} \rightarrow {}^3T_1g_{(P)}$ υ_3 , $^3A_2g_{(F)} \rightarrow {}^3T_1g_{(F)}$ υ_2 and $^3A_2g_{(F)} \rightarrow {}^3T_2g_{(F)}$ υ_1 which are a good evidence for octahedral geometry of Ni(II) complexes[169].

$[Cu(L^2)_2Cl_2]. H_2O$

The UV-Vis spectrum of Cu(II) complex, Fig. (3-71) and (3-72) showed additional absorption peak at (862) nm (11601) cm^{-1} was attributed to (d-d) spin-allowed electronic transitions type $^2Eg \rightarrow {}^2T_2g$, confirming distorted octahedral geometry about Cu(II) ion[170].

$[Zn(L^2)_2Cl_2]. H_2O$, $[Cd(L^2)_2 Cl_2]. H_2O$ and $[Hg(L^2)_2 Cl_2]. H_2O$

The electronic spectra of Zn(II), Cd(II), and Hg(II) complexes, Fig. [(3-73) - (3-78)] respectively, exhibit no peak in the visible region because of (d^{10}-system) of metal (II) ion, this is mean no (d-d) electronic transition happened [171] .

Table (3-25) Electronic spectral data for [L^2] complexes.

No.	Compounds	λ (nm)	υ^- (cm^{-1})	ε_{max} (molar^{-1} cm^{-1})	Assignment	Suggested structure
	[L^2]	270	37037	2738	($\pi \rightarrow \pi^*$)	-
		316	31646	3592	($\pi \rightarrow \pi^*$)	
9	$[VO(L^2)_2(SO_4)].H_2O$	270	37037	2888	Intra-ligand	Oh
		314	31847	4220	Intra-ligand	
		368	27174	1492	LMCT	
		497	20121	50	($^2B_2g \rightarrow {}^2A_1g$)	
		682	14663	60	($^2B_2g \rightarrow {}^2B_1g$)	
		813	12300	75	($^2B_2g \rightarrow {}^2Eg$)	
10	$[Mn(L^2)_2Cl_2].H_2O$	269	37175	2836	Intra-ligand	Oh
		318	31447	3780	Intra-ligand	
		366	27322	1444	MLCT	
		420	23809	18	($^6A_1g \rightarrow {}^4A_1g, {}^4Eg_{(G)}$)	
		484	20661	17	($^6A_1g \rightarrow {}^4T_1g_{(P)}$)	
		534	18727	18	($^6A_1g \rightarrow {}^4T_2g_{(G)}$)	
		736	13587	16	($^6A_1g \rightarrow {}^4T_1g_{(G)}$)	
		811	12330	18	($^6A_1g \rightarrow {}^4Eg_{(D)}$)	
11	$[Co(L^2)_2Cl_2].H_2O$	270	37037	2579	Intra-ligand	Oh
		301	33223	3977	Intra-ligand	
		359	27855	1329	MLCT	
		523	19120	29	($^4T_1g_{(F)} \rightarrow {}^4T_1g_{(P)}$)	
		678	14749	57	($^4T_1g_{(F)} \rightarrow {}^4A_2g_{(F)}$)	
		889	11428	22	($^4T_1g_{(F)} \rightarrow {}^4T_2g_{(F)}$)	

No.	Compounds	λ (nm)	υ⁻ (cm^{-1})	ε_{max} (molar^{-1} cm^{-1})	Assignment	Suggested Structure
12	$[Ni(L^2)_2Cl_2].H_2O$	268	37313	2756	Intra-ligand	Oh
		313	31949	4240	Intra-ligand	
		359	27855	1354	MLCT	
		428	23364	33	$(^3A_2g_{(F)} \rightarrow {}^3T_1g_{(P)})$	
		570	17544	31	$(^3A_2g_{(F)} \rightarrow {}^3T_1g_{(F)})$	
		811	12330	39	$(^3A_2g_{(F)} \rightarrow {}^3T_2g_{(F)})$	
13	$[Cu(L^2)_2Cl_2].H_2O$	269	37175	2722	Intra-ligand	Distorted Oh
		314	31847	4126	Intra-ligand	
		360	27778	1358	MLCT	
		862	11601	24	$(^2Eg \rightarrow {}^2T_2g)$	
14	$[Zn(L^2)_2Cl_2].H_2O$	270	37037	2866	Intra-ligand	Oh
		314	31847	4090	Intra-ligand	
		360	37778	1333	MLCT	
15	$[Cd(L^2)_2Cl_2].H_2O$	268	37313	2729	Intra-ligand	Oh
		317	31546	3589	Intra-ligand	
		364	27473	1423	MLCT	
16	$[Hg(L^2)_2Cl_2].H_2O$	270	37037	2974	Intra-ligand	Oh
		315	31746	3872	Intra-ligand	
		368	27174	1264	MLCT	

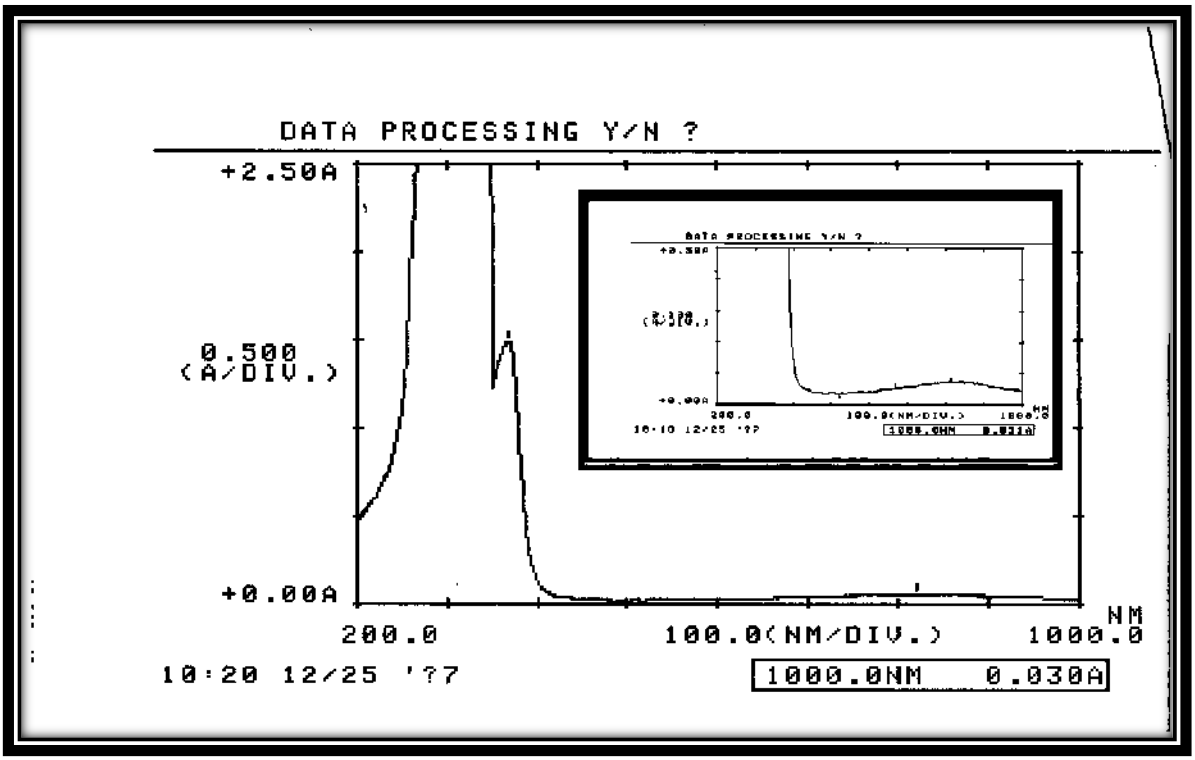

Fig.(3-63): Electronic spectrum of [VO $(L^2)_2(SO_4)$].H_2O (9) in 10^{-3}M.

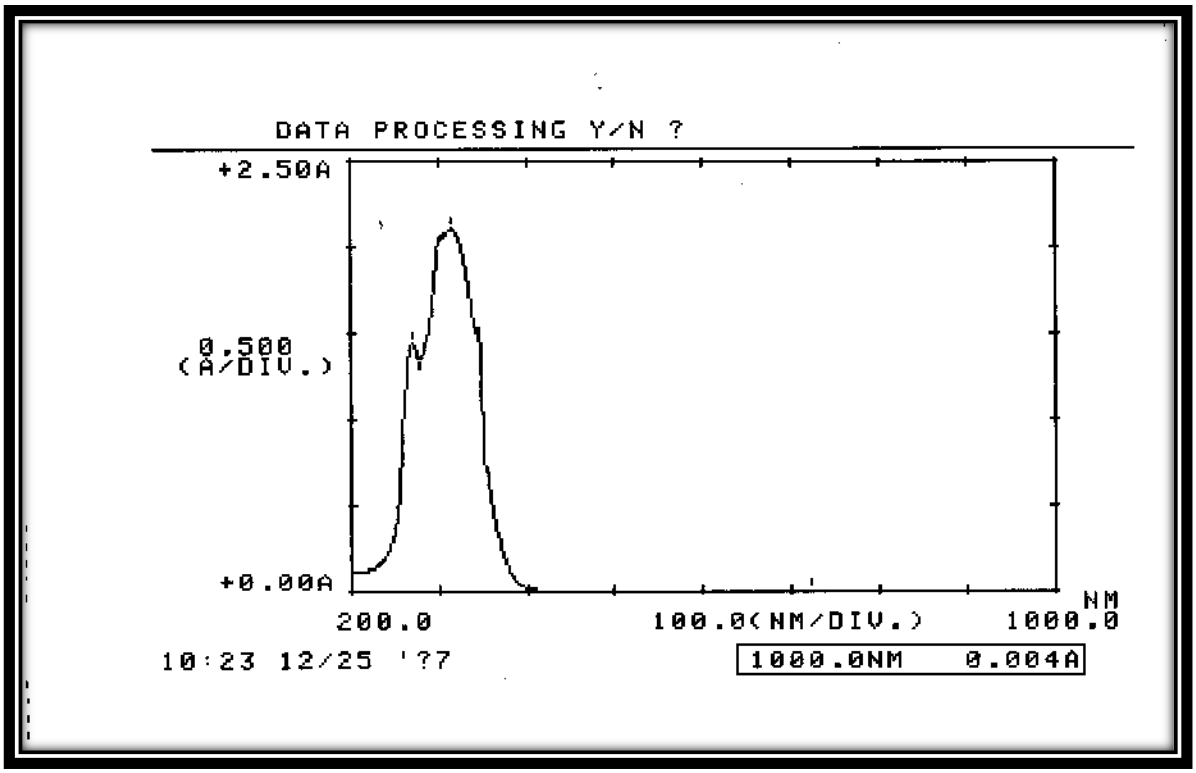

Fig.(3-64): Electronic spectrum of [VO $(L^2)_2(SO_4)$].H_2O (9) in $5x10^{-4}$M.

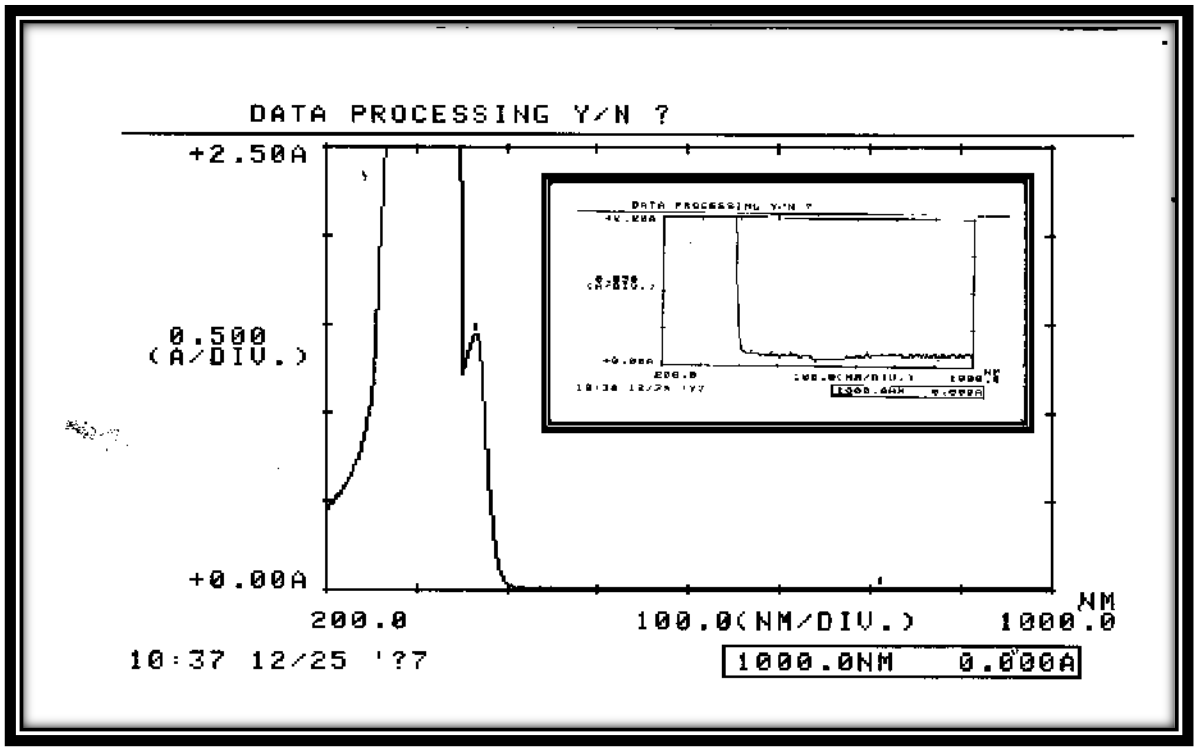

Fig.(3-65): Electronic spectrum of $[Mn(L^2)_2Cl_2].H_2O$ (10) in 10^{-3}M.

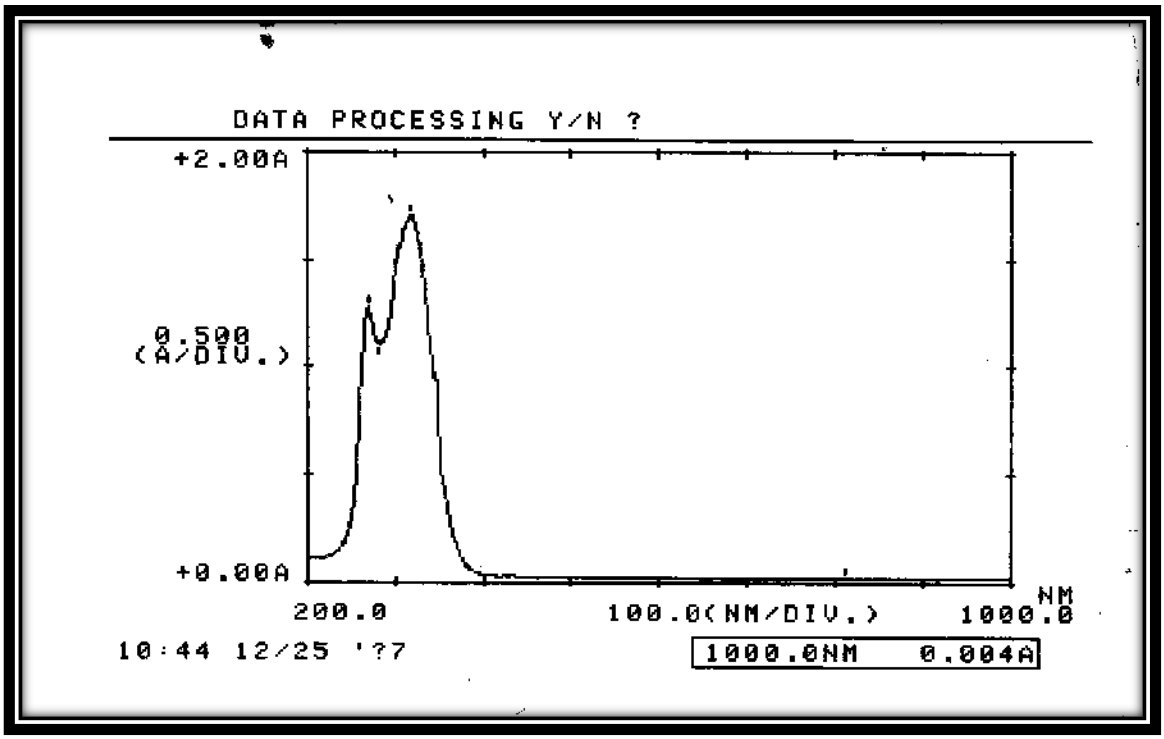

Fig.(3-66): Electronic spectrum of $[Mn(L^2)_2Cl_2].H_2O$ (10) in $4.5x10^{-4}$M.

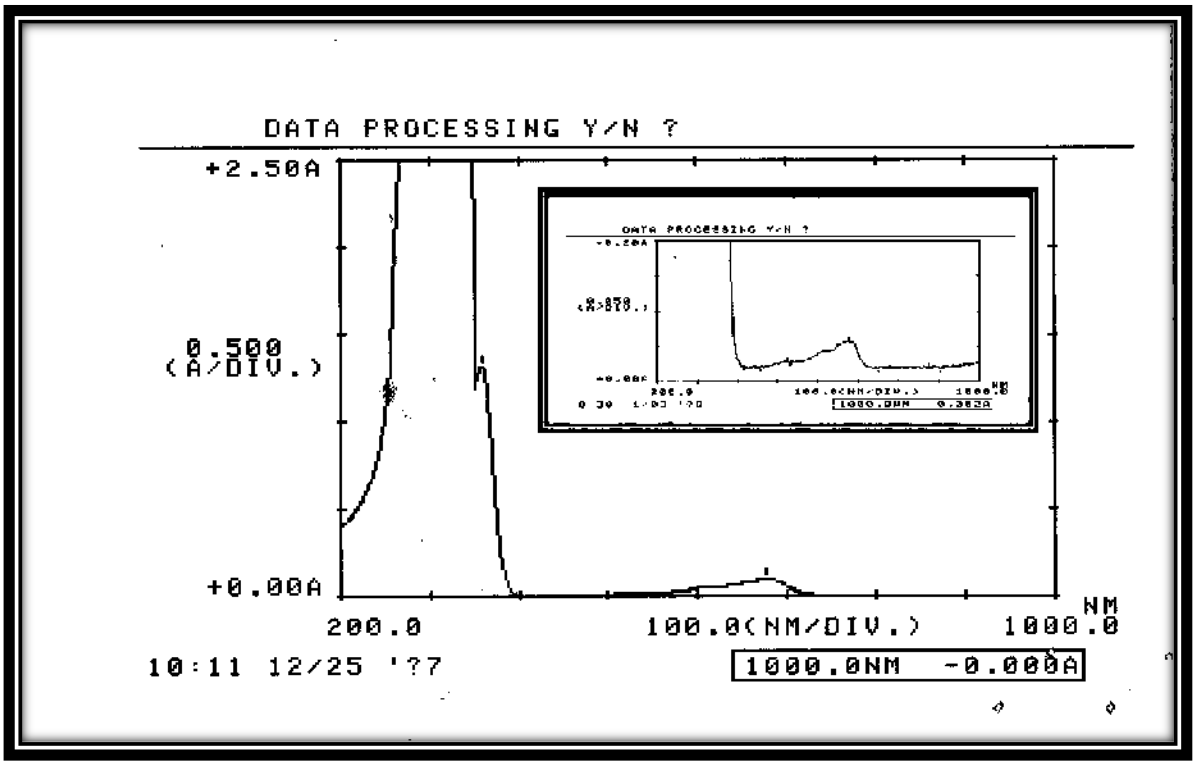

Fig.(3-67): Electronic spectrum of $[Co(L^2)_2Cl_2].H_2O$ (11) in 10^{-3}M.

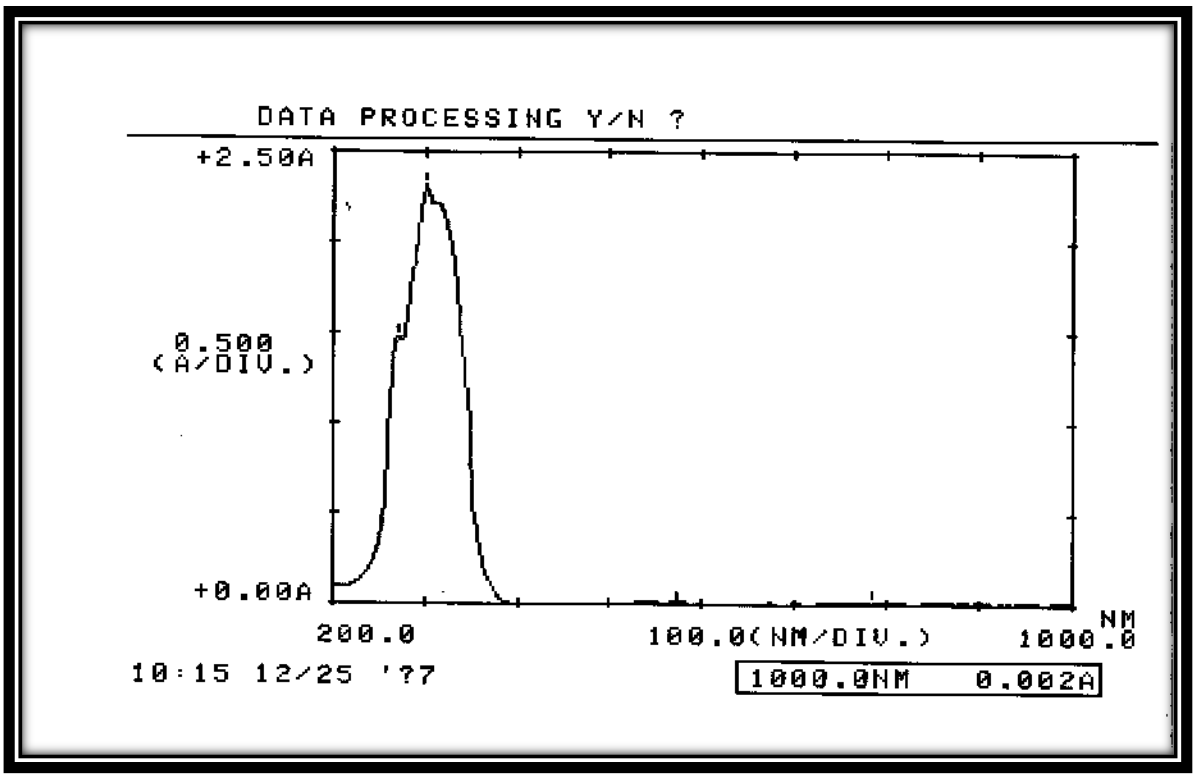

Fig.(3-68): Electronic spectrum of $[Co(L^2)_2Cl_2].H_2O$ (11) in $5.8x10^{-4}$M.

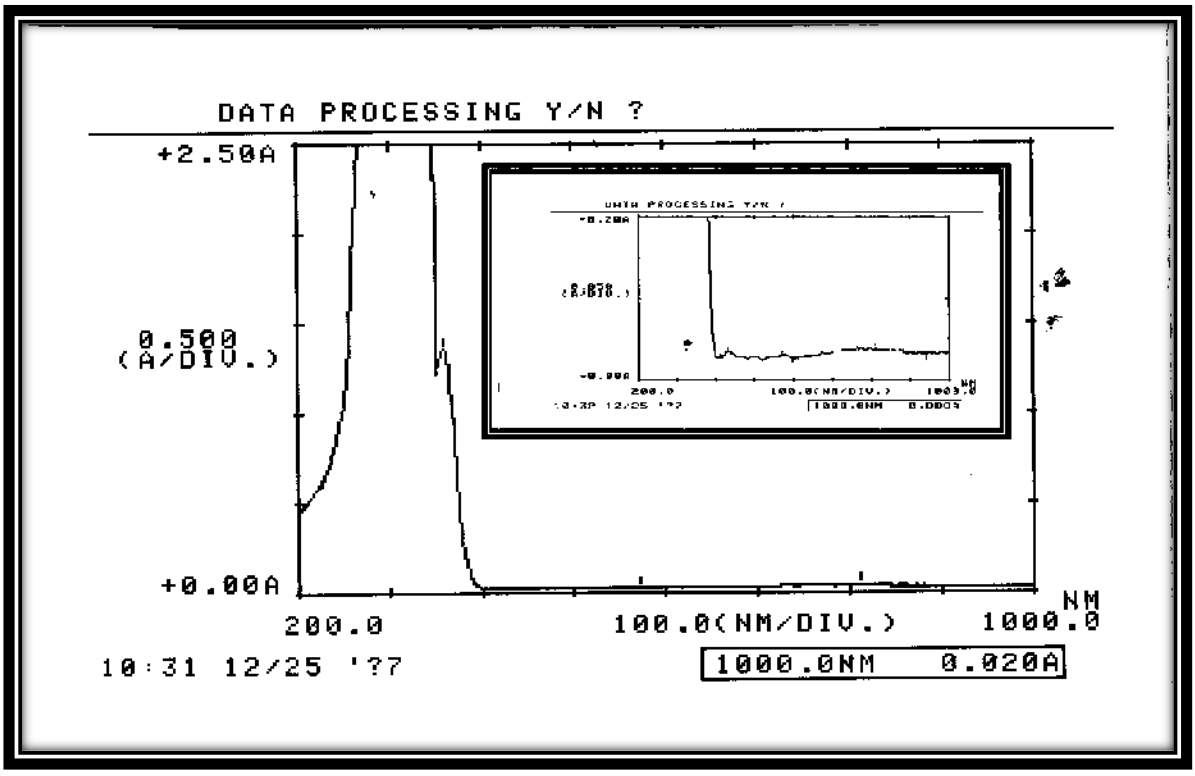

Fig.(3-69): Electronic spectrum of $[Ni(L^2)_2Cl_2].H_2O$ (12) in 10^{-3}M.

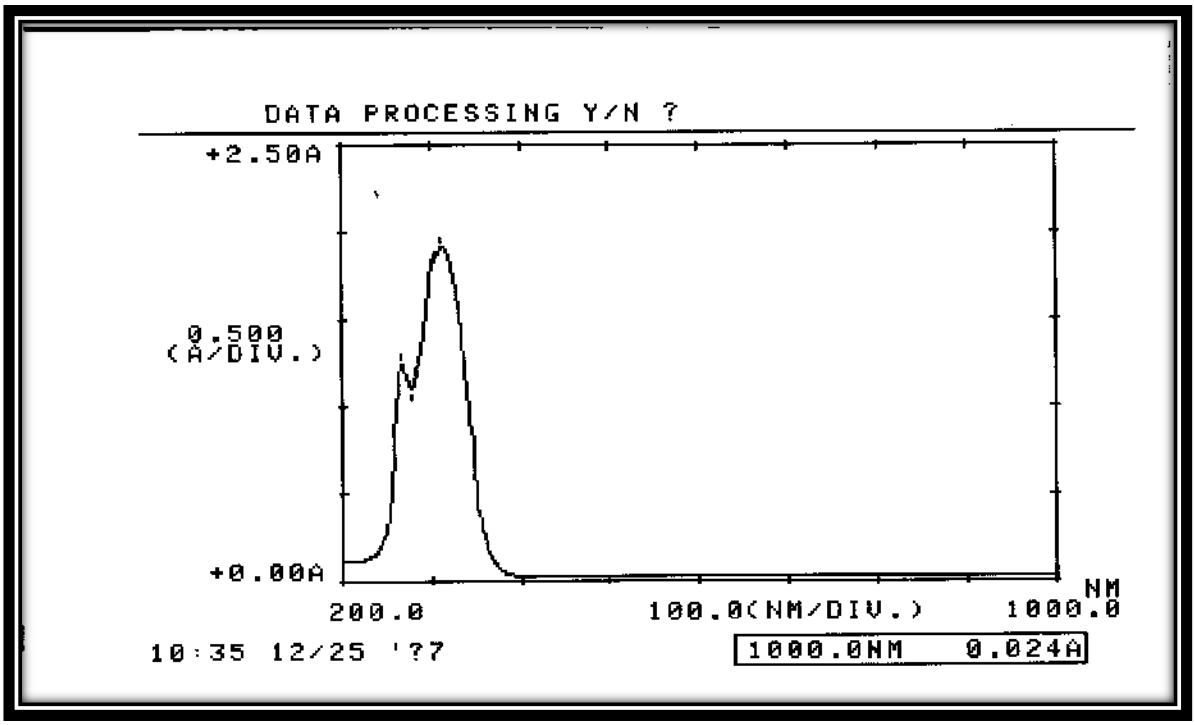

Fig.(3-70): Electronic spectrum of $[Ni(L^2)_2Cl_2].H_2O$ (12) in $4.5x10^{-4}$M.

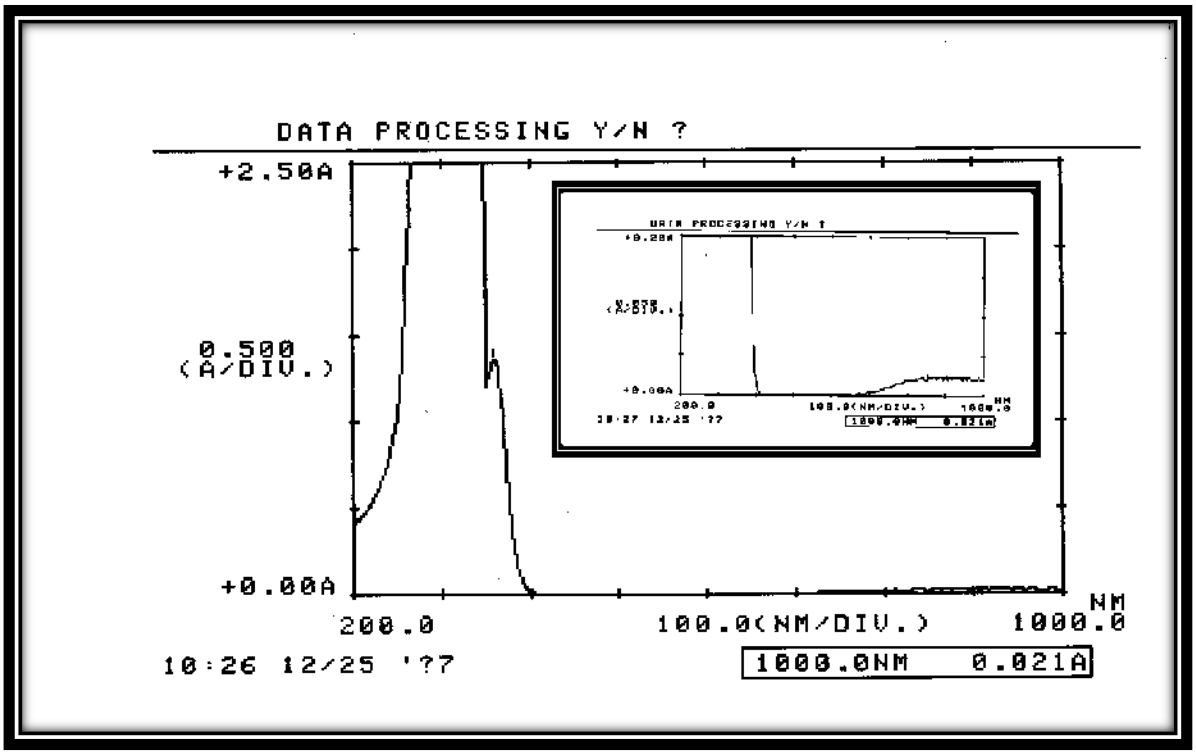

Fig.(3-71): Electronic spectrum of $[Cu(L^2)_2Cl_2].H_2O$ (13) in 10^{-3}M.

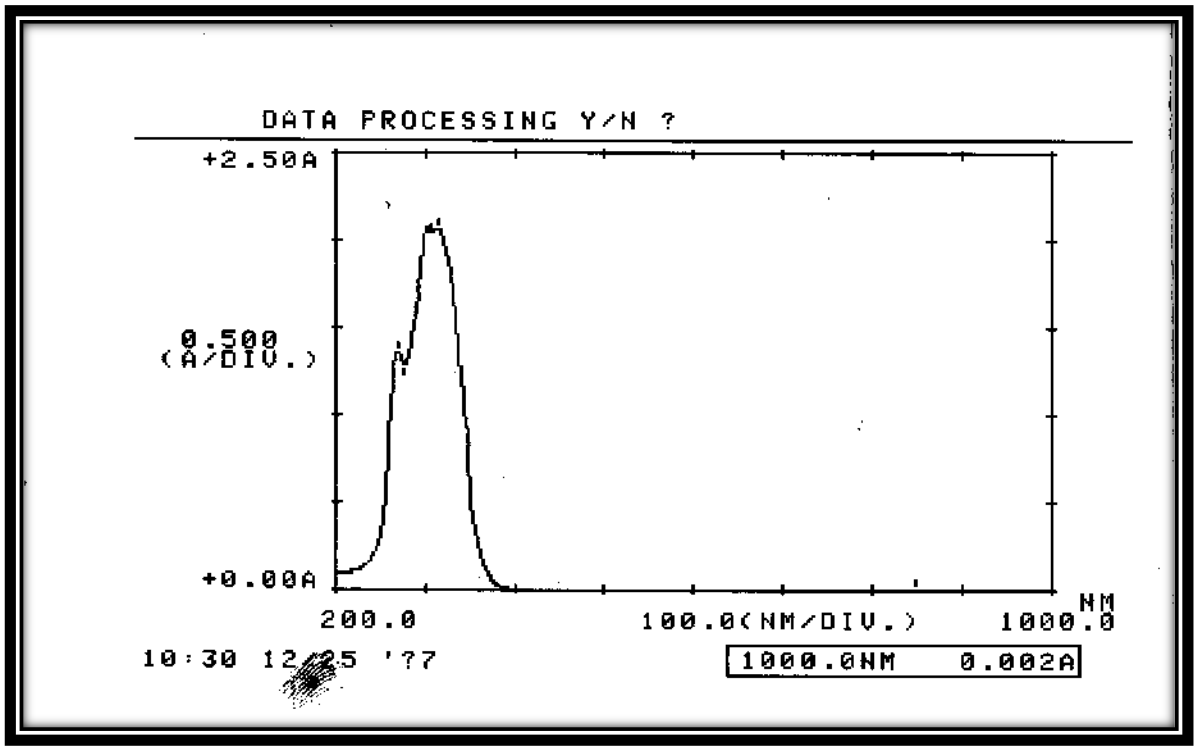

Fig.(3-72): Electronic spectrum of $[Cu(L^2)_2Cl_2].H_2O$ (13) in $5x10^{-4}$M.

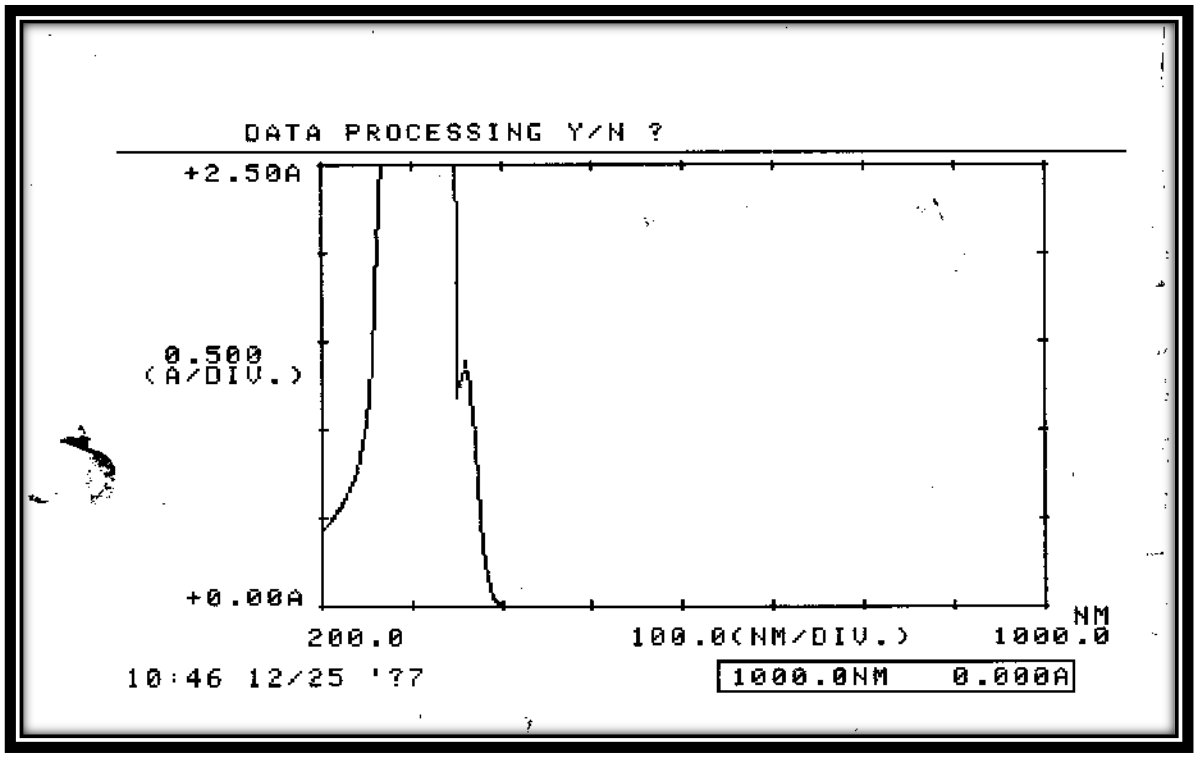

Fig.(3-73): Electronic spectrum of $[Zn(L^2)_2Cl_2].H_2O$ (14) in 10^{-3}M.

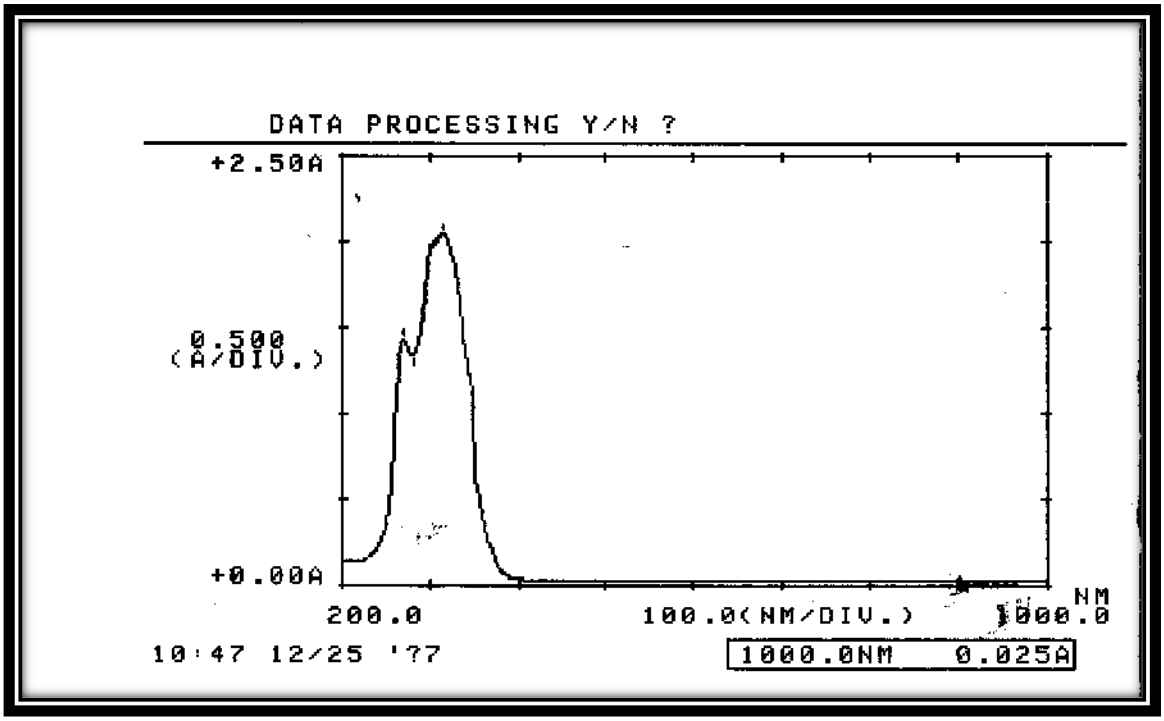

Fig.(3-74): Electronic spectrum of $[Zn(L^2)_2Cl_2].H_2O$ (14) in $5x10^{-4}$M.

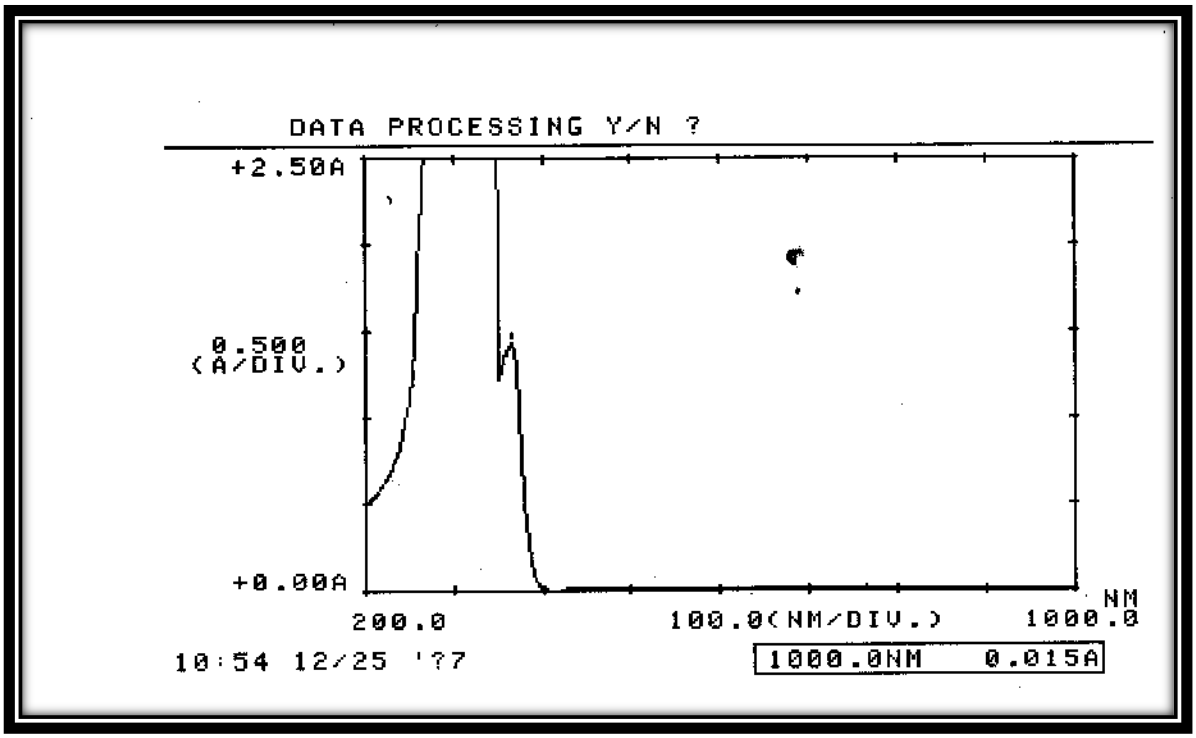

Fig.(3-75): Electronic spectrum of $[Cd(L^2)_2Cl_2].H_2O$ (15) in 10^{-3}M.

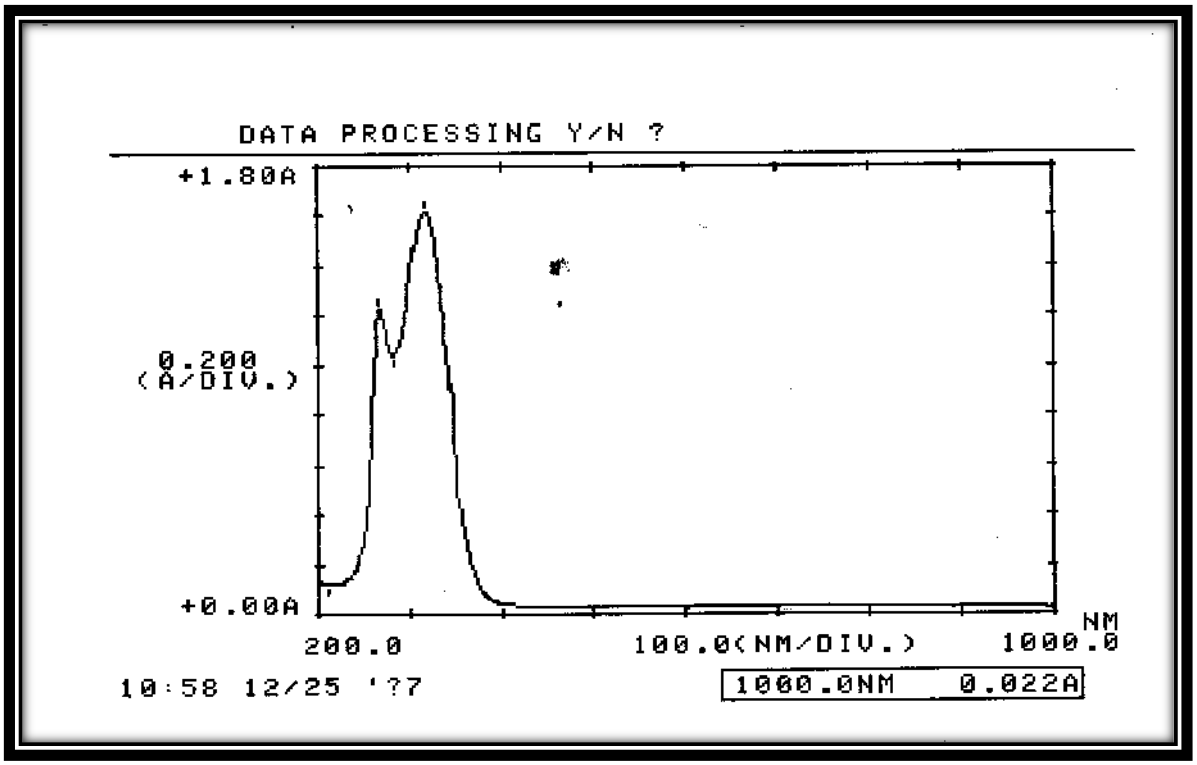

Fig.(3-76): Electronic spectrum of $[Cd(L^2)_2Cl_2].H_2O$ (15) in $4.5x10^{-4}$M.

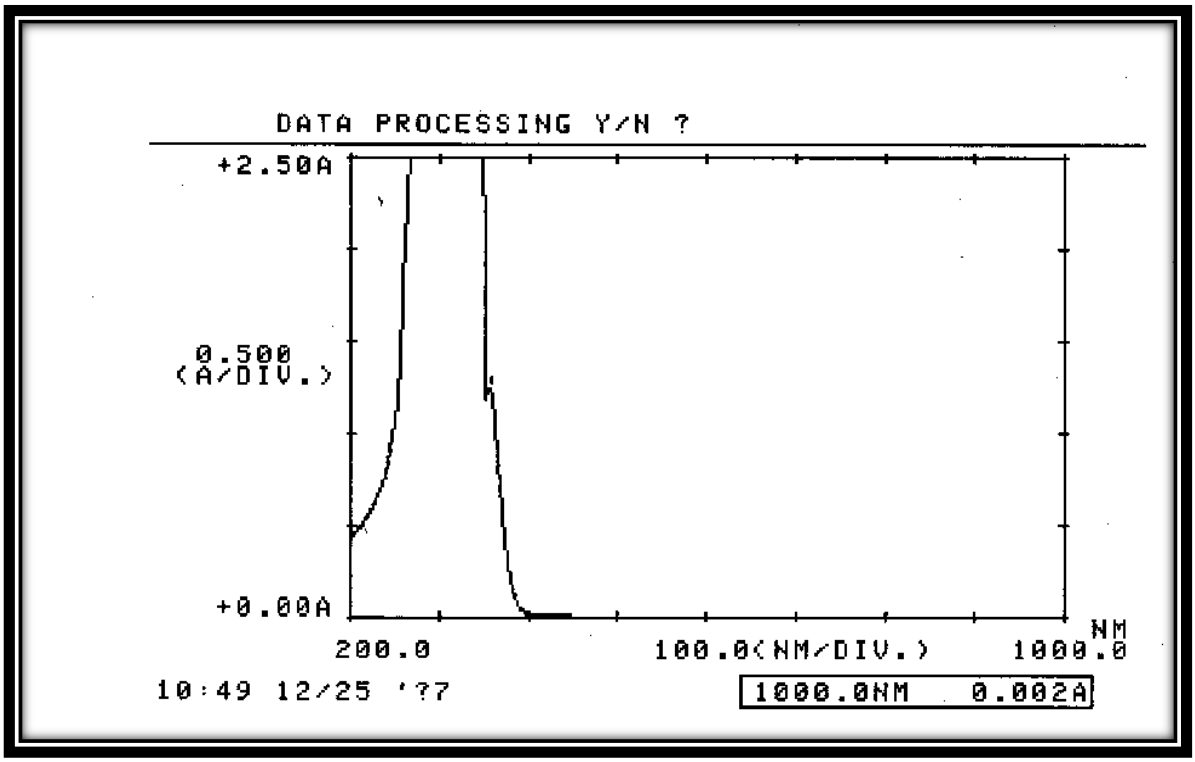

Fig.(3-77): Electronic spectrum of $[Hg(L^2)_2Cl_2].H_2O$ (16) in 10^{-3}M.

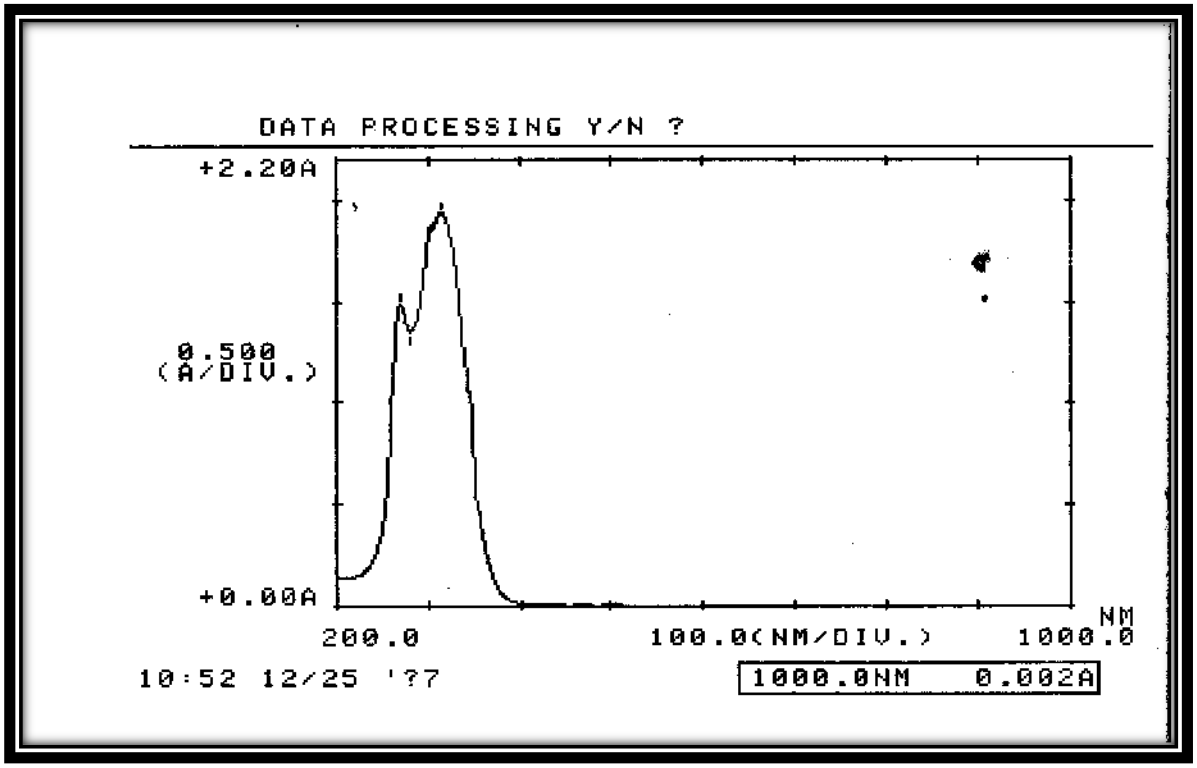

Fig.(3-78): Electronic spectrum of $[Hg(L^2)_2Cl_2].H_2O$ (16) in $5x10^{-4}$M.

(3.2.6.3) (UV.-Vis.) spectra of ligand's [L^3] complexes [(17)-(24)].

The electronic spectral data for synthesized complexes (17-24) were summarized in table (3-26) with electronic transitions and suggested geometrical formula. The electronic spectra for all synthesized complexes displayed three absorption peaks in the ultraviolet region. The first peak at range (266 –268) nm (37594 –37313) cm^{-1}, the second peak at range (301-316) nm (33222-31646) cm^{-1}, and the third peak at range (358-362) nm (27933 – 27624) cm^{-1} . The first two peaks were attributed to the intra-ligand $\pi \rightarrow \pi^*$, which exhibited bathochromic shift or hypsochromic shift when it comparison with that of free ligand this confirming the coordination of the ligand to the central metal ion[159] . While , the third peak was related to charge transfer electronic transition type (M→L) [55].

$[VO(L^3)_2(SO_4)].H_2O$

The electronic spectrum of VO(II) complex, Fig. (3-79) and (3-80) displayed three additional peaks. The first peak at (423) nm (23640) cm^{-1}, the second peak at (681) nm (14684) cm^{-1}, and the third peak at (809) nm (12261) cm^{-1} were attributed to (d-d) spin-allowed electronic transitions type $^2B_2g \rightarrow {}^2A_1g$, $^2B_2g \rightarrow {}^2B_1g$ and $^2B_2g \rightarrow {}^2Eg$, respectively suggesting octahedral geometry about VO(II) ion[63].

$[Mn(L^3)_2(H_2O)Cl]Cl.H_2O$

The UV-Vis spectrum of Mn(II) complex, Fig. (3-81) and (3-82) showed four new peaks. The first peak at (473) nm (21142) cm^{-1}, the second peak at (518) nm (19305) cm^{-1}, the third peak at (755) nm (11364) cm^{-1} and the fourth at (880) nm (9872) cm^{-1} were attributed to (d-d) spin-forbidden electronic transitions type $^6A_1g \rightarrow {}^4T_1g_{(p)}$, $^6A_1g \rightarrow {}^4T_2g_{(G)}$, $^6A_1g \rightarrow {}^4T_1g_{(G)}$ besides to $^6A_1g \rightarrow {}^4Eg_{(D)}$ respectively, indicating octahedral geometry around Mn(II) ion[172].

$[Co(L^3)_2(H_2O)Cl]Cl.H_2O$

The electronic spectrum of Co(II) complex showed three additional absorption peaks, Fig. (3-83) and (3-84). The first peak at (605) nm (16611) cm^{-1}, the second peak at (676) nm (14793) cm^{-1} and the third peak at (986) nm (10142) cm^{-1}were attributed to (d-d) spin-allowed electronic transitions type $^4T_1g \rightarrow {}^4T_1g_{(P)}\upsilon_3$, $^4T_1g \rightarrow {}^4A_2g_{(F)}\upsilon_2$ besides to $^4T_1g \rightarrow {}^4T_2g_{(F)}\upsilon_1$ respectively, characteristic octahedral geometry around Co(II) ion [173].

$[Ni(L^3)_2Cl]Cl.H_2O$

The electronic spectrum of Ni(II) complex, Fig. (3-85) and (3-86) displayed two new absorption peaks. The first peak at (727) nm (13755) cm^{-1} , the second peak at (500) nm (20000) cm^{-1} due to (d-d) spin-allowed electronic transitions type ($'A'_1 \rightarrow 'E'$) and ($'A'_1 \rightarrow 'E''$) which are a good evidence for trigonal bipyramid (tbp) geometry of Ni(II) complexes [174].

$[Cu(L^3)_2Cl_2].H_2O$

The UV-Vis spectrum of Cu(II) complex, Fig. (3-87) and (3-88) showed additional absorption peak at (923) nm (10834) cm^{-1} was attributed to (d-d) spin-allowed electronic transitions type $^2Eg \rightarrow {}^2T_2g$, confirming distorted octahedral geometry about Cu(II) ion [175].

$[Zn(L^3)_2Cl_2].H_2O$, $[Cd(L^3)_2Cl_2].H_2O$, and $[Hg(L^3)_2Cl_2].H_2O$

The electronic spectra of Zn(II), Cd(II), and Hg(II) complexes, Fig. [(3-98) - (3-94)] respectively, exhibit no peak in the visible region because of (d^{10}-system) of metal (II) ion . This is mean no (d-d) electronic transition happened [176].

Table (3-26): Electronic spectral data for [L^3] complexes.

No.	Compounds	λ (nm)	υ⁻ (cm^{-1})	ε_{max} (molar^{-1} cm^{-1})	Assignment	Suggested Structure
	[L^3]	263	38023	3075	($\pi \rightarrow \pi^*$)	-
		319	31348	3320	($\pi \rightarrow \pi^*$)	
17	$[VO(L^3)_2(SO_4)].H_2O$	266	37594	2593	Intra-ligand	Oh
		315	31746	3473	Intra-ligand	
		360	27778	1345	LMCT	
		423	23640	31	($^2B_2g \rightarrow {}^2A_1g$)	
		681	14684	34	($^2B_2g \rightarrow {}^2B_1g$)	
		809	12261	37	($^2B_2g \rightarrow {}^2Eg$)	
18	$[Mn(L^3)_2(H_2O)Cl]\ Cl .H_2O$	266	37564	2653	Intra-ligand	Oh
		316	31646	3490	Intra-ligand	
		358	27933	1307	MLCT	
		473	21142	10	($^6A_1g \rightarrow {}^4T_1g_{(P)}$)	
		518	19305	8	($^6A_1g \rightarrow {}^4T_2g_{(G)}$)	
		755	11364	4	($^6A_1g \rightarrow {}^4T_1g_{(G)}$)	
		880	9872	5	($^6A_1g \rightarrow {}^4Eg_{(D)}$)	
19	$[Co(L^3)_2(H_2O)Cl]Cl .H_2O$	266	37594	2765	Intra-ligand	Oh
		314	31847	2748	Intra-ligand	
		359	27855	1378	MLCT	
		605	16611	62	($^4T_1g \rightarrow {}^4T_1g_{(P)}$)	
		676	14793	78	($^4T_1g \rightarrow {}^4A_2g_{(F)}$)	
		986	10142	22	($^4T_1g \rightarrow {}^4T_2g_{(F)}$)	

No.	Compounds	λ (nm)	υ⁻ (cm^{-1})	ε_{max} (molar^{-1} cm^{-1})	Assignment	Suggested Structure
20	**$[Ni(L^3)_2Cl]Cl.H_2O$**	266	37594	2960	Intra-ligand	tbp
		312	32051	4174	Intra-ligand	
		359	27856	1348	MLCT	
		500	20000	12	('A'_1→'E'')	
		727	13755	11	('A'_1→'E')	
21	**$[Cu(L^3)_2Cl_2]. H_2O$**	266	37594	2684	Intra-ligand	Distorted Oh
		314	31847	3369	Intra-ligand	
		362	27624	1481	MLCT	
		923	10834	140	(^2Eg→^2T_2g)	
22	**$[Zn(L^3)_2Cl_2]. H_2O$**	267	37453	2716	Intra-ligand	Oh
		305	32787	3990	Intra-ligand	
		362	27624	1378	MLCT	
23	**$[Cd(L^3)_2Cl_2]. H_2O$**	268	37313	2825	Intra-ligand	Oh
		301	33222	4215	Intra-ligand	
		359	27855	1354	MLCT	
24	**$[Hg(L^3)_2Cl_2]. H_2O$**	267	37453	2658	Intra-ligand	Oh
		315	31746	3020	Intra-ligand	
		362	27624	1362	MLCT	

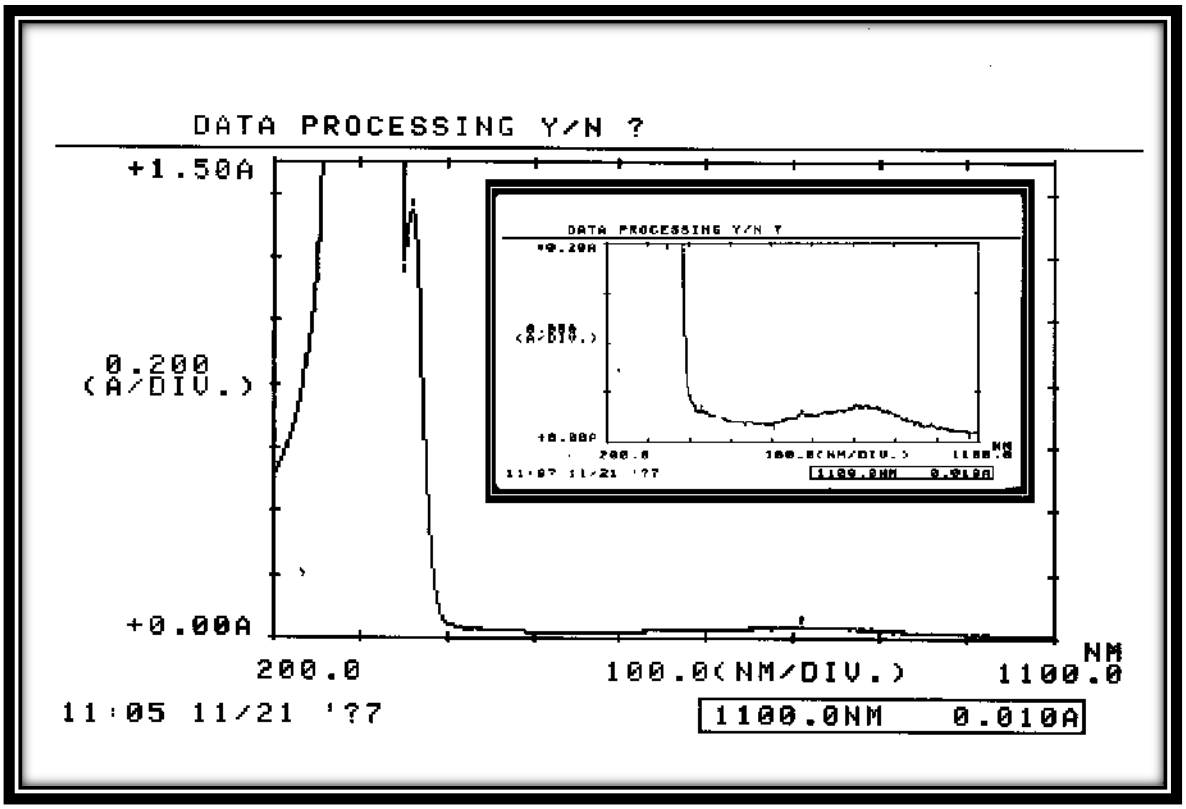

Fig.(3-79): Electronic spectrum of $[VO(L^3)_2(SO_4)].H_2O$ (17) in 10^{-3}M.

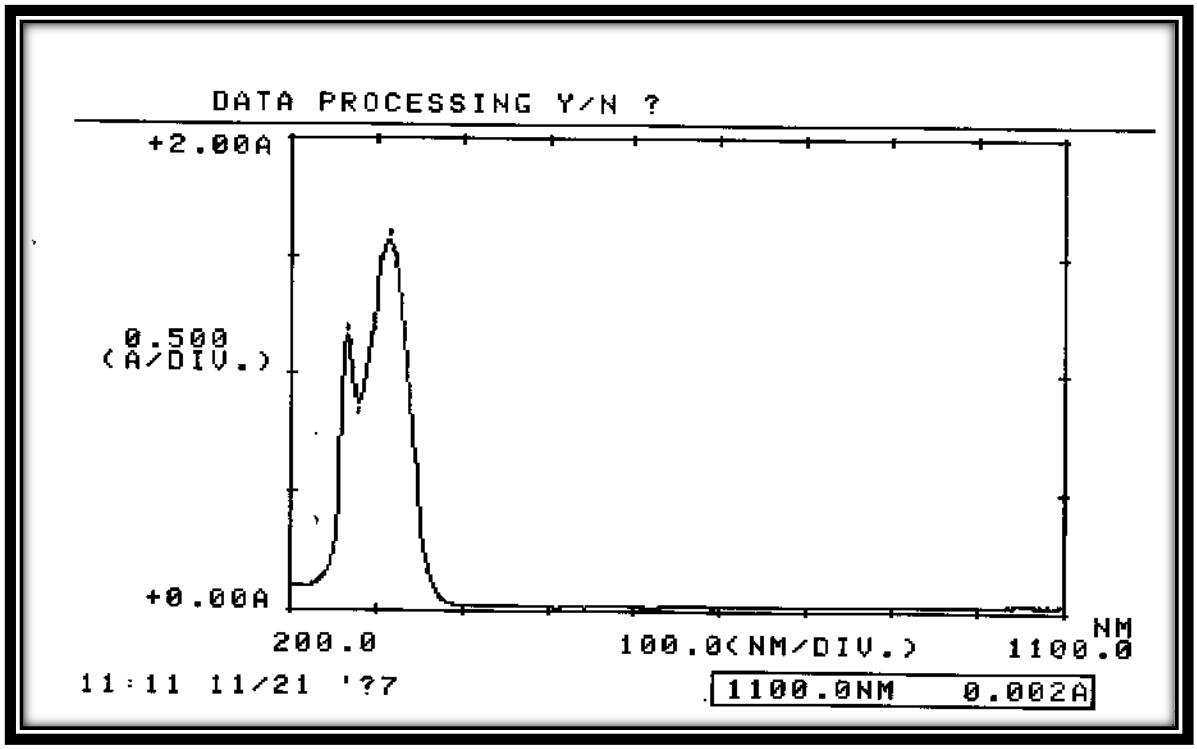

Fig.(3-80): Electronic spectrum of $[VO(L^3)_2(SO_4)].H_2O$ (17)in $4.5x10^{-4}$M.

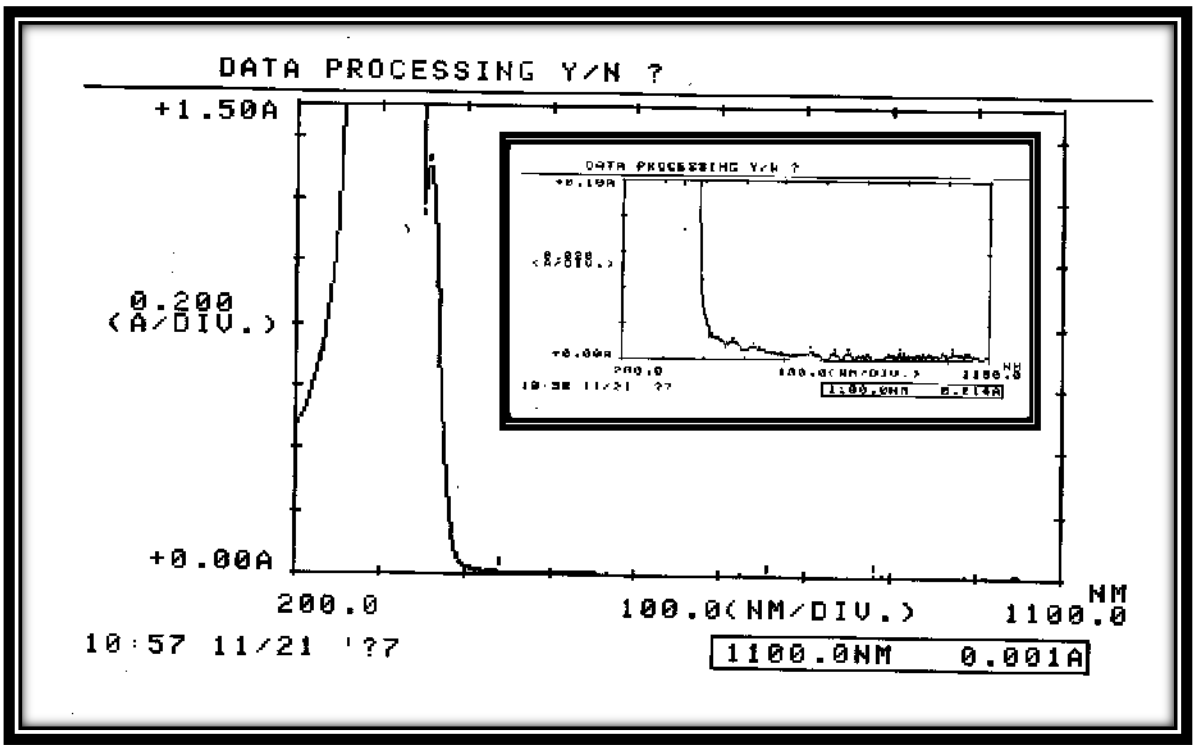

Fig.(3-81): Electronic spectrum of $[Mn(L^3)_2Cl_2].H_2O$(18) in 10^{-3}M.

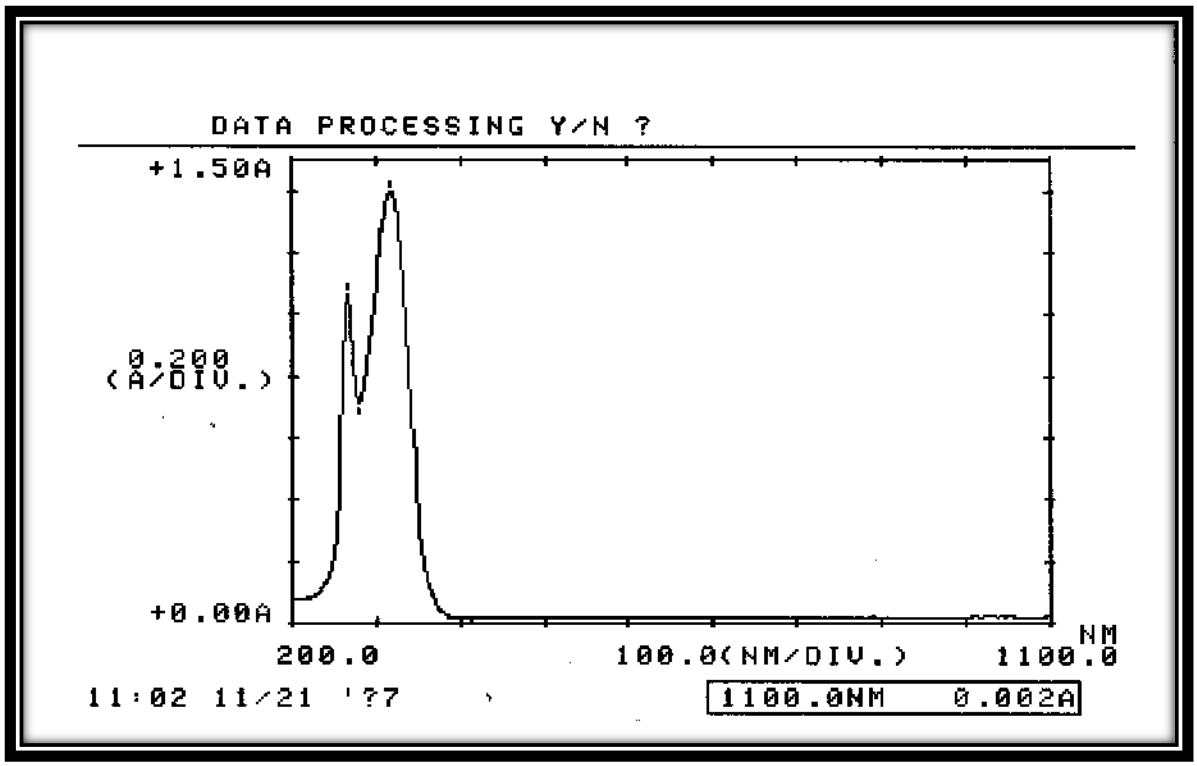

Fig.(3-82): Electronic spectrum of $[Mn(L^3)_2Cl_2].H_2O$(18) in $4x10^{-4}$M.

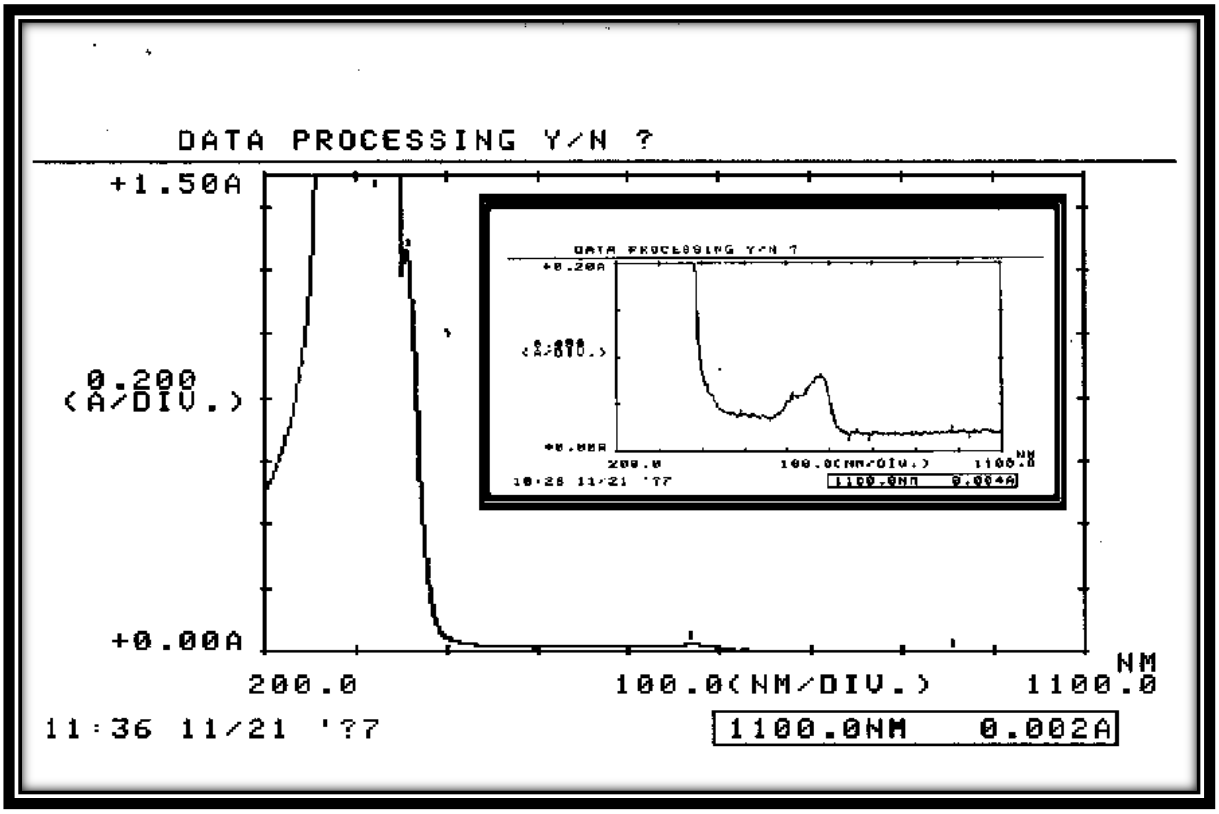

Fig.(3-83): Electronic spectrum of $[Co(L^3)_2Cl_2].H_2O$(19) in 10^{-3}M.

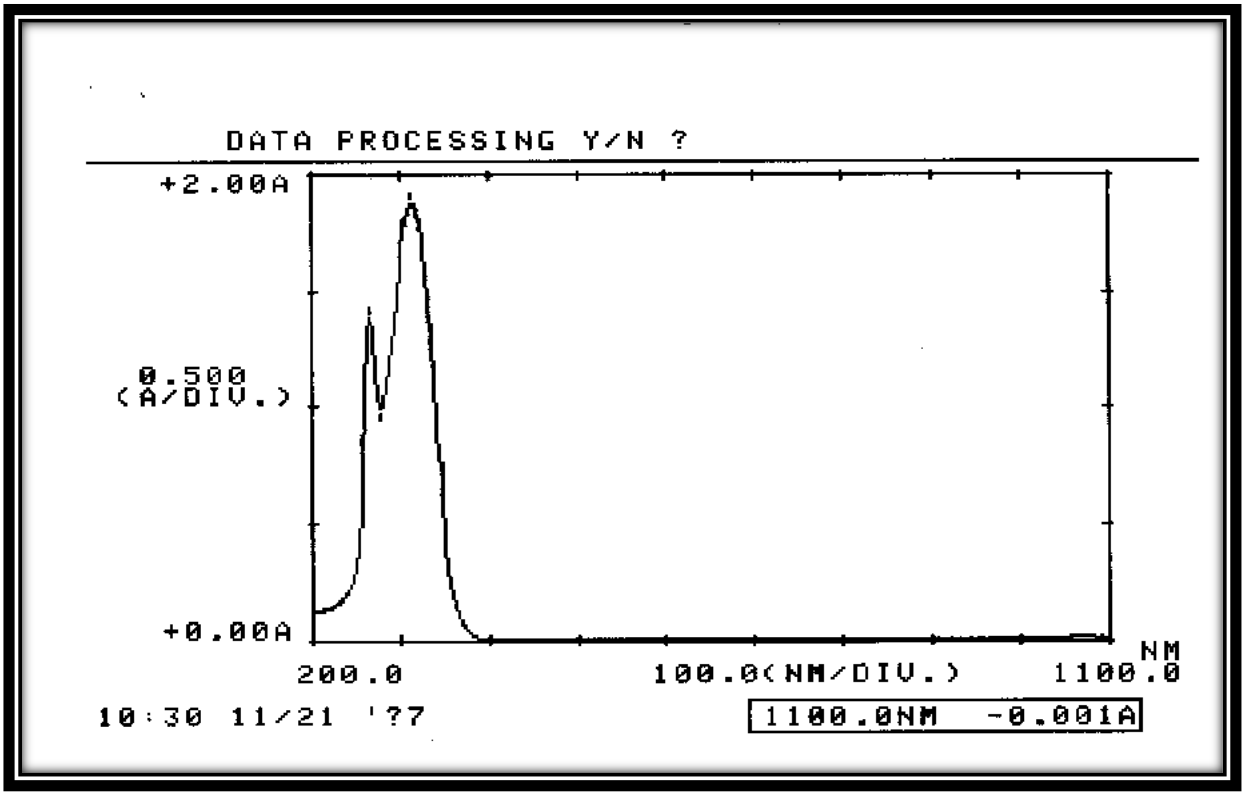

Fig.(3-84): Electronic spectrum of $[Co(L^3)_2Cl_2].H_2O$(19) in $5x10^{-4}$M.

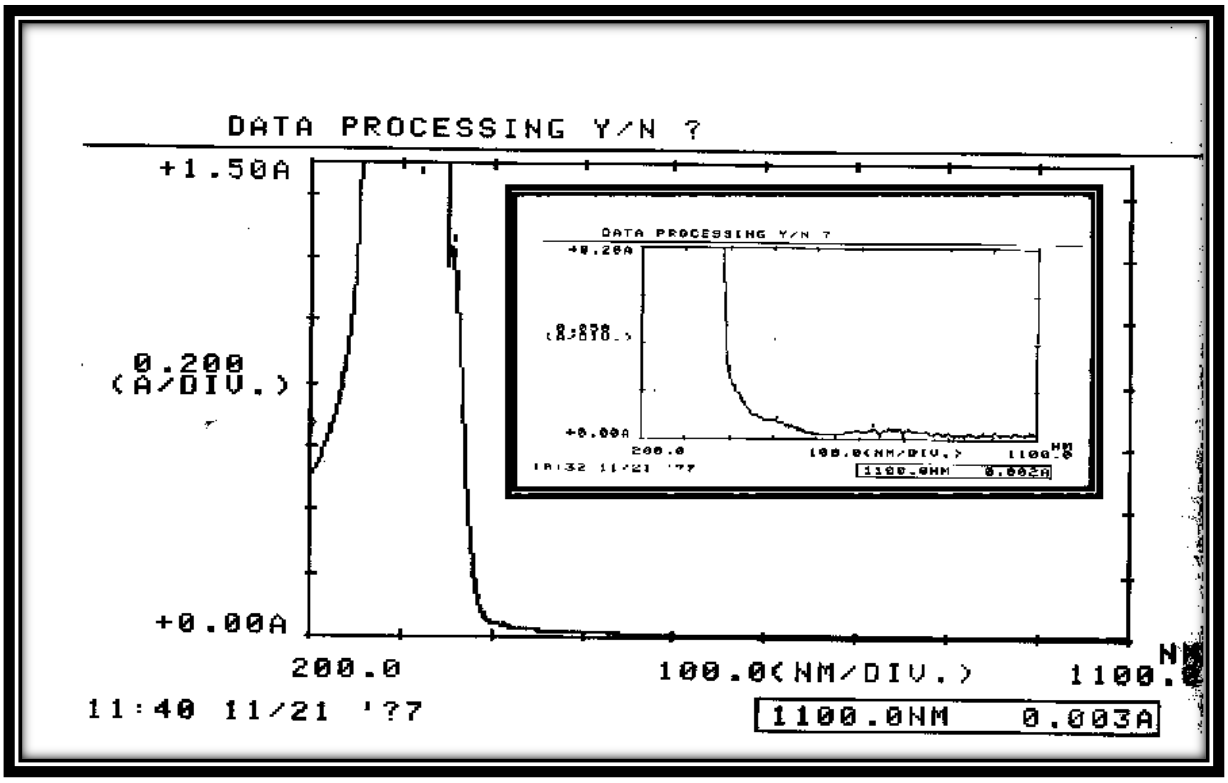

Fig.(3-85): Electronic spectrum of $[Ni(L^3)_2Cl]Cl.H_2O$(20) in 10^{-3}M.

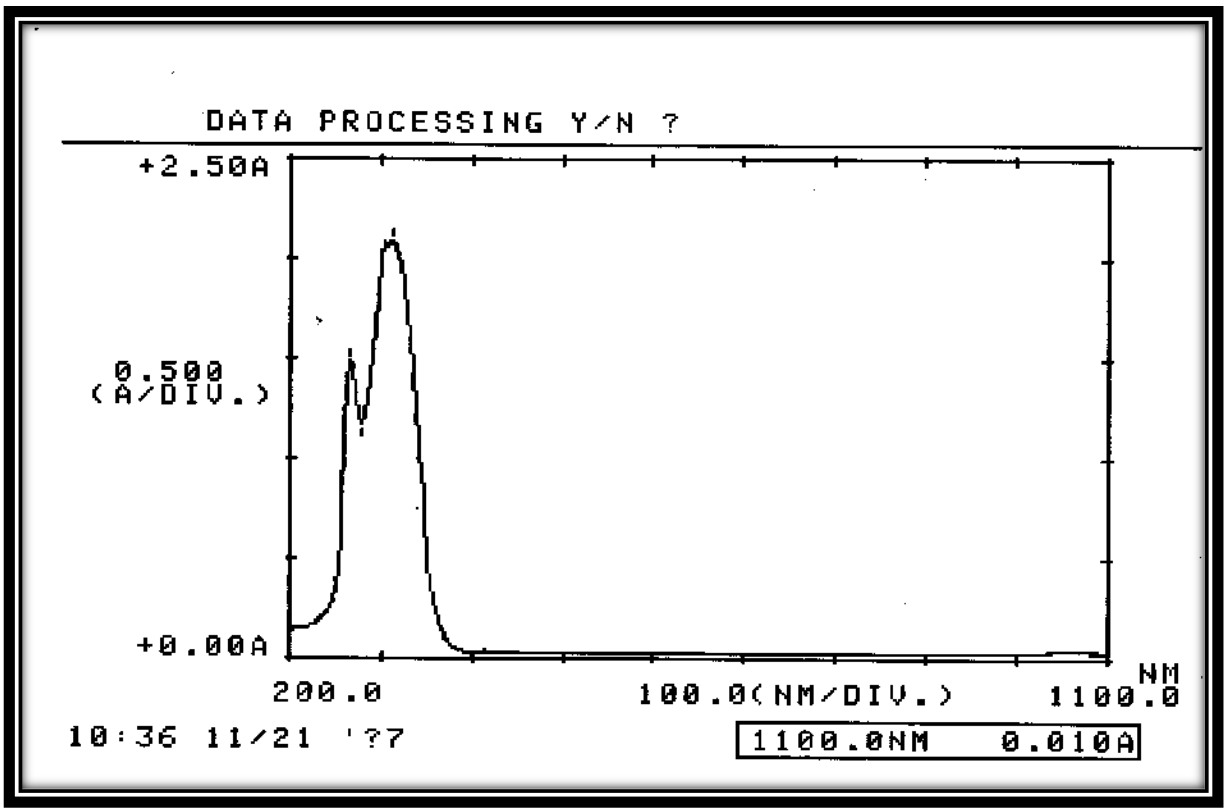

Fig.(3-86): Electronic spectrum of $[Ni(L^3)_2Cl]Cl.H_2O$(20) in $5x10^{-4}$M.

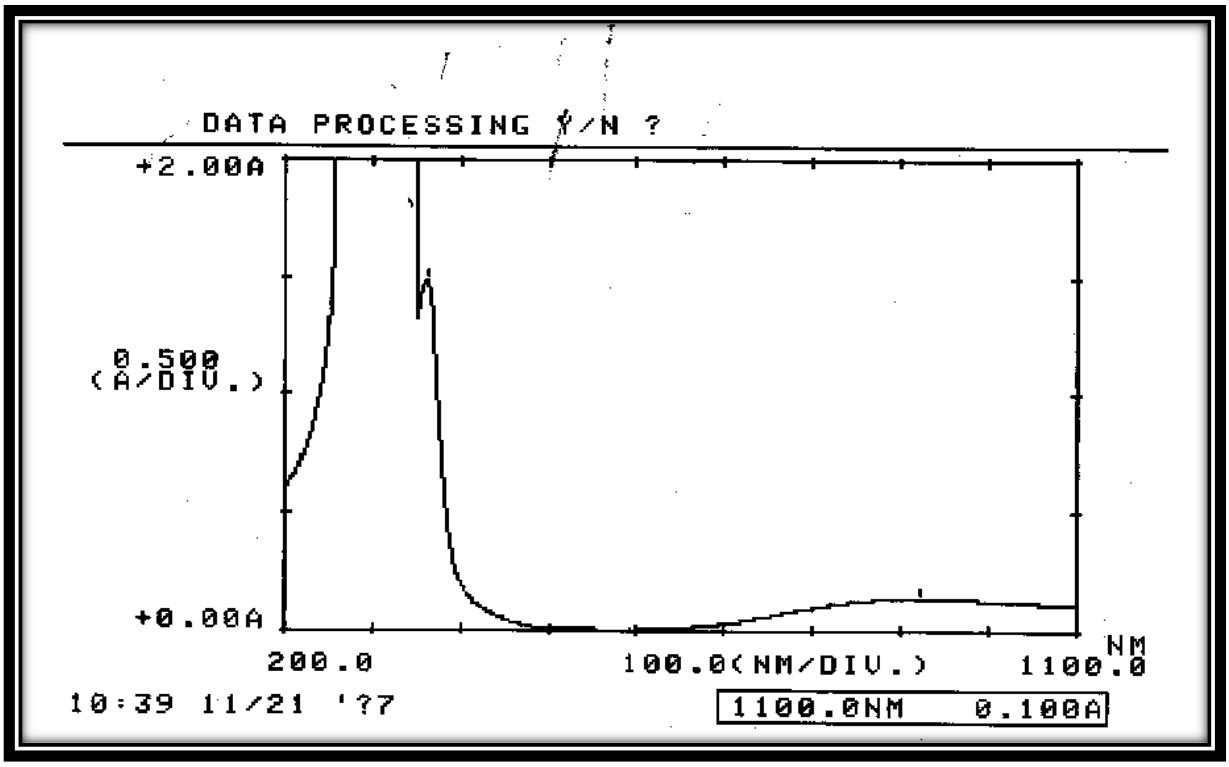

Fig.(3-87): Electronic spectrum of $[Cu(L^3)_2Cl_2].H_2O$ (21) in 10^{-3}M.

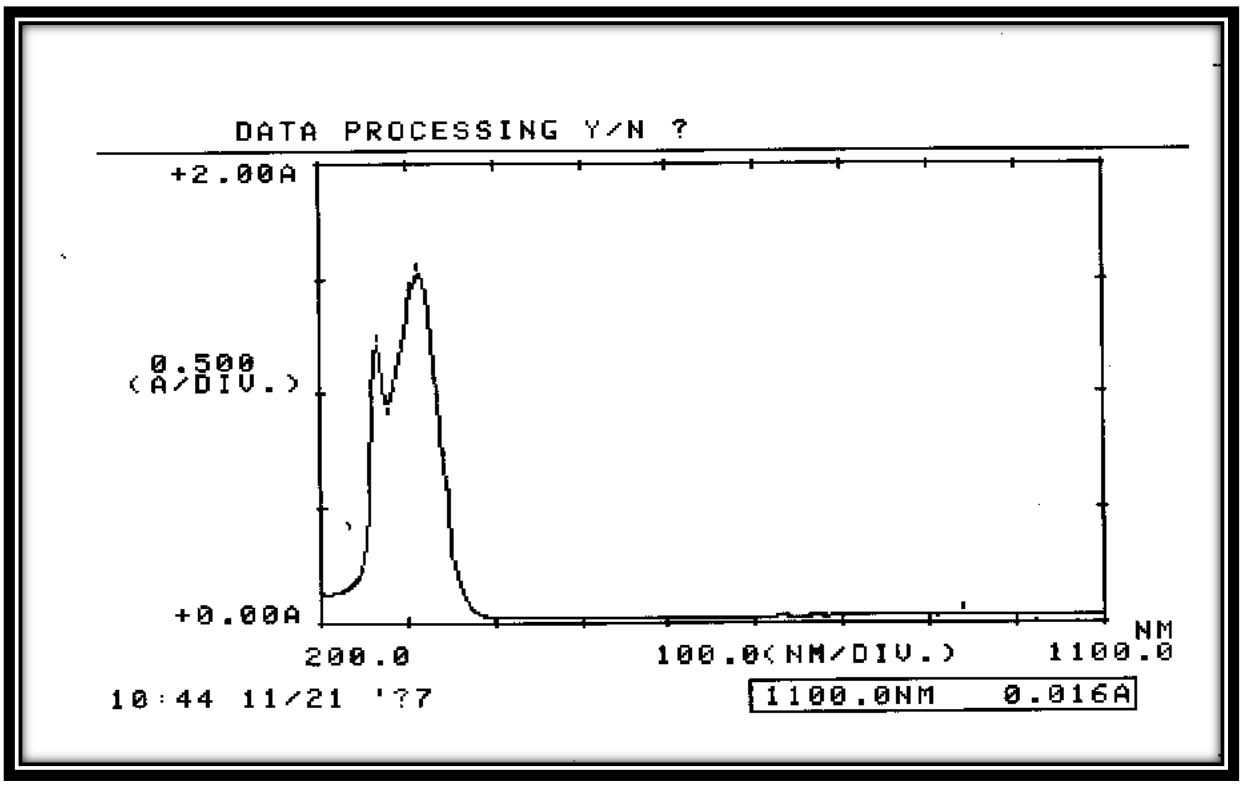

Fig.(3-88): Electronic spectrum of $[Cu(L^3)_2Cl_2].H_2O$ (21) in $4.5x10^{-4}$M.

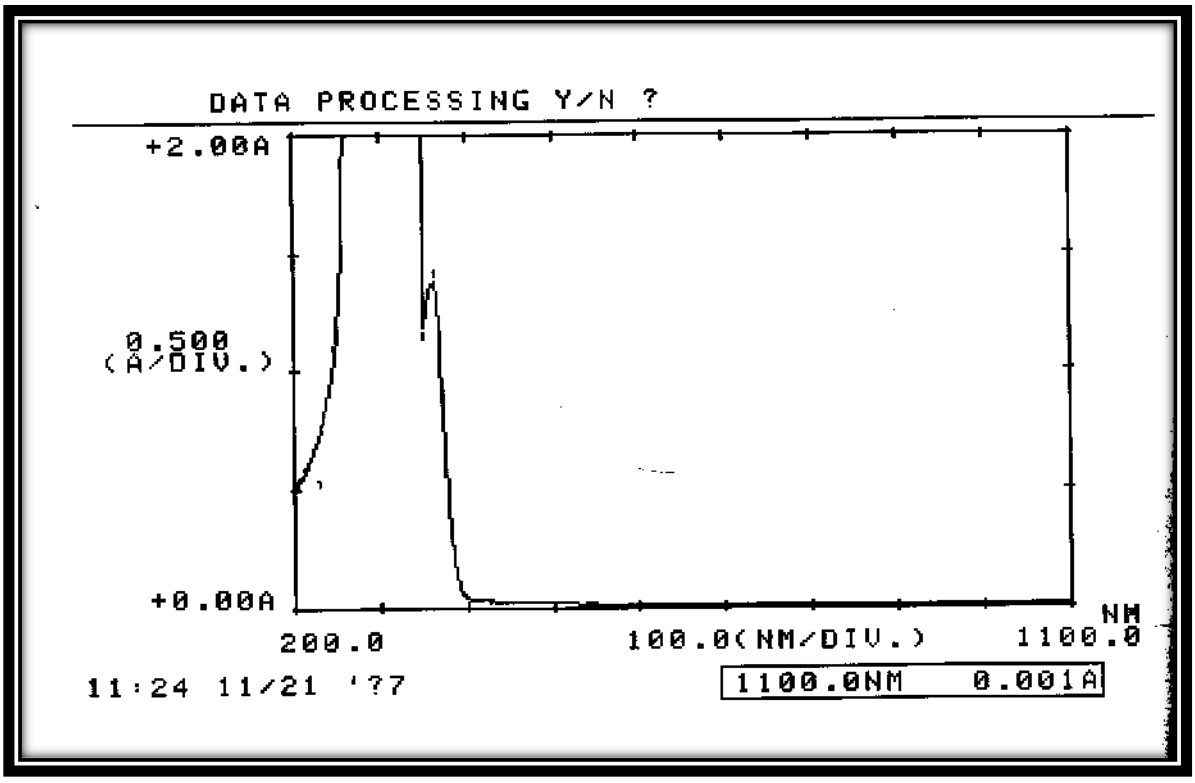

Fig.(3-89): Electronic spectrum of $[Zn(L^3)_2Cl_2].H_2O$ (22) in 10^{-3}M.

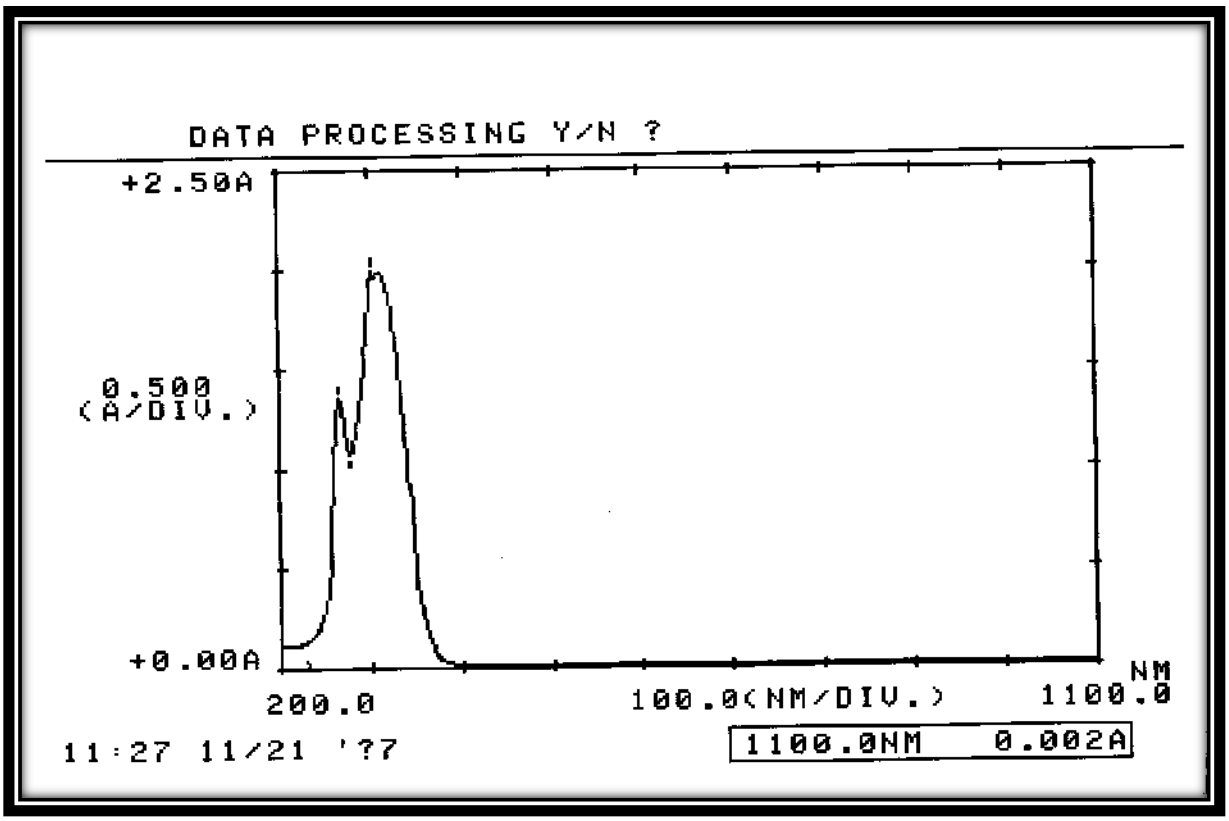

Fig.(3-90): Electronic spectrum of $[Zn(L^3)_2Cl_2].H_2O$ (22) in $5x10^{-4}$M.

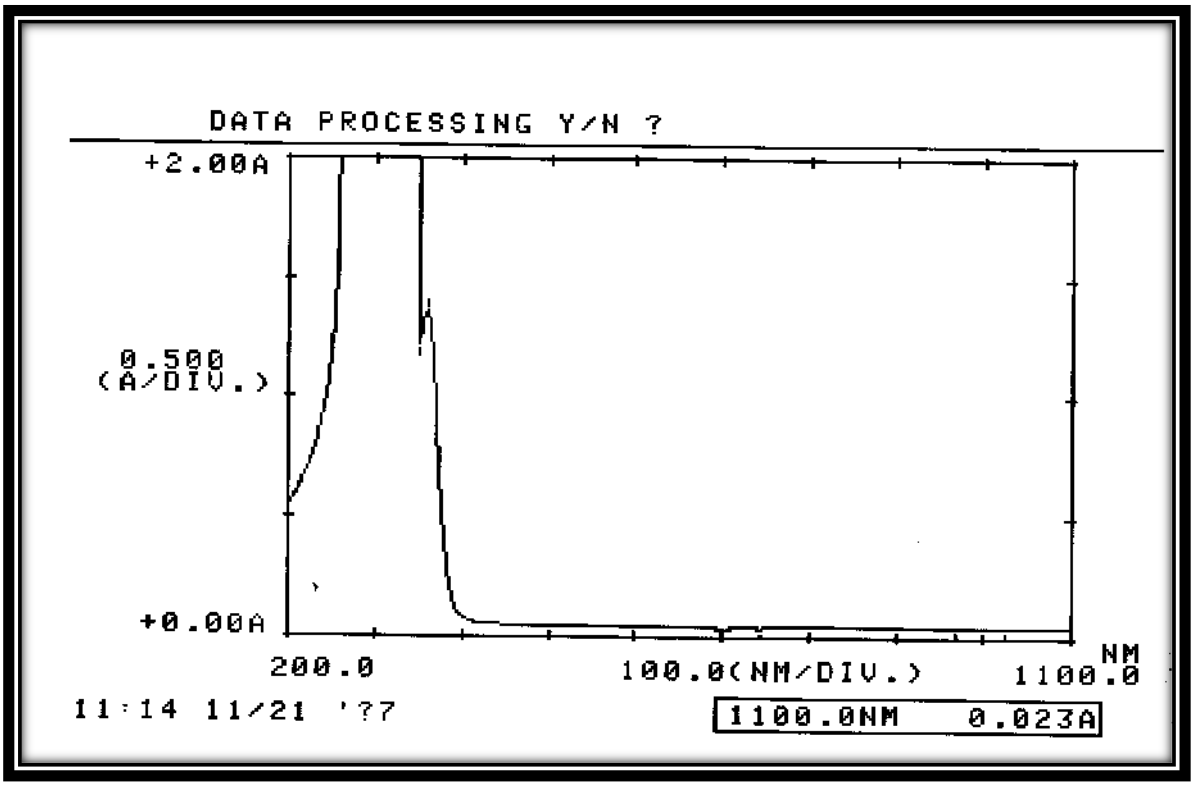

Fig.(3-91): Electronic spectrum of $[Cd(L^3)_2Cl_2].H_2O$ (23) in 10^{-3}M.

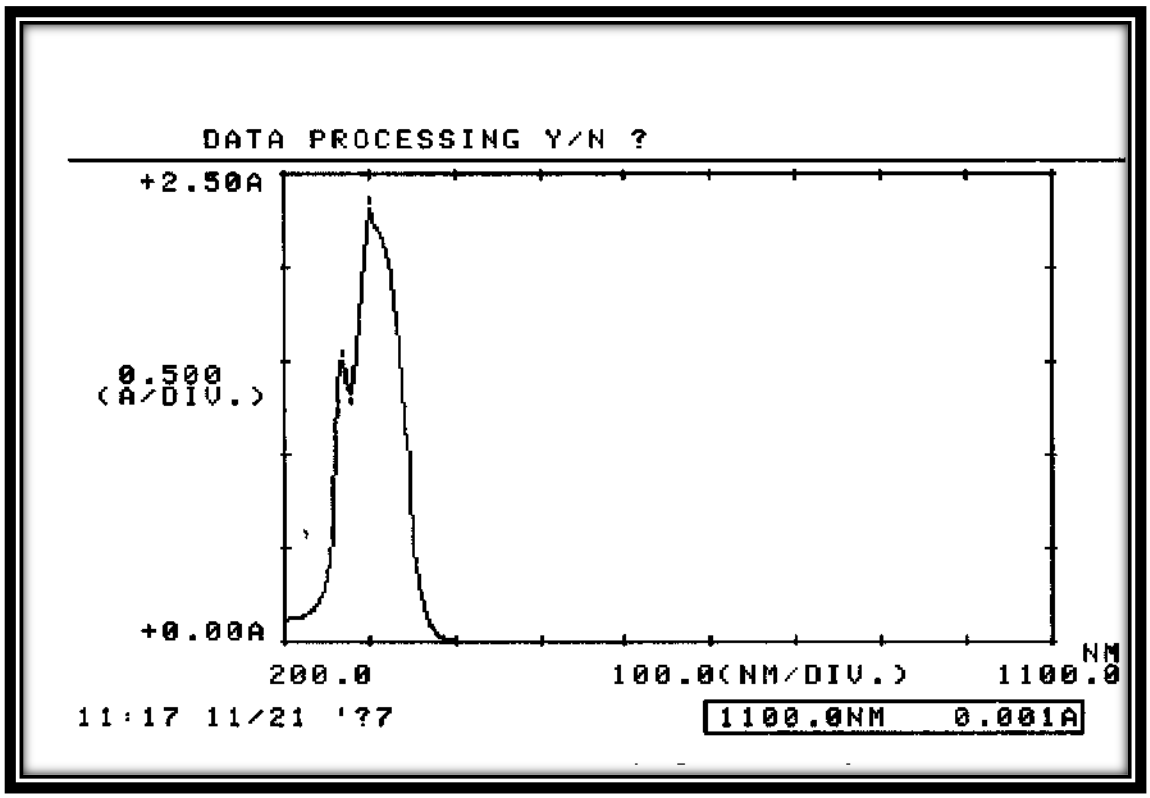

Fig.(3-92): Electronic spectrum of $[Cd(L^3)_2Cl_2].H_2O$ (23) in $5.5x10^{-4}$M.

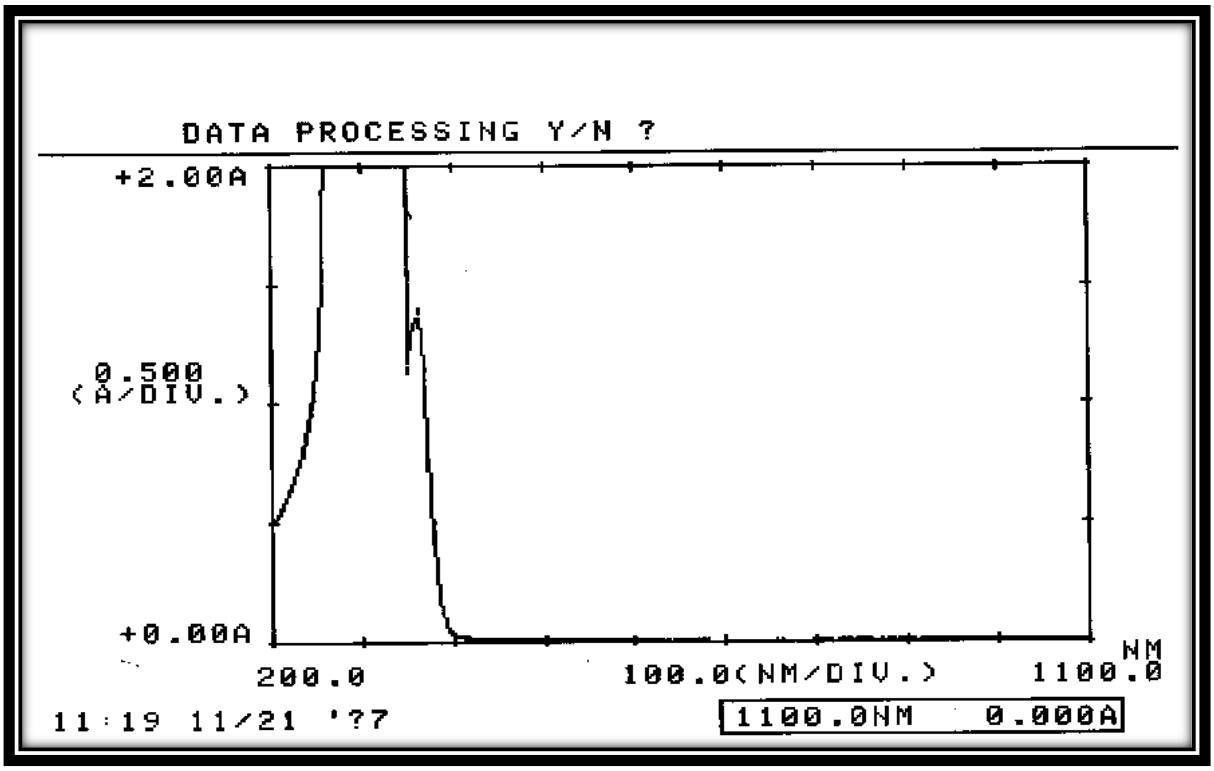

Fig.(3-93): Electronic spectrum of $[Hg(L^3)_2Cl_2].H_2O$ (24) in 10^{-3}M.

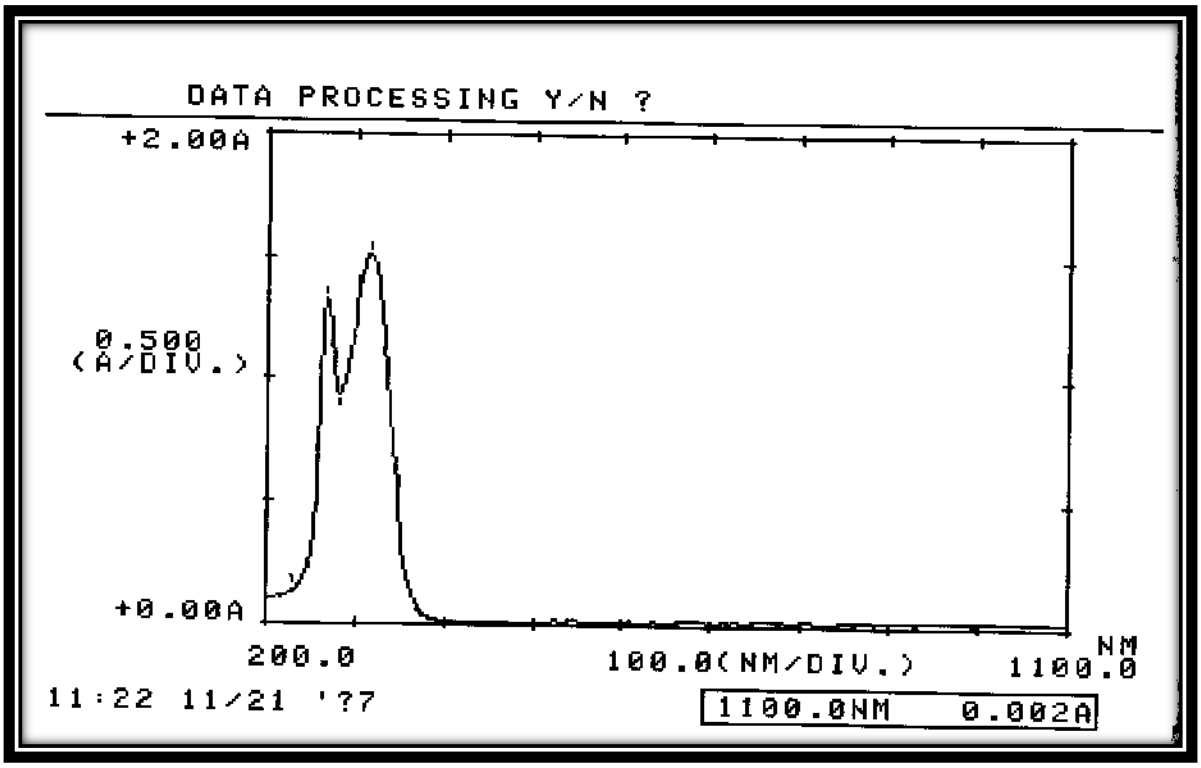

Fig.(3-94): Electronic spectrum of $[Hg(L^3)_2Cl_2].H_2O$ (24) in $5x10^{-4}$M.

(3.2.7) Thermal Analysis of Ligands Complexes:

Thermal decomposition data of some metal complexes are listed in Table (3-27). A range of analysis techniques including TGA (Thermo Gravimetric Analysis) and DSC (Differential Scanning Calorimetry) are used to study the title compounds in this work and their curves are discussed as follows:

(3.2.7.1) Thermal Decomposition of $[Cu(L^1)_2Cl_2].H_2O$

The thermogram for $[Cu(L^1)_2Cl_2].H_2O$ is placed in Fig.(3-95). In the TGA curve, peak recognized at 281.31 ºC is related to the loss of (H_2O , Cl_2 , C_8H_9NOS**)** portions, (det. = 4.765 mg, 23.829 %; calc. = 4.798 mg). The second step at 595.05 ºC that designated the loss of ($C_6H_4N_2OS$) fragment, (obs. = 2.832 mg, 14.179%; calc. = 2.852 mg). The final remainder of the compound that observed above 598.0 ºC is assigned to the ($CuC_{34}H_{25}N_7O_4$) , (det. = 12.343 , 61.715 %; calc. = 12.356 mg). The DSC analysis curve proved peaks at 89.6 , 133.2 , 163.6 , and 595.05 ºC refer to an endothermic decomposition process. Peaks observed at 267.0 , 302.1, 327.8 and 355.5 ºC were related to exothermic decomposition processes. The exothermic and endothermic peaks may demonstrate ignition of the natural ligand in an argon atmosphere . The last endothermic pinnacle may imply the metal-ligand bond breaking [177,178].

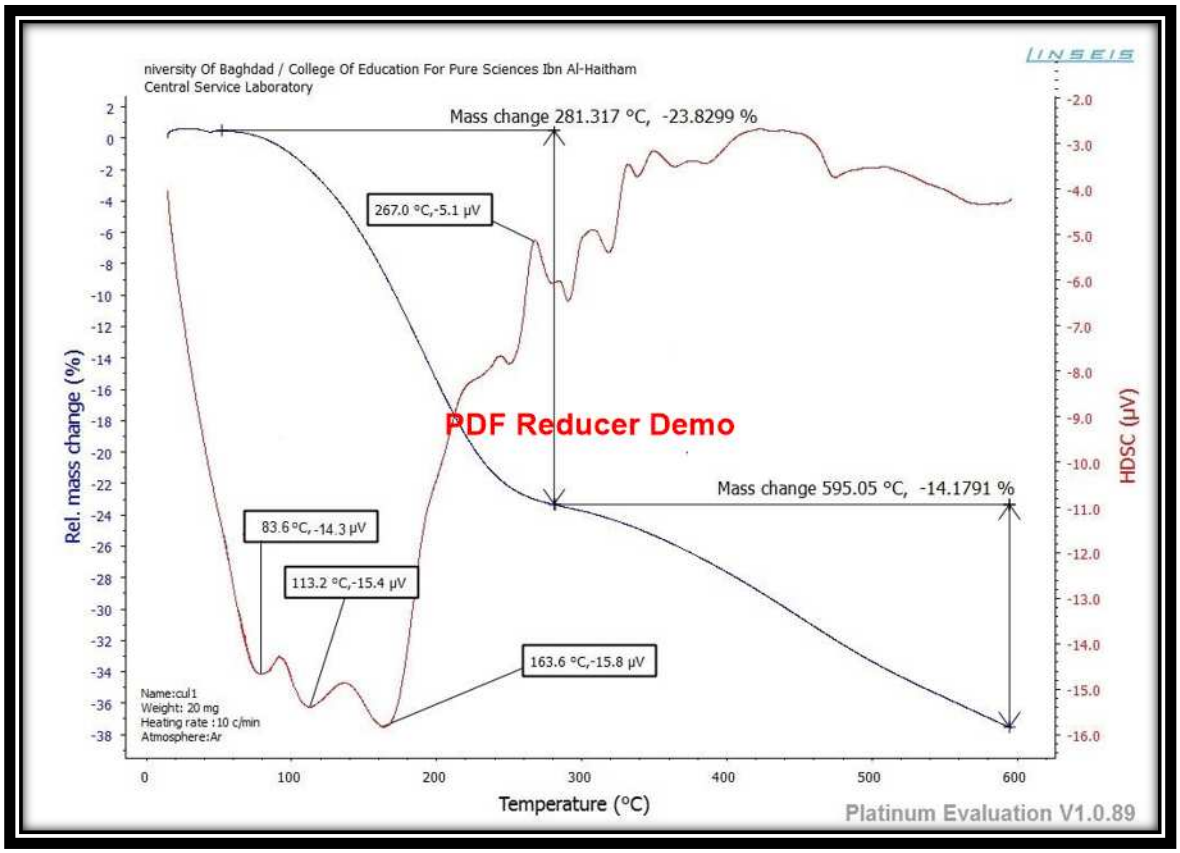

Fig. (3-95): (TGA and DSC) thermogram of $[Cu(L^1)_2Cl_2].H_2O$.

(3.2.7.2) Thermal Decomposition of $[Co(L^2)_2Cl_2].H_2O$

The thermogram for $[Co(L^2)_2Cl_2].H_2O$ is placed in Fig. (3-96). In the TGA curve, peak recognized detected at 248.61 ºC is related to the loss of (H_2O, Cl_2 , $C_7H_5N_2S$**)** portions, (det. = 4.726 mg, 23.632 %; calc. = 4.754 mg). The second step at 344.61 ºC that designated the loss of (3C , H_2) fragment , (obs. = 0.734 mg, 3.671%; calc. = 0. 759 mg). The third step at 595.57 ºC is related to the loss of ($C_4H_5N_3O_2S$) segments, (obs. = 3.158 mg, 15.792 %; calc. = 3.176mg) .The final remainder of the compound that observed above 598.0 ºC is assigned to the ($CoC_{32}H_{22}N_5O_2$) , (det. = 11.311, 56.556 %; calc. = 11.331 mg). The DSC analysis curve verified peaks at 56.2 , 133.3 , 188.6 and 595.5 ºC refer to an endothermic decomposition process. Peaks observed at 268.2 , 447.1 and 400.5 ºC were related to exothermic decomposition processes. The exothermic and

endothermic peaks may may demonstrate ignition of the natural ligand in an argon atmosphere . The last endothermic pinnacle may imply the metal-ligand bond breaking [179,180] .

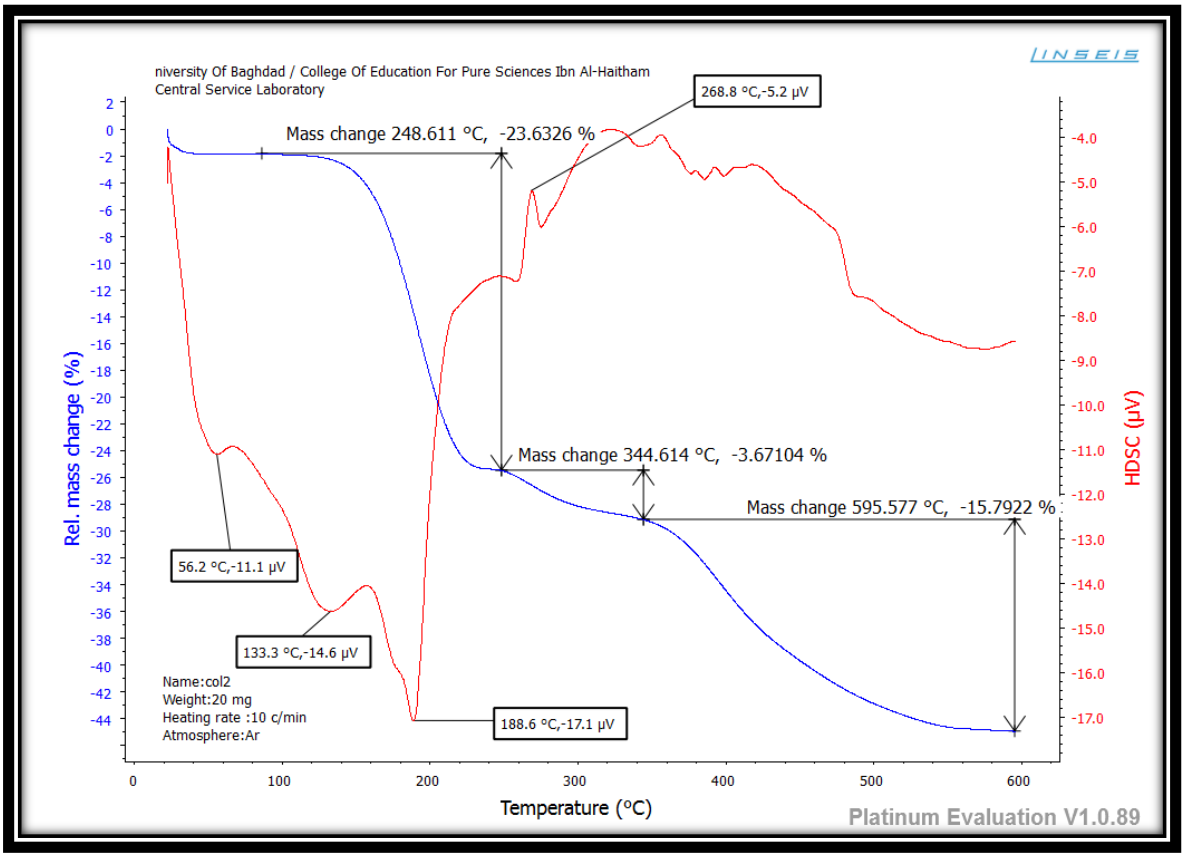

Fig. (3-96): (TGA and DSC) thermogram of $[Co(L^2)_2Cl_2].H_2O$.

(3.2.7.3) Thermal Decomposition of $[Mn(L^3)_2(H_2O)Cl]Cl.H_2O$.

The thermogram for $[Mn(L^3)_2(H_2O)Cl]Cl.H_2O$ is placed in Figure (3-97). In the TGA curve, peak recognized at 252.48 °C is related to the loss of ($2H_2O$, 2HCl , $2CH_4$, N_2 ,) portions , (det. = 3.308 mg, 15.036 %; calc. = 3.313 mg). The second step at 378.28 °C that designated the loss of (CO, C_3H_6) fragment , (obs. = 1.358 mg , 6.173%; calc. = 1.374 mg). The third step at 595.58 °C is related to the loss of ($C_{13}H_{12}N_2$, H_2) segments, (obs. = 3.864 mg , 17.566 %; calc. = 3.882 mg). The final remainder of the

compound that observed above 598.0 ºC is assigned to the ($MnC_{35}H_{18}N_8O_5$) , (det. = 13.439 , 61.045 %; calc. = 13.449 mg). The DSC analysis curve proved peaks at 96.4 , 135.4 , and 200.7 , 595.5 ºC refer to an endothermic decomposition process. Peaks observed at 268.2, 447.1 and 400.5 ºC were related to exothermic decomposition processes. The exothermic and endothermic peaks may demonstrate ignition of the natural ligand in an argon atmosphere. The last endothermic pinnacle may imply the metal-ligand bond breaking [181,182] .

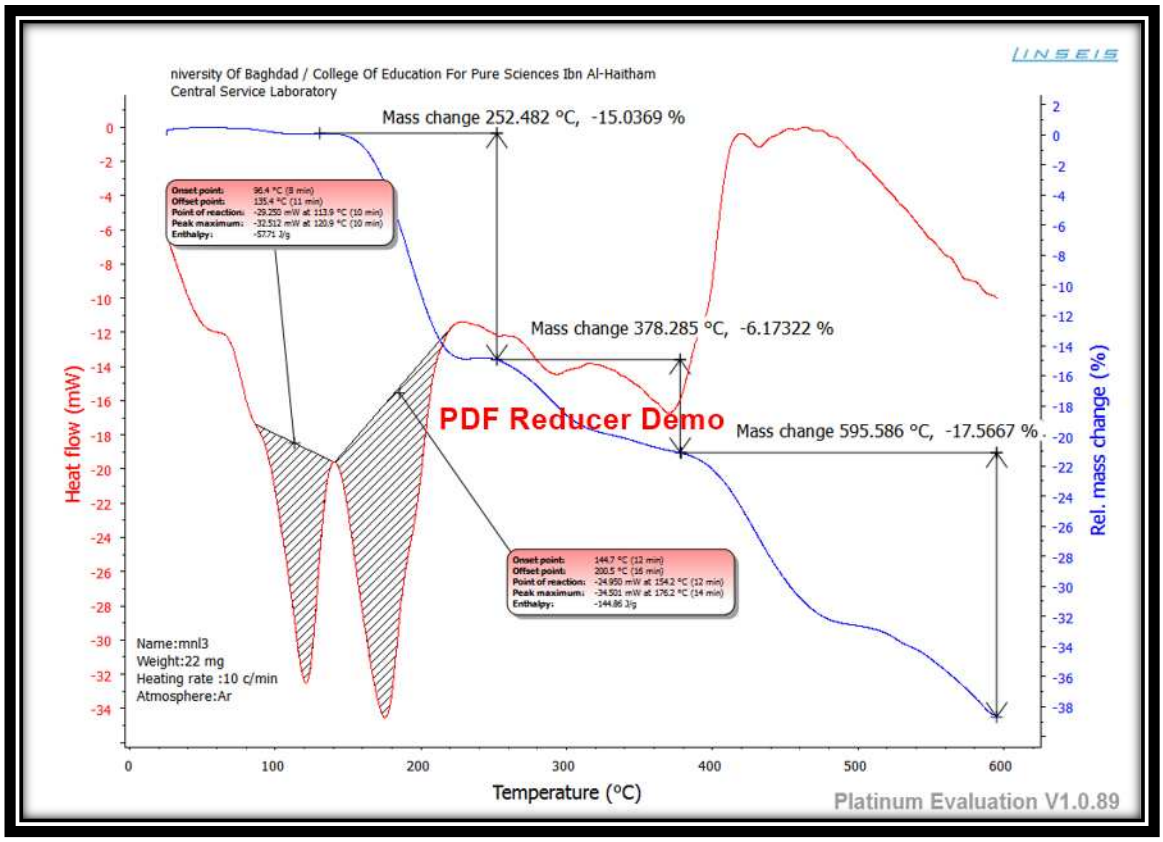

Fig. (3-97): (TGA and DSC) thermogram of $[Mn(L^3)_2(H_2O)Cl]Cl.H_2O$.

(3.2.7.4) Thermal Decomposition of $[Ni(L^3)_2Cl]Cl.H_2O$

The thermogram for $[Ni(L^3)_2Cl]Cl.H_2O$ is placed in Fig.(3-98). In the TGA curve, peak recognaized at 146.26 ºC is related to the loss of (H_2O, HCl ,$3H_2$**)** portions , (det. = 1.135 mg, 5.405 %; calc. = 1.146 mg). The

second step at 217.24 ºC that designated the loss of (HCl , $C_9H_6N_2O_2$) fragment , (obs. = 3.999 mg , 19.043%; calc. = 4.000 mg). The third step at 304.67 ºC is related to the loss of (CH_4, NH_3 , $3H_2$) segments, (obs. = 0.731 mg , 3.482 %; calc. = 0.743 mg). The forth step at 453.12 ºC is related to the loss of ($C_6H_3N_2O$) segments, (obs. = 2.241 mg , 10.674 %; calc. = 2.259 mg). The fifth step at 595.32 ºC is related to the loss of ($C_3H_4O_2$, C_2H_2) segments, (obs. = 1.840 mg , 8.763 %; calc. = 1.859 mg). The final remainder of the compound that observed above 598.0 ºC is assigned to the ($NiC_{33}H_{12}N_7O$) , (det. = 10.991 , 52.338 %; calc. = 11.004 mg). The DSC analysis curve proved peaks at 89.6 , 138.9 , 181.8 , 272.2 and 595.5 ºC refer to an endothermic decomposition process. Peaks observed at 297.7 and 312.9 ºC were related to exothermic decomposition processes. The exothermic and endothermic peaks may demonstrate ignition of the natural ligand in an argon atmosphere. The last endothermic pinnacle may imply the metal-ligand bond breaking [183,184].

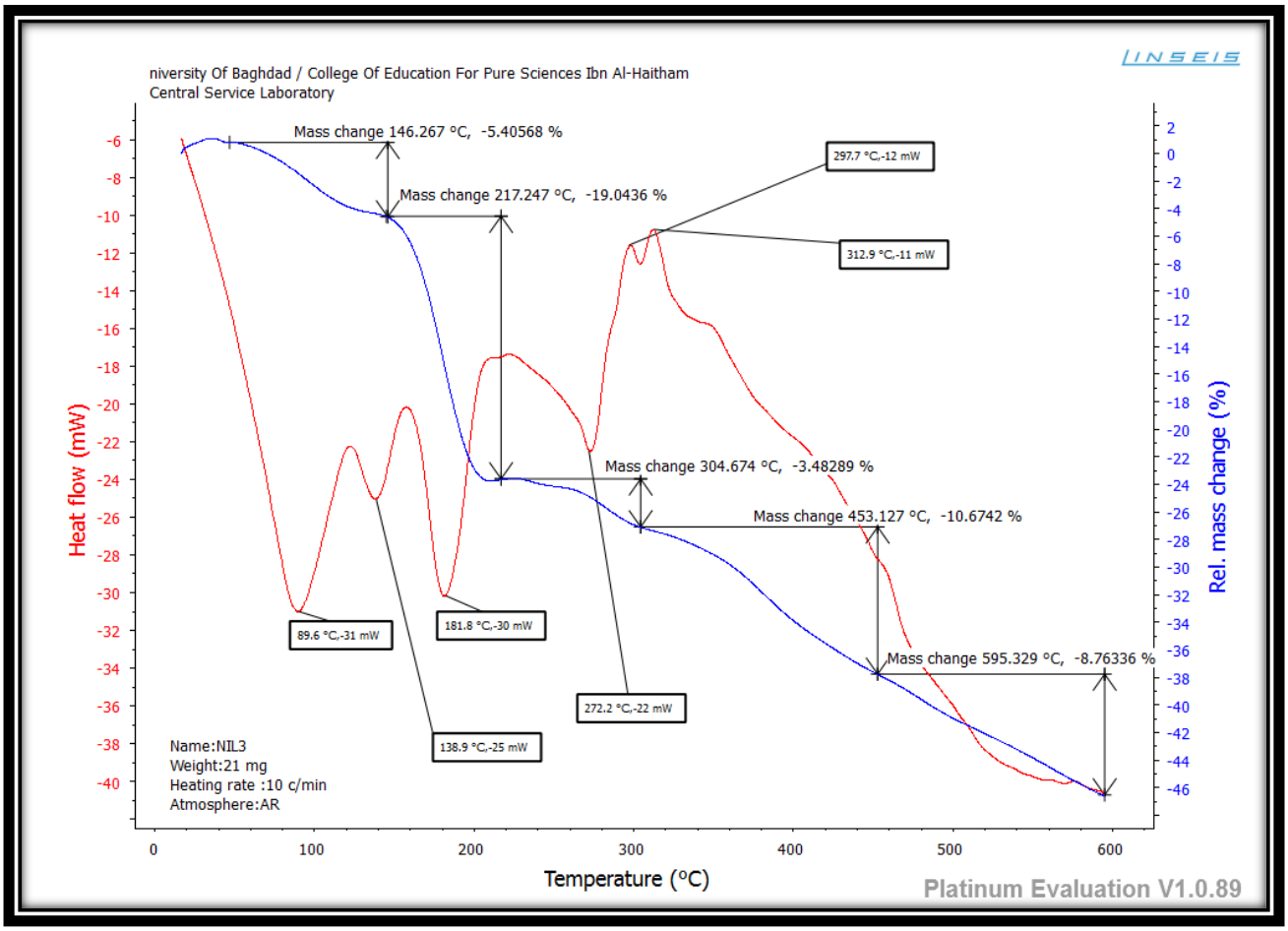

Fig. (3-98): (TGA and DSC) thermogram of $[Ni(L^3)_2Cl]Cl.H_2O$

(3.2.7.5) Thermal Decomposition of $[Hg(L^3)_2Cl_2].H_2O$

The thermogram for $[Hg(L^3)_2Cl_2].H_2O$ is placed in Figure (3-99). In the TGA curve, peak recognized at 271.81 ºC is related to the loss of (H_2O, Cl_2 , C_6H_5 , $C_{13}H_{13}N_3O$) portions , (det. = 5.959 mg, 31.365 %; calc. = 5.978 mg). The second step at 595.23 ºC that designated the loss of ($C_{11}H_{11}N_3O$, $C_8H_7N_3O_2$, $C_{13}H_{12}$) fragment , (obs. = 8.281 mg , 43.588%; calc. = 8.308 mg). The final remainder of the compound that observed above 598.0 ºC is assigned to the ($HgC_3N_3O_2$) , (det. = 4.720 , 24.8476 %; calc. = 4.727 mg). The DSC analysis curve proved peaks at 91.4 , 168.1 , 214.8 , 298.9 and 595.2 ºC refer to an endothermic decomposition process. Peaks

observed at 326.8 and 412.7 ºC were related to exothermic decomposition processes. The exothermic and endothermic peaks may demonstrate ignition of the natural ligand in an argon atmosphere. The last endothermic pinnacle may imply the metal-ligand bond breaking [185,186].

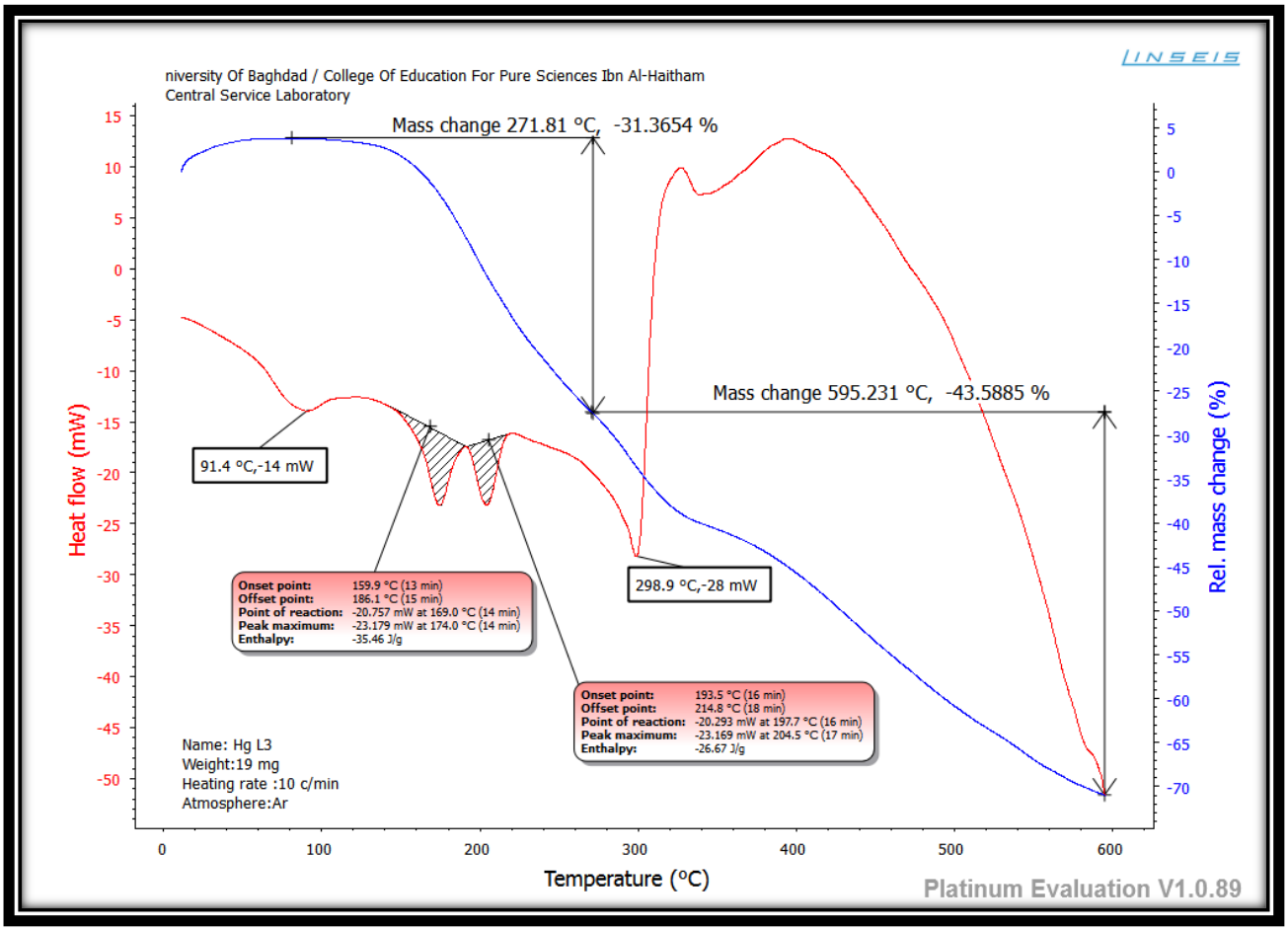

Fig. (3-99): (TGA and DSC) thermogram of $[Hg(L^3)_2Cl_2].H_2O$

Table (3-27): TG and DSC data for some ligand's complexes.

Complexes	Stage	Decomposition Temperature Initial-Final (°C)	Estimated (calculated)		Assignment
			Mass Loss	Total mass Loss	
$[Cu(L^1)_2Cl_2].H_2O$	1	83.1-281.3	4.765 (4.798)	7.597 (7.650)	- (H_2O+Cl_2 C_8H_9NOS)
	2	286.4-595.0	2.832 (2.852)		- ($C_6H_4N_2OS$) ($CuC_{34}H_{25}N_7O_4$)
$[Co(L^2)_2Cl_2].H_2O$	1	56.2-248.6	4.726 (4.752)	8.618 (8.687)	- (H_2O+Cl_2 $C_7H_5N_2S$)
	2	263.2-344.6	0.734 (0.759)		- (3C + H_2)
	3	344.6-595.5	3.158 (3.176)		- ($C_4H_5N_3O_2S$) ($CoC_{32}H_{22}N_5O_2$)
$[Mn(L^3)_2(H_2O)Cl]Cl.H_2O$	1	96.4 - 252.4	3.308 (3.313)	8.530 (8.569)	- (2H_2O+ 2HCl + 2CH_4+N_2)
	2	252.4 - 378.2	1.358 (1.374)		- (C_3H_6+CO)
	3	378.2 – 595.5	3.864 (3.882)		- ($C_{13}H_{12}N_2$+H_2) ($MnC_{35}H_{18}N_8O_5$)
$[Ni(L^3)_2Cl]Cl.H_2O$	1	89.6 -146.2	1.135 (1.146)	9.946 (10.010)	(H_2O + HCl +3H_2)
	2	146.6 -217.2	3.999 (4.003)		- (HCl+ $C_9H_6N_2O_2$)
	3	220.4 -304.6	0.731 (0.743)		- (CH_4 + NH_3+ 3H_2)
	4	304.6 - 453.1	2.241 (2.259)		- ($C_6H_3N_2O$)

	5	453.1-595.3	1.840 (1.859)		- (C_2H_2+ $C_3H_4O_2$) ($NiC_{33}H_{12}N_7O$)
$[Hg(L^3)_2Cl_2].H_2O$	1 2	91.4-271.8 271.8-595.2	5.959 (5.978) 8.281 (8.308)	14.240 (14.286)	- (H_2O+Cl_2 +C_6H_5+$C_{13}H_{13}N_3O$) -($C_{13}H_{12}$+ $C_{11}H_{11}N_3O$ +$C_8H_7N_3O_2$ ($HgC_3N_3O_2$)

(3.3) Conclusions and the proposed molecular structure for all prepared complexes [(1)-(24)].

According to the characterization data for new Schiff base (L^1) derived from MBZ with 2-amino-6-methoxybenzothaizol and its mono complexes, (L^2) derived from MBZ with 2-aminobenzothaizol and its mono complexes and (L^3) derived from MBZ with 4-APP and its mono complexes by FT- IR, U.V-Vis, atomic absorption, ^{1}H-NMR, ^{13}C-NMR, Mass, TGA, magnetic susceptibility, molar conductivity, elemental microanalysis, chloride content along with melting point, we found that:

1. The Schiff base (L^1) and (L^2) behave as bidentate ligand through N atom of imine group and N atom of four member ring with the central metal ions: (VO(II), Mn(II), Co(II), Ni(II), Cu(II), Zn(II), Cd(II) and Hg(II) forming complexes with general molecular formula: $[M(L)_2Cl_2].H_2O$ and $[VO(L)_2SO_4].H_2O$

2. The Schiff base (L^3) and behave as bidentate ligand through N atom of imine group and O atom of C=O group of five membered ring with the central metal ions: (VO(II), Mn(II), Co(II), Ni(II), Cu(II), Zn(II),

Cd(II) and Hg(II) forming complexes with general molecular formula: $[M(L^3)_2(X)(Y)]A.H_2O$ and $[VO(L^3)_2SO_4].H_2O$.

3. The octahedral geometrical structure was suggested for all synthesized complexes except the complex $[Ni(L^3)_2Cl]Cl.H_2O$ It showed the shape trigonal bipyramid (tbp) based on the characterization data using all previous techniques.

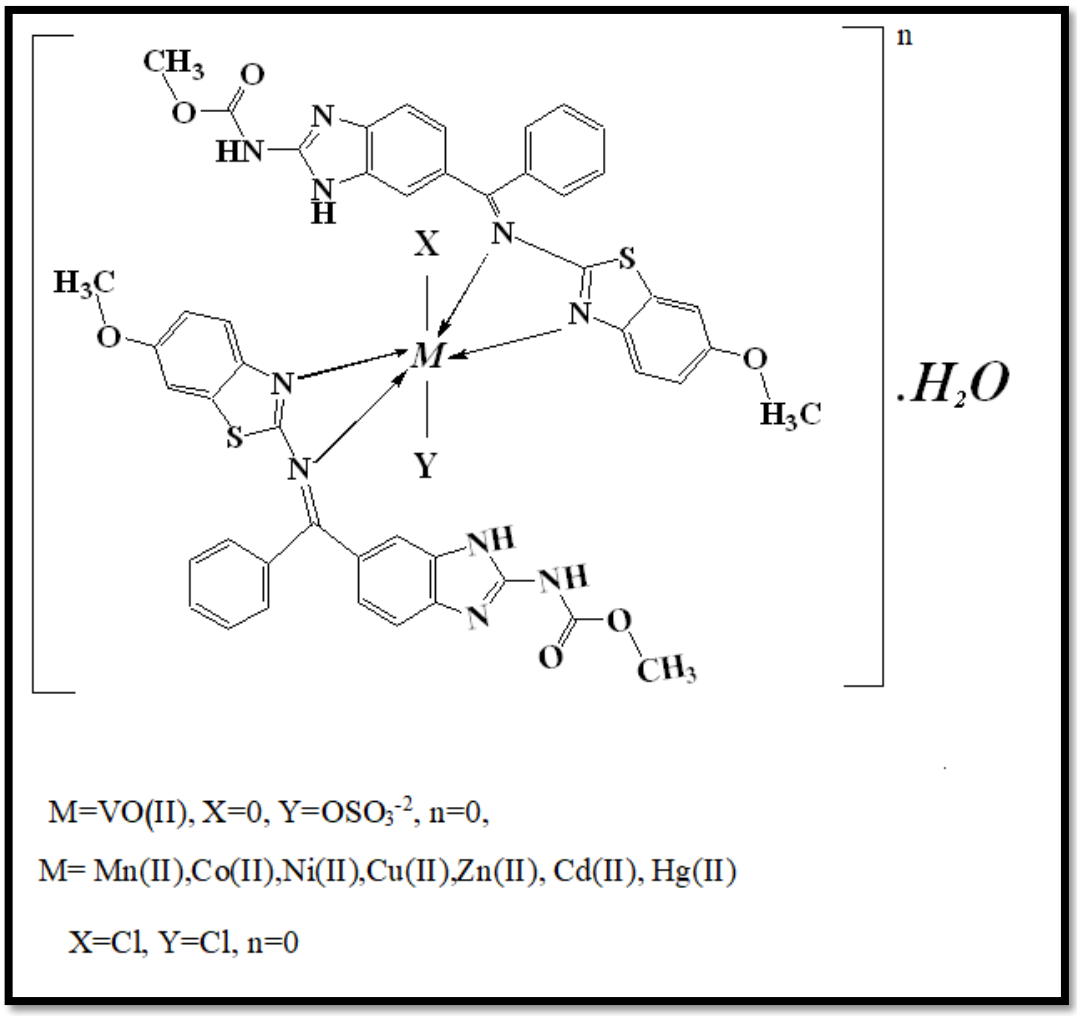

Fig.(3-100): The proposed geometrical structure of $[M(L^1)_2(X)(Y)].H_2O$

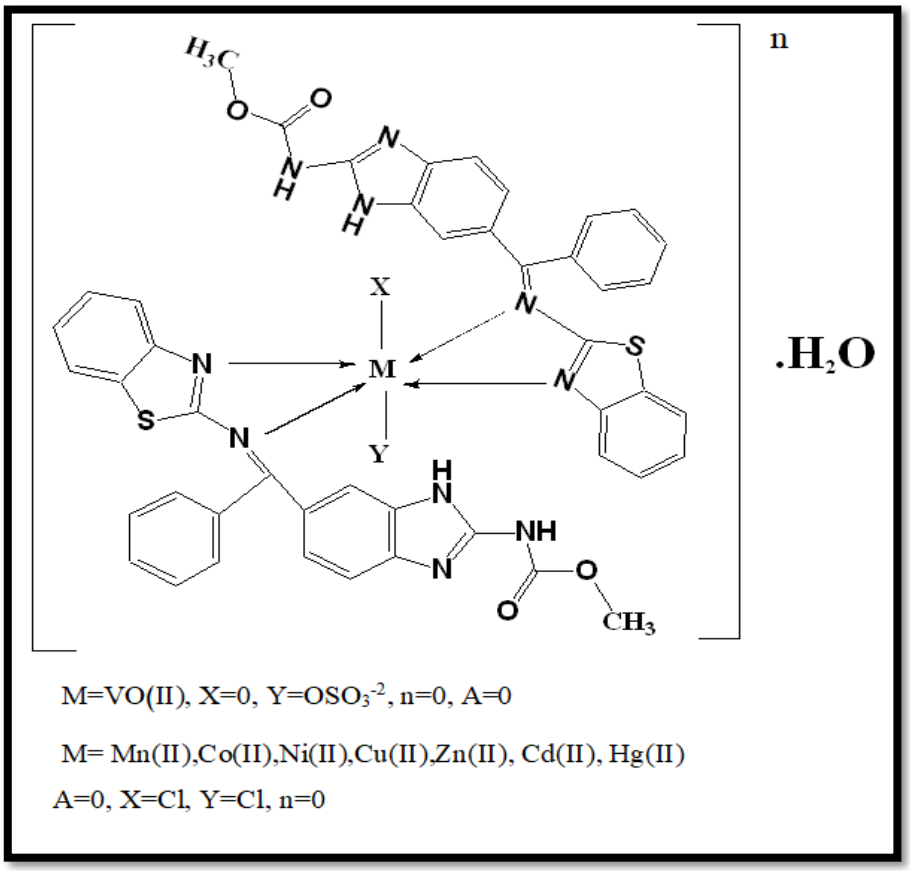

Fig.(3-101): The proposed geometrical structure of $[M(L^2)_2(X)(Y)].H_2O$

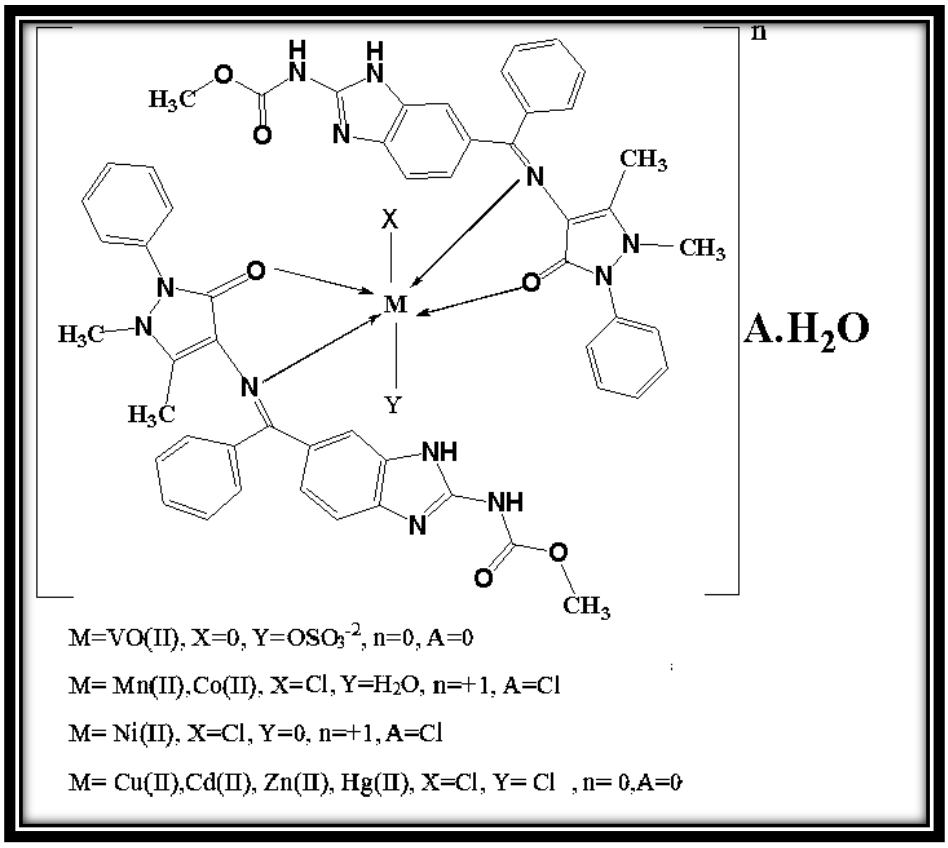

Fig.(3-102):The proposed geometrical structure of $[M(L^3)_2(X)(Y)]A.H_2O$

(3.4) Biological Activities:

The new synthesized ligands (L^1, L^2, L^3) and their complexes were tried against a range of bacterial strains (G^+ and G^-) and fungi species as follows:

(3.4.1) Bacterial Activity:

The synthesized ligands and their metal complexes were screened, for their antimicrobial activity against two bacterial strains (*Escherichia coli and Staphylococcus aureus*). This is to evaluate their potential antimicrobial activity. The job of DMSO in the biological screening was clarified by separate studies carried out with the solutions of DMSO alone, which showed no activity against bacterial strains [187]. The measured areas of inhibition against the growth of different microorganisms are listed in Table

(3-28) , Fig. (3-103) - (3-109) display the inhibition effect of the synthesized compounds on bacterial strains. The obtained data show that the title compounds have a different antimicrobial activity against the microorganisms. From the obtained data that displayed in the Table, the following key points are derived ;

More of complexes found to be actually more active towards tested bacterial strains, compared with the free ligands and the starting material, indicating complex formation improves antimicrobial activity. This could be related to the chelation effect that allow the involvement of the positive charge of the metal ion in complexes by the donor atoms present in the ligand. This will result in the π-electron distribution over the entire chelate ring that increases the lipophilic character of the metal chelate system. This will favour its mobility through the cell membranes [188,189] .

The obtained data show there is no trend regarding antibacterial activity of some the tested complexes. However, some common remarks have been observed and as follows;

a- The three ligands (L^1- L^3) showed no antimicrobial activity against *Staphylococcus aureus* [190].

b- The two ligands (L^1, L^2) showed antimicrobial activity against *Escherichia coli* [191] .

c- Mercury complexes for ligands (L^1, L^2 and L^3) have the higher antimicrobial activity, compared with other complexes. This may be related to its electronic configuration (d^{10} system) and/or its higher molecular weight, compared with other metal ions [192] .

The antimicrobial activity of the different compounds against different organisms depends on [193] :

a- Their impermeability of the microbial cells.

b- The difference in the ribosome of the microbial cells.

Table (3-28): Bacterial activity of the starting material, ligands and their complexes.

Compound	*Gram negative (G−)*	*Gram positive (G+)*
	E. Coli	*Staphylococcus*
DMSO (D)	-	-
MBZ (K)	14	-
AMBT (A_1)	19	12
ABT (A_2)	21	17
4-APP (A_3)	14	-
$[L^1]$	12	-
$[VO(L^1)_2(SO_4)].H_2O$	-	-
$[Mn(L^1)Cl_2].H_2O$	-	-
$[Co(L^1)Cl_2].H_2O$	-	-
$[Ni(L^1)_2Cl_2].H_2O$	-	-
$[Cu(L^1)_2Cl_2].H_2O$	-	-
$[Zn(L^1)Cl_2].H_2O$	-	-
$[Cd(L^1)Cl_2].H_2O$	-	-
$[Hg(L^1)Cl_2].H_2O$	27	44
$[L^2]$	13	-
$[VO(L^2)_2(SO_4)].H_2O$	14	16
$[Mn(L^2)_2Cl_2].H_2O$	18	22
$[Co(L^2)_2Cl_2].H_2O$	30	30
$[Ni(L^2)_2Cl_2].H_2O$	22	28
$[Cu(L^2)_2Cl_2].H_2O$	18	52
$[Zn(L^2)_2Cl_2].H_2O$	40	28

$[Cd(L^2)_2Cl_2].H_2O$	24	40
$[Hg(L^2)_2Cl_2].H_2O$	27	58
$[L^3]$	-	-
$[VO(L^3)_2(SO_4)].H_2O$	16	-
$[Mn(L^3)_2(H_2O)Cl]Cl.H_2O$	-	-
$[Co(L^3)_2(H_2O)Cl]Cl.H_2O$	25	23
$[Ni(L^3)_2Cl]Cl.H_2O$	21	23
$[Cu(L^3)_2Cl_2].H_2O$	15	27
$[Zn(L^3)_2Cl_2].H_2O$	22	35
$[Cd(L^3)_2Cl_2].H_2O$	29	36
$[Hg(L^3)_2Cl_2].H_2O$	27	37

Ecoli = ***Escherichia coli*** **Staph =** ***Staphylococcus***

Fig. (3-103): The effect of the starting material on Ecoli and Staph.

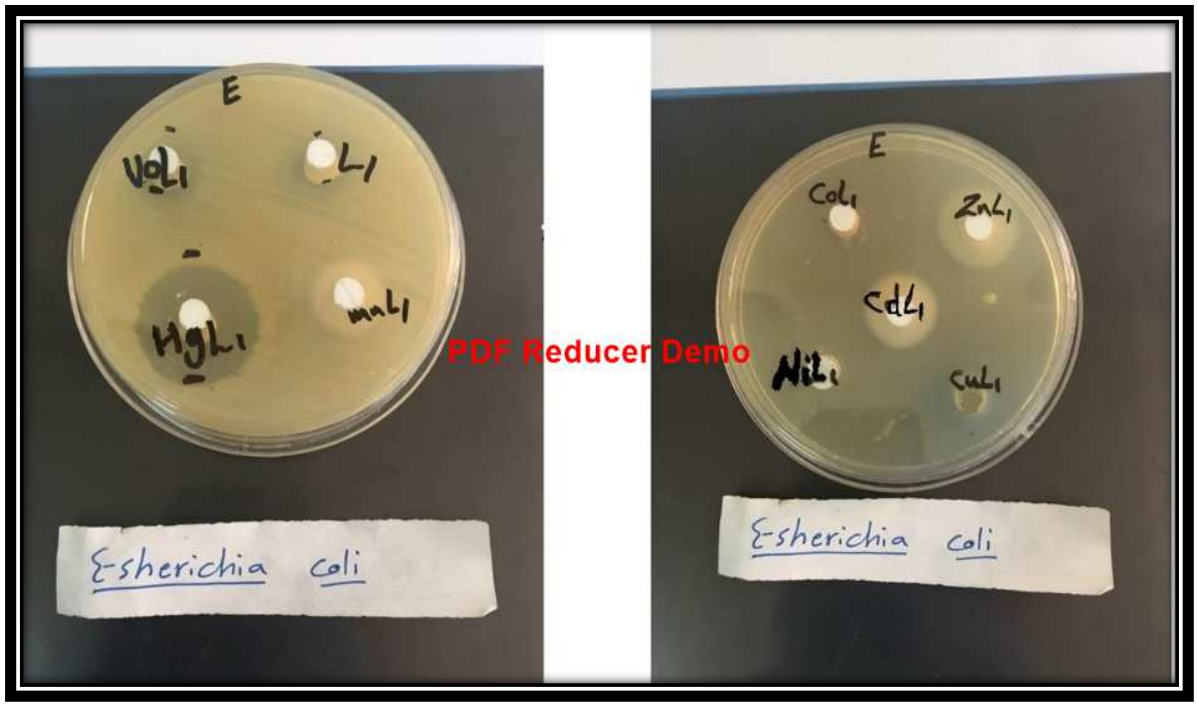

Fig. (3-104): The effect of (L^1) and it's complexes on (Ecoli).

Fig. (3-105): The effect of (L^1) and it's complexes on (Staph).

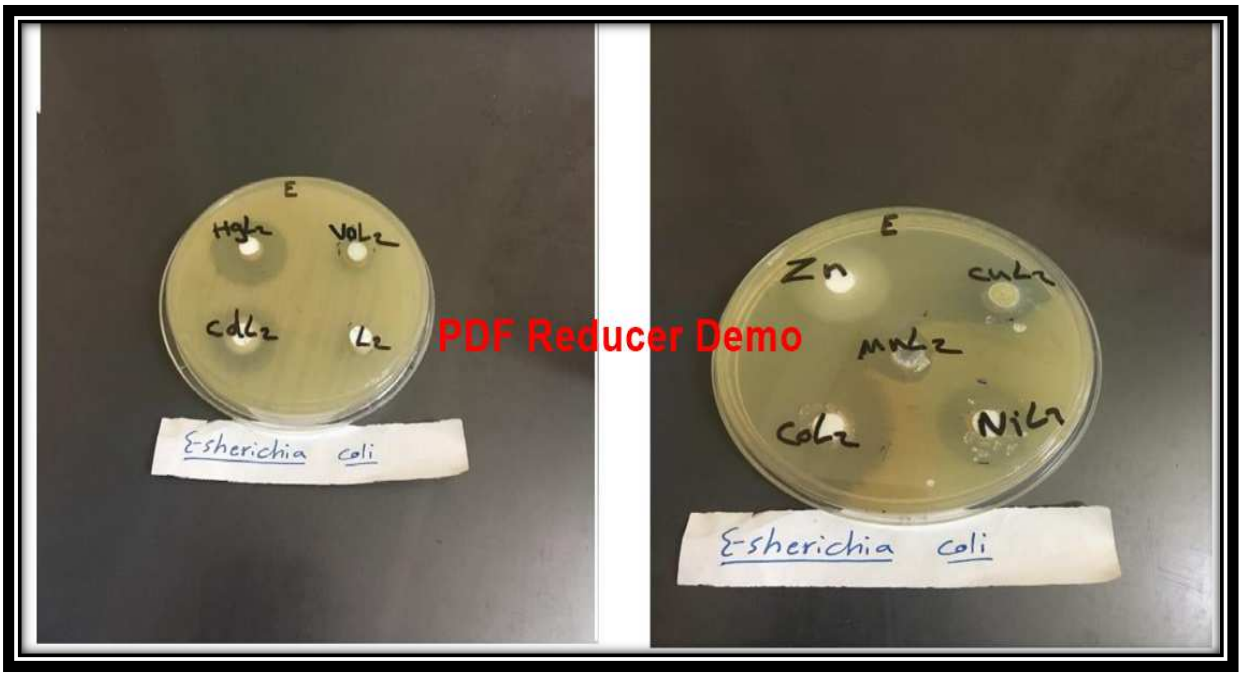

Fig. (3-106): The effect of (L^2) and it's complexes on (Ecoli).

Fig. (3-107): The effect of (L^2) and it's complexes on (Staph).

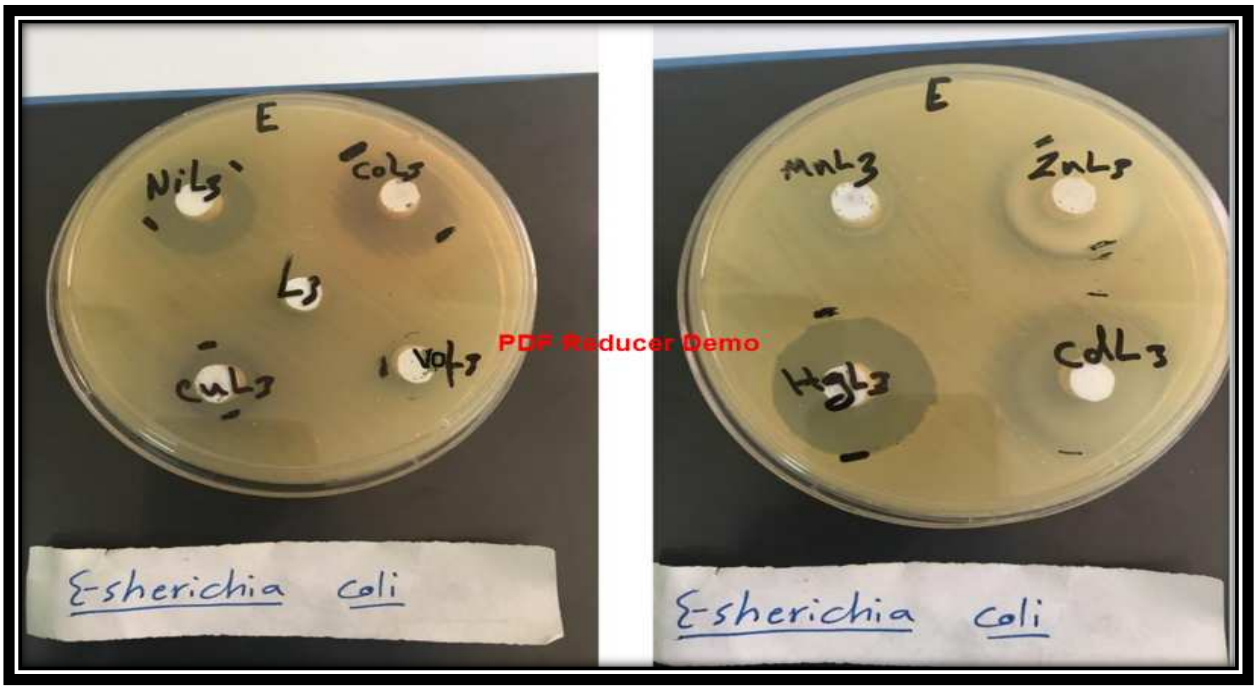

Fig. (3-108): The effect of (L^3) and it's complexes on (Ecoli).

Fig. (3-109): The effect of (L^3) and it's complexes on (Staph).

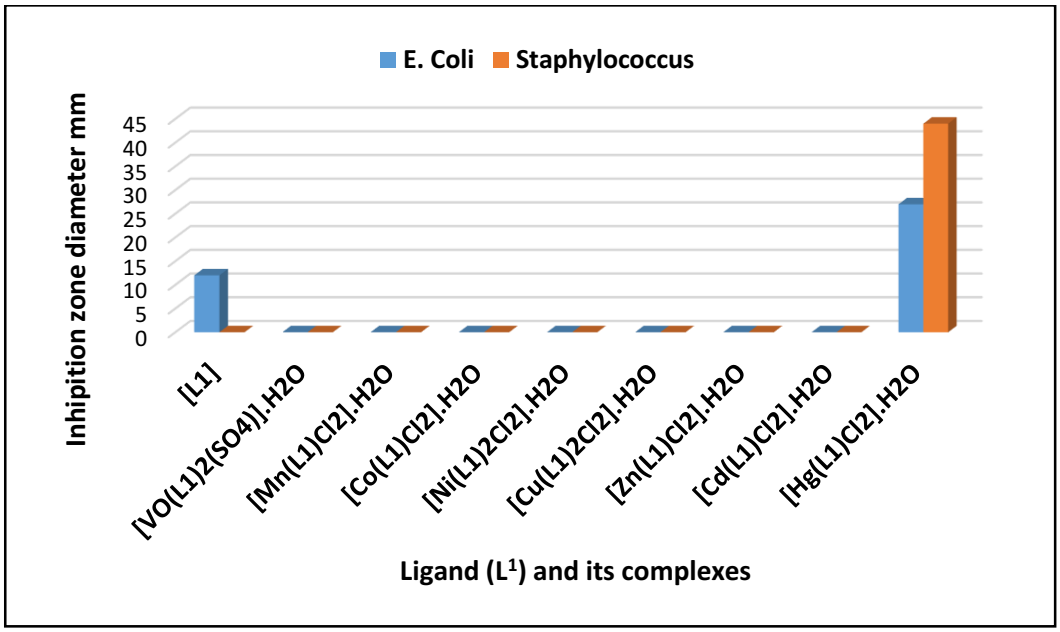

Fig. (3-110): Evolution of diameter zone (mm) of inhibition of (L^1) and its complexes against the growth of various bacterial strains.

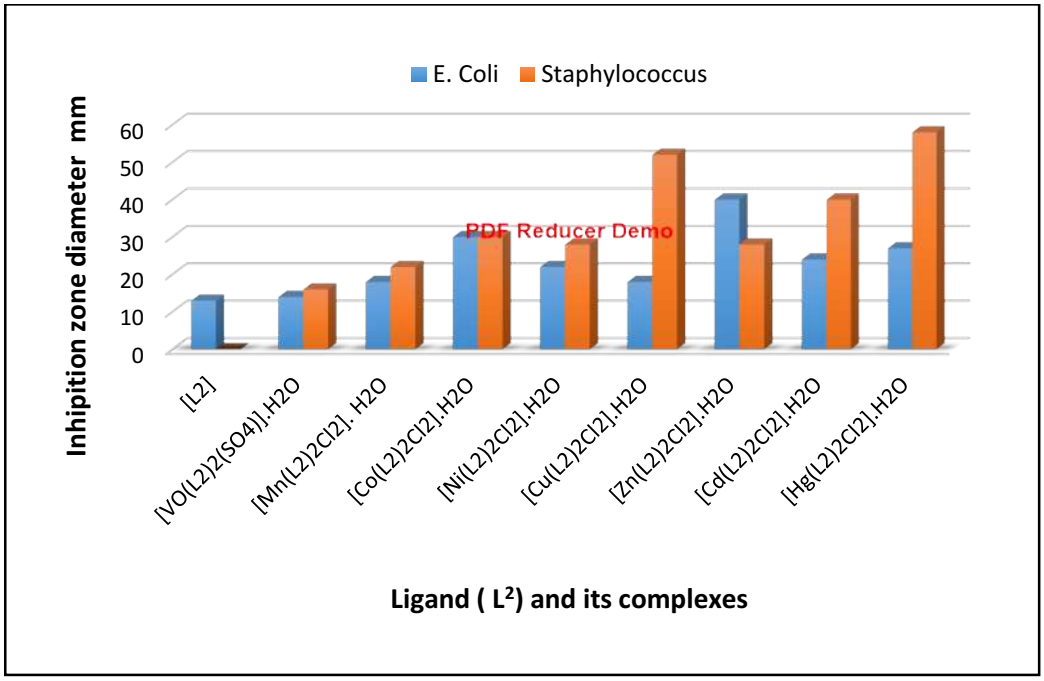

Fig. (3-111): Evolution of diameter zone (mm) of inhibition of (L^2) and its complexes against the growth of various bacterial strains.

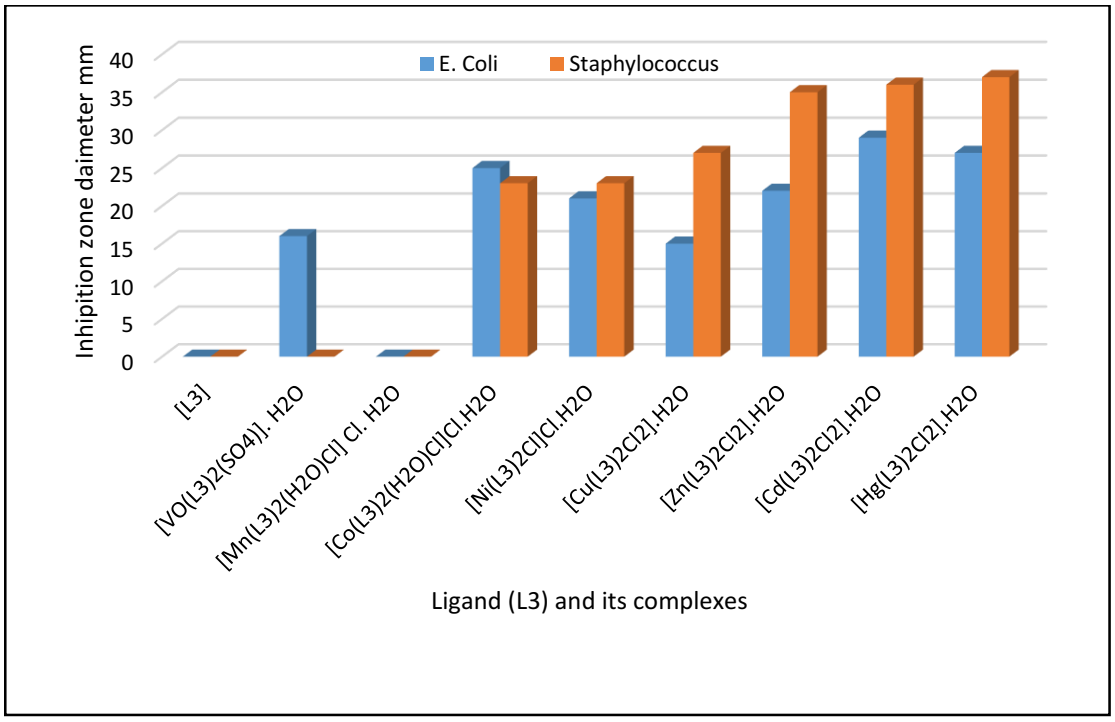

Fig. (3-112): Evolution of diameter zone (mm) of inhibition of (L^3) and its complexes against the growth of various bacterial strains.

(3.4.2) Fungi Activity:

The synthesized ligands and their metal complexes have been tested against one type of fungi (*Candida albicans*). Samples were dissolved in DMSO to provide a final concentration of (0.001) mg/ml. Fungi activity data against tested compounds are shown in Table (3-29). Fig. (3-107 to 3-110) display the inhibition capacity of the synthesized compounds on the tested fungi types. From the obtained data that included in the Tables, the following key points are concluded;

a-The (L^1-L^3) ligands displayed no-activity against *Candida albicans* [194]

b- More complexes of (L^1 –L^3) showed activity against *Candida albicans* [154]

c- Cadmium complexes of ligands ($L^1$and L^3) showed the higher activity, compared with the other complexes.

d- Nickel complexes for ligands (L^2) showed the higher activity, compared with other complexes [195] .

Generally speaking, the increase of the anti-fungal activity of complexes, compared with the ligands indicating that metal complexation improves the activity of the ligand. This may be described by the chelation concept [196] that explained that the delocalization of π electrons over the entire chelate sphere rises. This is due to which polarity of the ligand and the central metal atom decreases, and subsequently results in the infiltration of the complex through the lipid sheet of the cell membrane.

Table (3-29): Fungi activity of the starting material, ligands and their complexes.

Compounds	*C. albicans*
DMSO	**-**
MBZ (K)	**-**
AMBT (A_1)	**30**
ABT (A_2)	**-**
4-APP (A_3)	**28**
$[L^1]$	**-**
$[VO(L^1)_2(SO_4)].H_2O$	**-**
$[Mn(L^1)Cl_2].H_2O$	**12**
$[Co(L^1)Cl_2].H_2O$	**30**
$[Ni(L^1)_2Cl_2].H_2O$	**-**
$[Cu(L^1)_2Cl_2].H_2O$	**12**
$[Zn(L^1)Cl_2].H_2O$	**15**
$[Cd(L^1)Cl_2].H_2O$	**35**
$[Hg(L^1)Cl_2].H_2O$	**25**
$[L^2]$	**-**
$[VO(L^2)_2(SO_4)].H_2O$	**8**

$[Mn(L^2)_2Cl_2].\ H_2O$	**-**
$[Co(L^2)_2Cl_2].H_2O$	**24**
$[Ni(L^2)_2Cl_2].H_2O$	**30**
$[Cu(L^2)_2Cl_2].H_2O$	**12**
$[Zn(L^2)_2Cl_2].H_2O$	**-**
$[Cd(L^2)_2Cl_2].H_2O$	**27**
$[Hg(L^2)_2Cl_2].H_2O$	**23**
$[L^3]$	**-**
$[VO(L^3)_2(SO_4)].\ H_2O$	**-**
$[Mn(L^3)_2\ H_2OCl]\ Cl.\ H_2O$	**-**
$[Co(L^3)_2H_2OCl]Cl.H_2O$	**17**
$[Ni(L^3)_2Cl]Cl.H_2O$	**25**
$[Cu(L^3)_2Cl_2].H_2O$	**20**
$[Zn(L^3)_2Cl_2].H_2O$	**18**
$[Cd(L^3)_2Cl_2].H_2O$	**35**
$[Hg(L^3)_2Cl_2].H_2O$	**21**

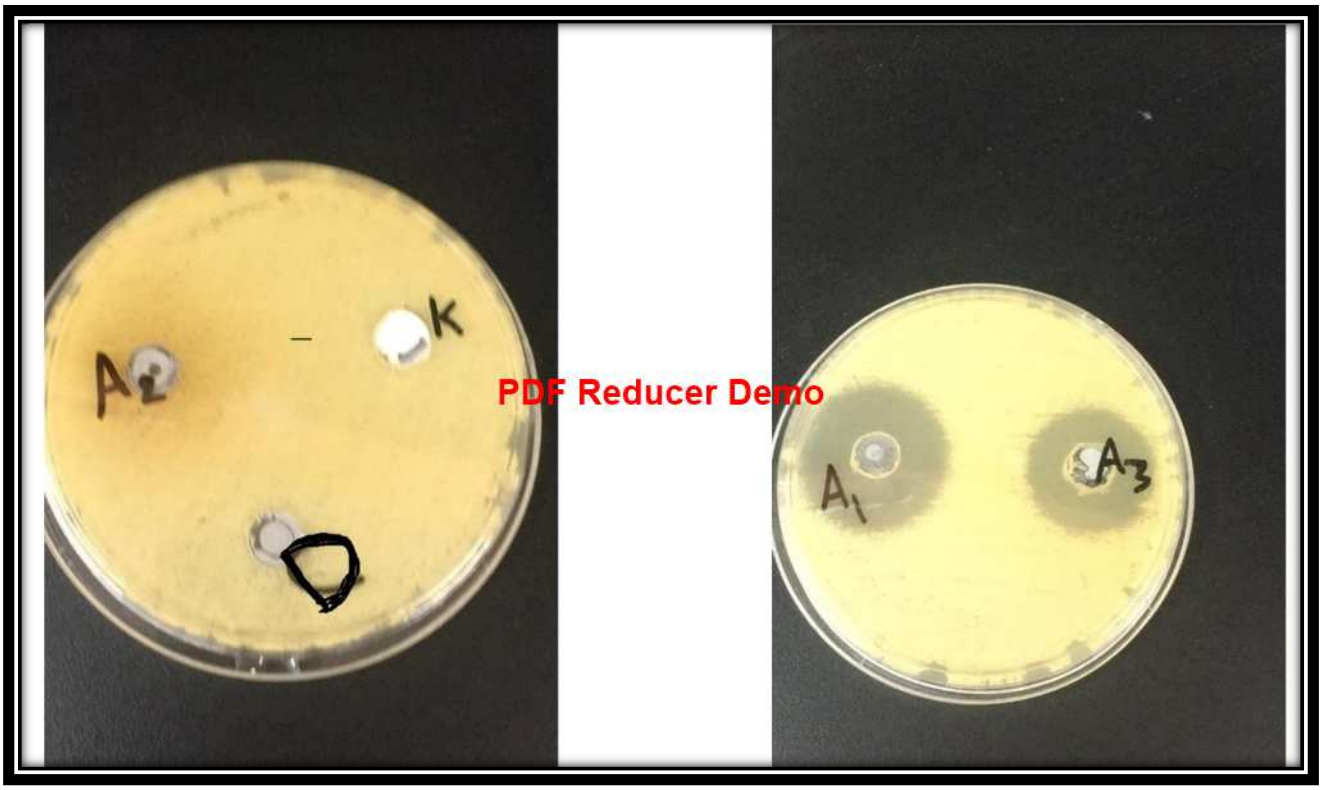

C.albicans* = *Candida albicans

Fig. (3-113): The effect of starting material on *C.albicans*.

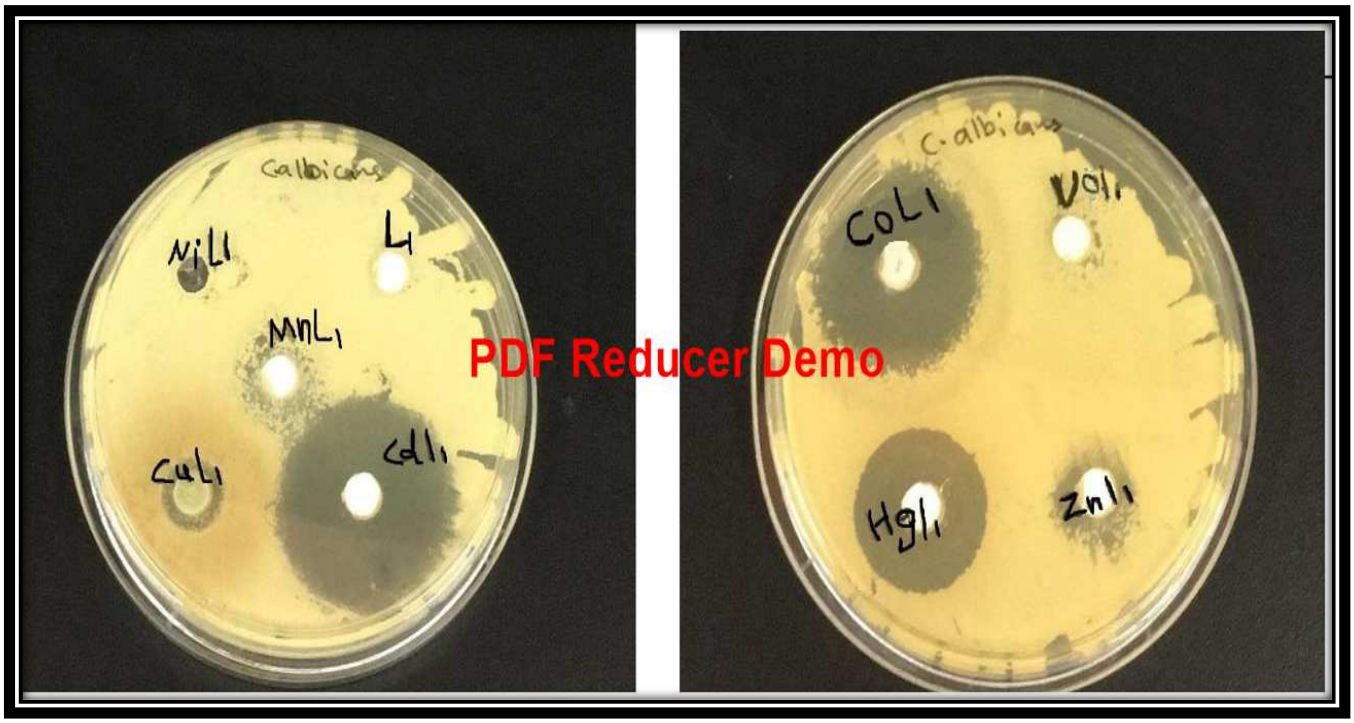

Fig. (3-114): The effect of (L^1) and its complexes on *C.albicans*.

Fig. (3-115): The effect of (L^2) and its complexes on *C.albicans*.

Fig. (3-116): The effect of (L^3) and its complexes on *C.albicans*.

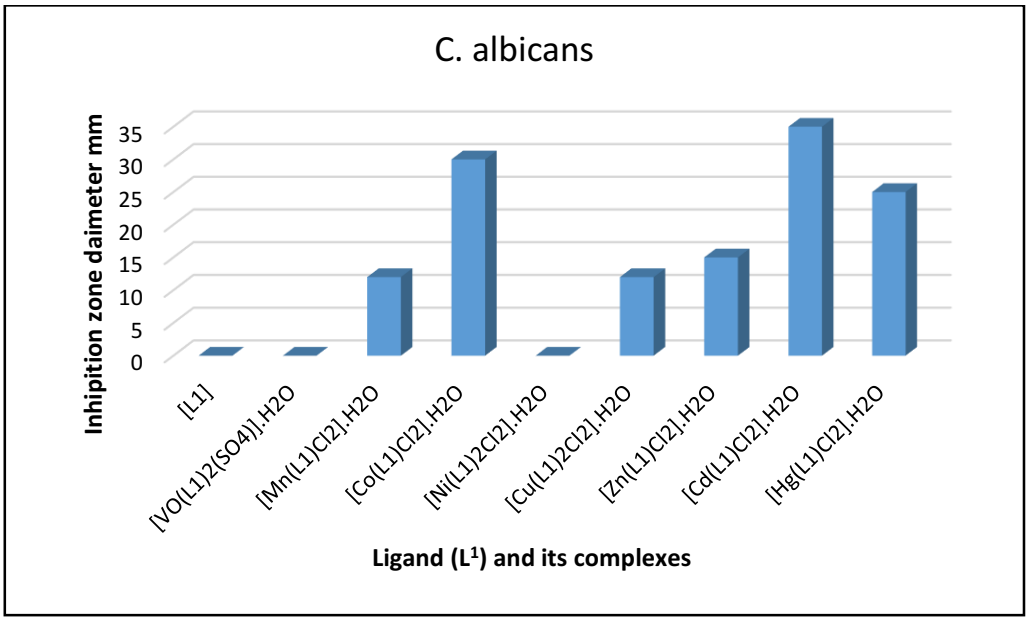

Fig. (3-117): Evolution of diameter zone (mm) of inhibition of L^1 and its complexes against the growth of various fungi strains.

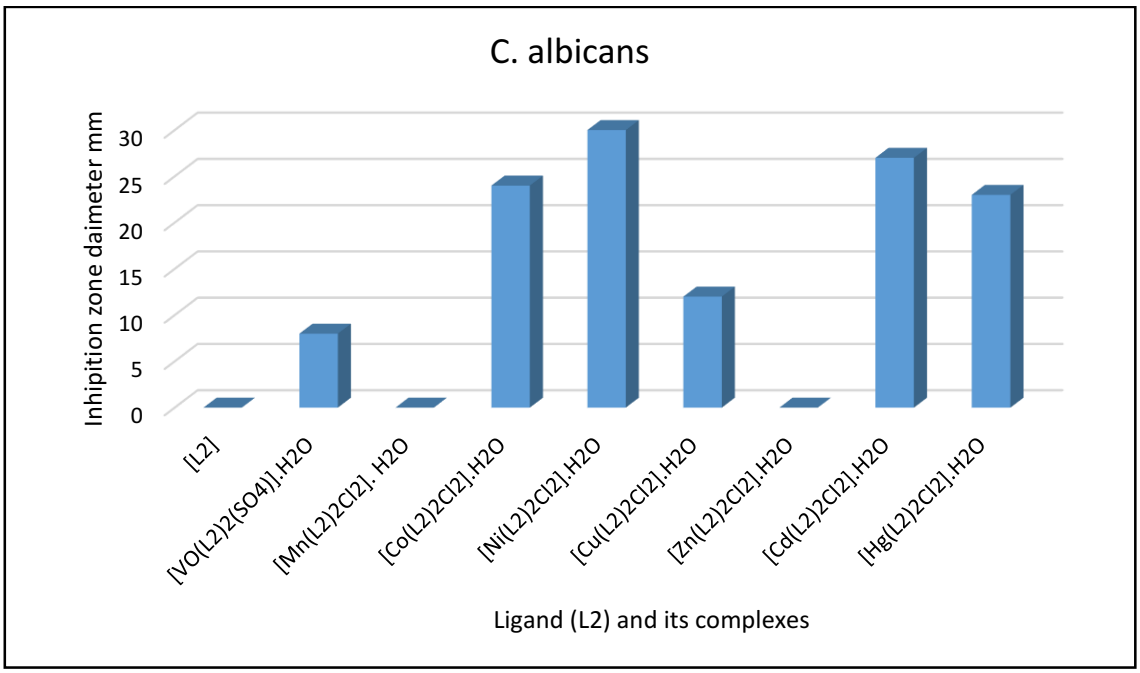

Fig. (3-118): Evolution of diameter zone (mm) of inhibition of L^2 and its complexes against the growth of various fungi strains.

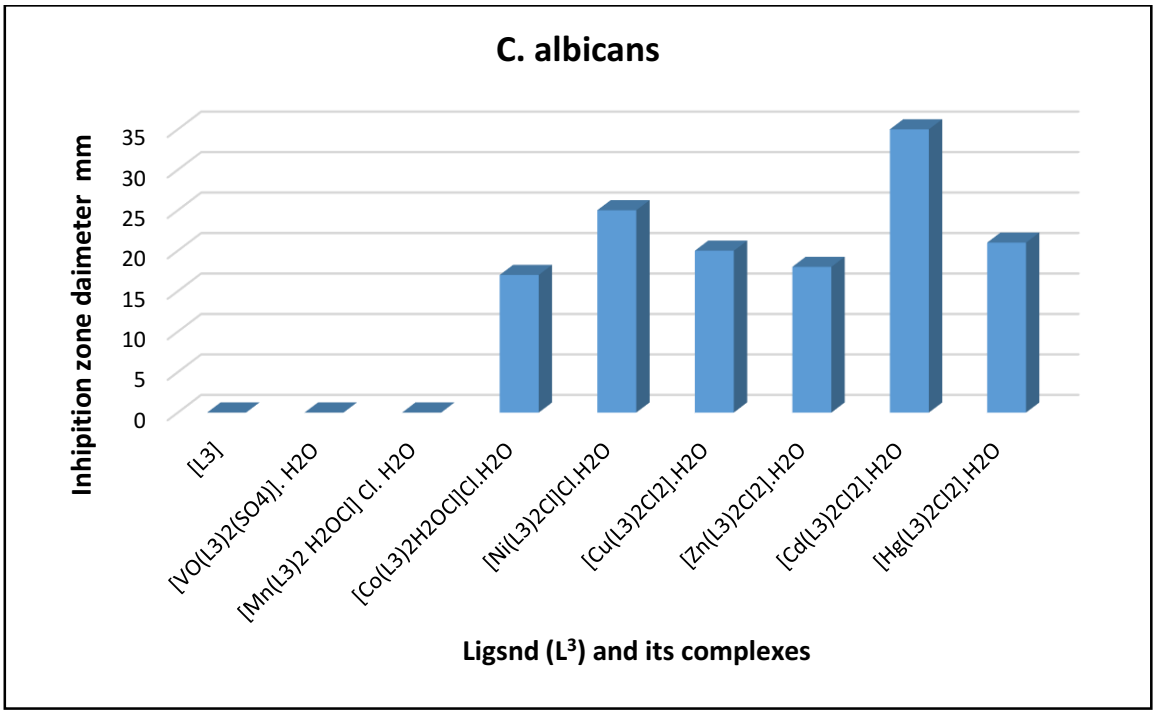

Fig. (3-119): Evolution of diameter zone (mm) of inhibition of (L^3) and its complexes against the growth of various fungi strains.

(3.5) Prospective studies

1- Preparation of new bidentate ligands with different substituents.

2- Synthesis of other complexes of Schiff base ligands (L) with some 4d and 5d row transition metals.

3- Studying the antioxidant activity for the ligands and their complexes.

4- Thermodynamic and kinetic studies for the ligands and their complexes

References

References:

1. N. Devi , Saurabh , D. Choudhary and S. L. Khokra ; *Europ. J. of Pharma. and Medic. Res.*, Vol. 3(11) , (2016) , 598-609 .
2. M. C. Murry ; "***Organic Chemistry***", 5th Ed., John wiley, New York , (2000) .
3. H. R. Marradiya and V. S. Patel ; *J. Serb. Chem. Soc.*, Vol. 67(1), (2002) , 17-25 .
4. R. O. Norman ; "***Principles of Organic Synthesis***", 2nd Ed., John Wiley and Sonc, New York , (1974) .
5. S. Jyothi , K. Sreedhar, D. Nagaraju and S.J. Swamy ; *Canadian Chem. Trans.*, Vol. 3 (4) , (2015) , 368-380 .
6. A.M. Abu-Dief and I. M. A. Mohamed ; *J. Basic Appl. Sci.*, Vol. 4, (2015) , 119-133 .
7. K. Rajasekar, T. Ramachandramoorthy and S. Balasubramaniyan ; *Chem. Sci. Trans*. 2(3), (2013), 877-882.
8. P. Tharmaraj , D. Kodimunthiri, C. D. Sheela and C.S. Shanmugapriya ; *J. Serb. Chem. Soc*. , Vol. 74 (8- 9), (2009) , 927- 938 .
9. K. B. Raj ; "***Heterocyclic Chemistry***", 4th Ed. New Age International publisher, New Delhi , (2010) .
10. A. F. Naasr Al- Hussainy and F. Abd Al.Hussaine Al-Rmah ; *AL-Qadisiya J. For Sci.* , Vol. 18 (2) , (2013), 168-183.
11. R.-Yuan Bai , V. Staedtke , T. Wanjiku , M. A. Rudek , A.Joshi , G. L. Gallia and G. J. Riggins ; *Clin. Cancer Res.* , Vol. 21(15) ,(2015) , 3462-3470 .
12. P. M. Ángeles , E. Begoña1 , T. Guillermo and N. Paola ; *J. of Pharm. and Pharmac.* , Vol. 4, (2016) 351-358 .

13. Z. Naderloo , A. Farahnak , A. Golestani , M. R. Eshraghian and M. B. M. Rad ; *J. of Par. Sci. (JPS)* , Vol. 7(1) , (2016) , 41-47 .
14. E. E. Elemike, A. P. Oviawe and I. E. Otuokere ; *Res. J. Chem. Sci*., Vol. 1 (8), (2011), 6-11 .
15. K. V. Kumar , K. Sunand , K. Ashwini , P. S. Kumar , S. Vishnu and A. Samala ; *Int. J. of Appl. Phar. Sci. and Res.* , Vol. 2(1) , (2017) , 8-14 .
16. R. K. Agarwal , I. Singh and D. K. Sharma ; *Bio. Chem. Appl*., Vol. 5(3) , (2006), 1-10 .
17. S. P. Bhutani ; "***Organic Chemistry***", 1st, Ed., Ane Books, India, (2007) .
18. M. Asiri and S. A. Khan ; *Molecules* , Vol. 15, (2010) , 6850-6858.
19. A.J. Jarad and S. S. Kadhim ; *Int. J. of Sci. and Res. (IJSR)* , Vol. 7 (4) , (2018) , 1291-1301 .
20. Sh.D. Dakore , V.T. Kamble and P. Pisal ; *Int. J. of Chem. Stud.* , Vol. 5(1) , (2017) ,110-113 .
21. M. Usharani , E. Akila , R. Ashokan and R. Rajavel ; *Int. J. of Pharma. Sci. and Heal. Care* ,Vol. 5(3) , (2013) ,1-11.
22. V. Sharma , D. Kumar Mehta, S. Bala , R. Das *; Int. J. of Uni. Pharm. and Bio Sci.* , Vol. 2(4) , (2013) , 241-257 .
23. J. Mohmed, R. R. Palreddy, A. Boinala, N. Narsimha, Sh. K. Gunda and S. Devi Ch ; *Int. J. of Pharm. Sci. and Res., IJPSR* , Vol. 7(3) , (2016) ,1103-1115 .
24. V. N. Telvekar, V. K. Bairwa, K. Satardekar and A. Bellubi ; *Bioorg. Med. Chem. Lett.* , Vol. 22, (2012) , 649–652 .

25. V. S. Padalkar, V. D. Gupta, K. R. Phatangare, V. S. Patil, P.G. Umape and N. Sekar ; *J. Saudi Chem. Soc*., Vol. 18, (2011), 262–268 .
26. K. N. Venugopala, M. Krishnappa, S. K. Nayak, B. K.Subrahmanya, J. P. Vaderapura, R. K. Chalannavar, R. M.Gleiser and B. Odhav ; *Eur. J. Med. Chem.*, Vol. 65, (2013), 295–303 .
27. A. Zablotskaya, I. Segal, A. Geronikaki, T. Eremkina, S.Belyakov, M. Petrova, I. Shestakova, L. Zvejniecea and V.Nikolajeva ; *Eur. J. Med. Chem.* Vol. 70, (2013), 846–856 .
28. S. Sarkar, J. Dwivedi and R. Chauhan ; *J. Pharm. Res.*, Vol. 7, (2013), 439 – 442 .
29. M. A. Azam, L. Dharanya, C. C. Mehta and S. Sachdeva ; *Acta Pharm.*, Vol. 63, (2013) ,19–30 .
30. C. Praveen, A. N. Kumar, P. D. Kumar, D. Muralidharan and P. T. Perumal ; *J. Chem. Sci.*, Vol. 124, (2012), 609–624 .
31. G. Mariappan, P. Prabhat, L. Sutharson, J. Banerjee, U.Patangia and S. Nath ; *J. Korean Chem. Soc.*, Vol. 56, (2012), 251–256 .
32. J. Cai, M. Sun, X. Wu, J. Chen, P. Wang, X. Zong and M. Ji ; *Eur. J. Med. Chem.*, Vol. 63, (2013), 702–712 .
33. M. M. Choi, E. A. Kim, H. G. Hahn, K. D. Nam, S. J. Yang,S. Y. Choi, T. U. Kim, S. W. Cho and J. W. Huh ; *Toxicology*, Vol. 239, (2007), 156–166 .
34. K. Arora and A. Parmar ; *Int. J. of Sci. and Res. (IJSR);* Vol. 4 (10) , (2015) 1603-1611 .
35. R. Haddad, E. Yousif and A. Ahmed ; *Sprin. plus*, Vol. 2, (2013), 510-518 .

36. A. dib ; *Int. J.of Chem. Tech Res.*,Vol. 5(1) , (2013), 204-211 .
37. W. Qin , Sh. Long , M. Panunzio and S. Biondi *Molecules* , Vol. 18(10) , **(**2013) , 12264-12289 .
38. M. B. Smith and J. March ; "***March's Advanced Organic Chemistry: Reactions, Mechanisms and Structure***", 6th ed., John Wiley & Sons, Inc., Hoboken, New Jersey, (2007) .
39. S.Konar, A.Jana, K.Das, S.Ray, S.Chatterjee and S.K. Kar ; *Inor. Chem. Acta* , Vol. 10 , (2013), 3951-3959 .
40. G. Y. S. K. Swamy and K. Ravikumar ; *J. of Stru. Chem.*, Vol. 52(1) , (2011), 208-211 .
41. K. Brodowska and E. Łodyga-CHRUŚCIŃSKA ; *CHEMIK* , Vol. 68(2) , (2014) , 129–134 .
42. S. Davagi and Y. Degani ; "***The Chemistry of Carbon Nitrogen Double Bond***" Ed. S. Patai John Wiley and Sons, Interscience, New York, (1970) .
43. N. Kumar, P. Sharma and A. Pareek ; *Inter. J. of Appl. Res.& Studs.*, Vol. 2(2),(2013),143-149 .
44. A. K. Sharma and S. Chandra; *Spectrochim. Acta Part A*, Vol. 78, (2011) 337–342 .
45. S. Patil, S. D. Jadhav and U. P. Patil ; Arch. Appl. Sci. Res., Vol. 4 (2) , (2012), 1074-1078 .
46. E. Erdem, E.Y. Sari, R. Kinlincarsian and N. Kabay ; *Trans. Met. Chem.* ,Vol. 9(2), (2008),125-136 .
47. B. H. Mehta and V. L. Chavan ; *Res. J. Chem. Environ*, Vol. 15(2), (2011), 57-61 .
48. Q. Wu, W.L. Chen, D. Liu, C. Liang, Y.G. Li, S. W. Lin and E. Wang ; *Dalton Trans*., Vol. 40(1), (2011), 56-61 .

49. W. R. Paryzek, V. Patroniak and J. Lisowski; *Coord. Chem. Rev*., Vol. 249 , (2005), 2156-2175 .

50. I.A. Hassan ; *Res. J. of Chem.Sci. ,* Vol. 3(12), (2013), 50-53 .

51. B. H. Nabeel and S.T. Farah ; *Res.J. of Chem. Sci.*, Vol. 2(6), (2012), 43-49 .

52. A. S. Kabeer , M. A. Baseer and N.A.Mote ; *Asian. J. Chem*., Vol. 13(2), (2001), 496–500 .

53. K. Rajasekar, T. Ramachandramoorthy and S. Balasubramaniyan ; *Res. J. of Chem.Sci. ,* Vol. 3(3), (2013) , 48-51 .

54. M. Abuyamine, R. S. Farag , I. Al-Sbbah and M. Elnawawy,; *Inorg. Chem.*, Accepted: 30 th September (2011).

55. A. A. Osowole , A. C. Ekennia , and B.O. Achugbu ; *Res. and Rev.: J. of Pharm. Ana. (RRJPA)* , 2(2) , (2013) ,1-5 .

56. S. M. Lateef and H. H. Alkam ; *DIALA J. of PUR. Sci.* , Vol. 10 (4) , (2014) , 40-58 .

57. M.M. Abd-Elzaher, M. M. E. Shakdofa , H. A. Mousa and S.A. Moustafa ; *SOP Tran. ON Appl. Chem.*, Vol. 1(1) (2014),42-52.

58. J. S. Sultan, S. M. Lateaf and Dh. K. Rashid ; *Ope. J.of Inorg. Chem.*, Vol. 5 (4) ,(2015), 102-111 .

59. Neelima , K. Poonia , S.Siddiqui, M Arshad and D. Kumar ; *Spectrochim. Acta*, Vol. 155 (15) , (2016), 146-154 .

60. E. K. Kareem , S. M. Lateef and A. A. Ali Drea ; *J. of Kufa for Chem. Sci.* , Vol. 1 (10) , (2015) , 74-85 .

61. S. Ravichandran and C.Murugesan ;*; Int. J. Chem. Tech. Res.*, Vol. 8(2), (2015), 937-943 .

62. M. Ravi, K.P. Chennam , B. Ushaiah1 , R. K. Eslavath ,Sh. Perugu , R. Ajumeera and Ch. S. Devi ; *J Fluoresc* , Vol. 25(5) ,(2015), 1279 –1296.

63. S. M. Lateef , B. M.Sarhan and W. A.J. Al-Saedi ; *Int. J. OF Eng. Sci. & Res. Tech. ,IJESRT,* Vol. 4(2) , (2015) , 606-620 .

64. J. J. Jadeja, M. B. Gondaliya, D. M. Mokariya and M. Shah; *Wor.Sci. New.,* Vol. 47(2), (2016), 123-150.

65. J. Joseph and G. B. Janaki ; *J. of Photochem. & Photobio., B: Biology,* Vol. 162 , (2016), 86‑92 .

66. S. M. El-Megharbel, A. S. Megahed and M. S. Refat ; *J. of Mol. Liq.,* Vol. 216 , (2016), 608–614 .

67. W. H. Mahmoud, R. G. Deghadi and G. G. Mohamed ; *J. Therm. Anal. Calorim. ;* Vol.127(3), (2017) , 2149-2171.

68. G. S. Padole-Gaikwad, R. D. Bagade, R. G. Chaudhary, M. P. Gharpure and H. D. Juneja ; *J. of the Chin. Adva. Mat. Soc. ,* Vol. 5(2) , (2017), 118–132 .

69. S. H. Kadhim, I. Q. Abd-Alla and Th. J. Hashim ; *Int. J.of Chem. Sci.* ; Vol. 15(1) 15, (2017) 1-7.

70. A.Ahlawat, V. Singh and S Asija ; *Chem. Pap.* , Vol. 71(11) , 2195 -2208 .

71. E. Th.Selvi and S. Mahalakshmi ; *Int. J. of Adv. Res. and Devel.*, Vol. 2(2), (2017), 51-56 .

72. Sh.M. Morgan, A.Z. El-Sonbati and H.R. Eissa ; *J.of Mol. Liq.,* Vol. (240), (2017), 752-776 .

73. N. Raman, Th. Chandrasekar, G. Kumaravel and L. Mitu ; *Appl. Organometal Chem.*, Vol. 32,(2018), 1-13.

74. Sh. Ibatte and B. More; Aayushi *Int. Inter. Res. J. (AIIRJ),* Vol. 5(1), (2018) 1-10 .

75. Neelimaab, K. Pooniaa and D. Kumara ; *Mat. Tod. : Proceedings*, Vol. 5, (2018), 1626–1634 .

76. A. Palanimurugan and A. Kulandaisamy ; *J. of Organ. Chem.* Vol. 861, (2018), 263-274 .

77. M.Bhavna, P.Krishna and A.Pralhad, *J. Mol. Cata.* , Vol. 75, (1992), 109 .

78. R. A. Al- Arajy; M. Sc. Thesis, Baghdad University, (2000) .

79. U. Caruso , B. Panunzi , A. Roviello and Angela Tuzi ; *Inor.Chem. Comm.* , Vol. 29 (2013) , 138–140 .

80. S.S.Abd EL-Rehim , M. A.M. Ibrahim and K.F.Khaled ; *J. of Appl. Electrochem.* , 29, (1999) , 593-599 .

81. A. U. Ezeoke , O. G. Adeyemi , O. A. Akerele and N. O.Obi-Egbedi ; *Int. J. of Electrochem. Sci.* , Vol. 7, (2012), 534-553 .

82. I. Danaeea , M. Gholamia , M. RashvandAveib and M. H. Maddahya; *J. of Indu. and Enginee. Chem.* , , Vol. 26(25) , (2015) , 81-94 .

83. P. M.P. Santos , A. M.M. Antunes , J. Noronha , E. Fernandes and A.l J.S.C. Vieira ; *Europ. J. of Medi.* Chem., Vol. 45 , (2010) , 2258–2264 .

84. P. S. Yadav , Devprakash and G. P. Senthilkumar ; *Int. J.of Pharma. Sci. and Drug Res.* , Vol. 3(1) (2011) , 01-07 .

85. S. Bondock, R. Rabie, H. A. Etman and A. A. Fadda; *Eur. J. Med. Chem.*, Vol. 43, 2122, (2008) .

86. S. E. Forest, M. J. Stimson and J. D. Simon; *J. Phys. Chem. B*, Vol. 103, 3963, (1999) .

87. G. Turan- Zitauni, M. Sivaci, F. S. Kilic and K. Erol; *Eur. J. Med. Chem.*, Vol. 36, 685, (2001) .

88. M. S. Collado, V. E. Manotorani, H. C. Goicoechea and A. C. Olivieri; *Talanta*, Vol. 52, 909, (2000) .
89. D. Sinha, A. K. Tiwari, S. Singh, G. Shukla, D. Mishra, H. Chandra and A. K. Mishra; *Eur. J. Med. Chem*., Vol. 43, 160, (2008).
90. P. S. Dixit and K. Srinivasan; *Inorg. Chem*., Vol. 27, (1988) .
91. R. E. Hester and E. M. Nourt; *J. Raman Spectrosc*., Vol. 11, 49, (1981).
92. Banerjee, P. Roy, K. Dhara, M. Manassero, J. Ratha and Pradyot ; Inorg. Chem. , Vol. 46, (2007), 2405-2412 .
93. B.L. Vallee and K.H. Falchuk ; Physiol. Rev. Vol. 73, (1993), 79.
94. C. J. Frederickson and D.W. Moncrieff ; Biol. Signals, Vol. 3, (1994), 127 .
95. C. J. Frederickson, Int. Rev. Neurobiol, Vol. 31, (1989), 145.
96. P.D.Zalewski, and S.H.Millard , *Int. J. Histochem. Cytochem*., Vol. 42, (1994), 877 .
97. P.D.Zalewski, and X.Jian , Fertil. Dev., Vol. 8, (1996), 1097.
98. T. Rosu, E. Pahontu, C. Maxim, R. Georgescu, N. Stanica and A. Gulea; *Polyhedron*, 30, 154, (2011) .
99. S. M. Pathani and K. C. Dash; *Ind. J. Chem*., Vol. 34, 904, (1995).
100. S. Tevin, F. Bedioui, M. G. Villegas and C. B. Charrelon; *Mater. Chem*., Vol. 7(6), 233, (1997) .
101. D. Trans; *The Royal Soc.of Chem.*, Vol. 4 (6), (2007),34-44.
102. U. Spichiger- Keller, "***Chemical Sesors and Biosensors for Medical and Biological Applications***", Wiley- VCH, Weinheim (1998) .

103. R. Gimenez, D. P. Lydon and J. L. Serrano; *Curr. Opin. Solid State and Mat.s Sci.* , Vol. 6(6), (2002) , 527-535 .

104. S. S. Bao, G. S. Chen, Y. Wang, Y. Z. Li. M. Zheng and Q. H. Luo; *Inorg. Chem*., Vol. 45, (2006) , 1124-1129 .

105. Z. Li, M. Fernandez and E.N. Jacobsen ; *Org. Lett*., Vol. 1(10), (1999) , 1611-1613 .

106. M. H. Faris and A. T. Numan ; *M.* Sc. Thesis in Baghdad University (2016).

107. S. Gunasekaran and D. Uthra ; *Asian J. of Chem.* , Vol. 20(8) , (2008), 6310-6324 .

108. D. Munirajasekhar, M. Himaja and V.M. Sunil ; *Int. Res. J. of Pharm.* IRJP, Vol. 2 (1) 2011 114-117 .

109. N. B. Patel and F. M. Shaikh ; *Saudi Pharm. J.* , Vol. 18 ,(2010), 129–136 .

110. G. Y. Yeap , B. T. Heng, N. Faradiana, R. Zulkifly, M. M. Ito,M. Tanabe and D. Takeuchi ; *J. of Mol.r Stru.* , Vol. 10(12) (2012) 1–11 .

111. B. G. Barare and K. Aslan ; thesis in the Morgan State University, May (2016) .

112. H. Ilkimen, C. Yenikaya, M. Sar, M. Bülbül, E. Tunca and H. Dal ; *J. of Enzy. Inh. and Med. Chem.* , Vol. 29(3) , Jun 2014 , 353-61 .

113. Y. A. El-Ossaily , R. M. Zaki , and S. A. Metwally ; J. Sci. Res., Vol. 6 (2), (2014), 293-307 .

114. D. M. Abd El-Aziz , S. E. H. Etaiw and, E. A. Ali ; *J. of Mol. Stru.* , Vol. 48 , (2013) 487–499 .

115. K. Rajasekar, T. Ramachandramoorthy and S. Balasubramaniyau; *Res. J. Chem. Sci.*, Vol. 3(3), 18 (2013), 48- 51 .

116. K. Rajasekar and T. Ramachandramoorthy; *Int. J. Pharm. Bio. Sci.*, Vol. 4(2), (2013), 271- 276 .

117. S.M. Lateef , B. M.Sarhan and W. A.J. Al-Saedi ; *DIALA J. of PUR.Sci.* , Vol. 12 (1) , (2016) ,10-27.

118. Sh. Baluja and S. Chanda ; *Rev. colomb. cienc. quim. farm.* , Vol. 45(2), (2016) , 201-218 .

119. I. Jirjees , S. A. Ali and, H. A. Mahdi ; *Int. J. of Scien. & Engin. Res.* , Vol. 6(11), (2015) , 735-743 .

120. B. Barare , M.Yıldız , H.Ünver and K. Aslan ; *Tatrahed. Lett.*, Vol. (57)5 , (2016), 537-542 .

121. J. Mohmed , R. R. Palreddy , A. Boinala , N. Narsimha , Sh.n K. Gunda and S. D. Ch ; *Int. J. Pharm. Sci. Res.* , Vol. 7(3) , (2016),1103-1115 .

122. A. Palanimurugan, V. Sudharkani and A. Kulandaisamy ; *J. of Nanosci.and Tech.* , Vol. 2(5) (2016) , 204–208 **.**

123. J. G. Smith ; ***"Organic Chemistry"*** , 1st ed , MC Graw-Hill , New York , (2006) , 522 .

124. Sie-T. Haa, Teck-M. Koh, Siew-L. Lee , Guan-Y. Yeap , Hong-Ch. Line and Siew-T. Ong ; *Liquid Crystals*, Vol. 37(5), (2010) , 547–554 .

125. Kok-L. Foo , Sie-T. Ha, Chien-M. Lin , Hong-Ch. Lin, Siew-L. Lee , Guan-Y. Yeap and, S. S. Sastry ; *Karbala Int. Journal of Mod. Sci.*, Vol. 1(2) , (2015) , 152-158.

126. F. A. Carey ***"Organic Chemistry"*** 6th ed , MC Graw-Hill , New York , (2006) .

127. A. Maruszewska and R.Podsiadły ; *Colora. Tech.* , Vol. 13 , (2014) , 243–249 .

128. A. J. Pearl and T.F.A.F. Reji; *Int. J. OF Adva. IN Phar., Bio. and Chem.* , *IJAPBC* , Vol. 3(2), 2014, 507-515 .

129. R. M. Silverstein, F. X. Webster and D. J. Kiemle ; ***"Spectrometric Identification of Organic Compounds***" , 7th ed , John Wiley and Sons , New York , (2005) .

130. M. M. Ghorab , M.G. El-Gazzar, and M. S. Alsaid ; *Int. J. Mol. Sci.* , Vol. 15(5) , (2014) , 7539–7553 .

131. M. Muthukkumar, M. Malathy and R. Rajavel ; *Der Chem. Sin.* , Vol. 6(11), (2015),12-20 .

132. J. Světlík , N. Pronayov , V. Frecer and D. Ciez ; *Tetrahedron,* Vol. 72 ,(2016) , 7620-7627 .

133. M. N. Bhoi, M. A. Borad, N. K. Panchal and H. D. Patel ; *Int. Lett. of Chem. , Physi. and Astron.* , Vol. 53, (2015), 106-113 .

134. R. B. Bennie , S. Th. David , M. S.Sakthi , S. A. J. Mary , M. S. ALakshmi , S. D. Abraham , C. Joel and R. Antony ; *Chem. Sci. Trans.*, Vol. 3(3), (2014) ,937-944 .

135. A.A.El-Asmy, T.Y.Al-Ansi and Y.M.Shaiba, *Trans.Meta.Chem*., Vol. 14**,** (1989), 446 .

136. W.J.Geary ;*Coord.Rev*., Vol. 7, (1971), 81 .

137. W. L. Jolly, **"*The synthesis and Characterization of Inorganic Compounds"***,1st Edn. ,Prentice- Hall of Canada, Canada (1970) .

138. F.A. Cotton and G. Wilkinson, ***"Advanceed Inorganic Chemistry"***4th Edn., John Wiley and Sons (1980) .

139. J.H. Huheey *"**Inorganic Chemistry: Principle of Structure and Reactivity** "* Harper International Edition, Harper and Row Publishers, New York (1994).

140. K. Bruger "***Coordination Chemistry Experimental Methods***", 1st Edn., Buther worth, London (1967) .

141. B.Anupama, M.Padmaja and C.G.Kumari; *E-J.Chem.*, Vol. 9(1), (2012) , 389-400 .

142. R.Buchanan and M.Mashuta ; J.Am.Chem.Soc., Vol. 11, (1989), 4497 .

143. M. A. Ali, A. H. Mirza, M. Nazimuddin, P. K. Dhar and R. J. Butcher; *Trans. Met. Chem*. Vol. 27, (2002), 27- 33 .

144. K. A. Maher and S. R. Mohammed ; *Int J Cur Res Rev* , Vol. 7 (2) ,(2015) , 6-16 .

145. S. A.Ahmed , A. O. Mohamed and A. A.Humada ; *Journal of Kirkuk University –Scie.c Stud.* , Vol. 4(2) ,(2009) , 37-45.

146. N. Raman , J. D. Raja and A. Sakthivel ; *J. Chem. Sci.*, Vol. 19(4) , (2007), 303–310 .

147. E. Schumann, J. Altman, K. Karaghiosoff and W. Beek; *Inorg. Chem*., Vol. 34, (2002) ,154- 165.

148. M. Shakir, S. Hanif , M.A. Sherwani , O. Mohammad , M. Azam and S. Al-Resayes ; *J. of Photochem. & Photobiol., B: Biology* , Vol. 157, (2016) , 39–56 .

149. Z. H. Abd El- Waheb, M. M. Mashaly and A. A. Faheim; *Chem. Pap*., Vol. 59(1), (2005), 25-36 .

150. A. A. Shabana , I. S. Butler , D. F.R. Gilson , B. J. Jean-Claude , Z. S. Mouhri , M. M. Mostafa and S. I. Mostafa ; *Inorg. Chim. Acta* , Vol. 23 (2014) , 242–255 .

151. A. S. Thakar, K. S. Pandya , K. T. Joshi and, A. M. Panch ; *E-J. of Chem.* , Vol. 8(4), (2011) , 1556-1565 .

152. N. Raman , S. Sobha and L. Mitu ; *J.l of Saudi Chem. Soc.* Vol. 17 , (2013) , 151–159 .

153. A. N. Al-Shareefi , S. H.i Kadhim and W. A. Jawad ; *J. of Appl. Chem.* ,Vol. 2(3) , (2013) , 438-446 .

154. D. Mohanambal and S. A. Antony ; *Res. J. of Chem. Sci.* , Vol. 4(7), (2014) , 11-17 .

155. N.M. Abdulkhader Jailani , A. Xavier and A. Mumtaj ; *J. of Advan. Appl. Scie. Res.*, Vol. 1(9) , (2017) , 39- 53 .

156. B. Anupama and C. G. Kumari; *Int. J.of Res. in Chem. and Envi.*, Vol. 3 (2) , (2013) ,172-180 .

157. P. Mangaiyarkkarasi, and S. A. Antony ; *Asian J. of Sci.and Tech.*, Vol. 5 (6) , (2014) , 340-347.

158. D.Mohanambal and S. A. Antony ; *Int. J. of Pharm. and Bio Sci.* , Vol. 5(3), (2014) ,600 – 611 .

159. A.R.Cowley, J.R.Dilworth, P.S.Donnelly and J.M.Whilte, *Inorg. Chem.*; Vol. 45, (2006), 496 .

160. B.Anupama, M.Padmaja and C.G.Kumari, *E-Journal of Chem.* ; Vol. 1, (2012) , 389-400 .

161. M.S.Suresh and V.Prakash ; *Inter.J.of the phys.sci.* ; Vol. 5(14), (2010), 2203-2211 .

162. N. Raman, S. Sobha and M. Selvaganapathy; *Int. J. of Pharm. and Bio Sciences* , Vol. 3 , (2012) , 251-267.

163. A. S. THakar , K. S. Pandya , K. T. Joshi and A. M. Panchol *; E-J. of Chem.,* Vol. 8(4), (2011),1556-1565 .

164. A. J. pearl and T. F. Abbs fen Reji ; *J. Chem. Pharm. Res* ,Vol. 5 (1) , (2013) , 115- 122 .

165. N. Lal and R. Kumar ; *Wor. J. OF Pharm. And Pharma. Sci.* , Vol. 5(7) , (2016) , 1747-1752 .

166. T. Mangamamba, M. C. Ganorkar, and G. Swarnabala ; *Int. J. of Inorg. Chem. ,* Vol.11(2), (2014) , 1-22.

167. K.O. Ogunniran , M.A. Mesubi , J.A. Adekoya , O.O. Siyanbola , AI Inegbinebor , O.O. Ojo , A.E. Adedapo , A. Edobor-Osoh , and T. Narender ; *Canadian J. of Pure and Appl. Sci.* , Vol. 9(2) , (2015) , 3519-3534 .

168. N. L. Obasi, C. O. Okoye, and O. A.Anaga ; *Chem. and Mater. Res.* , Vol. 6(3) , (2014) , 140-150 .

169. C. Leelavathy and S. A. Antony ; *Int. J.of Basic and Appl. Chem.Sci.* , Vol. 3 (4) , (2013), 88-95 .

170. S. S. Bhuyara , S. S. Kharkale-Bhuyarb , R. G. Chaudharyc , N. V. Gandhared , H. D. Junejaa and L. J. Paliwala ; *J. of the Chin. Advan. Mate. Soci* , Vol. 7(2) , (2015), 1-22 .

171. M. Shakir , S. Hanif , M. A. Sherwani , O. Mohammad , M. Azam and S. I. Al-Resayes ; *J. of Photochem. & Photobio. , B: Biology* , 157, (2016) , 39–56 .

172. P. Deshmukh , P. K. Soni , A. Kankoriya , A. K. Halve and R. Dixit ; *Int. J. Pharm. Sci. Rev. Res.*, Vol. 34(1), (2015) , 162-170 .

173. S.N. Chaulia ; *Der Pharm. Lettr.* , Scholars Research Library, Vol. 8 (21) , (2016), 55-74 .

174. A.B.P.Lever, "***Inorganic Electronic Spectroscopy second edition***", New York, (1984) .

175. A. M. N. Khaleel and M.I. Jaafar ; *J. of Appl. Chem. (IOSR-JAC)* , Vol. 9(8) , (2016), 4-11 .

176. R. Shakru ; *Int. J. of Conce. on Compu. and Inform. Techn.* ; Vol. 3(1) , 2015 , 52-56 .

177. M. Alias, H. Kassum and C. Shakir ; *J.of the Assoc. of Arab. Univ. for Basic and Appl. Sci.* , Vol. 15(2) , (2014), 28 – 34.

178. A.M. Nalawade , R.A. Nalawade , S.M. Patange and D.R. Tase ; *Int. J. of Engin. Sci. Inv.* , Vol. 2 (7) , July. (2013) , 01-04 .

179. A. A. Osowole ; *Int. J. of Inorg. Chem.* , Vol.4(12), (2011) , 7-12 .

180. M. S. Hossain , C. M. Zakaria and M. K. Zahan ; *J. OF Sci. Res.* , Vol. 9 (2), (2017) , 209-218 .

181. M.S.Suresh and V.Prakash ; *E-J. of Chem.* , Vol. 8(3), 2011 , 1408-1416 .

182. G. Nizami, P. Garg and Sh. Ahmad ; *Orien. J. OF Chem.* , Vol. 29 (4), (2013) , 1579-1584 .

183. J. Rani and Bheeter ; *Wor. J. OF Pharm. and Pharmac. Sci.. ;* Vol. 5(6) , (2016) ,895-904 .

184. M.S Suresh, and V.Prakash ; Int. J. of Curr.Res. , Vol. 3(2) , (2011) , 068-075 .

185. D. C. Onwudiwe and P. A. Ajibade ; *Int. J. Mol. Sci.* , Vol. 13(2) , (2012) , 9502-9513 .

186. H. H. Alganzory , S. A. Aly and T. A. Salem ; *J. of Chem. and Pharmac.l Res.* , Vol. 9(1) , (2017) , 133-144 .

187. A. Rahman, M. Choudhary and W. Thomsen, "***Bioassay Techniques For Drug Development***", Harwood Academic. Amsterdam. The Netherlands, (2001) .

188. R. V. Singh, R. Dwivedi and S. C. Joshi ; Trans. *Met .Chemi*., Vol. 29(1), (2004) , 70–74 .

189. E. I. Yousif and H. A. Hasan ; PhD. , Thesis in Baghdad University (2016) .

190. F. A. Al-Saif ; *Int. J. Electrochem. Sci*. , Vol. 8(3) , (2013) , 10424 – 10445 .

191. N. Gayathri and M.S. Suresh ; *Asian J. of Chem.* ; Vol. 29(3) , (2017), 541-546 .

192. N. Raman , J. D. RAJA and A Sakthivel ; *J. Chem. Sci.*, Vol. 119(4), (2007), 303–310.

193. R. Ramesh and S. Maheswaran , *J. Inorg. Biochem*., Vol. 96, (2003) ,457-462 .

194. V. Asati , N. K. Sahu, A. Rathore , S.Sahu and D.V. Kohli ; *Arabian J. of Chem.* , Vol. 8, (2015) , 495–499 .

195. I. P. Ejidike and P. A. Ajibade ; *Rev. Inorg. Chem.* , Vol. 35(4) , (2015) , 191–224 .

196. M. Balouiri. , M. Sadiki and S. K. Ibnsouda ; *J. of Pharmac. Analy.* , Vol. 6, (2016) , 71–79 .

الخلاصة

تضمن العمل تحضير ثلاث ليكاندات (L^1, L^2 and L^3) اثنان من نوع (N,N) وواحد نوع (N,O) والتي استعملت فيما بعد لتحضير المعقدات مع الايونات الفلزية وهذه الليكاندات هي :

[L^1]….. Methyl (E)-(6-(((6-methoxybenzo[d]thiazol-2-yl)imino) (phenyl) methyl)-1H-benzo[d]imidazol-2-yl) carbamate .

[L^2]….. Methyl (E)-(6-((benzo[d]thiazol-2-ylimino) (phenyl) methyl)-1H-benzo[d]imidazol-2-yl) carbamate.

[L^3]…..Methyl (E)-(6-(((1,5-dimethyl-3-oxo-2-phenyl-2,3-dihydro- 1H-pyrazol-4-yl)imino)(phenyl)methyl)-1H-benzo[d]imidazol-2-yl)carbamate.

تم تحضير هذه الليكاندات من مفاعله مكافئ واحد من (Mebendazole) مع مكافئ واحد لكل من 2-Amino-6-methoxy benzothiazole لليكاند الأول [L^1] و 2-Aminobenzothiazole لليكاند الثاني [L^2] ومع 4-Aminoantipyrine بالنسبة لليكاند الثالث [L^3].

(التفاعلات اجريت باستخدام الايثانول كمذيب والتصعيد العكسي ولمدة 30 ساعة لكل الليكاندات).

تم تشخيص الليكاندات باستخدام درجة الانصهار والتحليل الدقيق للعناصر وأطياف الأشعة تحت الحمراء وفوق البنفسجية–المرئيه وطيف الرنين النووي المغناطيسي وطيف الكتلة.

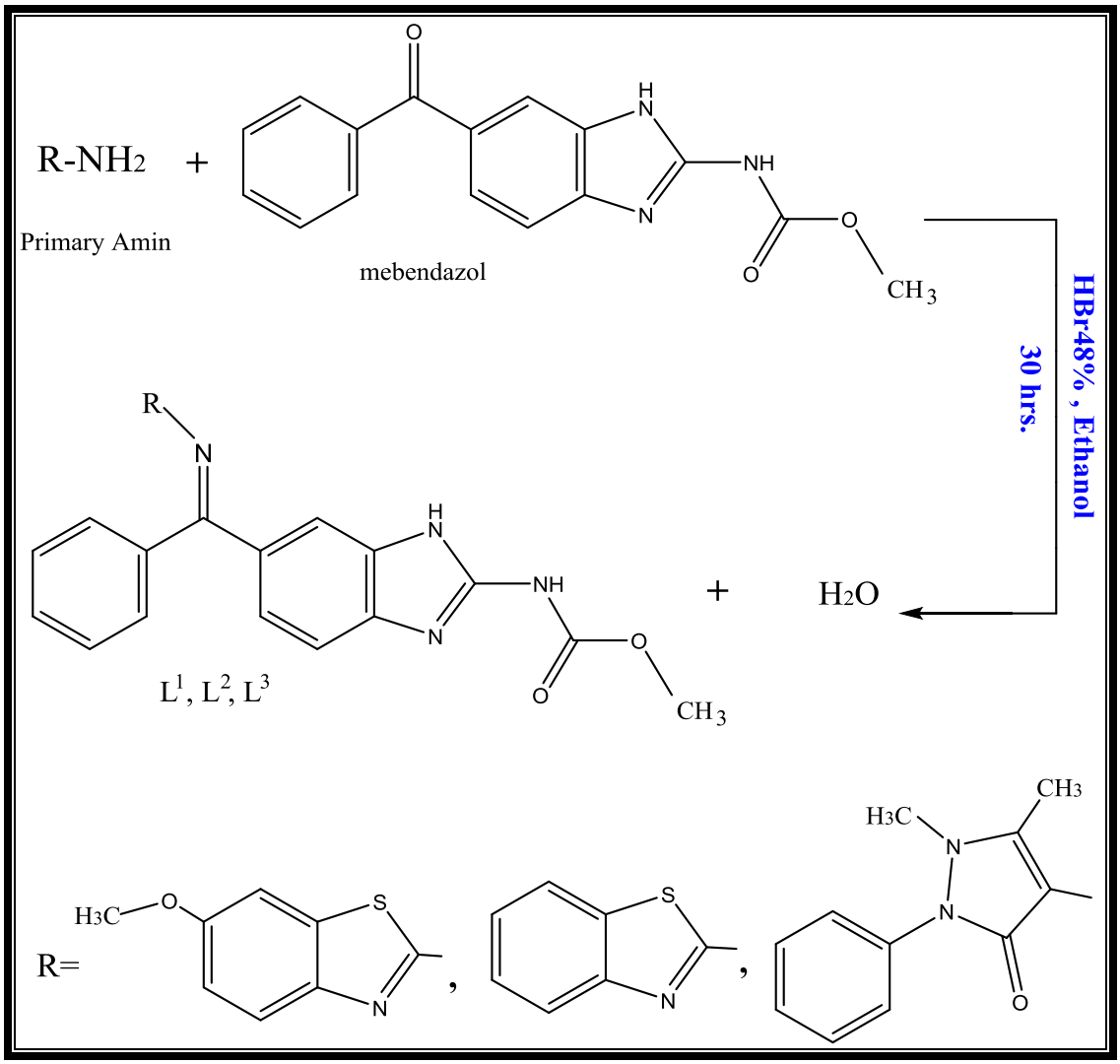

مخطط: يوضح تحضير الليكاندات (L^1 - L^3)

كما تضـمن البحث تحضـير سـلسـلة من المعقدات وذلك من خلال مفاعلة الليكاند مع أملاح: الفنادايل (II) والمنغنيز (II) والكوبلت (II) والنيكل (II) والنحاس (II) والخارصـين (II) والكادميوم (II) والزئبق (II) وباسـتخدام الاسـيتون كوسـط تفاعل لليكاندين الأول والثاني والميثانول لليكاند الثالث. شُـخصـت هذه المعقدات باسـتخدام درجة الانصـهار و التحليل الدقيق للعناصـر و الامتصـاص الذري اللهبي(A.A) و أطياف الأشـعة تحت الحمراء و فوق البنفسجية – المرئية و قياسات التوصيلة الكهربائية و محتوى الكلور والتحليل الحراري الوزني.

حيث اقترحت الصيغ الكيميائية العامة التالية : $A.H_2O$ $[M(L)_2(X)(Y)]$ حيث:

$L=L^1,L^2$

M=VO(II), X=0, $Y=OSO_3^{-2}$, A=0

M= Mn(II),Co(II),Ni(II),Cu(II),Zn(II), Cd(II), Hg(II)

A=0, X=Cl, Y=Cl,

$L=L^3$

M=VO(II), X=0, $Y=OSO_3^{-2}$, A=0

M= Mn(II),Co(II), X=Cl, Y= H_2O, A=Cl

M= Ni(II), X=Cl, Y=0, A=Cl

M= Cu(II) ,Cd(II) , Zn(II) , Hg(II) , X=Cl , Y= Cl , A=0

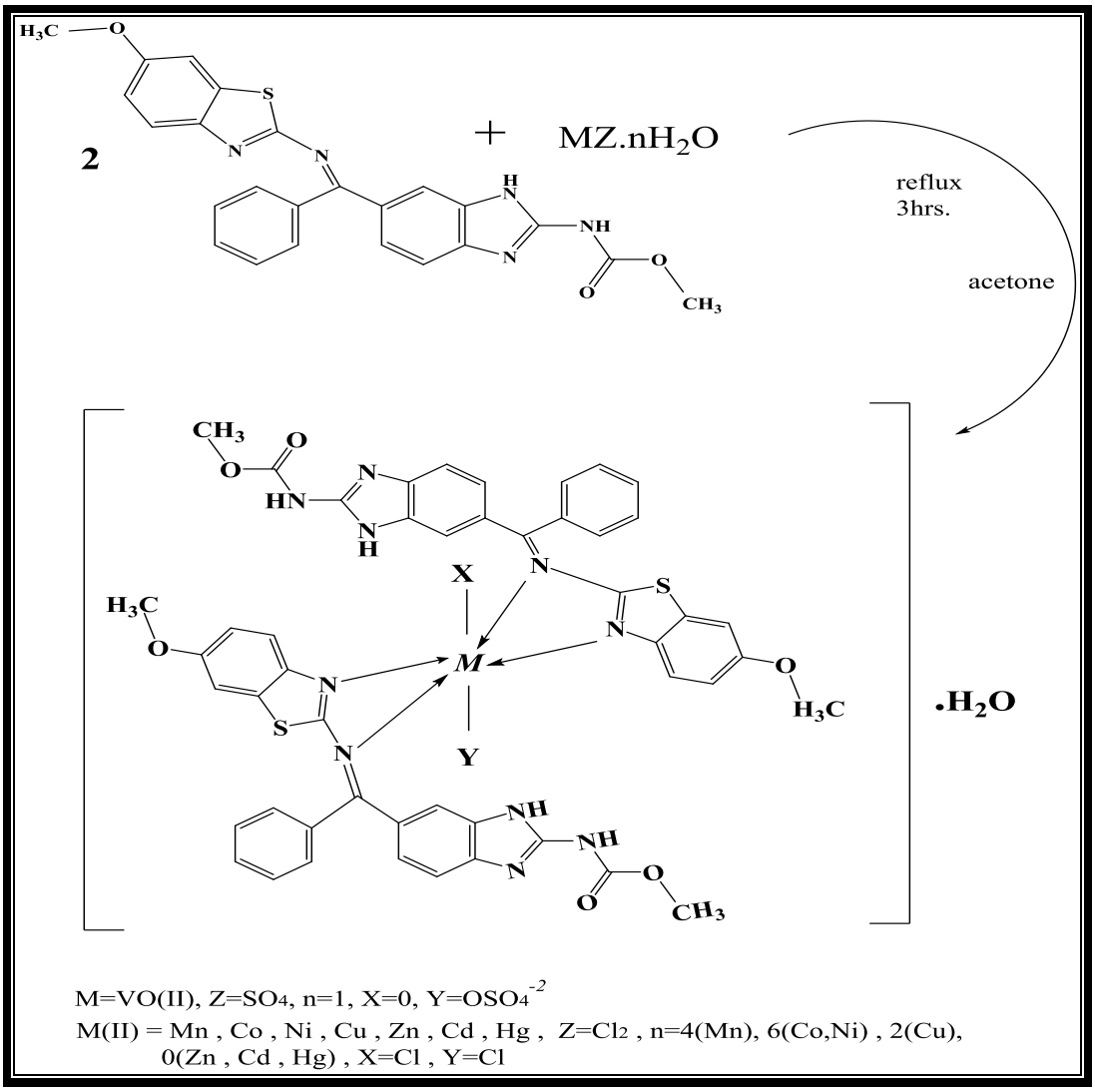

مخطط :يوضح تحضيرمعقدات الليكاند L^1

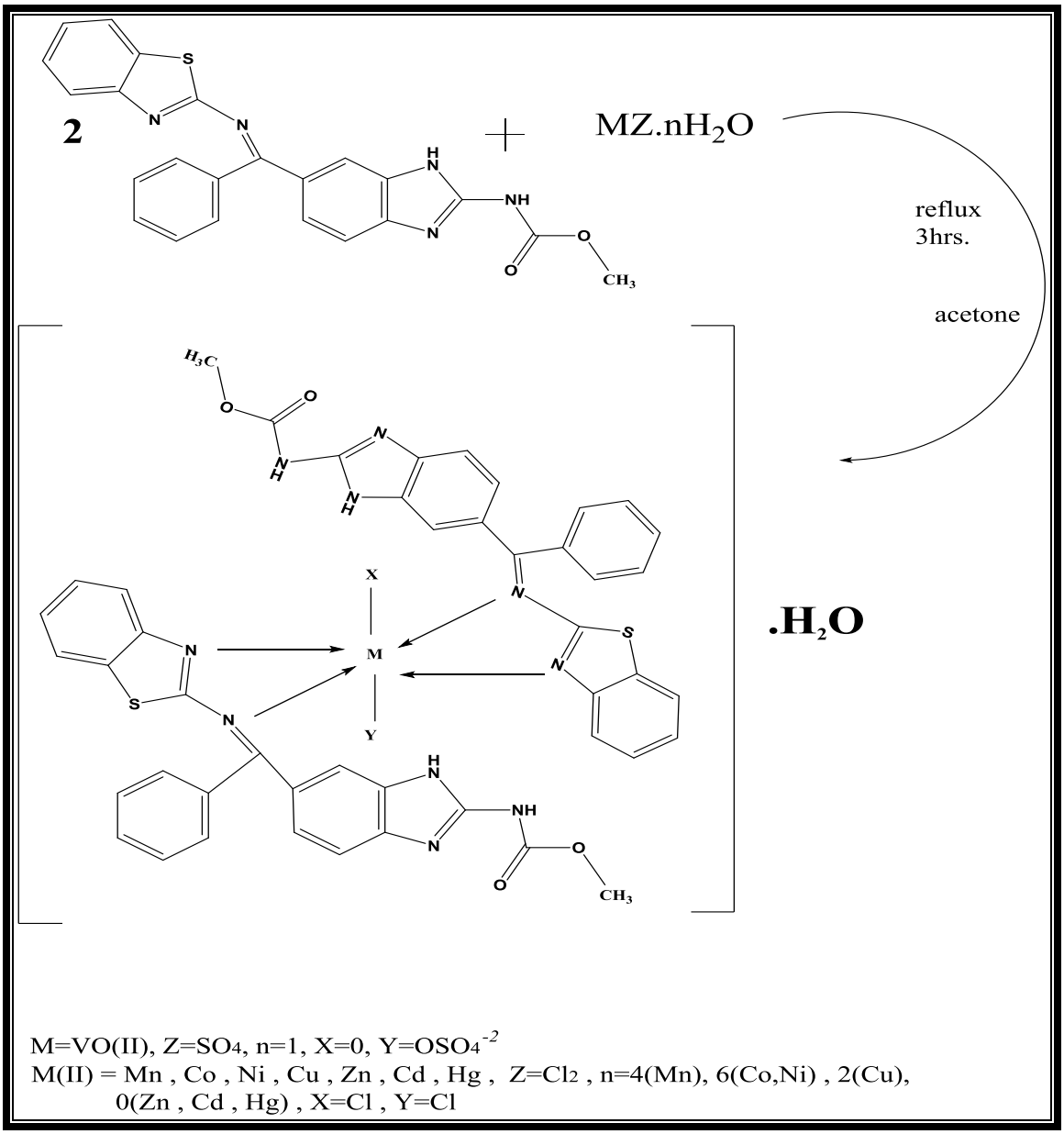

مخطط :يوضح تحضير معقدات الليكاند L^2

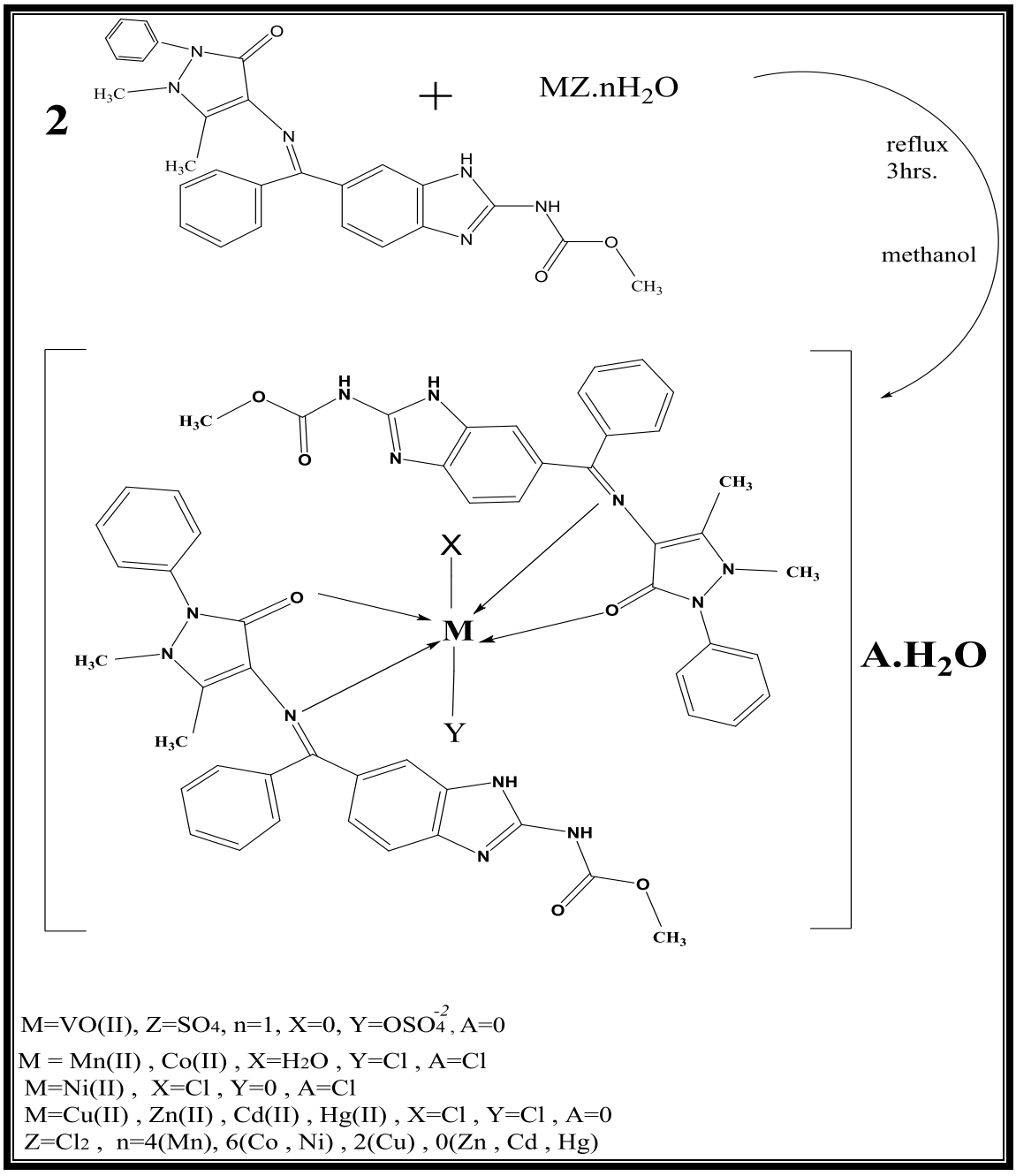

مخطط :يوضح تحضيرمعقدات الليكاند L^3

أظهرت أطياف الأشعة تحت الحمراء ان الليكاندات متعدده السن تسلك بصفتها ثنائيه التناسق. كما استخدمت أطياف الأشعة فوق البنفسجية – المرئية للمعقدات في دراسة التوزيع الفراغي لليكاند مع أيونات الفلزات. و باستخدام المعلومات المستحصلة من التحليل الدقيق للعناصر و الامتصاص الذري و التوصيلية الكهربائية و محتوى الكلور والتحليل الحراري الوزني بالإضافة الى القياسات الطيفية [الأشعة تحت الحمراء و فوق البنفسجية – المرئية]، اقترح ان الشكل الفراغي هو ثماني السطوح لجميع المعقدات ماعدا معقد الـ $[Ni(L^3)_2Cl]Cl.H_2O$ فقد اقترح الشكل ثنائي الهرم المثلثي.

تم تقدير الفعالية الحيوية لليكاندات والمعقدات المحضرة بالإضافة للمواد الأولية اتجاه نوعين من البكتيريا وهي :

(*Escherichia coli and Staphylococcus aureus*) ونوع واحد من الفطريات وهو (*Candida albicans*) وقد أظهرت النتائج ان المعقدات المحضرة لها فعالية حيوية مضادة للبكتيريا والفطريات المذكورة أعلاه اعلى مقارنة مع الليكاندات والمواد الأولية .

جمهورية العراق
وزارة التعليم العالي والبحث العلمي
جامعة بغداد
كلية التربية للعلوم الصرفة / أبن الهيثم
قسم الكيمياء

دراسة طيفية وتركيبية لقواعد شف جديدة ومعقداتها الفلزية وتقدير فعاليتها البايولوجية

أطروحة مقدمة إلى

كلية التربية للعلوم الصرفة/ ابن الهيثم – جامعة بغداد

وهي جزء من متطلبات نيل درجة الدكتوراه في فلسفة علوم الكيمياء

من قبل

شيماء احمد حسن الطائي

بكالوريوس كيمياء 2002

ماجستير كيمياء 2012

بأشراف

أ.د. ساجد محمود لطيف

1440هـ 2018 م